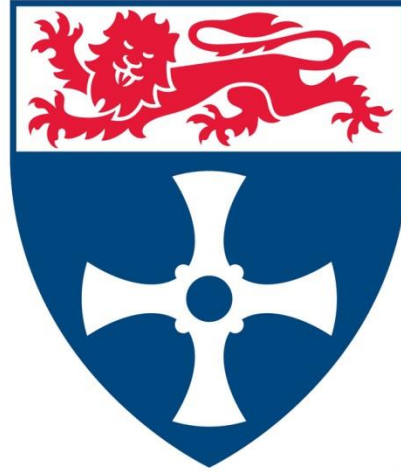


Using systems biology to investigate how age-related changes in TGF β signalling alter pro-inflammatory stimuli.



Newcastle
University

David Hodgson

Institute of Cellular Medicine (ICM)

Newcastle University

A thesis submitted in partial fulfilment of the requirements
for the degree of

Doctor of Philosophy

January 2018

Abstract

Osteoarthritis (OA) is a degenerative condition caused by dysregulation of multiple molecular signalling pathways. This dysregulation results in damage to cartilage, a smooth and protective tissue that enables low friction articulation of synovial joints. Matrix metalloproteinases (MMPs), especially MMP13, are key enzymes in the cleavage of type II collagen which is a vital component for cartilage integrity. Various stimuli have been identified as inducers of MMP expression such as excessive load, injury and inflammation.

Although previously considered a non-inflammatory arthritis, recent research has shown that inflammation may play an important role in OA development. A novel meta-analysis of microarray data from OA patients was used to create a cytoscape network representative of human OA. This enabled the identification of key processes in OA development, of which inflammation was prominent. Examining various different signalling pathways highlighted a role for transforming growth factor beta (TGF β) in protecting against pro-inflammatory cytokine-mediated MMP expression. Indeed, TGF β plays key roles in all facets of cartilage biology including development and maintenance of cartilage integrity. With age there is a change in the ratio of two TGF β type I receptors (ALK1/ALK5), a shift that results in TGF β losing its protective role in cartilage homeostasis. Instead, TGF β promotes cartilage degradation and this correlates with the spontaneous development of OA in murine models. However, the mechanism by which TGF β protects against pro-inflammatory responses and how this changes with age has not been extensively studied.

Mathematical modelling has previously revealed how stochastic changes in TGF β signalling during ageing led to the upregulation of MMPs. I have expanded the TGF β section of this model to incorporate the pro-inflammatory stimulus interleukin-1 (IL-1) + oncostatin M (OSM) in order to investigate how TGF β mediates MMP repression, specifically MMP-13. TGF β signalling appears to interact with the activator protein 1 (AP-1) complex, which has an important role in MMP upregulation. However, the model indicates this interaction alone is insufficient to mediate the full effect of TGF β , predicting it may also reduce MMP-13 mRNA stability. Furthermore, the model enabled me to predict how age alters these interactions; it suggested TGF β would provide limited repression with a prolonged inflammatory response.

Combining the modelled genes with the microarray network provided a global overview of how alterations in one pathway can affect others and lead to OA development. This study therefore demonstrates the power of combining computational biology with experimentally-derived data to provide insight into the importance of TGF β signalling, and how age-related changes can lead to cartilage damage and OA development.

Table of contents

Chapter 1. Introduction	1
1.1 Osteoarthritis	1
1.1.1 Tear, flair and repair	1
1.1.2 Cartilage	2
1.1.2.1 Extracellular matrix	2
1.1.2.2 Chondrocytes.....	5
1.1.2.3 Cartilage formation and maintenance	7
1.1.3 Subchondral bone.....	8
1.1.4 Mechanical stress	9
1.1.5 Aggrecanases.....	10
1.1.6 Collagenases	11
1.1.7 Inflammation	14
1.1.7.1 TGF β	15
1.1.7.2 Notch	17
1.1.7.3 PKC	18
1.1.7.4 Indian Hedgehog	19
1.1.7.5 Wnt/ β -catenin	19
1.1.7.6 IL-1 +OSM Pathway.....	20
1.2 Computational modelling	22
1.2.1 Advantages of a systems approach.....	22
1.2.1.1 Successes of modelling	22
1.2.2 Modelling complex systems	23
1.2.2.1 Petri network models	23
1.2.2.2 ODE models	24
1.2.2.3 Boolean network models	25

1.2.2.4 Other types of models.....	25
1.2.3 Stochastic simulations	25
1.3 Large scale bioinformatics analysis	26
1.4 Scope of thesis	27
1.5 Aims	29
Chapter 2 Methods	30
2.1 experimental methods	30
2.1.1 Molecular Biology Reagents	30
2.1.2 Chemicals and consumables.....	30
2.1.3 Cytokines and activating compounds	30
2.1.4 Cell line.....	31
2.1.5 RNA extraction	32
2.1.6 DNase1 treatment	32
2.1.7 Reverse-Transcription (RT)	33
2.1.8 TaqMan® qPCR	34
2.1.9 Preparation of whole cell lysates	37
2.1.10 Subcellular protein fractionation	38
2.1.11 SDS-Polyacrylamide Gel Electrophoresis (SDS-PAGE).....	39
2.1.12 Western blot	41
2.1.13 Small interfering RNA (siRNA) transfection	43
2.1.14 Lentiviral transfection.....	44
2.1.15 Adenovirus transfection	46
2.1.16 Live/dead viability/cytotoxicity assay	47
2.1.17 Stable plasmid transfection.....	48
2.1.18 Mini/maxi prep	50
2.1.19 Site directed mutagenesis	51

2.1.20 Colony PCR.....	53
2.1.21 In-fusion cloning.....	54
2.1.22 Ethidium bromide gel.....	55
2.1.23 Graph pad prism.....	56
2.2 Bioinformatics tools.....	57
2.2.1GEO.....	57
2.2.2 R.....	57
2.2.2.1 Bioconductor.....	57
2.2.3 ARACNE.....	58
2.2.4 Cytoscape.....	58
2.2.4.1 clusterMaker.....	58
2.2.5 DAVID.....	59
2.2.6 Creating a network of human OA.....	59
2.2.7 PhenomeScape.....	63
2.2.8 GSEA.....	64
2.2.9 MeV.....	64
2.3 Mathematical modeling tools.....	67
2.3.1 SBML.....	67
2.3.2 COPASI.....	67
2.3.2.1 Model simulation.....	67
2.3.2.2 Parameter scans.....	68
2.3.2.3 Extracting data.....	68
2.3.2.4 Events.....	68
2.3.2.5 Parameter estimations.....	69
2.3.3 Model justification.....	70
2.3.4 CellDesigner.....	78

2.3.5 Matlab.....	78
Chapter 3. Pathway selection in the context of inflammation/OA.....	80
3.1 Introduction.....	80
3.1.1 Chapter aims	80
3.2 Results.....	81
3.2.1 Bioinformatic analysis highlights Inflammations impotence in OA	81
3.2.2 Assessing the toxicity of activator compounds	83
3.2.3 Exploring the effect of activating specific pathways	87
3.2.4 Protective effect of TGF β	89
3.2.5 Bioinformatic validation of TGF β selection	95
3.3 Discussion	97
3.3.1 Activating compounds	97
3.3.2 TGF β selection	98
3.3.3 Summary	100
Chapter 4. Exploring the TGF β signalling pathway.....	101
4.1 Synopsis.....	101
4.2 Introduction.....	101
4.2.1 TGF β	101
4.2.2 TGF β activation	102
4.2.3 TGF β signalling	103
4.2.3.1 Canonical pathway	103
4.2.4 TGF β and cartilage.....	106
4.2.5 TGF β and bone	108
4.2.6 Changing role of TGF β with age.....	109
4.2.6.1 Pro-inflammatory interactions with TGF β signalling.....	109
4.2.7 Importance of TGF β in OA	111

4.2.8 TGF β specific modelling	115
4.2.9 Chapter aims	116
4.3 Results.....	117
4.3.1 TGF β -mediated repression is robust.	117
4.3.2 Importance of ALK5 in protection.....	121
4.4 Discussion	125
4.4.1 Pro-inflammatory interactions with TGF β signalling.....	126
4.4.2 Age-related changes to pro-inflammatory TGF β interactions	127
4.4.3 Summary	128
Chapter 5. Modelling the changing effects of TGF β on pro-inflammatory stimuli with age.	129
5.1 Introduction.....	129
5.1.1 ODE modelling for TGF β signalling.	130
5.1.2 Chapter aims	132
5.2 Model construction.....	133
5.2.1 IL-1+OSM	133
5.2.2 TGF β	135
5.3 Model parameterisation	137
5.3.1 Model fit with hypothesised AP-1 competitive inhibition.....	139
5.3.2 Model fit with only mRNA degradation.....	142
5.3.3 Model fit with both AP-1 inhibition and mRNA degradation	147
5.4 Model comparison	152
5.5 Model testing and predictions	159
5.5.1 TGF β -mediated repression after 6 hour exposure to cells.....	159
5.5.2 Importance of new protein synthesis	159

5.5.3 Increased signalling through ALK1 with age alters the TGF response to a pro-inflammatory stimulus.....	164
5.6 Discussion	167
5.6.1 Importance of <i>de novo</i> synthesis	168
5.6.2 Potential effect of ALK1 dominance.....	168
5.7 Summary	170
Chapter 6. Exploring the effects of ALK1 over-express in SW1353 cells.....	171
6.1 Introduction.....	171
6.1.1 Transient vs stable over-expression	171
6.1.1 Aims.....	172
6.2 Stable over-expression of ALK1	173
6.2.1 First attempt at stably over-expressing ALK1.	173
6.2.2 Creation of the pcDNA3.1_ALK1_HIS plasmid.....	178
6.2.3 Second attempt at stably over-expressing ALK1.	181
6.2.4 Adenoviral transduction	189
6.2.5 Lentiviral transduction.....	193
6.3 Discussion	197
6.3.1 Functionality of ALK1	197
6.3.2 Were SW1353 cells the correct cell type?	198
6.3.3 Future work.....	199
6.4 Summary	200
Chapter 7: Model predictions and theoretical interventions	201
7.1 Introduction.....	201
7.1.1 Theoretical therapeutic interventions.....	201
7.1.2 Alterations to the model	202
7.1.3 Chapter aims	202

7.2 Results.....	203
7.2.1 Therapeutic interventions.	203
7.2.1.1 Anti-TGF β treatment.....	204
7.2.1.2 Anti-ALK1 treatment	210
7.2.1.3 Pro-ALK5 treatment	212
7.2.1.4 Altering SMAD levels	214
7.2.2 TGF β reduces the impact of an inflammatory response whilst increasing stability.....	216
7.3 Discussion.	218
7.3.1 Incomplete removal of TGF β favours ALK1 signalling.....	218
7.3.2 Similarities between all theoretic interventions.	218
7.3.3 Stabilising the inflammatory response.	219
7.3.4 Summary	220
7.4 Future work.....	221
Chapter 8. Bioinformatic analysis provides insight into OA as a whole.....	222
8.1 Introduction.....	222
8.1.1 Chapter aims	223
8.2 Results.....	224
8.2.1 Knee osteoarthritis sub-networks.....	224
8.2.2 Bioinformatic analysis highlights the importance of inflammation in OA.	233
8.3 Discussion	234
8.3.1 Individual genes identified from PhenomeScape.....	235
8.3.1.1 PAPSS2.....	235
8.3.1.2 SPARC	236
8.3.1.3 XYLT1	236

8.3.1.4 FAM134B.....	237
8.3.1.5 Conclusions	237
8.3.2 Examining the context of my model in a global environment.....	237
8.3.2.1 TGFBR1 and SMAD1	238
8.3.2.2 JunB	238
8.3.2.3 c-Fos.....	238
8.3.2.4 Conclusions	239
8.3.2 Summary	240
Chapter 9 Final discussion.....	241
9.1 TGF β -mediated repression of IL-1+OSM-driven MMP-13 mRNA expression.....	241
9.1.1 How does TGF β mediate repression?	241
9.2 Alternative pro-inflammatory stimuli.....	241
9.3 Lack of MMP-13 in microarray data.....	242
9.4 Changing role of TGF β	243
9.4.1 ALK1/ALK5.....	243
9.4.2 Effects of clock genes.....	243
9.5 How TGF β links to key OA pathways	245
9.6 Therapeutic targets.....	246
9.7 Alterations with hindsight	246
9.7.1 ALK1 overexpression	247
9.7.2 Ambition in early stages	247
9.8 Future work.....	2478
9.8.1 Incorporating other pathways into the model	248
9.8.2 Exploring computational predictions	248
9.8.3 Importance of cycling TGF or clock genes incorporated into model ...	248

9.8.4 Examine model predictions experimentally.....	248
Chapter 10 Appendix	250

Acknowledgements

I would like to extend my sincerest thanks to my supervisors Dr Carole Proctor and Professor Drew Rowan for initially giving me the chance to do research, and for their continued support and advice throughout my PhD. In particular their commitments to helping me produce the best work I possibly can.

I would also like to express my gratitude to Professor Francesco Falciani whose expertise was a welcome addition to my research.

I am also grateful to the Centre of Integrated Research into Musculoskeletal Ageing (CIMA), Arthritis research UK and the Medical Research Council for funding my PhD.

I would also like to thank Dr Adrian Falconer, Alvaro Martinez Guimera, Neil McDonald, Ciaran Welsh, Dr David Wilkinson, Dr Mari Arques Mengual, Dr Chun Chan, Dr Carmen Martin-Ruiz and Hua Lin. For the help, support and advice although out, which has helped guide my project to where it is now. I would also like to thank them and many others for helping making both institutes a pleasure to work in.

A thank you as well to Anne Metcalf for proof reading this thesis.

Thank you as well to my Sisters, Gemma and Sarah for their support and love throughout my life and career. Also thanks to my brother in law Jim as well as my nephews and niece Grace, Christopher and Arthur who have made my life happier.

A special thanks to my girlfriend Beth whom has been a pillar of support throughout my PhD.

Finally I would like to express my deepest gratitude to both my parents and my Auntie Edie. Without whom none of this would ever have been possible, words cannot express my gratitude.

List of Figures

Chapter 1

Figure 1.1 Internal structure of articular cartilage.....	3
Figure 1.2 Transition from homeostasis to osteoarthritis.	4
Figure 1.3 How anabolic and catabolic changes can affect cartilage.....	5

Chapter 2

Figure 2.1 ALK1 lentiviral plasmid.....	46
Figure 2.2 ComBat removes the batch effects in combined microarray data... .	62
Figure 2.3 Using MeV to determine differentially expressed genes.	66

Chapter 3

Figure 3.1 Top Cytoscape clusters in human OA.....	82
Figure 3.2 Effect of activating compounds on MMP-13 expression after 24 hours treatment.....	84
Figure 3.3 Exploration of cell death after 24 hour Sodium butyrate treatment. .	85
Figure 3.4 Percentage of cell death in SW1353 cells after 24h stimulation.	86
Figure 3.5 MMP-13 expression at 24 hours after treatment with various activating compounds	88
Figure 3.6. MMP-1/-13 expression after 6 hours of Bryostatin-1 treatment.....	88
Figure 3.7 Time course of MMP-13 expression across a range of stimulations.	90
Figure 3.8 Time course of MMP-1 expression across a range of stimulations. .	91
Figure 3.9 Effect of TGF β on IL-1+OSM induced MMP-13 expression.....	93
Figure 3.10 Effect of TGF β on IL-1+OSM induced MMP-1 expression.....	94
Figure 3.11 Key KEGG processes in Srt/ort mice.....	96

Chapter 4

Figure 4.1 An overview of TGF β signalling pathway in chondrocytes.	106
Figure 4.2 Interaction of cartilage maintenance pathways.....	108
Figure 4.3 The role of TGF β in new bone formation.	110
Figure 4.4 Various concentrations of TGF β repress IL-1+OSM-induced MMP expression at 24 hours.....	118
Figure 4.5 Effect of TGF β on IL-1+OSM induced MMP-13 expression.....	119
Figure 4.6 Effect of TGF β on IL-1+OSM induced MMP-1 expression.....	120
Figure 4.7 Level of ALK5 mRNA relative to ALK1 leading to downstream expression of TGF β specific genes after 2h treatment.....	121
Figure 4.8 Potency of ALK5 siRNA on SW1353 cells.....	122
Figure 4.9 Effect of ALK5 silencing on TGF β -mediated MMP-13 repression at 24h.....	123

Figure 4.10 Effect of siRNA transfection on TGF β -mediated MMP repression..	124
--	-----

Chapter 5

Figure 5.1 Network diagram showing species and reactions involved in the IL-1+OSM response.....	134
Figure 5.2 Network diagram showing all the species and reactions involved in the TGF β pathway..	136
Figure 5. 3 Network diagram showing species and reactions involved in the IL-1+OSM+TGF β model.	138
Figure 5.4 Fitting the model using only AP-1 competitive inhibition.	139
Figure 5.5 Effect of TGF β over 48 hour simulation..	140
Figure 5.6 Parameter estimation based on experimental data.....	141
Figure 5.7 Network diagram showing all species and reactions involved in the IL-1+OSM+TGF β model..	143
Figure 5.8 A simplified network diagram showing the key interactions between the IL-1, OSM and TGF β components.....	144
Figure 5.9 Using MMP-13 mRNA degradation to fit the model. A.....	146
Figure 5.10 Fitting the complete model to experimental data..	149
Figure 5.11 Complete model run for 48 hours \pm TGF β	150
Figure 5.12 Effects of mRNA degradation and AP-1 complex inhibition in the complete model.	151
Figure 5.13 Comparison of SMAD signalling and TGF β receptor expression in response to in active TGF β treatment.....	154
Figure 5.14 Comparison of AP-1 component profiles after IL-1+OSM simulation.	157
Figure 5.15 Comparing the formation of c-Fos/c-Jun Heterodimers during a 48 hour simulation.	158
Figure 5.16 6 hour pre-treatment with TGF β was enough to mediate repression of IL-1 and OSM effects.....	162
Figure 5.17 The effect of 6 hour emetine pre-treatment IL-1+OSM+TGF β signalling.....	163
Figure 5.18 Changing responses of TGF β to a pro-inflammatory stimulus over 20 months..	166

Chapter 6

Figure 6.1 Confirmation of site directed mutagenesis products.	174
Figure 6.2 TGF β type I receptors in stable cell lines.....	176
Figure 6. 3 Live-cell plasmid expression.....	177
Figure 6.4 ALK1 specific primers.	179
Figure 6.5 Linearisation of pcDNA3.1+ allows incorporation of ALK1 containing fragments.....	180

Figure 6.6 Colony PCR reveals the colonies that have incorporated the ALK1 expressing plasmid.	181
Figure 6.7 Linearisation of pcDNA3.1_ALK1_HIS plasmid.	182
Figure 6.8 TGF β type 1 receptor composition after second stable transfection.	183
Figure 6.9 Effect of ALK5 removal on ALK1 over-expressing SW1353 cells..	184
Figure 6.10 TGF β -mediated repression in ALK1 over-expressing SW1353 cells.	185
Figure 6.11 Effect of varying siALK5 concentrations on TGF β -mediated response.	187
Figure 6.12 How reduced ALK5 affects TGF β -mediated repression in ALK1 over-expressing SW1353 cells cells.	188
Figure 6.13. MMP-13 expression after TGF β treatment in ALK1 over-expressing SW1353.....	188
Figure 6.14 Comparison of the first and second pcDNA3.1_ALK1_HIS stable SW1353 cells.....	189
Figure 6.15 Effect of ALK1 adenoviral transduction on TGF β -mediated response at 2 hours.....	191
Figure 6.16 Protein expression after ALK1 adenoviral transduction..	192
Figure 6.17. Effect of ALK1 adenoviral transduction on ALK1 and MMP-13 expression	192
Figure 6.18 Protein expression after ALK1 lentiviral transduction.	193
Figure 6.19 ALK1 mRNA expression after ALK1 lentiviral transduction.....	194
Figure 6.20 Effect of ALK1 lentiviral transduction on TGF β -mediated response, at 2 hours.....	195
Figure 6.21 Effect of ALK1 lentiviral transduction on TGF β -mediated MMP-13 expression, at 72 hours.....	195
Figure 6. 22 Effect of ALK1 lentiviral transduction on TGF β -mediated MMP-13 expression at 6 days.	196

Chapter 7

Figure 7.1 Effects of an additional RUNX2 inactivation reaction, on my complete model.....	203
Figure 7.2 The effects of Anti-TGF treatment, starting at 6 months, on MMP-13 mRNA expression.	206
Figure 7.3 The effect of time delays on Anti-TGF treatment, starting at 6 months.	207
Figure 7.4 The effects of Anti-TGF treatment, at 15 months, on MMP-13 mRNA expression.....	208
Figure 7.5 The effect of time delays on Anti-TGF treatment, starting at 15 months.	209
Figure 7.6 The effects of Anti-ALK1 treatment, at 6 or 15 months, on MMP-13 mRNA expression.	211

Figure 7.7 The effects of ALK5 addition, at 6 or 15 months, on MMP-13 mRNA expression.	213
Figure 7.8 The effects of ALK5 addition, at 6 and 15 months, on MMP-13 mRNA expression.	214
Figure 7.9 The effects of altering SMAD4 expression, at 15 months, on MMP-13 mRNA expression.	215
Figure 7.10 Average behaviour of 100 stochastic model runs showing inherent variation in the system.	217

Chapter 8

Figure 8.1 Complete gene network, representative of human OA.	225
Figure 8.2 Knee OA specific sub-networks identified with PhenomeScape.	227
Figure 8.3 PhenomeScape sub-network; Cell adhesion.	228
Figure 8.4 PhenomeScape sub-network; Cellular response to insulin.	228
Figure 8.5 PhenomeScape sub-network; Membrane invagination.	229
Figure 8.6 PhenomeScape sub-network; Cell surface receptor signalling pathway.	229
Figure 8.7 PhenomeScape sub-network; Negative regulation of neural precursor cell proliferation.	230
Figure 8.8 PhenomeScape sub-network; Negative regulation of neuron apoptotic process.	230
Figure 8.9 PhenomeScape sub-network; Extracellular matrix organisation.	231
Figure 8.10 PhenomeScape sub-network; Response to organic cyclic compound.	231
Figure 8.11 PhenomeScape sub-network; Osteoclast differentiation	232
Figure 8.12 PhenomeScape sub-network; Positive regulation of angiogenesis.	232
Figure 8.13 Overlaying model genes to the complete OA network.	233

Appendix

Appendix 5.1 Network diagram showing species and reactions involved in the IL-1+OSM response.	252
Appendix 5.2 Network diagram showing all the species and reactions involved in the TGF β pathway.	253
Appendix 7.1 Degradation of Anti-TGF	254
Appendix 7.2 Effect of Anti-TGF on active TGF β	255
Appendix 7.3 Effect of Anti-TGF on inactive TGF β	255

List of table

Chapter 1

N/A

Chapter 2

Table 2.1 Primers and probes for TaqMan assays, human genes.....	37
Table 2.2 Antibodies used throughout this project.	43
Table 2.3 Details of publically available microarray data for OA patients.....	61
Table 2.4 Model species.	74
Table 2.5 Reactions and their rates in my complete model.	78

Chapter 3

Table 3.1 The concentration used for activator compounds before and after cell viability adjustments.....	84
---	----

Chapter 4

Table 4.1 How TGF β signalling components are altered during OA development.	114
---	-----

Chapter 5

Table 5.1 Change in TGF β -mediated repression of IL-1+OSM-driven MMP-13 expression, with age.....	166
--	-----

Chapter 6

Table 6.1 Stop codon introduction into the mEmerald-ALK1-N-13 plasmid. ...	175
--	-----

Chapter 7

N/A

Chapter 8

Table 8.1 Table of PhenomeScape phenotypes, with identifying numbers.....	226
---	-----

Abbreviations

Agent-based models	ABM
Activin A Receptor Like Type 1	ACVRL1/ALK1
A Disintegrin and Metalloproteinase with Thrombospondin motifs	ADAMTS
Aldehyde Dehydrogenase 1 Family Member L1	ALDH1L1
TGF β receptor 1	ALK5
Activator protein 1	AP-1
Ammonium Persulphate	APS
Algorithm for the Reconstruction of Accurate Cellular Networks	ARACNE
Brain and Muscle ARNT-Like 1	BMAL1
Bone morphogenetic proteins	BMPs
Bryostatin-1	Bro-1
Bovine serum albumin	BSA
Calcein-AM	Cal
Cytoplasmic extraction buffer	CEB
Casein kinase 1	CK1
Complex pathway simulator	COPASI
Circadian rhythm	CR
Clustered regularly interspaced short palindromic repeats	CRISPR
Database for Annotation, Visualization and Integrated Discovery	DAVID
DECipherment Of DNA Elements	DECODE
Dulbecco's modified Eagle's medium	DMEM
Double stranded	ds
Dishevelled	Dsh
Dithiothreitol	DTT
Dual specificity phosphatase	DUSP1
E2F transcription factor 1	E2F1
Enhanced chemiluminescence	ECL
Extracellular matrix	ECM
EGF-Like Domain Multiple 7	EGFL7
Extracellular signal-regulated kinases	ERK-1/2
Ethidium homodimer	Ethd
Reticulophagy Regulator 1	FAM134B
Foetal bovine serum	FBS
False Discovery Rate	FDR
Fibroblast growth factor	FGF
FOS like 1	FOSL1
Far upstream element	FUSE
Gene expression omnibus	GEO
Community clustering	GLay
Glioma-Associated Oncogene Homolog 1	Gli1
G-protein coupled receptor kinase	GRK2
Gene Set Enrichment Analysis	GSEA

Graphical user interface	GUI
Histone deacetylase 4	HDAC4
Hedgehog	Hh
Heat-inactivated	HI
Hypoxia inducible factor 1	HIF-1
Human Immunodeficiency Virus	HIV
Horseradish peroxidase	HRP
Notch intracellular domain	ICD
Inhibitor of DNA Binding 1	ID1
Early Response 2	IER2
Immediate early response 3	IER3
Interferon gamma	IFN- γ
Insulin-like growth factor 1	IGF
Insulin-like growth factor 1	IGF-1
Indian Hedgehog	IHH
Interleukin-1	IL-1
IL-1 receptor	IL-1R
IL-1 receptor antagonist	IL-1Ra
c-Jun N-terminal kinase	JNK
latency associated peptide	LAP
Lysogeny broth	LB
Lymphoid enhancer-binding factor-1	LEF-1
Linear programming	LP
Lysophosphatidylcholine	LPC
Lysophosphatidylethanolamine	LPE
LDL-receptor-related protein	LRP
latent TGF β binding protein-1	LTBP1
Mitogen-Activated Protein Kinase	MAPK
Membrane extraction buffer	MEB
Multiple Experiment Viewer	MeV
Mutual information	MI
Moloney Murine Leukemia Virus Reverse Transcriptase	MMLV
Matrix metalloproteinase	MMP
Multiplicity of infection	MOI
Mesenchymal stem cells	MSC
Nuclear Factor-Kappa B	NF- κ B
Receptor Subfamily 1 Group D Member 1	NR1D1
Osteoarthritis	OA
Ordinary differential equations	ODEs
Oncostatin M	OSM
Plasminogen activator inhibitor-1	PAI1
3'-Phosphoadenosine 5'-Phosphosulfate Synthase 2	PAPSS2
Protease-activated receptor 2	PAR-2
Phosphate buffered saline	PBS

Principle component analysis	PCA
Polyethersulfone	PES
Protein kinase c	PKC
Plasminogen Activator Urokinase Receptor	PLAUR
Petri nets	PN
Protein-protein interaction	PPI
Purmorphamine	Pur
Polyvinylidene fluoride	PVDF
Quantitative polymerase chain reaction	qPCR
Recombination signal binding protein for Ig kappa J	RBPjk
RNA-induced silencing complex	RISC
Reverse-Transcription	RT
Significance Analysis of Microarrays	SAM
Sodium butyrate	SB
Systems biology graphical notation	SBGN
Systems Biology Markup Language	SBML
Site direct mutagenesis	SDM
SDS-Polyacrylamide Gel Electrophoresis	SDS-PAGE
Sarcoma growth factor	SGF
Small interfering RNA	siRNA
NAD-dependent deacetylase sirtuin-2	Sirt2
Smoothened	Smo
The Secreted Protein Acidic and Cysteine Rich	SPARC
Tris-buffered saline-Tween	TBS-T
T-cell factor	TCF
Transforming growth factor	TGF
TGF β receptor type 2	TGFBR2
Transforming growth factor beta	TGF β
Transforming Growth Factor Beta Induce	TGF β I
Tissue inhibitors of metalloproteinases	TIMP
Tetramethylethylenediamine	TMED
Tumour necrosis factor-alpha	TNF- α
12-O-Tetradecanoylphorbol-13-Acetate	TPA
Thrombospondin	TS
Woodchuck hepatitis virus post-transcriptional Regulatory Element	WPRE
Xylosyltransferase 1	XYLT1

Chapter 1. Introduction

1.1 Osteoarthritis

1.1.1 Tear, flair and repair

Osteoarthritis (OA) is a spectrum of degenerative disorders that become much more prevalent with age, to the extent that more than half of people aged over 65 years suffer from the disease (Hugle et al. 2012). It is a debilitating condition that primarily affects knee, finger, spine and hip joints, with the resulting damage causing disability for sufferers. The result is significant pain during even the most simple of tasks which greatly diminishes the patient's quality of life. OA development was regularly accredited to a cumulative effect of load over a person's life which results in "wear and tear" of the joint (Radin et al. 1972). This led people to label OA as a natural consequence of ageing, meaning that development of potential treatments was improbable (Radin et al. 1972). The result of this is limited treatment with no therapies that directly target the disease; instead the focus is on relieving symptoms and improving function. This is done through the use of painkilling medication in combination with physical therapy, as well as educating the patient to manage their weight, with the last resort being total joint replacement (Park and Choi 2016).

Further research into OA has shown this idea of wear and tear to be inaccurate. Although age is the biggest contributing factor to OA development, it is a result of many age-associated changes, rather than the joint gradually wearing down over time. Current understanding is that it best fits the theory of "tear, flair and repair"(Hugle et al. 2012). In this explanation "tear" refers to what was previously thought to be the causes of OA such as obesity, excessive usage or misaligned joints. "Flair" encompasses the roles of inflammation and "repair" covers the ability of the joint to recover from damage or create new tissues. This change in thinking towards OA has led to more research and in recent years our understanding has greatly increased, making the possibility of therapeutic intervention much more credible. Where and when to target in OA progression remains difficult due to the multifactorial nature of OA development (van der Kraan and van den Berg 2008). OA has both mechanical and

molecular causes. Therefore, increasing knowledge of both these causes as well as how they interact will be key in developing therapies for OA.

Age can affect the “tear”, “flair” or “repair” components of development. Studies have demonstrated that a person’s gait as well as the morphology of their joint can change as they age, resulting in extra damage (Pai et al. 1997). They suggest this is a result of age-related muscle degeneration, especially around the joint region resulting in altered biomechanics that leads to damage (Waters and Baumgartner 2011). Obesity can be a major cause for OA, not just because of the excess load on joints, but also because of a change in cytokine expression that can result in OA development (Thijssen et al. 2014). Many older individuals are in situations where they have both obesity and altered biomechanics which can in turn exacerbate the effect obesity has.

1.1.2 Cartilage

The hallmark of OA development is the proteolytic degradation of articular cartilage, a resilient and smooth elastic tissue needed for the low friction movement of synovial joints (Mort and Billington 2001). The resulting damage leads to pain in patients during movement.

1.1.2.1 Extracellular matrix

Cartilage is made up of three regions: the superficial tangential zone, the middle transitional zone and the deep zone. All three of these regions are made up of different quantities of the primary components of cartilage: water, collagen, proteoglycan and non-collagenous proteins (Fig 1.1). Water is the most abundant making up 80% of the wet weight of cartilage (A. J. Sophia Fox et al. 2009). Water functions to transport nutrients and minerals through the cartilage as well as providing lubrication and structural support by supplying functional resistance in the tissue (Linn and Sokoloff 1965). Collagen is the most abundant structural macromolecule in the extracellular matrix (ECM). Type 2 collagen makes up 90-95% of collagen found but types 1,4,5,6,9 and 11 are also present, altogether making up 60% of the dry weight of cartilage (A. J. Sophia Fox et al. 2009). The less abundant collagens serve to stabilise the type 2 collagen structures (Maroudas 1979) (Fig 1.1). The role of collagens is to

stabilise the matrix whilst also providing tensile and shear strength to the tissue (Maroudas 1979). Proteoglycans are heavily glycosylated protein monomers. In articular cartilage they make up 10-15% of the dry weight and are divided into aggregating and nonaggregating proteoglycans (A. J. Sophia Fox et al. 2009). The most abundant is aggrecan, which provides cartilage with osmotic properties that allow it to resist compressive loads (Buckwalter et al. 1990). The nonaggregating proteoglycans interact with collagen to help facilitate a variety of functions such as fibrillogenesis and interfibril interactions (Buckwalter et al. 1990) (Fig1.1). Type 2 collagen fibrils form interwoven networks that provide tensile strength, whilst the proteoglycans embedded within the matrix draw in water that allows cartilage to resist compression (Dingle et al. 1987). Figure 1.1 illustrates how collagen and aggrecan interact in cartilage. Destruction of both collagen and aggrecan in OA sufferers means they suffer discomfort during activities that cause compression, such as walking, demonstrating why OA is such a debilitating condition (Silman AJ 2001; Park and Choi 2016).

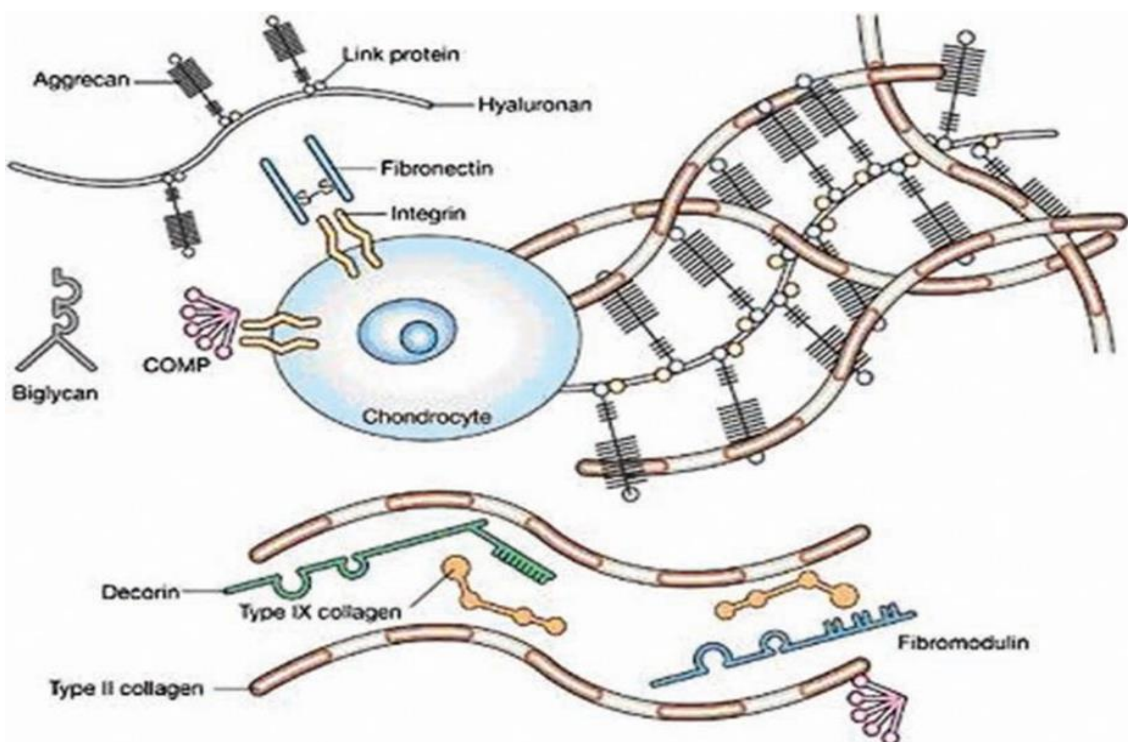


Figure 1 1 **Internal structure of articular cartilage.** Illustrates the interactions inside of the cartilage extra-cellular matrix. Type 2 collagen and Aggrecan are the largest components and interact to give cartilage its structure and properties. Taken from (Alice J. Sophia Fox et al. 2009)

Although proteoglycan degradation is problematic for cartilage, damage can be reversed after the removal of the stimulus (Mort and Billington 2001). Type 2 collagen, on the other hand, cannot be resynthesised so any damage to the tissue is irreversible (Mort and Billington 2001). The ability of cartilage to repair is low due to a lack of progenitor cells. As a result, mesenchymal stem cells are believed to be vital in the homeostasis and repair of the connective tissues (Chang et al. 2011). As we age there is a decrease in not only the amount of stem cells, but also their ability to propagate, which leaves joints less able to react to, or recover from, damage to the connective tissues (Chang et al. 2011). How the joint region changes is illustrated in Figure 1.2. A change in the bone and cartilage morphology leads to an obvious inflammatory response and exposed bone that can cause pain for the patient during movement.

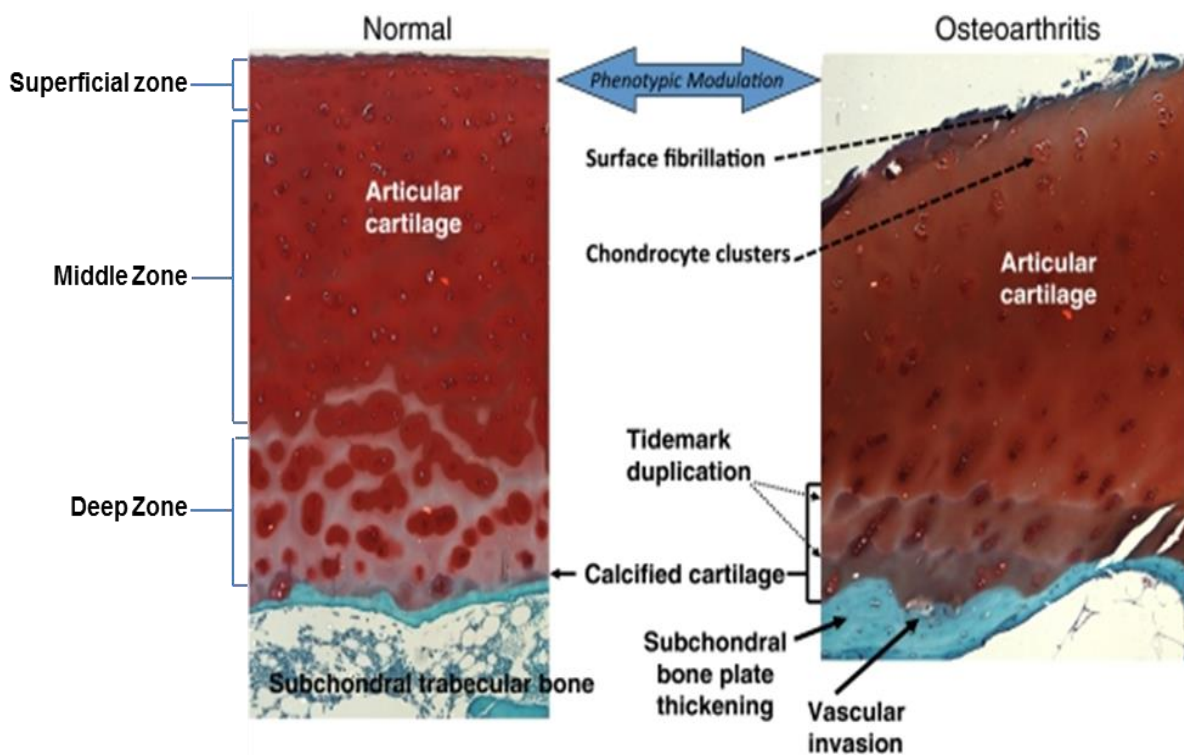


Figure 1.2 **Transition from homeostasis to osteoarthritis.** Healthy articular cartilage (left) undergoes a number of phenotypic changes resulting in the development of osteoarthritis. During OA development chondrocytes become activated instead of being quiescent. The resulting changes to all three of the cartilage regions as well as subchondral bone results in a painful joint that can no longer function as required. The increase in cartilage calcification, surface fibrillation and chondrocyte clusters all contribute to degradation in cartilage matrix. Adapted from Goldring (2012)

1.1.2.2 Chondrocytes

Chondrocytes are the only cell type found in healthy cartilage. They are highly specialised, secreting all the structural components of cartilage. This essentially localises chondrocytes, as the matrix they secret restricts their ability to migrate to other areas (Dingle et al. 1987). Restricted movement results in chondrocytes maintaining that area of cartilage. Throughout life, chondrocytes allow remodelling of cartilage by facilitating degradation then replenishing macromolecules (Buckwalter et al. 2005). They are responsible for cartilage homeostasis and must secrete both anabolic and catabolic molecules (Buckwalter et al. 2005). Throughout this thesis I will refer to anabolic and catabolic changes. Figure 1.3 summarises how these changes can cause or prevent cartilage damage. When this system becomes dysregulated most commonly, but not exclusively, by ageing or injury-based inflammation chondrocytes can no longer maintain or restore cartilage.

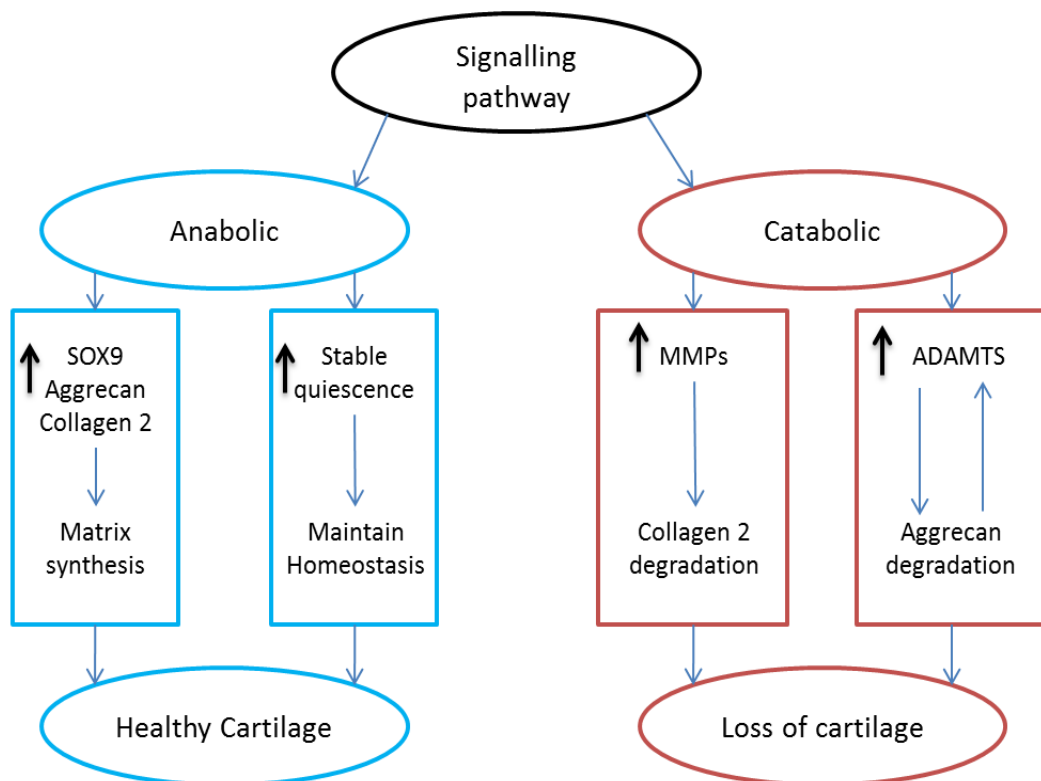


Figure 1.3 How anabolic and catabolic changes can affect cartilage. Signalling pathways can lead to the maintenance of healthy cartilage or its destruction. Stable quiescence refers to the state that healthy chondrocytes are held in, prior to terminal differentiation or hypertrophy. Aggrecan degradation is reversible whilst degradation of Collagen 2 is permanent.

Although proliferation in chondrocytes is rarely seen, even in healthy joints, there is a level of senescence induced with age. *In vitro* proliferation of cells from young donors differs to those from OA patients, the latter showing no signs of proliferation (Dozin et al. 2002). As proliferation is low, telomere shortening is not predicted to be the major driver of this senescence. Instead it is believed to be a result of oxidative stress, because reduced expression of oxygen scavengers such as superoxide dismutase has been shown in OA cartilage (Regan et al. 2005).

Evidence suggests age driven alterations in chondrocyte metabolism and signal transduction aligns with OA development (Cravero et al. 2009; Davidson et al. 2009). This is when degeneration of the articular cartilage and development of OA becomes evident.

Chondrocytes are an unusual cell type as they are in, and prefer, a constant state of hypoxia. These cells are exposed to oxygen ranging from 10% at the surface to less than 1% in the deep zones (Silver and Maroudas 1975). They produce more aggrecan and type 2 collagen under hypoxic conditions, and also have lower synthesis of cartilage-degrading molecules, when compared to normoxia (Strobel et al. 2010). Not just surviving, but thriving in these conditions, means that chondrocytes have had to develop regulatory pathways for hypoxic conditions. Hypoxia inducible factor 1 (HIF-1) is believed to be key in maintaining correct homeostasis in these conditions (Houard et al. 2013). Under normoxia HIF-1 levels are low because hydroxylation leads to ubiquitination and proteolytic inactivation, whereas hypoxic conditions allow HIF-1 levels to stay high. Inflammatory stimuli can also increase HIF-1 levels leading people to believe it is not just a hypoxia gene but a so-called “stress responder” that can help to maintain chondrocytes in unfavourable conditions (Mariani et al. 2014). Similarly to HIF-1, HIF-2 is upregulated under hypoxic conditions and appears to have an anabolic effect in cartilage, by signalling through SOX9 (Thoms et al. 2013). Conversely, it can also lead to catabolic changes and has been shown to have a role in OA development, upregulating a variety of matrix-degrading enzymes (Yang et al. 2010).

1.1.2.3 Cartilage formation and maintenance

The importance of cartilage combined with its limited ability to self-repair means that both its formation and maintenance must be tightly regulated, as any change to homeostatic conditions results in a significant loss that cannot be replaced (Mort and Billington 2001). Due to the importance of maintenance it is regulated with a high level of complexity by a multitude of interacting pathways. Dysregulation of these pathways often leads to OA-like phenotypes, so examining the maintenance pathways often highlights how distorted regular signalling can become during a multifaceted disease such as OA.

The transforming growth factor β (TGF β) superfamily, including bone morphogenetic proteins (BMPs), play a major role in chondrocyte phenotypic changes and differentiation progression. TGF β can hold chondrocytes in stable quiescence preventing terminal differentiation, whilst also leading to the upregulation of aggrecan and collagen type 2 production (Yang et al. 2001). BMPs are important in the regulation of all stages of chondrogenesis (Nishimura et al. 2012); their effect mainly being mediated through the master regulator of chondrogenesis SOX9 (Pan et al. 2008). BMP signalling can also activate chondrocyte proliferation and matrix synthesis, making the BMPs important in protecting against cartilage damage. Blocking BMP activity has been shown to result in increased damage for mouse models (Horiki et al. 2004; Lories et al. 2006). Conversely, both TGF β and BMP when bound to certain receptors can induce MMP-13 expression, as well as chondrocyte terminal differentiation leading to cartilage damage by signalling through SMADs 1/5/8 (Papathanasiou et al. 2012; Blaney Davidson et al. 2009). Insulin-like growth factor 1 (IGF-1) is a potent inducer of matrix metabolism, and introduction to monolayer or explant cultures induces a plethora of anabolic changes including: matrix synthesis, augmented proliferation and differentiation of progenitor cells, and maintenance of chondrocytes in hypertrophy (Papathanasiou et al. 2012; Fukumoto et al. 2003). IGF-1 introduction also blocks catabolic responses in both these cultures (Goodrich et al. 2007). IGF-1 and TGF β have been shown to interact. TGF β induces chondrogenesis but this effect is both strengthened and expanded upon addition of IGF-1, allowing greater matrix production than either

individually (Rosselot et al. 1994). TGF β can also increase the amount of IGF-1 receptors enhancing its impact (Yaeger et al. 1997). IGF-1 loses potency in old and OA tissues resulting in it no longer being able to reduce catabolic activity, although it can still result in some matrix synthesis when combined with BMP-7 (Loeser et al. 2002; Chubinskaya et al. 2007).

Other critical cartilage maintenance pathways are Wnt/ β -Catenin, Nuclear Factor-Kappa B (NF- κ B), Hedgehog (Hh)/Smoothed (Smo) and the Mitogen-Activated Protein Kinase (MAPK) Pathways. Wnt signalling is comprised of multiple proteins that mediate several Wnt pathways. Wnt/ β -Catenin however, has specific roles in chondrogenesis, chondrocyte differentiation and most importantly the cross-talk between cartilage and subchondral bone required for the development of both to form an effective joint (Usami et al. 2016). The relevant MAPK pathways are c-Jun N-terminal kinase (JNK), p38 and extracellular signal-regulated kinases (ERK-1/2). All three have distinct roles in cartilage matrix synthesis and homeostasis (Berenbaum 2004). NF- κ B is important in the remodelling of the extracellular matrix, as well as bone resorption (Rigoglou and Papavassiliou 2013). Hh is expressed as a response to mechanical stress (Ng et al. 2006) in the growth plate and has roles in chondrogenesis, chondrocyte proliferation and regulating the rate of hypertrophy (Chen et al. 2008). All of these pathways can lead to OA if dysregulated, either by an inability to perform their normal anabolic changes or because they lead to catabolic activity. Their interactions are very important in making sure they have the desired effect but if one or more are severely dysregulated it can lead to problems in the others. This is when OA development becomes apparent.

1.1.3 Subchondral bone

Subchondral bone refers to the bony components that lie distal to calcified cartilage. These are made up of both subchondral bone plate and subchondral trabecular bone (G. Li et al. 2013). Changes in subchondral bone can underpin both the initiation of OA as well as the progression towards late stage OA (G. Li et al. 2013). It is a very dynamic structure that has become adapted in order to

respond to mechanical forces and stresses, by means of bone modelling and remodelling (Yuan et al. 2014). Bone remodelling is essential to retain structural integrity, allowing the bone to repair damage and maintain homeostasis of calcium and phosphorous metabolism (Kini and Nandeesh 2012). The resorption and formation of bone occurs at specific sites and follows a well-defined sequence of events (Kini and Nandeesh 2012). In early OA an increase in bone remodelling and subchondral bone loss occurs, which results in an altered joint shape that can affect load transmission in a way that causes excess cartilage destruction (Guangyi Li et al. 2013). By late stage OA a further increase in bone remodelling, combined with a slow turnover, results in densification of the subchondral plate and eventually complete loss of cartilage (Yuan et al. 2014). These changes in bone structure also lead to the formation of osteophytes. These bony appendages that form as outgrowths of cartilage on bone under diseased conditions (van der Kraan and van den Berg 2007) cause discomfort in patients (Yuan et al. 2014).

1.1.4 Mechanical stress

The ability of articular cartilage to respond to mechanical simulation is important in maintaining joint integrity (Castrogiovanni and Musumeci 2016). It distributes force across the joint whilst also providing a smooth lubricated surface that can facilitate movement; all of this ultimately reduces damage (Castrogiovanni and Musumeci 2016). In response to mechanical simulation cartilage can produce both anabolic and catabolic molecules (Responte et al. 2012) (Fig 1.3). The duration or the extent of loading can affect its response, as well as the age of the tissue or its morphology (Responte et al. 2012). Components of the ECM are altered during loading. For example, water is gradually expelled from tissues. This is designed so cartilage can withstand a lifetime of cyclic loading (Coleman et al. 2013).

Chondrocytes have a pluripotent response to loading depending on its frequency and intensity. How they respond can be vital for chondrocyte survival (Buschmann et al. 1999). A sedentary life-style can cause static loading which results in little or no strain on the joint. Chondrocytes respond to this by both reducing protein synthesis but also increasing catabolic pathways resulting in

cartilage degeneration (Sanchez-Adams et al. 2014). In response to a normal load that is cycled throughout the day (not constant), chondrocytes will promote matrix synthesis, reduce proinflammatory pathways and also stimulate anti-catabolic pathways (Sanchez-Adams et al. 2014). In response to heavy load, either cyclic or acute, chondrocytes will increase matrix degradation, apoptosis and necrosis. An acute stimulus will also increase proinflammatory cytokines and inflammatory mediators (Sanchez-Adams et al. 2014). The transduction of strain into physiological responses is mediated in a number of ways including ion channels (Mobasheri et al. 2005), integrins (Millward-Sadler and Salter 2004) and internal structures such as cilia (Wann et al. 2012). These signals lead to activation of a number of pathways including, but not limited to, TGF β /Smad, FOS like 1 (FOSL1), Hedgehog signalling, E2F transcription factor 1 (E2F1) and protease-activated receptor 2 (PAR-2) signalling (S. Dunn et al. 2016; Correa and Lietman 2017; Sanchez-Adams et al. 2014). Latent TGF β can also be activated directly by the shearing of synovial fluid which happens during regular movement (Albro et al. 2012). The shear activation of TGF β appears important in the metabolic activity of cartilage, specifically synthesising DNA and ECM proteins, whilst also inhibiting the catabolic effects of IL-1, tumour necrosis factor-alpha (TNF- α) and more generally MMPs (Albro et al. 2012). It also induces the loss of proteoglycans (Albro et al. 2012), which as long as it is not in excess is useful for the normal turnover of healthy cartilage. All of these effects help to maintain the integrity of cartilage. Despite this, excess active TGF β can have negative effects leading to inflammation, cartilage damage and osteophyte formation. TGF β can also have these negative effects in aged tissue, without being in excess. It has been shown in aged tissue when joints are sufficiently loaded to activate TGF β , it signals through catabolic rather than anabolic signalling pathways (Madej et al. 2013)(Fig 1.3).

1.1.5 Aggrecanases

Aggrecanases are proteolytic enzymes that target large proteoglycans such as aggrecan. Early in OA development there is a degradation of aggrecan. Originally it was believed that Cathepsin D was the major aggrecanase that was responsible for this degradation, because of studies showing its activity was

upregulated in OA cartilage, and inhibition of it prevented cartilage degradation at pH5 (Sapolsky et al. 1973). Later it was discovered that OA cartilage has a neutral pH and Cathepsin D does not have any effect at neutral pH (Woessner 1973). Although now firmly established as collagenases, Matrix metalloproteinases (MMP)s were originally explored as important aggrecanases. This was because they were shown to not only degrade proteoglycans at neutral pH but also to be present in both cartilage and bone (Galloway et al. 1983). However, MMPs cleave proteoglycans at the Asn³⁴¹~Phe³⁴² bond (Fosang et al. 1996). It was later discovered that in the synovial fluid of OA patient the majority of Aggrecan fragments were cleaved at the Glu³⁷³~Ala³⁷⁴ rather than Asn³⁴¹~Phe³⁴² (Lark et al. 1995). It was also found that tissue inhibitors of metalloproteinases (TIMP) could not block the cleavage at this site, implying that something other than MMPs was cleaving proteoglycans in OA patients (Little et al. 2002).

This led to the discovery of A Disintegrin and Metalloproteinase with Thrombospondin motifs (ADAMTS), proteases which are zinc-dependant enzymes comprise of a N-terminal pro-domain, a catalytic domain, a disintegrin domain, one or more thrombospondin (TS) motifs, a cysteine-rich domain and a spacer domain of variable length (Kelwick et al. 2015). ADAMTS-4 was the first to be purified from IL-1-stimulated bovine cartilage (Tortorella et al. 1999) but since then many others have been discovered. ADAMTS 4 and 5 are considered to be the most activate aggrecanases and therefore most responsible for the Glu³⁷³~Ala³⁷⁴ cleavage in OA development (Sandy and Verscharen 2001; Little et al. 2007). Knocking out or blocking ADAMTS5 in mice leads to a reduction in OA severity (Glasson et al. 2005). The same is not true for ADAMTS-4 or -1 (Little et al. 2005; Glasson et al. 2004). However, there is some evidence that ADAMTS-4 is important in human cartilage degradation, making ADAMTS-4/5 the leading aggrecanase targets in OA drug development (Song et al. 2007).

1.1.6 Collagenases

Collagenases are enzymes that destroy peptide bonds in collagen, destroying extra-cellular structures in the case of OA cartilage. Whilst it is difficult to ascertain the exact order that cartilage matrix components are degraded,

studies suggest that Aggrecan protects from collagen degradation and must be degraded before collagen (Pratta et al. 2003). This being said, once collagen is degraded it cannot be reversed (unlike aggrecan) so any damage done is permanent. Fibrillar collagen can only be degraded by a relatively small number of mammalian enzymes; cathepsin K and MMPs -1,-8,-13 and -14 (Linda Troeberg and Hideaki Nagase 2012). MMP-13 is thought to be the collagenase that has the biggest role in OA development (Neuhold et al. 2001). It is upregulated in OA tissues and has been shown to induce spontaneous cartilage damage in mice, with MMP-13 null mice being protected against OA development (Little et al. 2009). It is believed that MMP-1 is also highly important but it is more difficult to study as the murine MMP-1 homolog varies greatly from human MMP-1 (Balbín et al. 2001). MMP activity is limited by their endogenous inhibitors TIMPs, which bind to and inhibit pro and active MMPs (Brew et al. 2000). The two domain TIMPs are a family made up of four proteins TIMP-1,-2,-3 and -4. TIMPs all have strong binding efficiencies for MMPs; some can also inhibit other molecules such as ADAMTS.

MMPs are calcium-dependent, zinc-containing endopeptidases, that are made up of three regions: one pro-peptide, the catalytic domain, and the haemopexin-like C-terminal domain linked by a hinge region (Massova et al. 1998). The pro-peptide is present on the newly synthesised MMPs (known as pro-MMPs) and must be cleaved in order for the enzyme to become active (Massova et al. 1998). The C-terminal domain is thought to be involved in protein-protein interaction. It determines substrate specificity and is also where TIMPs bind and regulate MMPs (Kjeldsen et al. 1993). Finally, the catalytic domain contains the active site which requires zinc to be bound to its three histidine residues found in the conserved sequence HEXxHxxGxxH (resulting in the name zinc-binding motif) (Cerdà-Costa and Xavier Gomis-Rüth 2014).

Due to the incredibly damaging effect of MMPs on collagen, drugs that inhibit them have long been desired in order to slow down or prevent OA progression (Wang et al. 2015). Problems arise because catalytic sites of MMPs are highly homologous, meaning drugs that target them are rarely specific and lead to off

target effects (Wang et al. 2015). MMP-13 is unique because it has a deep S1' subsite; this has been suggested as a target for more specific MMP-13 inhibitors (Wang et al. 2015). LS 1-0635 is an MMP-13 inhibitor that has proven chondroprotective effects. Unfortunately it causes noticeable musculoskeletal toxicity in rats (Janusz et al. 2006). PF152 is another inhibitor which in canine models reduced cartilage lesions, decreased biomarkers of type II collagen and aggrecan degradation and inhibited human cartilage degradation *ex vivo* in a dose-dependent manner (Settle et al. 2010). In some areas up to an 85% decrease in disease progression was seen (Settle et al. 2010). There is no denying that these drugs have chondroprotective effects in animal models. However, the off target effects need to be addressed before moving to human patients.

MMP-3, despite not being an active collagenase, is important to collagen destruction. It is highly upregulated in OA tissue and can activate pro-MMPs, making it important in activating latent MMP-1 and -13 (Swingler et al. 2009). Mice null in MMP-3 are protected against both collagen loss and aggrecan cleavage at Asn³⁴¹~Phe³⁴² (Van Meurs et al. 1999). Despite this, it has been shown that these null mice can develop more severe surgically-induced OA (Clements et al. 2003). Signifying MMP-3's role in OA is not as apparent as it initially appears. MMP-3, although important in activating both collagenases and aggrecanases appears to also have cartilage-protecting effects in some situations (Clements et al. 2003).

TIMP-3 is seen as the central inhibitor of cartilage degeneration as it can inactivate ADAMTS4 and 5 (Kashiwagi et al. 2001). Addition of TIMP-3 can limit cartilage damage for explant culture (Gendron et al. 2003), which is not seen when repeated with TIMP-1 or -2. TIMP-3 can also block cartilage degradation in a rat surgical model (Black et al. 2006). Reduced levels of TIMP-3 are seen in OA tissue with no change in mRNA, suggesting degradation of TIMP-3 is increasing with age in chondrocytes (Morris et al. 2010). TIMP-2 has little or no effect on explant culture whilst TIMP-1 can block glycosaminoglycan release but only in human explants (Gendron et al. 2003). TIMP-4 shows

decreased expression in OA tissues and a single nucleotide polymorphism has been linked to OA development (Lee et al. 2008). Unfortunately, despite all of this, the MMP inhibitory effect of TIMPs appears to be low in OA cartilage, with attempts to regulate MMP overproduction with TIMPs having little clinical effect (Clutterbuck et al. 2009).

1.1.7 Inflammation

It was originally believed that OA was a non-inflammatory arthropathy, but it has since been shown that inflammation plays both chronic and acute roles in the development of OA (Shen et al. 2017). Chronic low grade inflammation starts to develop as we age. This has been linked to pain and function in ageing adults that have OA (Stannus et al. 2013). The term inflamm-ageing was first presented by Franceschi et al. (2000) and refers to the increasingly pro-inflammatory environment that can occur with age. They proposed that the macrophage played a central role as the pro-inflammatory mediator, having a more potent effect as we age. Further studies have shown that there is more than just an increase in pro-inflammatory markers. Anti-inflammatory cytokine IL-10 is decreased in many patients, but there is an increase in several other anti-inflammatory markers (Morrisette-Thomas et al. 2014). Morrisette-Thomas et al. (2014) used principle component analysis to show how these markers correlated with disease. They found two groups, one that correlated with age, mortality and disease state, and another group that correlated with the innate immune system, age and chronic disease (including OA). Surprisingly, this second group was actually representative of protection from disease.

Morrisette-Thomas et al. (2014) suggested age-related inflammation will result in the upregulation of pro- and anti-inflammatory mediators and the balance of these factors will determine an individual's susceptibility to age-related disease.

Inflammation can drive the expression of collagenases and under normal conditions this can be important in the healthy turnover of matrix components. As shown by increased accumulation of type II collagen in MMP-13 knockout mice (Masaki Inada et al. 2004). However, a number of factors can contribute to increased inflammation with age, such as senescent cells which become more prevalent with age and also secrete inflammatory mediators (Greene and

Loeser 2015). Obesity contributes by increasing load on joints whilst also leading to adipose-induced inflammatory cytokine production (Greene and Loeser 2015). Age-related changes to joint tissues and surrounding bone can all be affected by age and this change can result in increased inflammation (Greene and Loeser 2015). Over-activity of chemokines can activate catabolic pathways and cause chondrocyte hypertrophy (Houard et al. 2013). Damaged matrix itself can also lead to the activation of Toll-like receptors, which in turn can upregulate pro-inflammatory mediators and reactive oxygen species leading to further damage (Houard et al. 2013).

Inflamed synovium and activated chondrocytes can result in the overproduction of cytokines and growth factors that can cause joint damage leading to OA development. The main pro- and anti-inflammatory cytokines in OA are considered to be; pro-inflammatory - IL-1, 6, 8, 15 and 17, TNF- α and anti-inflammatory- IL-4, 10, 11 as well as IL-1 receptor antagonist (IL-1Ra) (Rahmati et al. 2016). This is not an exhaustive list but they have all frequently been reported to be elevated in OA patients.

An increase in anti-inflammatory cytokines and growth factors such as IL-4,-10,-13 and TGF β is observed in synovial fluid taken from OA patients (Martel-Pelletier et al. 1999; Sutton et al. 2009). Their effect is mediated in a number of different ways to counteract the effect of the pro-inflammatory cytokines and growth factors. This includes feedback that reduces the expression of their opposite numbers, competing with receptors to reduce pro-inflammatory effects, and/or actively targeting downstream factors that may be produced (Sutton et al. 2009). The effect of anti-inflammatory cytokines or growth factors can be changed during injury or age. When this happens or the balance of anti to pro-inflammatory mediator changes in patients, OA begins to develop. Therefore, discovering the core reasons for these changes could be key in finding potential therapies for OA.

1.1.7.1 TGF β

TGF β signalling is unique in that it can have both catabolic and anabolic affects depending on which of its receptors it activates. In healthy cartilage TGF β

signals through both Activin A Receptor Like Type 1 (ACVRL1 or ALK1) and TGF β receptor 1 (ALK5). However, it predominantly signals through ALK5 which leads to Smad 2/3 phosphorylation which then blocks terminal differentiation, chondrocyte hypertrophy and also stimulates the production of matrix components (Blaney Davidson et al. 2009). Problems arise if the balance is switched towards ALK1 signalling which causes increased Smad 1/5/8 phosphorylation. This mediates the opposite effects to SMAD 2/3 leading to chondrocyte hypertrophy, terminal differentiation and matrix breakdown by MMPs such as MMP-13 (Blaney Davidson et al. 2009). Age has been suggested as the major driving factor for conversion from ALK5 to ALK1 signalling; highlighting how dysregulation can occur in the aging system (W. Hui et al. 2014). This change can also be mediated by crosstalk with other pathways: Wnt signalling, for example, has been shown to effect the expression of a number of proteins downstream that can skew TGF β signalling towards the catabolic ALK1 pathway (M. H. van den Bosch et al. 2014).

In OA development it has been shown on multiple occasions that the addition of TGF β can prevent cartilage breakdown by pro-inflammatory mediators such as IL-1 and OSM. This effect is believed to be the result of not only down regulation of MMPs but also maintaining levels of TIMPs (Hui et al. 2003, 2001, 2000). Despite the positive effect TGF β can have on cartilage, blocking its activity in an OA model results in a reduction of osteophyte formation (Scharstuhl, Glansbeek, et al. 2002), suggesting a negative effect in bone. Genetic studies have shown that mutations in in TGF β signalling can lead to OA susceptibility in patients. Microarray studies have also consistently highlighted the increase in ALK1/ALK5 ratio being important during OA development across a range of organisms.

The conflicting effects of TGF β make it a fascinating area of research. Its ability to protect the chondrocytes not only diminishes with age but an increase in ALK1 signalling makes it detrimental. This combined with its negative effects in bone make it an attractive target for combating OA. Understanding not only

where but at what time to target this TGF β signalling may be vital for developing therapeutics.

1.1.7.2 Notch

There are 4 notch single-pass transmembrane cell surface receptors (notch 1-4) which become activated upon binding with membrane ligands Delta-like 1,2 and 4 or jagged 1 and 2 (D'Souza et al. 2010). Once bound the notch receptor is cleaved by proteinases resulting in the Notch intracellular domain (ICD) being released into the cytoplasm. It then translocates to the nucleus where it forms a complex with the recombination signal binding protein for Ig kappa J (RBPjk), becoming active and inducing the expression of many downstream target genes (Kopan and Ilagan 2009).

The expression of notch-related molecules (notch, delta and jagged) was examined in cartilage dissected from both normal and osteoarthritic patients. These molecules were found to be greatly overexpressed in comparison to healthy tissue, with their peak expression localised to the most damaged areas (Mahjoub et al. 2012). Its involvement in OA was further confirmed by Sassi, Gadgadi, et al. (2014) who showed that blocking notch signalling in OA chondrocytes could reduce the presence of OA markers, including MMP-13, whilst simultaneously upregulating healthy cartilage indicators aggrecan and collagen 2.

How exactly the Notch pathway contributes to OA is unclear but it affects chondrocytes in a number of different ways. Differentiation has shown to be regulated by the RBPjk pathway (Kohn et al. 2012) playing a vital role in endochondral ossification (a key component of physiological skeletal growth). Dysregulation of Notch signalling can lead to chondrocytes undergoing hypertrophic differentiation, followed by the conversion of cartilage tissue into bone tissue. Ultimately this leads to destruction of the matrix as well as causing eroding of the joint surface (Hosaka et al. 2013). Results from transient and constant gain of function mice (Liu et al. 2015) showed that constant Notch signalling resulted in OA development, but transient activation could lead to

protection. Despite this, transient Notch activation increases damage in the event of injury.

1.1.7.3 PKC

Protein kinase c (PKC) represents a family of serine/threonine kinases that were first identified during the purification of kinases from bovine cerebellum (Takai et al. 1977) and have since been divided into 3 groups of isoforms; Conventional PKC (α , β _I, β _{II}, and γ), novel PKC (δ , ϵ , η , θ) and atypical PKC (ζ , ι) (Griner and Kazanietz 2007). PKC has been linked to multiple different processes that contribute to OA development. It has been shown to increase signalling in both early and late stage OA. A further increase during late stage suggests it may play a role in increasing chondrocyte apoptosis (Q. Chen et al. 2012).

Cartilage can be damaged during joint injury and this causes a release of fibroblast growth factor (FGF). This leads to activation of PKC, which through a series of cross signalling events leads to the upregulation of MMP-13 and further cartilage damage (Im et al. 2007). Similarly, PKC has been shown to play a role during inflammation-driven MMP-13 expression, as blocking its activity during treatment with the potent cytokine stimulus IL-1+OSM reduces the upregulation of MMP-13 (Litherland et al. 2010).

Despite this, PKC has been shown on multiple occasions to have a protective effect under mechanical strain. Both Hamanishi et al. (1996) and Yeh et al. (2009) showed that PKC was downregulated under mechanical stress in OA tissues. Hamanishi et al. (1996) experimentally induced mechanical strain in the knees of rabbits, which would normally lead to an OA like phenotype. However, adding a potent upregulator of PKC, 12-O-Tetradecanoylphorbol-13-Acetate (TPA) for three weeks post operation saw an almost complete preservation of cartilage. Yeh et al. (2009) looked at both SW1353 and osteoarthritic cells under varying levels of mechanical stress. They found that the levels of PKC fluctuated and this coincided with an increase in levels of plasminogen activator inhibitor-1 (PAI1), a gene which has a protective effect on chondrocyte cells.

1.1.7.4 Indian Hedgehog

Indian Hedgehog (IHH) binds to its receptor patched allowing the release of Smo protein into the cytoplasm. Smo can then move to the cilia where it is phosphorylated by casein kinase 1 (CK1)/ G-protein coupled receptor kinase (GRK2). This phosphorylation leads to a series of downstream signalling events that result in an activated version of the transcription factor Glioma-Associated Oncogene Homolog 1 (Gli1), which can then increase the expression of a number of different genes that lead to OA development such as: MMP-13, Runx-2 and Col10a1.

The primary cilium is present in chondrocytes and serves as a mechanosensory organelle that can transduce mechanical signals into a biological response (Shao et al. 2012). One such response is an increase in IHH expression. This is almost exclusively linked to an increase in hydrostatic pressure; thus provides evidence of a mechanism by which abnormal loading (obesity or injury) can result in OA development. It has been demonstrated on a multitude of occasions that increasing the pressure on chondrocyte cell cultures leads to an upregulation of IHH. The increased IHH correlates with changes in chondrocyte morphology and OA progression by increasing expression of genes that leads to cartilage degradation and chondrocyte hypertrophy (Wei et al. 2012; Shao et al. 2012). By creating chondrocyte-specific knockout mice Zhou et al. (2014) demonstrated that IHH has a causative role in OA, rather than just being an artefact of increased pressure on the joint. These mice showed significantly less cartilage damage as well as a reduction in key OA markers MMP-13 and Col10a1.

The IHH signalling pathway represents an exciting opportunity for future study as it is the primary biological response to increased mechanical stress. As mechanical stress can have both positive and negative effects, understanding IHH signalling may provide an insight into how pathway regulation is altered under different forms of stress.

1.1.7.5 Wnt/ β -catenin

Wnt genes have consistently been some of the most highly expressed in OA tissues (Hopwood et al. 2007; Meng et al. 2005). This dysregulation of Wnt

signalling has been linked with early and late OA (Sassi, Laadhar, et al. 2014). The Wnt/ β -Catenin pathway has an effect on chondrocyte differentiation, cartilage matrix catabolism and chondrocyte apoptosis (Luyten et al. 2009).

β -catenin is central to canonical Wnt signalling and under normal conditions is ubiquitinated for destruction by GSK-3 β (M. Wang et al. 2011). However, when Wnt binds to Frizzled and its co-receptors LDL-receptor-related protein (LRP) 5/6, it leads to alterations in the downstream signalling of both Dishevelled (Dsh) and Axins 1/2, resulting in the deactivation of GSK-3 β (M. Wang et al. 2011). This in turn allows the survival of β -catenin which migrates to the nucleus where it binds Lymphoid enhancer-binding factor-1 (LEF-1) / T-cell factor (TCF), causing an upregulation of target genes (M. Wang et al. 2011).

Genetic studies have shown that people with altered Frizzled proteins are more susceptible to the development of certain forms of OA (Loughlin et al. 2004). Mice models expressing chondrocyte specific constitutively active β -Catenin demonstrated the role it can have in OA development (Wawra et al. 2007). After 8 months these mice had many OA phenotypes including a complete loss of articular cartilage (Wawra et al. 2007). β -Catenin appears to mediate its affect through controlling chondrocyte maturation, osteophyte formation and MMP-13 expression (Wawra et al. 2007). Despite this, there are reports that suggest high levels of β -Catenin may not be a cause of OA, but rather a consequence. Normal chondrocytes require low levels for certain functions. OA driven dedifferentiation may then lead to increased β -Catenin attempting to re-establish these functions (Chun et al. 2008). Wnt/ β -catenin also has reported interactions with a number of other pathways linked to OA such as: Indian hedgehog and TGF β (Mariani et al. 2014; Baarsma et al. 2011).

1.1.7.6 IL-1 +OSM Pathway

IL-1 is a multifunctional cytokine; it induces many systematic changes, altering gene expression in processes such as metabolism, neurology and endocrinology (Dinarello 1988). It is a potent pro-inflammatory stimulus that may be the principal cytokine in OA development as it results in the

upregulation of many matrix-degrading enzymes (Bellehumeur et al. 2009), in particular MMP-1 and -13. It can also stimulate its own upregulation by chondrocytes (Bellehumeur et al. 2009). IL-1Ra is produced to provide inhibition to IL-1 but reduced levels lead to damage and OA progression (Abramson and Amin 2002). Many drug studies have attempted to reduce the effect IL-1 has in joints, predicting that blocking its effect will reduce, if not elevate, OA in patients (Jotanovic et al. 2012).

OSM is a pleiotropic cytokine that belongs to the IL-6 group of cytokines, regulating growth in a number of cell lines (Cawston et al. 1995). It signals through a series of cell surface receptors containing the protein gp130 (Richards 2013). OSM upregulates chondroprotective elements such as TIMPs and was originally believed to provide protection against IL-1-mediated cartilage destruction. However, this was shown to be inaccurate as combining the two cytokines results in an increase in MMP production (Cawston et al. 1995) as well as increased cartilage damage. Raised levels of OSM were detected in rheumatoid and osteoarthritis synovial fluid correlating with joint inflammation (Cawston et al. 1998; Tsuchida et al. 2014). Blocking OSM also alleviates cartilage damage (Plater-Zyberk et al. 2001). This is because although OSM does not lead to damage alone it can synergise with IL-1, TNF- α and also retinoic acid, increasing the inflammatory response and damage caused by any of these pro-inflammatory mediators individually (Shingleton et al. 2006; Cawston et al. 1995; Hui et al. 2003).

IL-1 alone can result in a rapid release of proteoglycans in cartilage, and this effect is obviously damaging but can be reversed upon the removal of stimulus. The combined effect of IL-1 and OSM is more damaging as it has been shown to result in the destruction of more than 90% of collagen from bovine cartilage at 14 days (Milner et al. 2001). This degradation of collagen cannot be reversed and is most likely mediated by the potent increase and activation of MMPs by IL-1 and OSM, namely MMP-1/-13.

1.2 Computational modelling

1.2.1 Advantages of a systems approach

The complexity of the interactions between inflammatory pathways, along with their changing effects over time, will be difficult to fully ascertain but computational modelling may be a tool that could provide a wealth of information. Mapping the understood parts of the pathway and attempting to represent the unknown elements to replicate results can provide us with a testable hypothesis as well as a much deeper understanding of the importance of certain components. Searching for these interactions experimentally would not only be expensive but also labour intensive for potentially few results. Although model construction can be laborious and time consuming they provide an in-depth look at the pathways as well as a cost effective method of testing drug compounds or exploring pathway interactions. It has the added advantage that it can capture the two different states of the same system. Stochastic simulations can capture the changing nature of a system and highlight the moment when it changes from one form of signaling to another, whether this effect is gradual or instant.

1.2.1.1 Successes of modelling

Development of pharmaceutical interventions can be aided greatly by modelling for three major reasons. (i) They can show novel molecular functions by capturing signaling behaviors that would not normally be obvious. (ii) It allows you to change conditions with relative ease i.e. concentration of a receptor which would be very difficult to alter experimentally. You can then gain an understanding of what changes these effects may have with a smaller investment of both time and money. (iii) They provide an extensive overview of the signaling pathway, documenting many proteins involved, as well as how they interact. This can serve as a useful reference for anybody working in a similar area.

Past studies have used models in complex situations to gain solutions for various problems. Zhao et al. (2013) developed models that allow them to study individual cancer subtypes with the same model structure. Using these they looked at three different breast cancer metastases: brain, lung and bone. They

identified that for each metastasis there were different protein and drug targets. By comparing them they found some targets specific to all of them. After validating these targets experimentally they found two current drugs that could be repositioned for treatment of these cancers: Sunitinib (for which a clinical study is now at stage 2) and Dasatinib (Zhao et al. 2013). AstraZeneca also improved a cancer drug Iressa by linking the efficacy of the drug to impaired receptor internalisation and reliance on downstream AKT signalling (Hendriks et al. 2006). As well as directly finding drug targets, modelling can aid in the design of optimal functioning drugs. Antisense oligonucleotides can work as targets to RNA to have beneficial effects. However, their design is confusing as chemical modifications can increase potency normally, but sometimes making them smaller and lower affinity can have a similar effect. Pedersen et al. (2014) made a model of their binding that allowed a better understanding of this finding in what they called the “optimal binding affinity”. Experiments supported their finding allowing them to advise the best way to apply modifications to create potent oligonucleotide drugs.

1.2.2 Modelling complex systems

Simulating complex biological pathways is a goal that can be difficult to achieve and because of this there have been a number of approaches utilised to facilitate model development. Deciding which of these approaches to follow is not always obvious, as multiple techniques can be used for the same problem. These techniques include ordinary differential equations (ODEs), Boolean network, Petri nets (PN), linear programming (LP) based model and agent-based models (ABM) (Ji and Yan 2017). A good model must be sufficient in replicating the data it was built upon and formulating predictions on independent data. Prior understanding of the previously mentioned methods can allow one to make a justified model that can generate sensible hypotheses for further study.

1.2.2.1 Petri network models

PN type models have been used to model systems such as EGF signalling (Lee et al. 2006). They work by having two nodes; places and transitions (commonly represented as circles and boxes). Places change in the model through the use of transitions; they can be either inputs or outputs of transitions (known as arcs).

Each arc has a required number of tokens to be activated. Signalling cascades are represented by imputing a number of tokens as a signalling input. These can then be separated throughout the model to form outputs. PN can be used to simulate signalling pathways and gene regulatory networks concurrently, asynchronously, distributed, parallel, non-deterministically, and stochastically. They are limited as they cannot simulate deterministically and their primitive conception means graphical representation can be confusing. This means models must be optimized, making large systems difficult to simulate at this time.

1.2.2.2 ODE models

ODE modelling utilizes a series of differential equations to capture all available kinetic information for a biological system. Increasing computation power has allowed these types of models to become more viable and as a result they have grown into the most commonly used type of modelling for looking at time dependant alterations in biological systems (Resat et al. 2009). ODE models work by representing biological molecules as species. These species can then interact with each other but every reaction has an associated function. Functions take into account the speed of the reaction (using parameters), as well as the initial concentration of all molecules involved. The species continue to interact with each other and the equations are constantly solved over a time frame. This allows us to measure the change in species concentrations over time, showing the systems behaviour. How the species interact can be represented by a number of different rate laws: the law of mass action, Hill function, and Michaelis-Menten Kinetics (Ji and Yan 2017). Which law is used can change the behaviour of the model as well as how we can simulate it, so choosing the correct rate law is important in creating an accurate model. The advantage of ODE modelling is that it can accurately predict the kinetic changes in small networks. They can also test how abnormal interactions can alter such a system (i.e. for disease or for treatments). Their main weakness is that they require a lot of computing power so for larger networks it becomes very difficult to use accurately, especially if some parameters are unknown and estimation techniques must be used.

1.2.2.3 Boolean network models

Boolean network models are a special case of discrete dynamic models. Their structure is a series of nodes that are represented by 1 or 0 to denote active or inactive. A discrete time variable is then used to determine the state of each node as time progresses. Boolean functions are used to determine the state of each node, using logic operators AND, OR and NOT to produce an effect. The network states can be updated by synchronisation. (Wang et al. 2012).

Alternatively they can be updated by asynchronisation, where the state of a node is determined by the combination of the states of its parent nodes at a given time point (Wang et al. 2012). These types of networks lie between static and continuous dynamic models making them a tractable and powerful approach to modelling large-scale biological systems. A major advantage of Boolean networks is they do not require parameters, making them useful for describing large scale systems dynamically and allowing intervention predictions, as well as modelling poorly understood systems. However, Boolean networks only allow us a limited biological insight due to their inherent qualitative nature to both time and the state of the nodes.

1.2.2.4 Other types of models

Both LP and ABM are unique techniques that have, on rare occasions, been adapted to model biological systems. LP is important in mathematics and has been adapted to modelling by incorporating some Boolean methods, making it a parameter-free system. ABM is mainly used in cancer models for examining specific inputs on the system as a whole but is limited by variability and multiple models need to be tested to make conclusions (Daub and Merks 2015).

1.2.3 Stochastic simulations

Computational models are typically run deterministically. This type of simulation has known inputs that result in a unique but uniform set of results. Every deterministic run gives the same output and they are used to explore signalling behaviours and underlying mechanisms. Biology however, is not that simple and stochastic simulations provide a way of modelling the inherent variation of biological systems. Stochastic simulations add variation to all the reactions in the model meaning that every run of the model is different. This allows one to

better understand the random variation that can occur in your system, and also uncover random dynamic signalling that may go unnoticed in a deterministic simulation. For example, if a receptor was to spontaneously signal earlier than expected it could cause a totally unexpected output and this would only be discovered by stochastic simulation.

The Gillespie algorithm was first presented in 1976 and has since become a powerful tool in computational modelling (Gillespie 1976). The algorithm allows you to simulate variation as it works by the principle that molecules in a vessel must collide in order for a reaction to take place. It assumes that collisions are frequent but proper energy and orientations are infrequent. This means that the concentration of a given substrate affects the chance that it will react, but does not guarantee that the most abundant molecules will always interact. When simulating a model it takes your initial inputs, then randomly generates which reaction will occur. The chance of a reaction occurring will be based proportionally on the number of substrate molecules. It will then update the time step and recalculate the chances of a reaction occurring based on the updated molecule numbers. This will continue until the time scale is exceeded or the number of reactants reaches zero.

The nature of the algorithm means that it is normally used for systems when the molecular numbers are low, as with higher numbers the variation is reduced and the output is similar to deterministic simulations. The Gillespie algorithm is regularly used but not the only option; stochastic simulation can also be performed using the Gibson and Bruck, direct or Corana algorithms, all of which are available through COPASI. Hybrid systems also exist that allow stochastic simulations at low molecule numbers but changes to deterministic when they reach a higher molecule number set prior to the simulation.

1.3 Large scale bioinformatics analysis

Increasingly, next generation sequencing is becoming both powerful and inexpensive, meaning we can generate a large volume of data for disease in a time scale previously unimaginable (Schadt et al. 2010). This has led to an increase in microarray data being publically available through online databases

i.e. gene expression omnibus (GEO) (R. Edgar et al. 2002). Surprisingly, the exponential growth in available data has not coincided with a shift in our understanding of biology. This is a result of discovering new areas of importance such as genetic variability, epigenetic modifications, and post-transcriptional regulation mechanisms (Davidsen et al. 2016). It is also because our ability to analyse these data has not progressed at the same speed as its generation. For a multifactorial disease such as OA understanding all the ways it can develop is incredibly difficult. Although computational modelling is helping to understand the complexities of disease, other facets of systems biology are also proving to have a powerful role. Next generation sequencing for OA allows us to look at a number of potential causes at once. However, the problem is now how to analyse all of these data. Finnson et al. (2012) assembled a list of microarray data (Table.1.1) from OA patients and highlighted the difference in TGF β throughout these studies. It demonstrated a common problem, that microarray data between two studies may show completely different results. This means that we have to validate findings and also really think about how we analyse microarray data. New ways of understanding microarray data may be beneficial for a range of diseases. Meta-analyses are a combination of multiple studies that have been useful in identifying common behaviours in both cancer (D. R. Rhodes et al. 2004) and more generally responses to chemical stress (Schuttler et al. 2017). OA has a number of publically available datasets and collaborating with Francesco Falciani's group in Liverpool I have created a meta-analysis of these to create an overview of OA. This analysis has highlighted a lot of interesting pathways and genes that may drive future work into the development of OA. Overlaying my model genes to this array has also allowed us to develop a more global understanding of how my model functions in a way that, to my knowledge, has not been performed before.

1.4 Scope of thesis

OA is a very debilitating disease that affects a large proportion of the ageing community. Cartilage degradation is the hallmark of OA progression and is ultimately caused by the proteolytic cleavage of type II collagen (Mort and Billington 2001). The collagenases MMP-1 and MMP-13 have major roles in this

process. Under normal conditions inflammation can upregulate these collagenases, leading to the normal turnover of matrix components and helping to maintain cartilage homeostasis (Masaki Inada et al. 2004). However, with age, injury or genetic mutation, inflammatory pathways can become chronically activated, resulting in an over-expression of collagenases and cartilage damage (Shen et al. 2017).

As described in this chapter there are numerous inflammatory pathways that can lead to cartilage damage, many of which are still not fully understood. Currently there are no therapeutic treatments that directly target OA progression. Thus, a better understanding of the basic biology leading to OA development will hopefully reveal areas for drug targets. As chondrocytes are the only cell type in cartilage (Dingle et al. 1987) it is important to understand how they react to, and regulate, inflammatory responses. In particular how inflammatory pathways drive the upregulation of MMP-13, which is believed to be the most important MMP in cartilage damage (Neuhold et al. 2001). Exploring the effect activating these pathways will have on a chondrocyte cell line should help me understand how MMP-13 is regulated by chronic inflammation.

Computational modelling provides a method of studying complex systems with reduced expense, whilst also allowing easy control of a system that may be difficult to manipulate experimentally. Making use of these computational techniques to better understand inflammatory pathways may be pivotal in developing therapeutic targets. Building a model requires experimental data, not only to provide information on the network structure but also for model calibration and to test model predictions. The data generated in chondrocyte cell lines can provide data around which to build a model of inflammation as well as provide a model for testing theoretic hypotheses.

All areas of systems biology are growing in popularity and with increasing computational power and reduced cost they are becoming more viable as powerful tools in understanding biological processes. Public repositories provide a wealth of microarray studies, and new techniques can provide a way of

extracting useful information from these data. Meta-analyses of publically available OA datasets provide a way of looking at OA in a novel way. Exploring these types of analysis can provide insight into the key OA process as well as the genes that are responsible for driving them.

1.5 Aims

1. Use a novel meta-analysis of publically available microarray data to build a network representative of OA in humans. Then use this to explore key processes in the development of OA.
2. Explore the effect activating inflammation related pathways has on a chondrocyte cell line. Use these findings to create experimental data for model construction and calibration.
3. Build a dynamic mathematical model representative of inflammatory damage in chondrocytes. Explore how the model output changes with age and injury.
4. Based on the findings design experiments that can test model predictions. If the predictions are correct move on to look at therapeutic targets in a model that incorporates ageing. However, if the predictions are not supported by experimental data then modify the model accordingly.
5. Use the network representative of human OA to examine how components in the computational model may interact with other genes, and pathways important in OA development.

Chapter 2 Methods

2.1 experimental methods

2.1.1 Molecular Biology Reagents

For plasmid preparation, mini/maxi-prep kits were obtained from Qiagen (Hilden, Germany). All custom primer oligonucleotides were synthesised by Sigma-Aldrich (St. Louis, USA) or Applied Biosystems (Warrington, UK). Plasmid sequencing was undertaken by Source Bioscience (Nottingham, UK). For molecular cloning, all restriction endonucleases and their buffers were obtained from Thermo Fisher (Loughborough, UK). Ligation was undertaken using an In-Fusion HD kit from Clontech (Mountain View, USA). The QuikChange site-directed mutagenesis kit was bought from Agilent (California, United States). Both the LIVE/DEAD® Viability/Cytotoxicity and Subcellular Protein Fractionation Kits were bought from Thermo Fisher (Loughborough, UK). Amersham ECL Prime Western Blotting Detection Reagents were purchased from GE Healthcare (Chicago, USA). PCR clean up kits were bought from Qiagen (Hilden, Germany).

2.1.2 Chemicals and consumables

All reagents were obtained from Sigma-Aldrich (St. Louis, USA) unless stated otherwise. All cell culture medium was obtained from Thermo Fisher (Loughborough, UK) unless stated otherwise. Dulbecco's Phosphate buffered saline (PBS) was obtained from both Sigma-Aldrich (St. Louis, USA) and Thermo Fisher (Loughborough, UK). Unless otherwise stated, all cell culture dishes, flasks and plates were manufactured by Corning (New York, USA) and purchased from Sigma-Aldrich or VWR International (Radnor, USA).

2.1.3 Cytokines and activating compounds

IL-1 α was a gift from Dr Keith Ray (GlaxoSmithKline, Stevenage, UK) and is dissolved in Dulbecco's Modified Eagle's medium, sterile filtered with a 0.22 μ m polyethersulfone (PES) filter then stored at -20°C until use. Recombinant OSM was made in-house at a concentration of 60 μ g/ml in PBS with 0.1% (w/v) bovine serum albumin and stored at -80°C until use.

Sodium butyrate and Purmorphamine were bought from Sigma-Aldrich (Poole, UK) . Bryostatin-1 and QS11 were purchased from Tocris bioscience (Bristol, UK) and finally TGF β was from Peprotech (Rocky Hill, USA). All compounds were made up in DMSO except for TGF β which was made up in acetic acid.

2.1.4 Cell line

Background: SW1353 chondrosarcoma cell lines were purchased from the American type culture collection. The cells originate from a primary grade II chondrosarcoma of the right humerus, obtained from a 72 year old female Caucasian. They were cryopreserved in culture medium supplemented with 10% DMSO.

Reagents:

- Serum-containing media: Dulbecco's modified Eagle's medium (DMEM)-F12, 10 % (w/v) foetal bovine serum (FBS), 2mM L-glutamine, 200IU/ml penicillin, 200 μ g/ml streptomycin.
- Serum-free media: DMEM-F12, 2mM L-glutamine, 200IU/ml penicillin, 200 μ g/ml streptomycin.
- Trypan blue
- Trypsin
- PBS

Method: Prior to use SW1353 cells were resurrected from cryopreservation by rapidly thawing at 37°C, the adding 9ml of Serum-containing media. The tube was then centrifuging at 1100x g for 5 minutes and the supernatant was discarded. The dry pellet was then resuspended in 12ml Serum-containing media and moved to a T75 flask. Cells were passaged at least once prior to use. To passage the cells they were allowed to grow until around 90% confluent, which normally takes around 3 to 4 days. The cells were then washed with PBS, before incubating for 5 minutes at 37°C with 2mL trypsin, a serine protease that detaches the adhered cells from the plate. 8ml of Serum-containing media was then added to inhibit trypsin and the cells were moved to a 12ml tube, then centrifuging at 1100x g for 5 minutes. The supernatant was removed and the dry pellet resuspended in 10ml Serum-containing media. Cells

were then counted by mixing 10 μ L of cell suspension with 10 μ L of trypan blue. This was then added to the chamber of a Fuchs Rosenthal haemocytometer. Four (normally the corners) squares were then counted and an average cell count taken. Cells were then plated out as required for experimental design. One sixth of the cells were also moved to a fresh T75 with 11ml Serum-containing media to continue growing the cell line. Cells were typically retained for around 18-22 passages. Plated out cells were cultured in Serum-containing media and prior to treatment were serum starved overnight in Serum-free media.

2.1.5 RNA extraction

Background: In order to measure gene expression in a monolayer cell culture the mRNA must first be extracted and stabilised. RNA is highly unstable so to avoid degradation all steps were performed on ice and a commercially available buffer was used.

Reagents:

- Cells-to-cDNA II Cell Lysis Buffer (Thermo Fisher, Loughborough, UK)
- PBS

Method: For gene expression experiments the cells were always cultured in a 96 well plate. After stimulation cells were placed on ice and the media was removed and discarded, the cells were then washed with ice-cold PBS. After which 30 μ L of Cells-to-cDNA II Cell Lysis Buffer was added to the cells, which were then scratched with a pipette tip for 10 seconds to help break the cell membrane. The buffer/lysate mix was then moved to a 96 well PCR plate and heated at 75°C for 15 minutes in a PCR thermocycler. This process inactivates RNases to help protect RNA from degradation. The lysates were then DNase1 treated, stored at -80°C or reverse transcribed immediately thereafter.

2.1.6 DNase1 treatment

Background: After RNA extraction the lysates will contain not only RNA but also genomic DNA. When qPCR primers do not span an exon-exon boundary, or if

there are pseudogenes for the target in the genome, this can lead to DNA being amplified instead of cDNA. PCR products generated from the genomic DNA will be indistinguishable from those amplified from cDNA. However, treatment with DNase1 will remove genomic DNA prior to Reverse-Transcription preventing amplification. The RNA is still highly unstable so all steps were performed on ice.

Reagents:

- RNase-free, DNase1 (Thermo Fisher, Loughborough, UK)
- RNase and DNase-free water

Method: 1µl of water was mixed with 1µl of DNase1 per treatment well. 2µl of this mix was then added to each well of the lysates generated during RNA extraction, and then incubated for 15 mins at 37°C. After which the lysates were heated for 5 minutes at 75°C, this inactivated the DNase1, preventing it from effecting the reverse transcription products. The lysates were then stored at -80°C or reverse transcribed immediately thereafter.

2.1.7 Reverse-Transcription (RT)

Background: For quantification the mRNA extracted must be converted to cDNA. cDNA differs from genomic DNA in the same way mRNA differs from RNA, this is that the introns have been spliced out. Commercially available reverse transcription enzymes contain a ribonuclease H activity to prevent the transcription of RNA, ensuring the production of cDNA.

Reagents

- Moloney Murine Leukemia Virus Reverse Transcriptase (MMLV), 200units/µL (Thermo Fisher, Loughborough, UK)
- 5x First Strand buffer (250mM Tris-HCl (pH 8.3), 375mM potassium chloride, 15mM Magnesium Chloride) (Thermo Fisher, Loughborough, UK)

- Random Hexamers (NNN NNN), 0.2µg/µL (Integrated DNA Technologies, Coralville, USA)
- RNase and DNase-free water
- 100mM Dithiothreitol (DTT) (Thermo Fisher, Loughborough, UK)
- dNTPs, 2.5mM each (Thermo Fisher, Loughborough, UK)
- RNaseOUT™ Recombinant Ribonuclease Inhibitor, 40units/µL (Thermo Fisher, Loughborough, UK)

Method: Mix one comprised of; 3 µl dNTPs and 1 µl random hexamers (0.2µg/µl). Mix two comprised of: 4µl of 5 times first strand buffer, 2µl DTT, 0.125µl RNase OUT, 0.5µl MMLV and 1.375µl water. Both mixes were made in advance for the number of wells being reverse transcribed then stored on ice. For the reverse transcription, 4µl per well of mix 1 was added to 8µl of lysate generated during RNA extraction. This mix was then heated at 70°C for 5 minutes. Immediately afterwards the sample was chilled on ice and stayed ice-cold whilst 8µl of mix two was added using a repeater pipette. This mix was then returned to the PCR block for 50 minutes at 37°C for transcription, then a further 15 minutes at 70°C to denature the enzyme activity of MMLV. The resulting cDNA was stored at -20°C until use or at 4°C for short term storage.

2.1.8 TaqMan® quantitative polymerase chain reaction (qPCR)

Background: Taq polymerases uses oligonucleotide primers to replicate the cDNA generated during reverse transcription. Primers are ideally designed to be in different exons close to, or spanning, an exon boundary preventing any amplification of residual genomic DNA. If this is impossible DNase treatment prior to reverse transcriptions allows the use of single exon spanning primers. A probe is also added that contains a fluorophore coupled to the 5' end and a fluorescence quencher at the 3' end. A laser in the qPCR machine will excite the fluorophore but only when the quencher is not present. When Taq polymerase extends the new strand, its 5' to 3' exonuclease activity cleaves the probe, thus separating the fluorophore from the quencher and a signal can be detected. The relative fluorescence can then be measured to quantify the amount of cDNA in the sample. Increased cDNA may be the result of increased

cell numbers or RNA extraction efficiency in a particular culture so to normalise for this an endogenous control must be used. The $\Delta\Delta CT$ method then allows fold change quantification of the gene of interest relative to another condition (normally control). Throughout this thesis I will use GAPDH and 18s as indigenous controls, unless stated other.

Reagents:

- TaqMan® Gene Expression Master Mix (Thermo Fisher, Loughborough, UK)
- TaqMan™ Fast Advanced Master Mix (Thermo Fisher, Loughborough, UK)
- RNase and DNase-free water
- Oligonucleotide primers 30 μ M (Applied Biosystems, Warrington, UK and Sigma-Aldrich, Poole, UK)
- Oligonucleotide probes 30 μ M (Applied Biosystems, Warrington, UK and Sigma-Aldrich, Poole, UK)

Protocol: The primers were designed using Primer Express software version 1.0 (Applied Biosystems, Warrington, UK) or the universal probe library (Roche, Burgess Hill, UK). The sequences of primers used in this thesis are shown in Table.2.1. A master mix was created initially for the number of wells required containing; 4.5 μ l of TaqMan Gene Expression or Fast Master Mix, 0.1 μ l probe, 0.2 μ l forward and reverse primers. 20 μ l of cDNA sample generated during reverse transcription were then diluted in 30 μ l of water; there was also a further 25-fold dilution for 18S samples. 5 μ l of this diluted sample was then moved to an optical bottom 96-well qPCR plate (Applied Biosystems, Thermo Fisher) along with 5 μ l of the master mix. The relative gene expression of these samples was then determined using either a Lightcycler (Roche, Burgess Hill, UK) or a 7900HT PCR system (Applied Biosystems, Warrington, UK). Cycling conditions;

Normal assay

1. Initial denaturation stage of 95°C 10 minutes
2. 40 cycles of 95°C for 15 seconds then 60°C for 60 seconds.

Fast assay

1. Initial denaturation stage of 95°C 30 seconds
2. 40 cycles of 95°C for 1 second then 60°C for 15 seconds

Analysis: Comparing CT values from different genes can show you the relative level of one gene compared to the other. To do this gene X is simply divided by gene Y, after normalisation. However, when comparing CTs determined from the Roche probe library another step must first be added to confirm the binding efficiency of the probes. Samples are diluted 1/2, 1/4, 1/8, 1/16 and 1/32 and qPCR ran with the given primers. A slope is then determined for the CT values. After which, the CT values are altered by subtracting the endogenous control then dividing by the slope. This must be repeated for the comparison gene and these altered CT values are then used to determine the relative concentrations.

Primer	Sequence
MMP-13	Forward 5'AAATTATGGAGATGCCATT'3 Reverse 5'TCCTTGGAGTGGTCAAGACCTAA'3 Probe 5'CTACAACCTGTTTCTTGTTGC'3
MMP-1	Forward 5'AAGATGAAAGGTGGACCAAATT3' Reverse 5'CCAAGAGAATGGCCGAGTTC3' Probe 5'CAGAGAGTACAACCTTACATCGTGTGCGGCTC3'
18s	Forward 5'CGAATGGCTCATTAAATCAGTTATGG'3 Reverse 5'TATTAGCTCTAGAATTACCACAGTTATCC'3 Probe 5' TCCTTTGGTCGCTCGCTCCTCTCCC'3
GAPDH	Forward 5'GTGAACCATGAGAAGTATGACAAC'3 Reverse 5' CATGAGTCCTTCCACGATACC'3 Probe 5' CCTCAAGATCATCAGCAATGCCTCCTG'3
ALK5	Forward 5' GCAGACTTAGGACTGGCAGTAAG'3 Reverse 5' AGAACTTCAGGGGCCATGT'3 Probe Roche probe library probe #5 (Roche, Basel, Switzerland)
ALK1	Forward 5' AGACCCCCACCATCCCTA'3 Reverse 5' CGCATCATCTGAGCTAGGC'3 Probe Roche probe library probe #71 (Roche, Basel, Switzerland)
ID1	Forward 5' CCAGAACCGCAAGGTGAG'3 Reverse 5' GGTCCCTGATGTAGTCGATGA'3 Probe Roche probe library probe #39 (Roche, Basel, Switzerland)
PAI1	Forward 5' AAGGCACCTCTGAGAACTTCA'3 Reverse 5' CCCAGGACTAGGCAGGTG'3 Probe Roche probe library probe #19 (Roche, Basel, Switzerland)

Table 2.1 **Primers and probes for TaqMan assays, human genes.**

2.1.9 Preparation of whole cell lysates

Background: In order to measure the protein content of a cell via SDS-PAGE they must first be lysed. Full lysis of cells releases proteins from all compartments to give you the complete protein content. The lysis buffer is designed in order to effectively lyse cell whilst also inhibiting proteases and phosphatases. This produces the maximal yield, whilst maintaining protein phosphorylation states. Whole cell lysis can be performed on monolayer cultures or suspended cells.

Reagents:

- RIPA buffer; 150mM Sodium chloride, 1% Triton X-100 (v/v), 0.5% sodium deoxycholate (w/v), 0.1% SDS (v/v), 50mM Tris (w/v) pH8 and 1 Complete protease inhibitor Mini tablet/10 ml of buffer.
- PBS

Monolayer culture method: 6 well plates or 10cm dishes were lysed, after appropriate stimulations, by removal of media followed by washing with ice cold PBS. 100µl of ice cold RIPA buffer was then added to the cells on ice. The cells were incubated on ice for 30 minutes, whilst constantly being moved by an orbital shaker. A cell scraper was then used to ensure full lysis of the cells and the resulting lysates were moved to a 1.5ml microcentrifuge tube. The samples were then centrifuged at 12,000g for 20 minutes at 4°C. The supernatant was then moved to a clean 1.5ml microcentrifuge tube and stored at -80°C or used immediately.

Suspended cell method: Following trypsinisation 1 million SW1353 cells were placed into a 1.5ml microcentrifuge tube, then centrifuged at 500g for 5 minutes. The media was then removed and the cells were washed with ice cold PBS. After which 100µl of ice cold RIPA buffer was then added to the cells on ice. The cells were then vortexed at full speed for 10 seconds then incubated on ice for 30 minutes, whilst constantly being moved by an orbital shaker. The samples were then centrifuged at 12,000g for 20 minutes at 4°C. The supernatant was then moved to a clean 1.5ml microcentrifuge tube and stored at -80°C or used immediately.

2.1.10 Subcellular protein fractionation

Background: Fractionation of subcellular proteins allows the separation of membrane, cytoplasmic, chromatin-bound, cytoskeletal and nuclear soluble extracts from monolayer or suspended cells. The first buffer causes selective permeabilisation and the release of cytoplasmic components. The second reagent can then dissolve plasma, mitochondria and ER-golgi membranes whilst leaving behind the nuclear membrane. This pellet must then be recovered in order to allow the third agent to yield the soluble nuclear extract. To release

chromatin bound nuclear proteins the third buffer must be supplemented with a micrococcal nuclease. Finally the remaining reagent can be added to extract the cytoskeletal proteins. These extract can then as separate protein extracts and processed.

Reagents:

- Subcellular Protein Fractionation Kit (Thermo Fisher, Loughborough, UK).
- PBS

Method: Following trypsinisation 1 million SW1353 cells were placed into a 1.5ml microcentrifuge tube, then centrifuged at 500g for 5 minutes. The media was then removed and the cells were washed with ice cold PBS. The amount of buffer used is then governed by the size of the packed cell volume. For adherent cells this is normally estimated. However, as I knew I was using one million cells and it is known that this equates to around 10 μ l packed cell volume, the relevant amounts were used. 100 μ l of ice cold cytoplasmic extraction buffer (CEB) containing protease inhibitors was added to the dry pellet and then incubated at 4 $^{\circ}$ C, whilst constantly being moved by an orbital shaker for 10 minutes. The samples were then centrifuged for 5 minutes at 500g. The supernatant (cytoplasmic extract) was then moved to a clean pre-chilled 1.5 microcentrifuge tube and stored at -80 $^{\circ}$ C. 50 μ l ice-cold membrane extraction buffer (MEB) was then added to the remaining pellet and vortexed at the highest setting for 5 seconds. The samples were then then incubated at 4 $^{\circ}$ C, whilst constantly being moved by an orbital shaker for 10 minutes. The supernatant (membrane extract) was then moved to a clean pre-chilled 1.5 microcentrifuge tube and stored at -80 $^{\circ}$ C. At this point the pellet can be further treated to extract more protein but as I only required the membrane I omitted the remaining steps and discarded the pellet.

2.1.11 SDS-Polyacrylamide Gel Electrophoresis (SDS-PAGE)

SDS-PAGE allows the separation of protein samples bases solely on the size of the proteins. SDS plays a crucial role in insuring no factors but size effects migration through the gel by binding to the denatured protein, preventing the

formation of secondary or tertiary structure. The binding of SDS also imparts a slightly negative charge on the proteins removing any natural variation in charge that proteins have. Boiling the samples at 105°C denatures the protein to allow comprehensive binding of SDS. β -mercaptoethanol is also added to the samples to ensure primary structures and also reduce disulphide bridges.

Once the samples have been charged and linearised they can be ran through a polyacrylamide gel in a tank containing tris-glycine running buffer. An electric current is run through the gel with the anode at the bottom, and cathode at the top. This causes the now negatively charged proteins to migrate down the gel. The gel is split into the “stacking gel” and the “resolving gel” the stacking gel is above the resolving gel and due to a lower percentage of acrylamide has a larger pore size. Movement through the part of gel is therefore due to current rather than size meaning large and small proteins migrate together. Proteins become trapped in the stacking gel between chloride ions (from the gel) which move faster and glycine (from the buffer) which moves slower, the glycine essentially then pushes the protein into a desired band at the top of the resolving gel. The lower pH of the resolving gel then causes the glycine and chloride ions to move much faster through the gel, leaving the proteins to separate based on size. The resolving gel has smaller pores and so this retards the progression of larger proteins.

Reagents:

- Resolving gel; 375mM Tris pH 8, 0.1% (w/v) SDS, 12% (v/v) Acrylamide/Bis-acrylamide.
- Stacking gel; 125mM Tris pH 6.8, 0.1% (w/v) SDS, 4% (v/v) Acrylamide/Bis-acrylamide.
- Ammonium Persulphate (APS) 0.2% (w/v)
- 5x Laemmli Buffer: 625mM Tris pH 6.8, 50% (v/v) Glycerol, 10% (w/v) SDS, 5% (v/v) β mercaptoethanol, 0.025% Bromophenol blue.
- Running buffer 25mM Tris, 192mM Glycine, 0.1% (w/v) SDS.
- Tetramethylethylenediamine (TMED)

Method: Whole cell or membrane specific protein samples were mixed 4 parts to 1 in 5x laemmli buffer and boiled at 105°C for 3 minutes. The SDS page gels where made in house and were set using 20µl TEMED and 60µl APS. Once set the gels were then loaded into a Bio-Rad Mini-PROTEAN Tetra cell tank with running buffer. Between 10-30µl of the SDS protein samples were then loaded into the gels along with 5µl of a pertained protein ladder (Thermo Fisher, Loughborough, UK), so the size of the proteins could be determined after Western blot. The gel was then ran at between 140-200V until the bromophenol blue had reached the bottom of the gel, this took approximately two hours. Western blot was then performed to visualise the protein.

2.1.12 Western blot

Background: Western blotting is a technique that allows the visualisation of specific proteins following SDS-PAGE. The proteins are transferred from the acrylamide gel to either polyvinylidene fluoride (PVDF) or nitrocellulose membrane. The transfer takes advantage of the negative charge imparted on the proteins by SDS. The membrane must be first activated, the gel and membrane are then held tightly together and an electric current causes the proteins to move onto the membrane. The activated membrane has a high affinity for proteins, so to prevent any further proteins binding and leading to non-specific binding (from the antibody in later steps) it must first be blocked with milk. The membrane is then incubated with an antibody against the protein of interest. The excess is washed away and the membrane is then incubated with a secondary antibody against the primary antibody. This secondary antibody is conjugated to the horseradish peroxidase (HRP) enzyme, and enhanced chemiluminescence (ECL) can then allow visualisation of the protein. HRP can covert luminol to its oxidised form in the presence of hydrogen peroxide, this reaction produces light as a by-product, which can be detected on x-ray film in an imaging hood. The amount of protein present in the band will be directly relative to the amount of light observed. Meaning western blotting is a semi-quantitative method for a single band but cannot be directly compared to separate blots or different protein bands on the same blot.

Reagents:

- Transfer Buffer: 39mM glycine, 48mM Tris-base, 0.0375 % (w/v) SDS and 20 % (v/v) methanol
- Tris-buffered saline-Tween (TBS-T): 10mM Tris-HCl pH 7.4, 0.15M NaCl and 0.2 % (v/v) Tween-20
- Non-fat dry milk (Marvel brand)
- HRP-conjugated secondary antibody (Dako, Agilent Technologies, Santa Clara, USA)
- ECL reagents
- Bovine serum albumin (BSA)
- PVDF or nitrocellulose membrane
- Methanol

Method: Transfer was performed using a semi-dry method throughout this project. 4 pieces of blotting paper were cut to the size of the gel being transferred; these were then placed into transfer buffer. The membrane was cut marginally smaller and activated by being placed in methanol, then moved to transfer buffer. A sandwich was made with the components: in order, two pieces of blotting paper, the membrane, the gel and then two more pieces of blotting paper. Any bubbles in the sandwich were removed with a roller. It was then secured and moved to electroblotter from BioRad (Hercules, USA).

Electroblotting was undertaken at 80 mA per gel for 1.5 hours. The membrane was then washed three times in TBS-T before being left in 5% milk for 2 hours at room temperature. After which, the membrane was again washed three times in TBS-T for 5 minutes, before being left overnight at 4°C in primary antibody (table 2.2). The primary antibody was diluted to manufacturer-recommended concentration in 5% BSA in TBS-T with 0.02% sodium azide. The next morning the membrane was washed three times in TBS-T for 5 minutes. The relevant secondary antibody was then added at 1:2000 concentration, in 5% milk. The secondary antibody was left for 1 hour, then followed by three final wash steps with TBS-T for 5 minutes. The membranes were treated with the ECL reagents and visualised using a Gbox EF Gel Documentation System with Genesnap software (Syngene, Cambridge, UK).

Antibody	Source	Manufacturer	Product code
ALK1	Anti-Mouse	Thermo Fisher, Loughborough, UK	PA5-14921
ALK5	Anti-Rabbit	Abcam, Cambridge, UK	ab31013
GAPDH	Anti-Rabbit	Abcam, Cambridge, UK	ab8245
HIS-tag	Anti-Rabbit	Abcam, Cambridge, UK	ab18184

Table 2.2 **Antibodies used throughout this project.**

2.1.13 Small interfering RNA (siRNA) transfection

Background:

siRNA transfection allows the short-term silencing of a specific gene of interest. It takes advantages of a process that is normally important in protecting the cell against viral infection. The silencing is mediated by double stranded (ds)RNA which is delivered intracellularly using lipid vesicles that can permeate the cell membrane. Once in the cell the dsRNA is cleaved by the enzyme endoribonuclease Dicer which leaves 21-23bp siRNAs. These in turn bind to the RNA-induced silencing complex (RISC). This is a ribonucleoprotein which incorporates the siRNA and uses it as a template to target mRNA. Once the target mRNA is found a protein in the RISC, called Argonaute, then activates and cleaves the mRNA. This can essentially silence the specific gene in a given cell population. After transfection, cells can be either harvested to test transfection efficiency, or treated further to test the effect gene silencing will have on the cells response to stimuli.

Reagents:

- Dharmacon ON-TARGET plus SMARTpools (Thermo Fisher, Loughborough, UK).

- Dharmacon ON-TARGET plus Non-targeting pool control siRNA (Thermo Fisher, Loughborough, UK).
- DharmaFECT Transfection reagent (Thermo Fisher, Loughborough, UK).
- 5x siRNA resuspension buffer (Thermo Fisher, Loughborough, UK).
- Serum-containing medium: DMEM-F12, 10 % (w/v) FBS, 2mM L-glutamine, 200IU/ml penicillin, 200µg/ml streptomycin.
- Antibiotic- and serum-free medium: DMEM-F12, 2mM L-glutamine.
- Serum-free medium: DMEM-F12, 2mM L-glutamine, 200IU/ml penicillin, 200µg/ml streptomycin.
- PBS
- RNase-free water

Method: SW1353 cells were cultured in 96 or 6 well plates until they had reached 50-70% confluency. siRNA including the non-targeting siRNA controls were made up at a final concentration of 100nM, from a 20µM stock, using 1x siRNA resuspension buffer, diluted in RNase-free water. DharmaFECT transfection reagent (0.2µl/well of 96-well plate or 3.2µl/well of 6-well plate) was added to antibiotic- and serum-free medium (10µl/well of a 96-well plate or 160µl/well of a 6-well plate). In a separate container the volume of siRNA required for the desired transfection concentration was made up to 10µl/well (96 well) or 160µl/well (6 well) with Anti-biotic and Serum-free medium. Both DharmaFECT and siRNA were left for 5 minutes, then combined and left for a further 20 minutes all at room temperature but under sterile conditions. 90µl/well (96 well) or 1440µl/well (6 well) of serum-containing medium was then added. Cells were washed and then 100µl/well (96 well) or 1600µl/well (6 well) of the final mixture was added to the cells and left for 24 hours. After which, they were washed with PBS, serum starved overnight and then subsequently harvested or further treated.

2.1.14 Lentiviral transfection

Background: lentivirus is a type of retrovirus that can lead to chronic and deadly diseases such as the Human Immunodeficiency Virus (HIV), which causes AIDS. All retroviruses have a single stranded RNA genome with reverse

transcriptase activity. Lentiviruses also have a viral envelope that helps to facilitate the incorporation of their viral genome into host DNA, allowing it to replicate within the host cell. Taking advantage of this system allows the transient overexpression of proteins in cell lines. Lentiviral vectors use a highly modified version of the HIV-1 virus. There are three generations of vectors the 1st generation present a significant biosafety risk, the 2nd generation are much safer and sufficient for most experiments, but the 3rd generation has the maximal biosafety. This project uses a commercially available “ready to use” lentivirus from Vigene (Rockville, USA). It contains: C-terminal FLAG and Myc protein tags, a Woodchuck hepatitis virus post-transcriptional Regulatory Element (WPRE), a SV40 and CMV promoter region as well as ampicillin resistance. Figure 2.1 gives an overview of the plasmid. Hexadimethrine bromide (commercial brand name Polybrene) neutralises the affect that charge has on transduction, to increase efficacy.

Reagents:

- Polybrene (Sigma-Aldrich, Poole, UK).
- HI-Serum-containing medium: DMEM-F12, 10 % (w/v) Heat-inactivated (HI)-FBS (made by heating FBS at 56°C for 30 minutes), 2mM L-glutamine, 200IU/ml penicillin, 200µg/ml streptomycin.
- Serum-free medium: DMEM-F12, 2mM L-glutamine, 200IU/ml penicillin, 200µg/ml streptomycin.

Method: SW1353 cells were cultures in 96 or 6 well plates until they had reached 50-60% confluency. 5µl of polybrene was added to 10ml of HI-Serum-containing medium. 100µl/well (96 well) or 2ml/well (6 well) of this mixture was then transferred to a clean container. Lentivirus was then thawed slowly on ice and the relevant amount for the desired MOI added to the mixtures. Any remaining lentivirus was stored at 4°C, as freeze-thawing vastly reduces potency. 100µl/well (96 well) or 2ml/well (6 well) was added to cells and they were incubated at 37°C for 24 or 48 hours. After which, they were washed with PBS, serum starved overnight and then subsequently harvested or further treated.

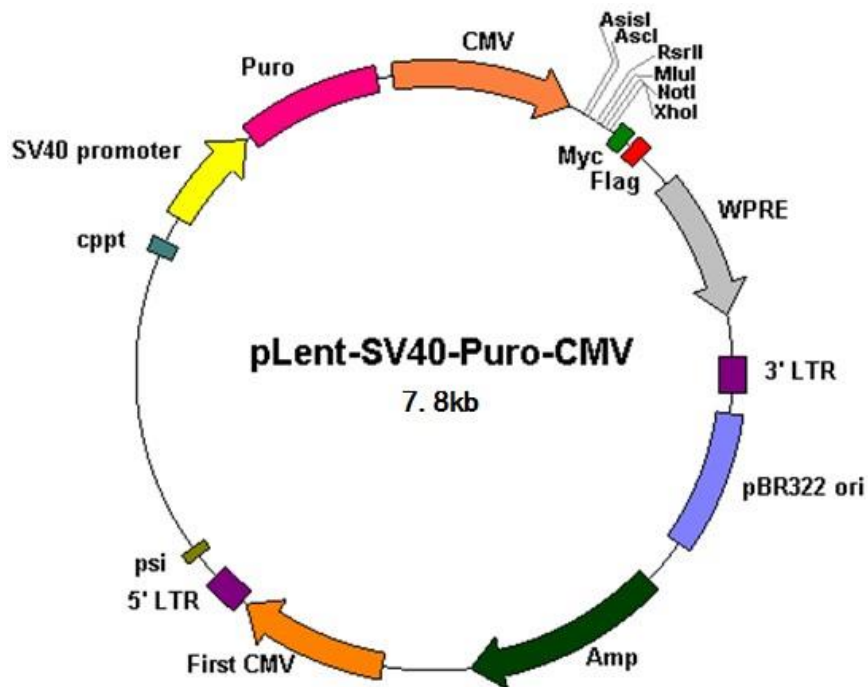


Figure 2.1 ALK1 lentiviral plasmid.

2.1.15 Adenovirus transfection

Background: Adenoviruses are the largest non-enveloped viruses and contain double stranded DNA. They are able to replicate in the host cell's nucleus using the cells own replication machinery. This means adenoviral DNA does not incorporate into the host genome. A replication deficient adenovirus is used for the transfection. This allows your gene of interested to be transfected into the cell with a high efficiency and then shuttled to the nucleus, where it will be overexpressed. As the gene cannot integrate into the genome it is lost during cell division, the high transfection efficiency will allow for this but it means cells should be at a higher seeding density than for siRNA or lentiviral transduction. The adenovirus used through this project was a gift from Prof Peter van der Kraan (Radboud, Nijmegen, Netherlands).

Reagents:

- Serum-containing medium: DMEM-F12, 10 % (w/v) FBS, 2mM L-glutamine, 200IU/ml penicillin, 200µg/ml streptomycin.

- Serum-free medium: DMEM-F12, 2mM L-glutamine, 200IU/ml penicillin, 200µg/ml streptomycin.
- PBS

Method: SW1353 cells were cultured in 96 or 6 well plates until they had reached >70% confluency. Adenovirus was then thawed slowly on ice and the relevant amount for the desired concentration added to Serum-containing medium. The cells were washed with PBS. Then 100µl/well (96 well) or 1ml/well (6 well) of the adenovirus containing medium was added to the cells and left for 24 or 48 hours. After which, they were washed with PBS, serum starved overnight and then subsequently harvested or further treated.

2.1.16 Live/dead viability/cytotoxicity assay

Background: The LIVE/DEAD® Viability/Cytotoxicity Kit for mammalian cells provides two probes that work simultaneously to stain a given population for alive and dead cells. Calcein-AM (Cal) is used to measure alive cells, it is a non-fluorescent precursor which can enter cells but only fluoresces (at excitation ~494 nm, emission ~517 nm) when cleaved by intracellular esterase, which is only present in live cells. Ethidium homodimer (Ethd) is used to measure the dead cells as it can only enter cells when they have damaged membranes. It then binds to nucleic acid, which results in a 40-fold increase in fluorescence (at excitation ~528 nm, emission ~617 nm).

Reagents:

- LIVE/DEAD® Viability/Cytotoxicity Kit
- PBS

Method: The assay usually requires that you test different concentrations of Cal and Ethd for your given cell type. However, our group has already done this for SW1353 cells so it was not necessary to replicate this. SW1353 cells were plated and treated under normal conditions until they would have ordinarily been harvested. Prior to treatment both chemicals were removed from the freezer and warmed to room temperature. Cells were then washed with PBS. A solution of PBS was then made that contained Cal at 0.5µM and Ethd at 2.5µM. This

was then lightly vortexed to ensure mixing. 100µl/well of this mix was added to cells and left in a dark cupboard for 5 minutes. The mixture was then removed and the cells left in PBS. Each lane was then photographed on a Zeiss Axiovert 200M inverted microscope (Carl Zeiss AG, Oberkochen, Germany) at the different wavelengths, as well as one image on bright field.

Analysis: Using a representative area for each given well I counted the live and dead cells. I then added the values together to get the total cell count. I also counted all of the cells using the bright field image to confirm it matched the total cell count. After which, I divided the number of dead cells by the total cell count and multiplied this by 100 to get a percentage of cell death.

2.1.17 Stable plasmid transfection

Background: A stable cell lines is one that has incorporated a plasmid into its genome, resulting in a stable over-expression of a protein of interest. This plasmid will also include a gene for antibiotic resistance, which is used to select the cells that have successfully incorporated the plasmid. Culturing transfected cells in medium containing the antibiotic will result in the death of all cells not expressing the plasmid. The surviving cells can then be cultured as normal but in medium containing this antibiotic. This means that all surviving cells should be expressing your gene of interest, removing the variability between cells which is seen with a transient transfection. If for any reason the plasmid stops being expressed the antibiotic will ensure these cells die, so there is no chance of you continuing with cells that no longer express the plasmid. As the cells are all expressing the gene they can be treated in the same way as wild-type, allowing treatment to be done immediately.

Reagents:

- DMEM-F12, supplemented with 10% FBS and 2 mM L-glutamine but no antibiotics.
- 50mg/mL G418 in ddH₂O, filtered with 0.22µm PES filter.
- FuGene HD (Promega, Wisconsin, United States)
- Serum-containing medium: DMEM-F12, 10 % (w/v) FBS, 2mM L-glutamine, 200IU/ml penicillin, 200µg/ml streptomycin.

- Serum-free medium: DMEM-F12, 2mM L-glutamine, 200IU/ml penicillin, 200µg/ml streptomycin.
- Selective medium: DMEM-F12, 10 % (w/v) FBS, 2mM L-glutamine, 400 µg/mL G418.
- PCR clean up kit
- Restriction enzymes and relevant buffers.

Method: I used two different plasmids throughout this thesis, the first was mEmerald-ALK1-N-13 and was a gift from Michael Davidson (Addgene plasmid # 53981). The second was created in-house using the pcDNA3.1 plasmid (Thermo Fisher, Loughborough, UK). Both plasmids were selected for with the antibiotic G418. Prior to transfection the plasmid should be linearised. For this a 100µL reaction was set up contain 10µg plasmid and 50 units of either *MfeI* or *Pvu1* (depending on the plasmid) along with the relevant buffer, these were then incubated for 4 hours at 37°C. An ethidium bromide gel was used to confirm the digestion had been successful. The remaining product was then purified using a PCR clean up kit, as per the instructions. A 6 well plate was seeded with 200,000 SW1353 cells then incubated overnight in Serum-containing medium. Plasmid DNA (2.75µg) was combined at a 1:3 ratio with 8.25µL FuGene HD and 137.5µL of Serum-free medium. A control was also created that had water instead of the plasmid. These mixtures were vortexed at full speed for 5 seconds then left for 10 minutes at room temperature, before being added to the cells along with 4ml of Serum-containing medium. After 24 hours the treatment medium was removed and replaced with Serum-containing medium overnight. The following day the medium was replaced with selective medium, this was then replaced every 2-3 days until the control cells were dead and the treated cells were fully confluent. Each well of the plate was then split and transferred to a T25 flask until confluent. They were then split and transferred to a T75 flask. After which, they could be treated the same as wild-type SW1353 cells but incubated in selection medium instead of Serum-containing medium. It is important to note that typically you need to test various concentrations of G418 for your specific cell type. However, this had already been done by our group for SW1353 cells.

2.1.18 Mini/maxi prep

Background: QIAprep Spin Miniprep Kits are designed to isolate high-purity plasmid DNA. Allowing the extraction of high quality DNA from bacterial cultures. The mini-prep results in lower quantities of DNA but is cheaper, allowing you to reduce risk when testing if a plasmid is as desired. The Maxi-prep then allows much higher quantities of DNA to be produced, allowing you to make sufficient plasmid DNA for regular transfection.

Reagents

- QIAprep Spin Miniprep Kit
- QIAprep Spin Maxiprep Kit
- QIAvac 24 Plus
- Antibiotic containing Lysogeny broth (LB) medium, autoclaved to prevent any unintended growth, also containing Kanamycin at 50mg/ml.
- DNase-free water.

Method: Three 50ml mixtures were made containing: the LB medium with no bacteria, bacteria containing the plasmid of interest or bacteria resistant to an alternative antibiotic. Bacteria were transferred to the tubes by pressing the colony with a 20 μ L pipette tip and then moving the tip to the medium, all under sterile conditions. The tubes were then incubated at 37°C overnight with agitation at 225-250 rpm in an orbital incubator. The following day only the bacteria containing the plasmid of interest should have grown.

Mini-prep: This tube is spun at 5400xg for 10 minutes at 4°C and the supernatant discarded. The pellet was then resuspended in 200 μ L P1 buffer and transferred to a 1.5ml microcentrifuge tube. 200 μ L P2 buffer was added and mixed by inverting gently. This was followed by adding 350 μ L P3 buffer and mixed by inverting gently. The tube was then spun at 17,900g for 10 minutes at 4°C. The QIAvac 24 Plus filtering system was then used on the lysates. Lysates were passed through the column and then the eluant was discarded. Endotoxin removal wash was then eluted through the column. This was then followed by buffer PE to wash. The DNA was then eluted into a clean 1.5ml microcentrifuge tube using DNase-free distilled water, extra time was taken to ensure the

column was completely dry. The eluted DNA could then be analysed on a Nanodrop ND 1000 spectrophotometer (Thermo Fisher, Loughborough, UK) to determine purity and concentration.

Maxi-prep: All the bacteria containing medium was then added to 250ml of fresh LB medium and incubated at 37°C overnight with agitation at 225-250 rpm in an orbital incubator. This tube was spun at 5400xg for 10 minutes at 4°C and the supernatant discarded. The pellet was then resuspended in 12ml resuspension buffer and vortexed until there were no clumps remaining. 12ml of lysis buffer was then added and inverted 3-5 times. After which, it was left for 3 minutes. I then added 12ml of neutralising solution and spun at 17,900g for 20 minutes at 4°C. The QIAvac 24 Plus filtering system was then used on the lysate, with larger columns than used from the Mini-prep. Lysates were passed through the column and then the eluant was discarded. Endotoxin removal wash was then eluted through the column. This was then followed by buffer PE to wash. The DNA was then eluted into a clean 1.5ml microcentrifuge tube using DNase-free distilled water, extra time was taken to make sure the column was completely dry. The eluted DNA was then run on a Nanodrop ND 1000 spectrophotometer to detect purity and concentration. Plasmids were then stored at -20°C until use.

2.1.19 Site directed mutagenesis

Background: QuikChange site-directed mutagenesis from Agilent Technologies (California, USA) allows you to make single nucleotide changes.

Oligonucleotides are used that have an almost identical sequence to the region of interest, but also contain the relevant mutation(s). These bind to the plasmid of interest and a high fidelity DNA polymerase can then replicate both plasmid strands. However, the ends of the plasmid cannot be joined leaving it with staggered nicks. DpnI endonuclease is added to the samples as it targets specifically methylated and hemi-methylated DNA resulting in it degrading the parental strand (without the mutation). The DNA must then be transformed into bacteria in order to fix the nicks. It can then be harvested from these cells at a much higher quantity and ready for transfection.

Reagents:

- QuikChange site-directed mutagenesis kit
- “Stellar” E. coli (Clontech, California, USA)
- SOC medium
- Oligonucleotide primers
- DNase-free water
- dNTPs, 2.5mM each
- Kanamycin (50mg/ml) containing agarose plates

Method: Created a 50 μ L reaction made up of 10x reaction buffer, 5-50ng plasmid, 125ng of forward and reverse primers, 0.5 μ L dNTP mix, 0.5 μ L *PfuTurbo* DNA polymerase and water. This mix was then added to a PCR block and run using the following cycle:

1. Initial denaturation stage of 95°C 30 seconds
2. 12 cycles of 95°C for 30 seconds then 55°C for 1 minute and finally 68°C for 7 minutes (1 minute per kb of plasmid length).

The samples were then transferred to ice for 2 minutes to cool the reaction. 0.5 μ L of 20,000 units/ml DpnI was then added to the reactants and gently mixed. The samples were then transferred to a water bath at 37°C, for 1 hour. During this I gently thawed “Stellar” E. coli on ice, 25 μ L was then transferred to two clean 1.5ml microcentrifuge tube. 1 μ L of water was added to 1 tube, and 1 μ L of treated DNA was added to the other. The tubes were then swirled to mix and left on ice for 30 minutes. The samples were then carefully placed in a water bath for 1 minute at 48°C, then transferred to ice for 2 minutes. In sterile conditions 500 μ L of SOC medium was added to each tube and they were incubated at 37°C for 1 hour with agitation at 225-250 rpm in an orbital incubator. The mixture was then spread on Kanamycin (50mg/ml) containing agarose plates and left for 16 hours at 37°C. Any colonies could then be mini-prepped and sent for sequencing to check the mutation was as desired. More information on specific gene changes and primers used will be given in chapter 6.

2.1.20 Colony PCR

Background: Colony PCR is a simple and quick method of determining if an insert has successfully incorporated into a plasmid. Cells are lysed to release the DNA, allowing plasmids to serve as templates for an amplification reaction. Primers can either flank the insert or copy the entire plasmid. The amplified DNA can then be run on a gel to determine if insert is present.

Reagents:

- Master mix per reaction: 0.3mM dNTPs, 0.5 μ M of each forward and reverse primers, 1.5mM MgCl₂, 0.25 units recombinant Taq polymerase (Thermo Fisher, Loughborough, UK) in the supplied buffer.
- DNase-free water.

Method: 10+ colonies were chosen from an antibiotic containing agar plate. The colonies were selected by pressing them with a 20 μ L pipette tip then moving that tip to an Eppendorf tube containing 100 μ L sterile water. The tube was then heated for 3 minutes at 98°C. 1 μ L of this DNA-containing water was then added to 9 μ L of master mix. The reactants were then transferred to a PCR block with cycling conditions:

1. Initial denaturation stage of 94°C 2 minutes
2. 35 cycles of 94°C for 45 seconds, 42°C for 30 seconds and 72°C for 90 seconds
3. Final elongation of 72°C for 10 minutes

The products of this cycling were then run on a 1% agarose gel with ethidium bromide. If the primers were flanking the gene then any products showed that the insert was present. If the primers replicated the full plasmid then the DNA ladder would show the molecular weight, which will be higher if the insert is present. If the fragment was as expected the sample was then mini-prepped and sequenced. More information on specific gene changes and primers used will be given in chapter 6.

2.1.21 In-fusion cloning

Background: In-Fusion Cloning Kits by Clontech (California, USA) are designed to allow fast cloning of a fragment, or fragments of DNA into a vector. Primers are designed that flank the gene of interest but leave overhangs of 15-bp that have known restriction enzyme sequences at the end. A restriction enzyme can then be used to cut your plasmid of interest leaving compatible ends of both your plasmid and gene fragment. The In-Fusion Enzyme then allows the DNA fragment to fuse into the plasmid efficiently and precisely by recognizing 15-bp overlaps at their ends. The resulting plasmid should be seamless with no unwanted base pairs so can be used immediately.

Reagents:

- In-Fusion cloning kit
- “Stellar” E. coli (Clontech, California, USA)
- Master mix per reaction: 0.2mM dNTPs, 0.5 μ M of forward and reverse primers and 0.5 units of Q5 polymerase, in Q5 polymerase buffer
- SOC medium.
- PCR clean up kit.
- DNase-free water.
- Kanamycin (50mg/ml) containing agarose plates.
- Restriction enzymes and relevant buffers.

Method: Two mixes were made containing template DNA (1ng) and master mix, to a 25 μ L total volume. The reactants were then transferred to a PCR block with one of two cycling conditions 64 $^{\circ}$ C or 72 $^{\circ}$ C, as advised by the protocol:

64 $^{\circ}$ C cycle:

1. Initial denaturation stage of 98 $^{\circ}$ C 30 seconds
2. 30 cycles of 98 $^{\circ}$ C for 10 seconds, 56 $^{\circ}$ C for 15 seconds and 64 $^{\circ}$ C for 15 seconds
3. Final elongation of 64 $^{\circ}$ C for 2 minutes

72 $^{\circ}$ C cycle:

1. Initial denaturation stage of 98°C 30 seconds
2. 30 cycles of 98°C for 10 seconds, 56°C for 15 seconds and 72°C for 15 seconds
3. Final elongation of 72°C for 2 minutes

The plasmid was then double digested with two restriction enzymes. 1µg of the plasmid was incubated for 4 hours at 37°C with 20 units of each restriction enzyme in 50µL reactions with relevant buffer (New England Biolabs, Ipswich, USA). The products were subsequently purified using a PCR clean up kit, as per instructions. Both the products of the DNA fragments and cut plasmid were then run on a 1% agarose gel with ethidium bromide to verify both have worked. I found the 72°C cycle samples gave a stronger signal so continued with them samples and discarded the samples from the 64°C cycle. 50ng of cut plasmid and 100ng of insert were then incubated with the relevant In-Fusion kit component at 50°C for 15 minutes, in a 10µL reaction. During this Stellar™ E. coli were gently thawed on ice. After which, 25µl were transferred to two clean 1.5ml microcentrifuge tubes. In 1 tube 1µl of water was added and the other 1µl of treated DNA. The tubes were swirled to mix and then left on ice for 30 minutes. The samples were then carefully placed in a water bath for 1 minute at 48°C then transferred to ice for 2 minutes. In sterile conditions 500µl of SOC medium was added to each tube and they were left at 37°C for 1 hour with agitation at 225-250 rpm in an orbital incubator. The mixture was then spread on Kanamycin (50mg/ml) containing agarose plates and left for 16 hours at 37°C. Any colonies could then be mini-prepped and sent for sequencing to check the mutation was as desired. More information on specific gene changes and primers used will be given in chapter 6.

2.1.22 Ethidium bromide gel

Ethidium bromide gels are used to visualise DNA by utilising agarose gel electrophoresis to separate the samples by size. The gel contains ethidium bromide which can intercalate with DNA, allowing it to be visualised under UV-light.

Reagents:

- TAE buffer: 40mM Tris-base, 0.11% (v/v) Acetic acid, 1mM EDTA in ddH₂O.
- Ethidium bromide (10mg/mL).
- Agarose.

Method: A 1% agarose gel was made by adding 1g of agarose to 100ml of TAE buffer and dissolving in a microwave until boiling. This mixture is then allowed to cool before adding 1 μ L ethidium bromide in a hood. The solution was then added to a gel tray and left to solidify. The gel was then placed in a running tank that was full with TAE buffer and 1 μ L of ethidium bromide. Samples were loaded and the gel was run at 110V for approximately 30 minutes (until the dye in the DNA ladder reached the end of the gel). Gels were then visualised using a Gbox EF Gel Documentation System with Genesnap software (Syngene, Bangalore, India).

2.1.23 Graph pad prism

GraphPad Prism is commercial scientific 2D graphing and statistics software published by GraphPad Software, Inc. It has an intuitive interface that allows the plotting of graphs but also statistical analyses of all data. It was used for the plotting and statistical analysis of my experimental data.

2.2 Bioinformatics tools

A range of bioinformatic tools have been used throughout this thesis. Making use of publically available microarray data helped to guide the initial experiments and has provided direction for future work. Sections 2.2.1 through to 2.2.5 explain the programs that were used to create a cytoscape network of OA, as described in 2.2.6.

2.2.1GEO

The gene expression omnibus (GEO) is a publically available international repository run by the National Center for Biotechnology Information (Ron Edgar et al. 2002). It archives and freely distributes microarray, next-generation sequencing, and other high-throughput functional genomic data sets. GEO stores and provides all details of the study, a link to any associated publications as well as raw data files, processed data, and descriptive metadata, which are indexed, cross-linked, and searchable. The database can be searched according to any property of the data for example: organism, cell type, treatment or disease.

2.2.2 R

R is a computational language used for statistical computing and graphics. Originally it was developed by Bell Laboratories (formerly AT&T, now Lucent Technologies) by John Chambers and colleagues (Team 2013). It is an open source software with a wide variety of statistically and graphical techniques. It also has a variety of “packages” that can be added to tailor it to your specific needs. It allows the incorporation, storage and manipulation of large data files making it ideal for manipulating microarray data. Some of the R packages were also useful for combining multiple microarray data files. Bioconductor is a package that I used regularly.

2.2.2.1 Bioconductor

An open source package designed to provide tools of the analysis and comprehension of high-throughput genomic data (Gentleman et al. 2004). It allows for data to be taken directly from GEO or imported from your own data files. It provides the “RMA” function which computes the RMA (Robust Multichip Average) expression measure described in (Irizarry et al. 2003), providing a

quick and uniform way to normalise microarray data. It also contains the function “ComBat” which allows user to correct for batch effects, when the reasons for the batch effects are known. The methodology used is described in (Johnson et al. 2007).

2.2.3 ARACNE

The Algorithm for the Reconstruction of Accurate Cellular Networks (ARACNE) is a novel algorithm that uses mutual information (MI) to quantify interaction between genes (Margolin et al. 2006). This number quantifies the "amount of information" obtained about one random variable, through the other random variable. In this case the variable is gene expression and how much the change in one gene effects the expression of another. MI is scored between zero and one, with one being the highest. How the expression of one gene corresponds to another is used for your data to determine interactions and their MI values. The data processing inequality is then used to remove the majority of indirect candidate interactions that is inferred by co-expression methods. The algorithm provides a way of using microarray data to expose the functional mechanisms that underlie the cellular processes.

2.2.4 Cytoscape

Cytoscape is an open source software platform used primarily for the visualisation of molecular interaction networks, whilst also integrating gene expression profiles and other state data (Shannon et al. 2003). Cytoscape core distribution provides a basic set of features for data integration, analysis, and visualization. Allowing you to change how the network is visually presented as well as sorting the data by whatever value you have used to quantify interactions. For example when looking at MI you can sort the data so that any interactions with an MI lower than a set threshold are deleted. This helps to identify the strongest interactions in the data. Additional features can be added to Cytoscape, known as apps. Throughout this thesis I have used two “clusterMaker” and “PhenomeScape”.

2.2.4.1 clusterMaker

clusterMaker is an open source Cytoscape app that contains multiple different clustering algorithms, which allow you to locate distinct clusters of genes in your

network that interact with each other (Morris et al. 2011). These can then be presented as hierarchical groups of nodes that can be exported to other programs to determine the processes governed by this specific group of genes. Community clustering (GLay) was used as it is powerful tool that can quickly identify groups of genes that interact exclusively with each other (Su et al. 2010). It then presents these clusters in a uniform order, with the largest cluster at the beginning followed by smaller clusters, leading to single genes at the end.

2.2.5 DAVID

The Database for Annotation, Visualization and Integrated Discovery (DAVID) is an integrated biological knowledgebase that contains analytical tools for extracting biological meaning from gene lists (Huang et al. 2009). It requires a gene input list containing common identifiers, such as official gene symbols. The DAVID Bioinformatics Resources consists of five integrated, web-based functional annotation tool suites: the DAVID Gene Functional Classification Tool, the Functional Annotation Tool, the Gene ID Conversion Tool, the Gene Name Viewer and the DAVID NIAID Pathogen Genome Browser. I made use of the DAVID Gene Functional Classification Tool, which allows functional annotation clustering of a gene list based on enriched biological themes. This means by using pre-selected biological themes, such as GO term or KEGG pathways, the system can then look for terms that contain a significant number of your gene list. This provides an idea of biological functions your gene list could be responsible for.

2.2.6 Creating a network of human OA

To create a network overview of human OA I collected publically available OA microarray data from GEO. I searched GEO using the keyword “osteoarthritis” then selected the relevant affymetrix samples. Table 2.3 shows the samples that were used for the rest of the analysis of these I only used the diseased samples and got 50 samples overall from 5 different studies. The samples are not identical but they are close enough that I could consider them representative of the same disease. The data was first imported into R and normalised using the RMA function, which is built into Bioconductor. R was then used to combine the data, change the gene names to “official gene names” and

take the average of any duplicate genes in the samples. The expression data from all the samples were tested using a principle component analysis (PCA) analysis, which is also built into Bioconductor. PCA tests for variability between samples and showed that the samples from the same experiment clustered together (Fig 2.2A). This is unsurprising as slight changes in the experimental technique as well as how the samples were processed most likely led to minor changes. ComBat was then used to remove these batch effects. It was run for all the samples under the assumption that the some changes could be the result of experimental variation between samples. Figure 2.2B shows a PCA after running ComBat for which the gene sets have a less clustered pattern.

After batch corrections I put the samples through ARACNE which determined how all of the genes interact with each other and the strength of these interactions. ARACNE was run using the command line, by directing my combined data to the programme and setting a p value cut off. The following script was used “-i corrected-data.txt -p 1e5 -o outfile.adj -h C:\aracne “.The resulting data was then imported into Cytoscape and clustered with the GLay algorithm (clusterMaker) to provide an overview of OA as a network. Selecting any of these clusters gave me a gene list that could then be analysed using DAVID to determine the biological function of that cluster. The analysis of these clusters is shown in chapter 3. It is important to note that this analysis was run at the end of 2015 so any protein links established since then will not have been included in the analysis.

Number of samples	Array type	Tissue	Reference
19	Affymetrix Human Genome U133 Plus 2.0 Array	synovial membrane	(Q. Wang et al. 2011)
10	Affymetrix Human Genome U133A Array	synovial membrane	(Woetzel et al. 2014)
10	Affymetrix Human Genome U133A Array	synovial tissue	(Woetzel et al. 2014)
6	Affymetrix Human Genome U133A Array	synovial membrane	(Woetzel et al. 2014)
5	Affymetrix Human Genome U133 Plus 2.0 Array	synovial biopsy samples	(Toukap et al. 2007)

Table 2.3 Details of publically available microarray data for OA patients.

Relevant details of all microarray samples combined to create the cytoscape OA network. Although three share the same reference, they were created by three separate groups that were collaborating for that publication.

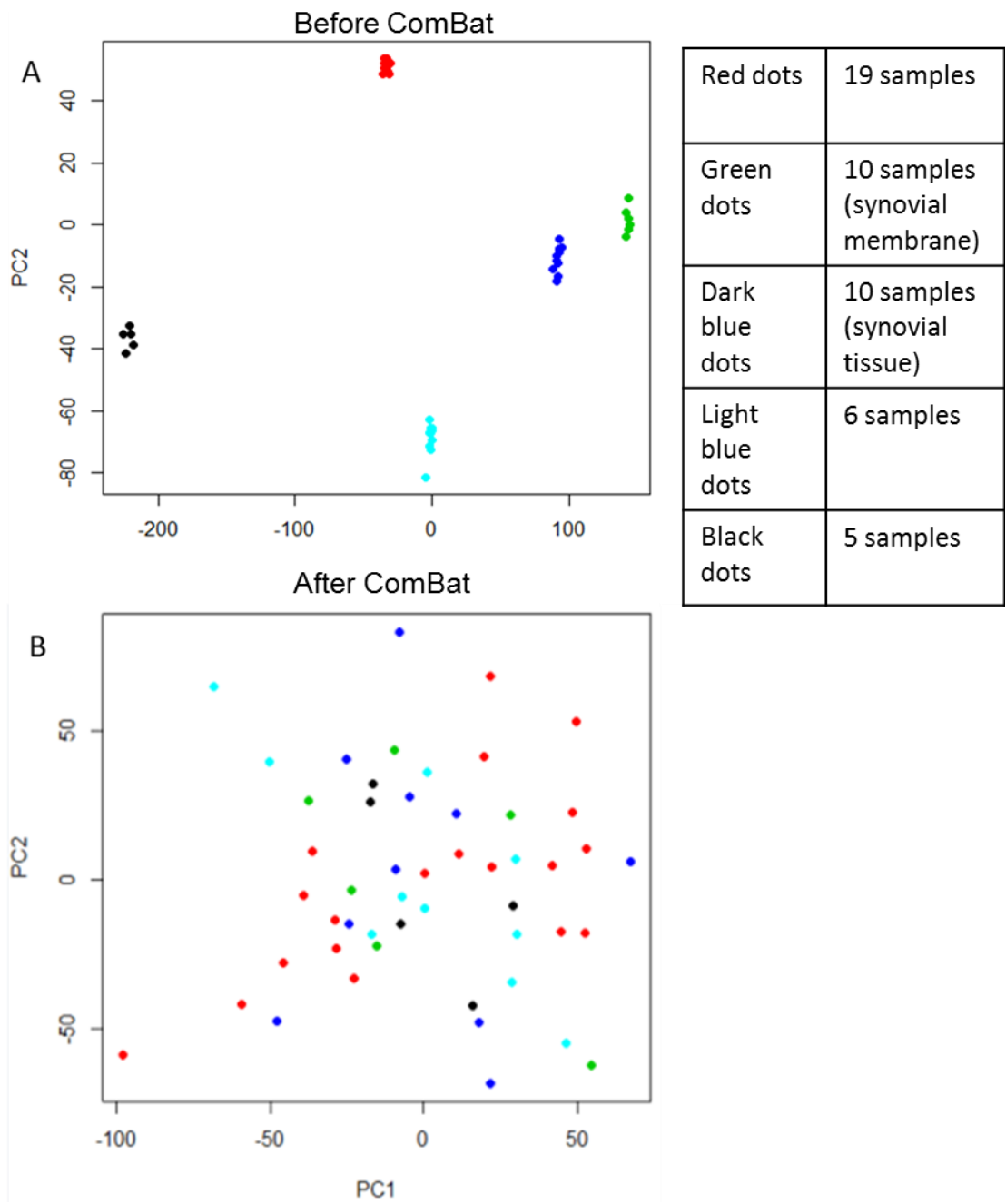


Figure 2.2 **ComBat removes the batch effects in combined microarray data.** Principle component analysis (PCA) which separates the samples presented in table 2.3 based on their variance. A) PCA analysis on the samples, after they had been normalised and combined. B) PCA of the same samples after running ComBat to remove batch effects.

2.2.7 PhenomeScape

PhenomeScape is an open source Cytoscape app that enables the identification of active sub-networks, by looking at groups of differentially expressed genes that are physically interacting (Soul et al. 2016). What makes it unique is that it also links these sub-networks to human and animal disease, by using gene expression studies that show changes in genes leading to disease like phenotypes. There is an option to only look for phenotypes relevant to a disease of interest and in an animal of interest.

PhenomeScape requires a protein-protein interaction (PPI) network for which I used the cytoscape network described in section 2.2.6. Manual selection of phenotypes of interested is then required. These phenotypes are taken from UberPheno (Köhler et al. 2013) and include human, mammalian and zebrafish studies. Finally PhenomeScape requires analysed expression data with gene symbols, fold change and P-values is required. There is an OA dataset built into cytoscape that I used for this analysis (S. L. Dunn et al. 2016). This expression dataset is linked to the original PPI network by gene symbols. PhenomeScape works by a two-step process as described in Soul et al. (2016) first ranking the protein-protein interactions based upon the phenotypes chosen. It then uses these genes and phenotypes as the starting points to find other closely related phenotypes, and also uses their known associations to aid the analysis. Activity scores are calculated based on the gene and phenotype interaction and high scoring groups of interacting proteins are identified as sub-networks. There is then a final test to make sure a sub-network of that size could not have that level of differential expression by chance. The networks also show the top enriched GO term associated with them genes to give an indication of the function of that sub-network. I ran the programme for human phenotype with the default parameters: network size (10), number of random networks (1000), minimum p value (0.05) and minimum size (4). More information on this analysis will be given in chapter 8.

PhenomeScape contains zebrafish and mammalian phenotypes which were used in this study despite being linked to human diseases. This was because UberPheno have designed them to be comparable. To do this they used mouse

or zebrafish datasets to infer gene-phenotype interactions in there human orthologues, when human data was unavailable. This was justified in (Köhler et al. 2013).

2.2.8 GSEA

Gene Set Enrichment Analysis (GSEA) is a computation method used to determine if a gene list significantly up or down regulates a biological state, such as chromosomal modifications, pathway regulations or cell division (Subramanian et al. 2005). Taking microarray data sets and running them through the GSEA programme allows you to find process that are affected by their gene profiles. For example KEGG pathways have known genes that affect them, if a significant number of genes are upregulated in your profile the relevant KEGG pathway will appear in the output. The programme also takes into account the change in regulation when determining significance. So if one of the genes in the pathway is upregulated 2-fold it will carry more weight, compared to another upregulated 0.5-fold. The GSEA programme also ranks the genes showing which genes are responsible for that pathway being significantly regulated and which are not. This gives you an idea of the biological processes that are occurring in your samples and which genes from your data are responsible for this. I have ran differentially expressed gene lists through GSEA to determine their biological function but also because it allows you to explore what genes are responsible for that function being significantly upregulated. This will be demonstrated in chapter 3.

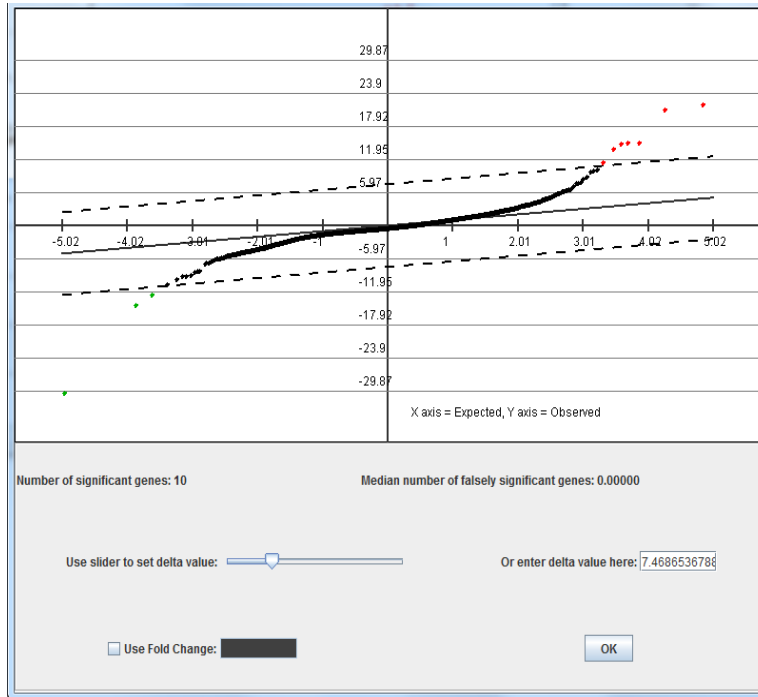
2.2.9 MeV

Multiple Experiment Viewer (MeV) is an open source cloud based application that allows analysis, visualization, and stratification of large genomic data (Saeed et al. 2003). MeVs built in PCA function allows you to assess the variability between samples, from this you can see if any of the samples are outliers and need to be removed from the samples. Significance Analysis of Microarrays (SAM) analysis can also provide a list of differentially expressed genes between sets of samples. It also provides an estimate of the False Discovery Rate (FDR), allowing for the removal of genes that are most likely there by chance. How stringent this is, is not set and can be changed

accordingly. Its design has the advantage that before setting this value you can look at the distribution of your genes and so can alter to a level relevant for what you require.

MeV was used through this thesis for determining differential genes in any microarray data not present in table 2.3. The array data was initially normalised using the Bioconductor function RMA, this normalised data was then moved to MeV where the built in PCA allowed for outliers to be removed. PCA clusters each of patient samples so that if one sample does not cluster with others it can be removed from the analysis. The differentially expressed genes were then determined using SAM. Figure 2.3A shows an example of the distribution of the genes. Figure 2.3B shows the delta values from the same gene list. 0.622 is the highest value with an FDR less than 10%, so re-running the SAM with this delta value provides a list of differentially expressed genes.

A



B

	Delta	Median false	90th %ile false	# sig. genes	FDR(%) Median	FDR(%) 90th %ile
Original Data	0.322	374.043	1,700.300	2007	13.347	63.000
Cluster Manager						
Gene Cluste						
Sample Clus	0.547	321.124	1,547.308	2580	12.447	59.973
Gene Cluste	0.572	274.793	1,346.805	2361	11.639	57.044
Sample Clus	0.597	241.243	1,183.847	2214	<u>10.896</u>	53.471
Analysis Results	<u>0.622</u>	207.692	1,040.858	2093	9.923	49.730
Data Source	0.647	182.130	873.107	1943	9.374	44.936
PCA - sampl	0.671	157.367	761.272	1828	8.609	41.645
SAM (2)	0.696	131.006	656.627	1696	7.724	38.716
SAM Grap	0.721	115.030	568.758	1591	7.230	35.748
SAM (1)	0.746	95.858	511.243	1483	6.464	34.474
Delta tab	0.771	80.680	470.503	1372	5.881	34.293
Expressio	0.796	65.503	441.746	1274	5.142	34.674
Centroid	0.820	57.515	408.195	1203	4.781	33.931
Expressio	0.845	51.923	371.450	1128	4.603	32.930
Table Vie	0.870	47.130	339.497	1082	4.356	31.377
Cluster Ir	0.895	41.538	296.361	1027	4.045	28.857
General I	0.920	35.947	251.627	979	3.672	25.702
SAM (3)	0.945	34.349	226.864	934	3.678	24.290
SAM (4)	0.970	30.355	208.491	890	3.411	23.426
SAM (5)	0.994	26.361	187.722	843	3.127	22.268
SAM (6)	1.019	25.562	178.935	813	3.144	22.009
SAM (7)	1.044	23.965	165.355	781	3.068	21.172
07-Sep-2015	1.069	19.172	147.781	723	2.652	20.440
PCA - genes	1.094	16.775	141.391	706	2.376	20.027
Script Manager	1.119	15.976	130.207	681	2.346	19.120
History	1.144	15.178	115.828	635	2.390	18.241
History Log	1.168	13.580	104.645	611	2.223	17.127
	1.193	11.982	94.260	594	2.017	15.869
	1.218	11.183	88.669	565	1.979	15.694
	1.243	9.586	85.473	542	1.769	15.770
	1.268	8.787	75.089	515	1.706	14.580
	1.293	8.787	70.296	495	1.775	14.201

Figure 2.3 Using MeV to determine differentially expressed genes. A) SAM analysis of an entire microarray gene list. It is intentionally set with a high delta value so only highly significantly enriched genes will be found. B) The delta values from the SAM analysis performed in A. The black line indicates where the FDR becomes less than 10%. The delta value in the red circle gives the value where all genes underneath have a FDR less than 10%. Re-running SAM with this cut off will then result in a gene list where all significantly enriched genes have a less than 10% FDR.

2.3 Mathematical modeling tools

2.3.1 SBML

All the models in my thesis were encoded in the Systems Biology Markup Language (SBML), a machine-readable format that is based on XML - (Hucka et al. 2003). SBML models are comprised of compartments, species and reactions. Compartments are what the reactions take place in for example nucleus. They have an initial volume that helps determine the speed of reactions. Species are what react, and are representative of proteins or complexes. The initial concentrations of species need to be set. Reactions refer to interactions between species (i.e. phosphorylation events), how these interact is via rate laws.

2.3.2 COPASI

Complex pathway simulator (COPASI) is a software application for simulation and analysis of biochemical networks and their dynamics (Stefan Hoops et al. 2006). It supports computational models in SBML format and allows time dependant simulations that can be deterministic, stochastic or a hybrid. The model is created in a graphical user interface (GUI) format which allows you to insert reactions and specify the rate laws. COPASI will then automatically convert the reactions into a set of differential equations. I created a model by modifying two previously published models in COPASI. I then combined the models and made any further modifications that were required in order to fit the model to experimental data. COPASI allows for the model to be run using a variety of different units. However as I was looking for patterns rather than exact concentrations I used particle numbers for the species concentrations. Particle number is normally depicted with the letter N and literally refers to the number of constituent particles in the system. COPASI has a number of built in tools for simulating and analysing models. I used the following tools to create and investigate the model:

2.3.2.1 Model simulation

Simulations involve solving the system of coupled differential equations that constitute the model. COPASI allows for the deterministic or stochastic simulation of the model. The deterministic simulations were run using the

simulation algorithm LSODA (Petzold 1983). Simulations were configured with parameters: Duration (1440), Interval Size (1), Relative Tolerance (1e-06), Absolute Tolerance (1e-12), Max Internal Steps (10000). Stochastic simulation were run using the direct method, which uses the Gillespie algorithm (Gillespie 1976). Simulations were configured with the Max internal step set at 1000000, random seed was not used. Simulations were run using COPASI version 4.20.

2.3.2.2 Parameter scans

Parameter scans allow the user to vary the value of a parameter or particle number of a species. The scan will increase the value or concentration from the minimum to the maximum values in a stepwise manner simulating the model at each increase. The minimum, maximum and number of simulations are set by the user. I used these parameter scans to alter the starting concentration of TGF β in the model. This allowed me to compare simulation data to experimental data as explained in chapter 5.

2.3.2.3 Extracting data

Although COPASI offers a way to visualise the data generated within it, these are normally rudimentary with no way to generate high quality figures. COPASI allows you to extract the data as a comma-separated values file that can then be moved to other programmes for visualisation.

2.3.2.4 Events

Events are state transitions of the model that require a condition to be triggered. They consist of two parts a trigger, such as a specific time, which signals for the event to take place. The second part is at least one assignment, which modifies the model; this is normally a change in concentration of one of the species. At the exact moment that the trigger changes from false to true the assignment will take effect. The assignment can affect multiple species in the model. It is also possible to have multiple events in the same simulation. Events were used to alter the concentration of species in the model after time zero. For example IL-1+OSM rather than being present initial in the model, was introduced at 6 hours in the simulation shown in chapter 5.

2.3.2.5 Parameter estimations

Background: The original choice of model variables can be determined from past literature, or if feasible measured experimentally. Unknown variables are normally estimated. However, parameter estimation provides a way of optimising the model to fit experimental data, by altering the parameters to allow the model to fit the data with reduced error. The algorithms for parameter estimation work by measuring the distance between model observables and data measurements at given time points. They then compute a solution by assigning and changing parameter values that minimise the distance between model predictions and experimental results. How this is accomplished depends on the algorithm that is used. These algorithms can be classified as either global or local. Global estimations aim to find the minimal distance by altering the parameter values over a large search space and once a lower minimum distance has been found the estimation starts to focus on these parameters. These algorithms can be very accurate as they search a large area. However, they also have a high demand on computational power and time. There is also a chance that they can focus on the wrong local minima, missing the optimum parameter values. Local algorithms focus on reducing the minimal distance, by finding new parameters close to the original starting values of the model. This has the advantage of being much faster but comes at the expense of excluding the majority of parameter sets. These algorithms are regularly used to improve a model that already has a reasonable fit to the data. Both types of algorithms allow you to select which parameters can be estimated.

Method: To parametrised my model I used a common technique of combining an initial global parameter scan followed by a local scan. I used the genetic algorithm for the global estimation. It works by randomly creating different parameter sets, the top ranking sets then progress to the next population being only marginally altered. The second population then contains the original sets combined with a new set of randomly assigned parameters, again the highest ranking parameter sets move on to the next generation. This is continued for a number of generations set at 1000. The amount of parameter sets that move through each generation is also set at 20. Once this has finished the highest

ranking parameter set is then further optimised using the local algorithm, Hook and Jeeves. This works by choosing parameters and randomly increasing or decreasing them, it then analyses if this positively impacts the models fit to the data if it does then the change remains, if not it is reversed. This is repeated for a number of iterations chosen were 50. For my model I was fitting MMP-13 data and since this gave a variable fold change, I instead fit to the percentage of repression. This was possible as the MMP-13 expression pattern under IL-1+OSM treatment had already been established in the model I started with. Knowing this I then used my generated data to determine the level of repression necessary at each time point and created a file for which that was true. For example at 24 hours the molecular number for MMP-13 with IL-1+OSM treatment was 109. I knew from my data that when TGF β was present this should be reduced 42%, so at 24 hours the value was 63. This was repeated for all known time points and the IL-1+OSM+TGF β model was fit to that data.

2.3.3 Model justification

Throughout this thesis I have used COPASI to modified and expanded upon two previously published models (Wang Hui et al. 2014; Proctor et al. 2014) in order to assess how these systems interact during ageing. The models were simplified but to still fit the same profiles. They were simplified in order to reduce the computational burden. In order to achieve this some assumptions had to be made, which marginally changed the structures. These changes are shown in chapter 5 and, as explained there, the simulation profiles still match the output in the previous models. However, there were some simplifying assumptions still in place from the original models that should be mentioned. These were justified in the supplementary data in (Wang Hui et al. 2014) and the main text of (Proctor et al. 2014).

The first model simplification is that TGF β is not turned over and so it can only be added to the model in the initial conditions or via an event. This simplification was left in place as TGF β can enter the system for a variety of reason and incorporating these into the model would have added significant complexity. Instead TGF β is inactivated and activated in the model but never lost. Any active TGF β that enters the system is then inactivated, in a process that

degrades ALK5 and SMAD7. ALK1 can also be degraded if TGF β is bound to an ALK1/ALK5 heterodimer. Inactive TGF β can then be activated by Integrin, a species in the model that can convert inactive TGF β to active. MMP-2 could also activate TGF β in the original model but this was removed as it had no effect on my combined model. It is known that TGF β can be activated by many biological components such as plasmin, F-spondin or MMP-2/-9 (Yu and Stamenkovic 2000; Attur et al. 2009) as well natural detergents such as lysophosphatidylethanolamine (LPE) and lysophosphatidylcholine (LPC) (Gay et al. 2004). For simplification integrin is representative of all mechanisms of TGF β activation. The TGF β driven increase in MMP-13 mRNA is driven by RUNX2, which is activated by phospho-SMAD1 and inactivated by phospho-SMAD2. This is a simplification as RUNX2 can be inactivated by other means (Jonason et al. 2009). However, as we are specifically interested in how TGF β affects RUNX2, having just phospho-SMADs affecting its activation gives us an insight into how their effect on RUNX2 changes with age. It is also important to note that SMAD2 in the model represents both SMAD2/3, and SMAD1 represents SMAD1/5/8.

The model works through the assumption that IL-1+OSM-driven MMP-13 expression is a result of c-Fos/c-Jun heterodimers and c-Jun homodimers. Our group has recently published that this may be a simplistic view as ATF3 appears to be important in the upregulation (Chan et al. 2017). However, it is clear that c-Fos/c-Jun heterodimers have a significant effect on ATF3 upregulation (Chan et al. 2017), so it is reasonable to assume that blocking c-Fos/c-Jun in the way predicted in the model would have the same effects. The model also allowed TGF β to affect the stability of MMP-13 mRNA. This was required for the model to fit experimental data. The justification behind including this instead of alternatives will be discussed in more detail in chapter 5.

The combined model uses mass action kinetics excluding equations for homodimer formation, where mass action has been altered to allow for the fact that the initial molecule cannot bind to itself. Normally during heterodimerisation one molecule binds to another so the reaction can be determined as $X*Y*k1$.

Where X is the concentration of molecule X, Y is the concentration of molecule Y and k1 is the rate constant. However, during homodimerisation one X molecule cannot bind to itself so has to be $X*(X-1)*k1$, the minus one take into account that the second molecule is taken from the overall concentration not including the first. This reaction must also be time be halved to account for the fact that both molecules are from the same pool so becomes $X*(X-1)*0.5*k1$. An example is for c-Jun dimerization which has the equation: " $k1*(cJun_P)*(cJun_P-1)*0.5$ ". Only one compartment was used for the model. The complete list of species and reactions in the combined model can be seen in tables 2.4 and 2.5.

Species	Description	Initial amount (particle number)
IL1	IL-1	100
Jnk_p	Phosphorylated form of Jnk	0
Jnk	Jnk	100
IL1R	IL-1 receptor	100
IL1RR	IL-1 bound to receptor	0
IL1RR.int	IL-1 bound to receptor and internalised	0
cJun	c-Jun	100
cJun_P	Phosphorylated form of c-Jun	0
cJun_dimer	c-Jun dimer	0
OSM	OSM	1000
OSMR	OSM receptor	100
OSMRR	OSM bound to receptor	0
Jak1	Jak1	100
Jak1_P	Phosphorylated form of Jak1	0
Stat3_nuc	Stat3 in the nucleus	0
cFos_mRNA	c-Fos mRNA	0
Stat3_cyt	Stat3 in the cytoplasm	75
cFos	c-Fos	0
p38	p38	100
p38_P	Phosphorylated form of p38	0
cFos_P	Phosphorylated form of c-Fos	0
cFos_cJun	c-Fos/c-Jun heterodimer	0
Block	A dummy species to represent 3 proteins (see chapter 5)	0
MMP13_mRNA	MMP-13 mRNA	0
Integrin	Integrin but also representative of all mechanisms of TGF β activation	0
Source (fixed particle number)	A fixed pool for the creation of new molecules	1
Sink (fixed particle number)	A fixed pool for the degradation of molecules	1
Alk5	ALK5	500
Tgfb_A	Active form of TGF β	0
Tgfb_I	Inactive form of TGF β	200
Alk5_dimer	ALK5 homodimer	0
Alk1	ALK1	300

Alk1_Alk5	ALK1/ALK5 heterodimer	0
Tgfb_Alk5_dimer	Active TGF β bound to an ALK5 homodimer	0
Smad7	SMAD7	0
Tgfb_Alk5_dimer_Smad7	Active TGF β bound to an ALK5 homodimer and SMAD7	0
Tgfb_Alk1_Alk5	Active TGF β bound to an ALK1/ALK5 heterodimer	0
Smad2	SMAD2	600
Smad2_P	Phosphorylated form of SMAD2	0
Smad2_P_Smad4	Phosphorylated form of SMAD2 bound to SMAD4	0
Smad4	SMAD4	600
Runx2_A	Active form of RUNX2	0
Runx2_I	Inactive form of RUNX2	100
Smad1	SMAD1	600
Smad1_P	Phosphorylated form of SMAD1	0
Smad1_P_Smad4	Phosphorylated form of SMAD1 bound to SMAD4	0
Tgfb_Alk1_Alk5_Smad7	Active TGF β bound to an ALK1/ALK5 heterodimer and SMAD7	0
JunB_mRNA	JunB mRNA	0
JunB	JunB	0
JunB_cJun	JunB bound to c-Jun	0
Dummy	A dummy species (see chapter 5)	0
Dummy_mRNA	Dummy species mRNA	0
A	Protein needed to drive dummy production	100
A_P	Protein needed to drive dummy production phosphorylated	0
Anti-TGF	A antibody representative of 1D11 (see chapter 7)	0

Table 2.4 **Model species.** The names and initial amounts (particle numbers) of all species in my complete model, as well as description of what the species represents.

Reactions	Parameter values
IL1 → sink	0.0134 s ⁻¹
Jnk + IL1RR.int → Jnk_P + IL1RR.int	0.0000707 mol ⁻¹ s ⁻¹
Jnk_P → jnk	0.00117 s ⁻¹
IL1 + IL1R → IL1RR	0.0000156 mol ⁻¹ s ⁻¹
IL1RR → IL1 + IL1R	0.000456 mol ⁻¹ s ⁻¹
IL1RR → IL1RR.int	0.000526 s ⁻¹
IL1RR.int → IL1RR	0.000109 s ⁻¹
cJun + JNK_P → cJun_P + JNK_P	0.000518 mol ⁻¹ s ⁻¹
cJun_P → cJun	0.0101 s ⁻¹
2 * cJun_P → cJun_dimer	0.0000346 mol ⁻¹ s ⁻¹
cJun_dimer → 2 * cJun_P	0.00598 s ⁻¹
OSM + OSMR → OSMRR	0.00000565 mol ⁻¹ s ⁻¹
OSMRR → OSM + OSMR	0.000146 s ⁻¹
OSM → Sink	0.0049 s ⁻¹
Jak1 + OSMRR → Jak1_P + OSMRR	0.0000115 mol ⁻¹ s ⁻¹
Stat3_cyt + Jak1_P → Stat3_nuc + Jak1_P	0.000255 mol ⁻¹ s ⁻¹
Jak1_P → Jak1	0.000113 s ⁻¹
Stat3_nuc → Stat3_cyt	0.00517 s ⁻¹
cFos_mRNA → sink	0.00193 s ⁻¹
Stat3_nuc → Stat3_nuc + cFos_mrna	0.0373 mol ⁻¹ s ⁻¹
Stat3_nuc + Jak1_P → Jak1 + Stat3_nuc	0.00000252 mol ⁻¹ s ⁻¹
cFos_mRNA → cFos_mRNA + cFos	0.000638 s ⁻¹
cFos → sink	0.0000893 s ⁻¹
p38 + IL1RR.int → p38_p + IL1RR.int	0.000103 mol ⁻¹ s ⁻¹
p38_p → p38	0.000375 s ⁻¹
p38_p + cFos → p38_p + cFos_P	0.0000123 mol ⁻¹ s ⁻¹
cFos_P → cFos	0.0249
cFos_P + cJun_P → cFos_cJun	0.0000517 mol ⁻¹ s ⁻¹
cFos_cJun → cFos_P + cJun_P	0.0000381 s ⁻¹
cJun_dimer → cJun_dimer + Block	0.000209 s ⁻¹
cFos_cJun → cFos_cJun + Block	0.00418 s ⁻¹
Block → sink	0.0000182 s ⁻¹

Block + IL1RR.int \rightarrow Block + IL1R	0.000181 mol ⁻¹ s ⁻¹
Jnk_P + Block \rightarrow Jnk + Block	0.000351332 mol ⁻¹ s ⁻¹
Stat3_nuc + Block \rightarrow Stat3_cyt + Block	0.00291 mol ⁻¹ s ⁻¹
cFos_P + Block \rightarrow cFos + Block	0.0000658 mol ⁻¹ s ⁻¹
cJun_dimer \rightarrow MMP13_mRNA + cJun_dimer	0.00154 s ⁻¹
cFos_cJun \rightarrow MMP13_mRNA + cFos_cJun	0.000475 s ⁻¹
MMP13_mRNA \rightarrow Sink	0.00000348 s ⁻¹
Source \rightarrow Integrin	0.000000226 mol s ⁻¹
Integrin \rightarrow Sink	0.000509 s ⁻¹
Source \rightarrow Alk5	0.00000259 mol s ⁻¹
Tgfb_I + Integrin \rightarrow Tgfb_A + Integrin	0.000832 mol ⁻¹ s ⁻¹
Tgfb_A \rightarrow Tgfb_I	0.0309 s ⁻¹
2 * Alk5 \rightarrow Alk5_dimer	0.000119 mol ⁻¹ s ⁻¹
Alk5_dimer \rightarrow 2 * Alk5	0.000743 s ⁻¹
Alk1 + Alk5 \rightarrow Alk1_Alk5	0.0000765 mol ⁻¹ s ⁻¹
Alk1_Alk5 \rightarrow Alk1 + Alk5	0.0105 s ⁻¹
Tgfb_A + Alk5_dimer \rightarrow Tgfb_Alk5_dimer	0.0000354 s ⁻¹
Tgfb_Alk5_dimer \rightarrow Tgfb_A + Alk5_dimer	0.00000111 s ⁻¹
Tgfb_Alk5_dimer + Smad7 \rightarrow Tgfb_Alk5_dimer_Smad7	0.0000165 mol ⁻¹ s ⁻¹
Tgfb_Alk5_dimer_Smad7 \rightarrow Tgfb_Alk5_dimer + Smad7	0.00000164 s ⁻¹
Tgfb_Alk5_dimer_Smad7 \rightarrow Tgfb_I	0.0000206 s ⁻¹
Tgfb_A + Alk1_Alk5 \rightarrow Tgfb_Alk1_Alk5	0.00000477 mol ⁻¹ s ⁻¹
Tgfb_Alk1_Alk5 \rightarrow Tgfb_A + Alk1_Alk5	0.00000156 s ⁻¹
Tgfb_Alk5_dimer + Smad2 \rightarrow Tgfb_Alk5_dimer + Smad2_P	0.0000312 mol ⁻¹ s ⁻¹
Smad2_P + Smad4 \rightarrow Smad2_P_Smad4	0.000053 mol ⁻¹ s ⁻¹
Smad2_P_Smad4 \rightarrow Smad2_P + Smad4	0.0109 s ⁻¹

Smad2_P → Smad2	0.0088 s ⁻¹
Smad2_P_Smad4 → Smad2_P_Smad4 + Smad7	0.00000894 s ⁻¹
Runx2_A + Smad2_P_Smad4 → Runx2_I + Smad2_P_Smad4	0.000717 mol ⁻¹ s ⁻¹
Alk5 → Sink	0.000000345 s ⁻¹
Tgfb_Alk1_Alk5 + Smad1 → Tgfb_Alk1_Alk5 + Smad1_P	0.0000169 mol ⁻¹ s ⁻¹
Smad1_P → Smad1	0.000217
Smad1_P + Smad7 → Smad1 + Smad7	0.000377 mol ⁻¹ s ⁻¹
Smad1_P + Smad4 → Smad1_P_Smad4	0.000047 mol ⁻¹ s ⁻¹
Smad1_P_Smad4 → Smad1_P + Smad4	0.0177 s ⁻¹
Runx2_I + Smad1_P_Smad4 → Runx2_A + Smad1_P_Smad4	0.00166 mol ⁻¹ s ⁻¹
Runx2_A → mmp13_mrna + Runx2_A	0.00000159 s ⁻¹
Source → Alk1	0.00000488 mol s ⁻¹
Alk1 → Sink	0.000000017 s ⁻¹
Tgfb_Alk1_Alk5 + Smad7 → Tgfb_Alk1_Alk5_Smad7	0.265 mol ⁻¹ s ⁻¹
Tgfb_Alk1_Alk5_Smad7 → Tgfb_Alk1_Alk5 + Smad7	0.00076 s ⁻¹
Tgfb_Alk1_Alk5_Smad7 → Tgfb_I	0.00000977 s ⁻¹
Smad7 → Sink	0.00797 s ⁻¹
Smad2_P_Smad4 → Smad2_P_Smad4 + JunB_mRNA	0.0000171 s ⁻¹
JunB_mRNA → JunB_mRNA + JunB	0.000852 s ⁻¹
JunB_mRNA → Sink	0.0000148 s ⁻¹
JunB → Sink	0.00924 s ⁻¹
p38 + Smad1_P_Smad4 → p38_P + Smad1_P_Smad4	0.000019 mol ⁻¹ s ⁻¹
JunB + cJun_dimer → cJun_P + JunB_cJun	0.00000138 mol ⁻¹ s ⁻¹
JunB + cJun_P → JunB_cJun	0.000697 mol ⁻¹ s ⁻¹
JunB_cJun → JunB + cJun_P	0.0000337 s ⁻¹
cFos_cJun + JunB → JunB_cJun +	0.00000675 mol ⁻¹ s ⁻¹

cFos_P	
Smad2_P_Smad4 → Smad2_P_Smad4 + A_P	0.0000142 s ⁻¹
A_P → Dummy_mRNA + A_P	0.0000146 s ⁻¹
Dummy_mRNA → Dummy	0.0000154 s ⁻¹
Dummy + mmp13_mrna → Dummy	0.00000107 mol ⁻¹ s ⁻¹
Dummy_mRNA → sink	0.0000386 s ⁻¹
Dummy → sink	0.0000322 s ⁻¹
A_P → A	0.000379 s ⁻¹
Runx2_A → Runx2_I	0.001 s ⁻¹
Alk1 + Anti-TGF → Anti-TGF	0.000000549 mol ⁻¹ s ⁻¹
Anti-TGF → Sink	0.000035 s ⁻¹
Tgfb_A + Anti-TGF → Anti-TGF	0.000000549 mol ⁻¹ s ⁻¹

Table 2.5 **Reactions and their rates in my complete model.** The reactions and parameter values in my complete model.

2.3.4 CellDesigner

CellDesigner is a structured diagram editor for drawing gene-regulatory and biochemical networks (Funahashi et al. 2003). The programme has built in tools that allow you to display biological pathways with the systems biology graphical notation (SBGN) (Le Novere et al. 2009). SBGN is a visual language for systems biology and was designed to create a consistent and unambiguous standard notation for biological networks. The diagrams are then stored in SBML, which means that the structure can be moved to other programmes. Also models designed in another programme can be moved to CellDesigner, though this normally results in a cluttered diagram that is difficult to rearrange. Throughout this thesis I have used CellDesigner for any model schematic.

2.3.5 Matlab

MATLAB is a proprietary programming language developed by MathWorks, primarily for numerical computing, but also has a wide range of additional tools (MathWorks Inc., Natick, MA, 2016). I used it for analysing and plotting the model output. The programme allows the import of large data files and the

construction of high quality figures. I wrote scripts to generate the plots, as this enabled me to re-use and adapt the scripts for different figures. So creating figure in Matlab is much more efficient than other tools such as Excel.

Chapter 3. Pathway selection in the context of inflammation/OA

3.1 Introduction

Although it is becoming more established, there is still some debate about the importance of inflammation in OA (Berenbaum 2013). Future research into inflammatory pathways in the context of OA will hopefully enable us to fully understand its role in development of disease. I chose five pathways; TGF β , Wnt/ β -catenin, IHH, PKC and Notch, all of which, as described in chapter 1, have established roles in inflammation-driven joint damage. Activating compounds were used to examine the affect these pathways had on the expression of MMP-13. The aim was to create computational models for all of the pathways. I could then examine how these pathways interact with each other as well as how they contribute to the inflammatory response in OA development. Building a model requires an area of focus to act as an anchor to base the model design around. MMP-13 was used as it is vital for cartilage degradation and all of the pathways have a reported effect on its expression.

3.1.1 Chapter aims

- Use bioinformatic tools to justify the selection of inflammatory pathways.
- Look at the affect of activating the five pathways: TGF β , Wnt/ β -catenin, IHH, PKC and Notch, on both cell viability and the expression of MMP-13, after 24 hours. Then explore in more detail any interesting observations made.

3.2 Results

3.2.1 Bioinformatic analysis highlights Inflammations impotence in OA

The development of OA is typically a result of many changes within the tissue. This makes it difficult to identify the major factor driving the progression of this disease. To address this I took microarray data from 50 OA samples (chapter 2.2.6) and using a series of bioinformatic tools created a clustered Cytoscape network representative of OA in humans (Fig 3.1). DAVID analysis of the clusters allowed me to better understand the function of each cluster, of which 2 of the top 6 clusters represented inflammation. Tight clustering means each node has multiple connections to other nodes, suggesting that there is a lot of crosstalk between the genes in that cluster. In the case of both inflammatory clusters there was an area of tightly clustered genes, suggesting many of these genes interact with each other. This highlighted the importance of inflammation in OA development, as well as the level of crosstalk between inflammatory genes (Fig 3.1).

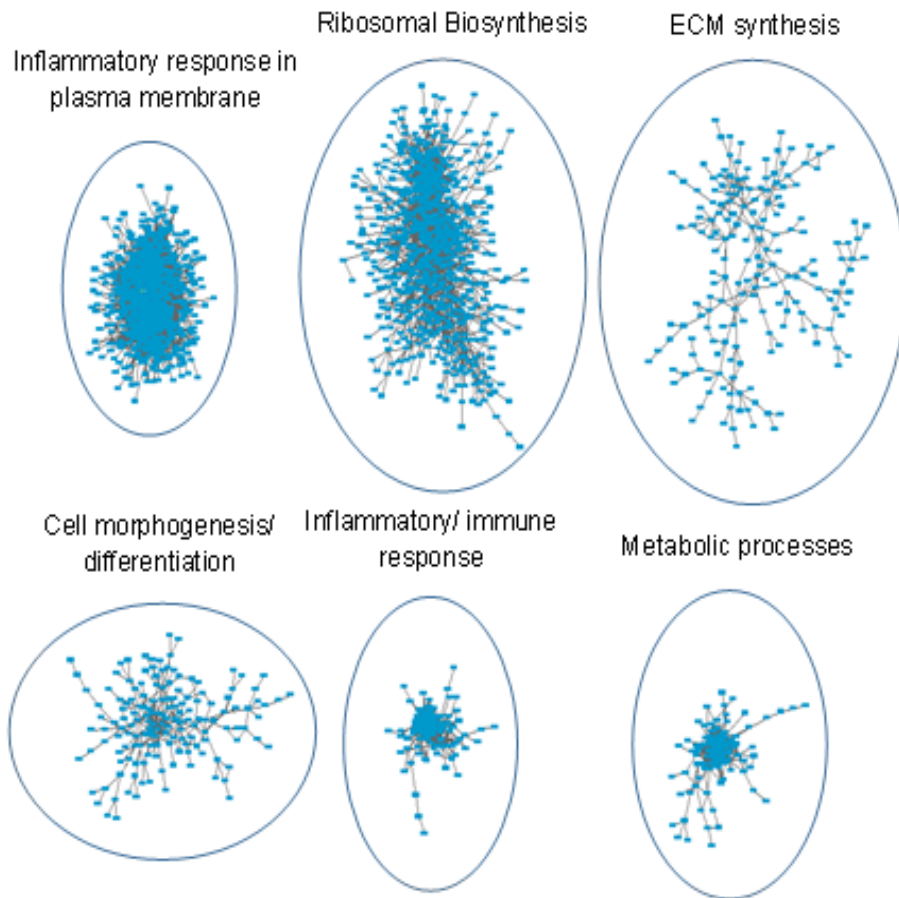


Figure 3.1 **Top Cytoscape clusters in human OA.** Affymetrix microarray data from 50 knee OA patients were collected from the GEO database, normalised, and the differentially expressed genes combined. ARACNE then inferred the interactions between these genes providing mutual information (MI) values that could be visualised using Cytoscape. The nodes (blue dots) represent differentially expressed genes and the edges are the MI values. Using clusterMaker these genes were then clustered based on MI values. DAVID analysis was then used to determine what each of the clusters represent. The six largest clusters are presented along with what they represent.

3.2.2 Assessing the toxicity of activator compounds

In order to examine some of the pathways that appear important in OA development I obtained five activating compounds: sodium butyrate (SB), a Notch activator; Purmorphamine (Pur), a IHH activator; Bryostatin-1 (Bro-1), a protein kinase C (PKC) activator; QS11, a Wnt/ β -catenin activator; and an active form of TGF β (Table 3.1). Figure 3.2 shows the effect all the compounds had on SW1353 cells at 24 hours. Only QS11 and SB have a significant effect on MMP13 expression at this time point (Fig 3.2). The variability of the response as shown by the standard deviations was high for both of these compounds (Fig 3.2). This could be traced to the raw data where the average CT value for the loading control gene (18S rRNA) was higher with irregular variation in cells treated with some of the compounds, compared to control cells. For example the average CT for 18S in QS11-treated samples was 20.1 ± 1.28 compared to 18.1 ± 0.47 in control. This showed there was less total mRNA and that the amount was highly variable, both of which was most likely a result of cell death.

Concentrations at which to use these compounds were taken from published literature (Table.3.1). I used a live/dead assay to assess the toxicity. This assay allowed me to visualise the number of live cells against the level of dead cells. Taking a representative sample I then counted the cells and worked out the percentage of cell death. Figure 3.3 shows an example of the live/dead assay for four concentrations of SB. It was clear that there were substantially more live cells at 1mM than the original 20mM concentration.

Quantifying this cell death allowed me to alter the original concentrations of all the compounds so that there was a similar level of cell death to the control cells. Figure 3.4A shows this specifically for the quantifications of SB and this same process was applied to all compounds (data not shown). Figure 3.4B shows the cell death of the compounds at the corrected concentrations (Table.3.1). I found that Pur and Bro-1 were non-toxic at $0.5\mu\text{M}$ and 20nM respectively, whilst SB had to be 1nM (Table.3.1). All other compounds remained at their original concentrations. It is also worth noting that DMSO alone did not seem to induce additional cell death, so it is the compounds themselves that were mediating the

observed effects (Fig 3.4B). TGF β was the only compound that increased cell viability, reducing the 14.9% cell death seen in control cells to 6.7% (Fig 3.4B).

Pathway Activators	Activated Pathway	Original Concentration	Corrected Concentrations
Sodium butyrate (SB)	Notch	20mM	1mM
QS11	Wnt/ β -catenin	2.5 μ M	2.5 μ M
Purmorphamine (Pur)	Indian hedgehog	4 μ M	0.5 μ M
TGF β	TGF β	0.15 μ M	0.15 μ M
Bryostatin-1 (Bro-1)	Protein kinase C	100nM	20nM

Table 3.1 The concentration used for activator compounds before and after cell viability adjustments.

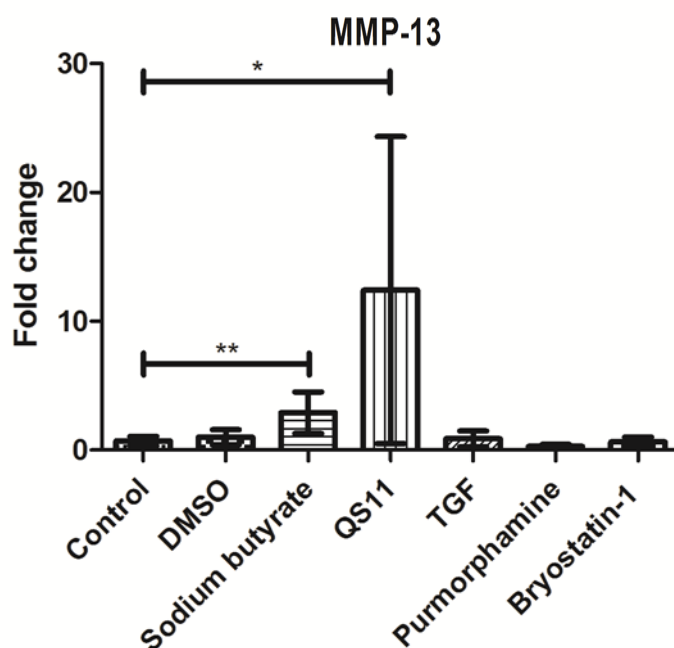


Figure 3.2 **Effect of activating compounds on MMP-13 expression after 24 hours treatment.** SW1353 cells were stimulated for 24 hours with SB (20mM), QS11 (2.5 μ M), Pur (4 μ M), TGF β (0.15 μ M), Bro-1 (100nM), or DMSO as a vehicle control. qPCR was then performed on the isolated mRNA to measure MMP-13 expression. Data are presented as fold change relative to control (mean \pm SD, n=6). Statistics calculated using unpaired Student's t-test, where * $p < 0.05$; ** $p < 0.01$.

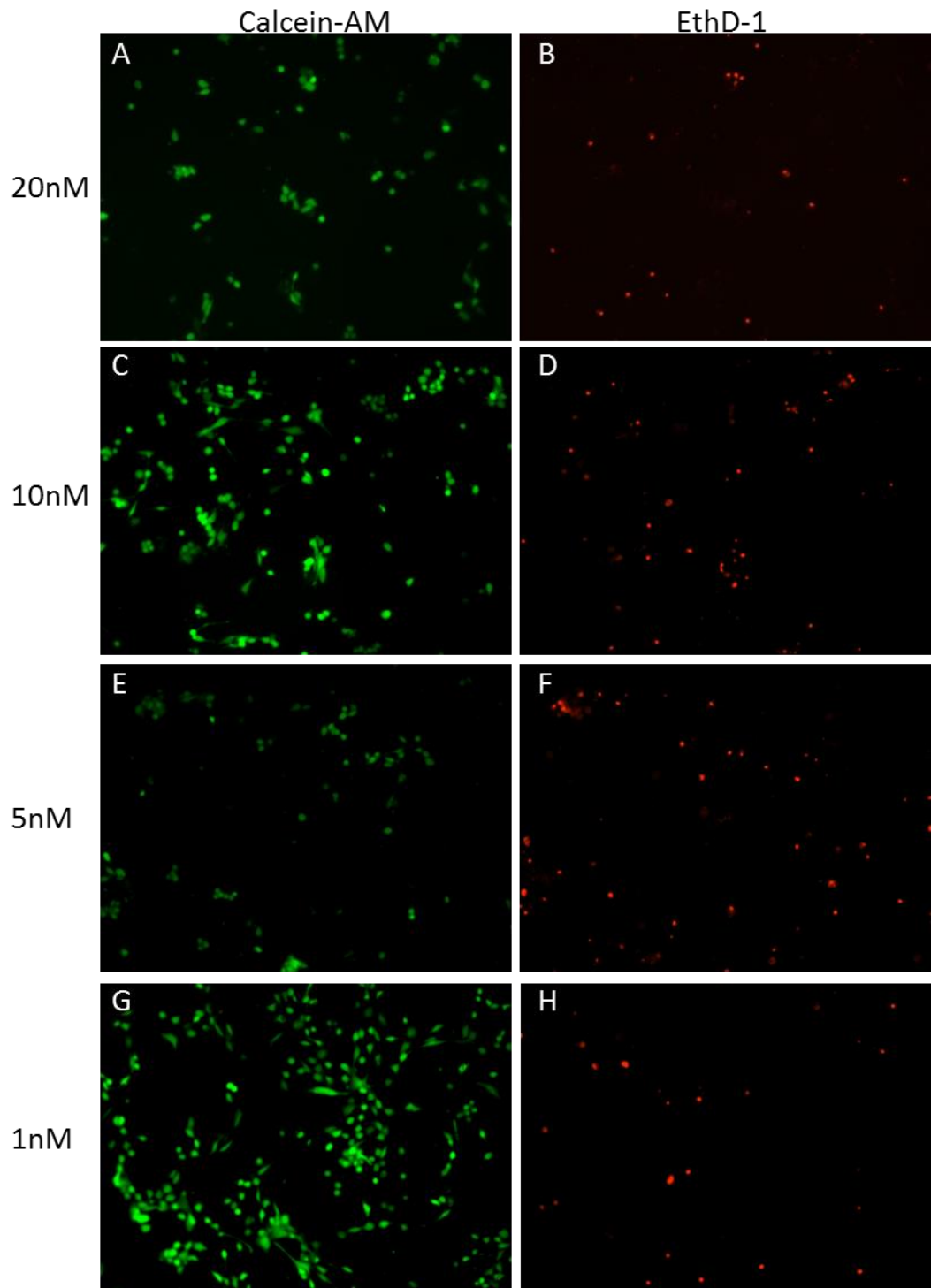


Figure 3.3 Exploration of cell death after 24 hour Sodium butyrate treatment. SW1353 cells were serum starved overnight and then treated with SB for 24 hours at 20mM, 10nM, 5nM, 1nM. Calcein-AM stains only live cells, whereas EthD-1 stains only dead cells. The Calcein-AM and EthD-1 images are both taken from the same sample on the same field of view but under different fluorescent filters. Data are representative of two experiments using separate SW1353 cell populations.

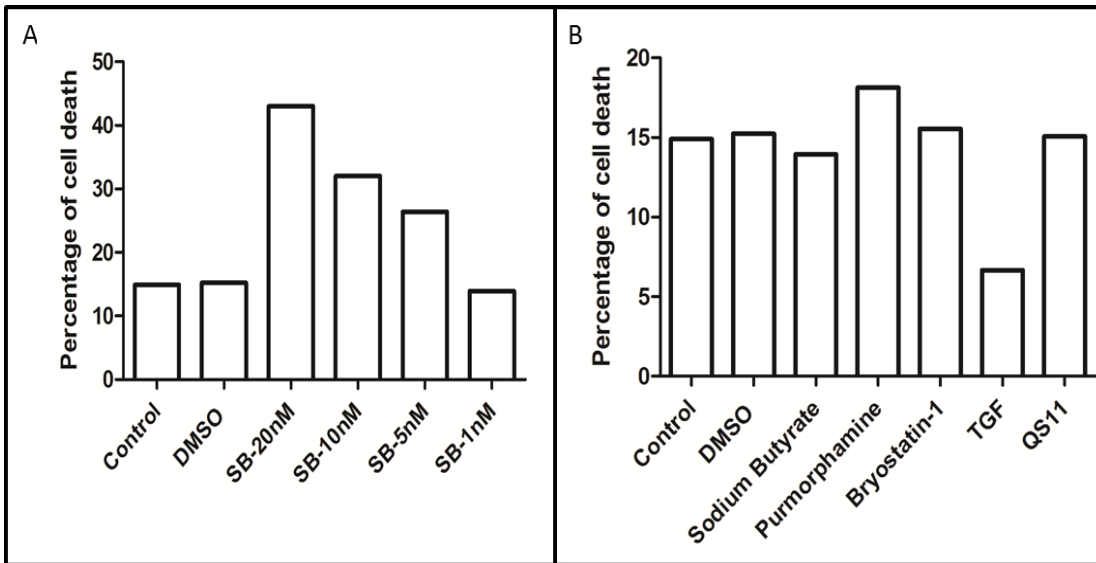


Figure 3.4 Percentage of cell death in SW1353 cells after 24h stimulation. SW1353 cells were stimulated for 24 hours with A) SB at 20mM, 10nM, 5nM, 1nM or DMSO as a vehicle control. B) SB (1mM), QS11 (2.5µM), Pur (0.5µM), TGFβ (0.15 µM), Bro-1 (20nM) or DMSO. Live/dead assays were performed to quantify the number of alive and dead cells in a population after treatment. Data are presented as number of dead cells divided by total cell count x 100, defined as percentage cell death. Data are representative of two experiments using separate SW1353 cell populations.

3.2.3 Exploring the effect of activating specific pathways

Once a non-toxic concentration had been established, I re-tested the effects of the compounds at 24 hours. IL-1 and OSM were also included in these experiments, as our group has previously explored their potent upregulation of MMP-13 in detail and so would provide a reference point for the potency of the various stimuli. The ability of TGF β to protect against cell death (Fig 3.4B) highlighted some work done previously by our group, which showed TGF β could protect against inflammatory stimuli (Hui et al. 2003; Hui et al. 2000). This work had not yet been followed up by our group and repression had only been previously shown in Northern blots. Therefore I also included IL-1+OSM+TGF β to better quantify the levels of repression of MMP-13 mRNA.

In this second experiment QS11 lost the upregulation of MMP-13 (Fig 3.5) that was previously seen (Fig 3.2). A potent effect was seen by IL-1+OSM and this was significantly repressed by TGF β addition (Fig 3.5A). Pur appeared to upregulate MMP-13 but this effect was not significant. Only SB and Bro-1 compounds had a significant effect on MMP-13 expression (Fig 3.5B). This effect was similar to that of IL-1 alone (Fig 3.5B).

If Bro-1 was activating PKC I would have expected a more significant increase in MMP-13 than was seen (Fig 3.5B). The small increase contradicted work performed earlier by our lab and others on PKC (Litherland et al. 2010). Re-evaluating when to look at PKC activation suggested it may have a stronger effect over a shorter time scale (6 hours) and at different concentrations. When run for 6 hours at various concentrations Bro-1 caused a much more potent increase in MMP-13 expression (Fig 3.6A). The expression of MMP-13 varied considerably across the concentrations, with a large standard deviation on many of the samples (Fig 3.6A). There was a prodigious increase in MMP-1 expression which was also considerably less variable, although it did appear to peak at 10 and 30nM above all other concentrations (Fig 3.6B).

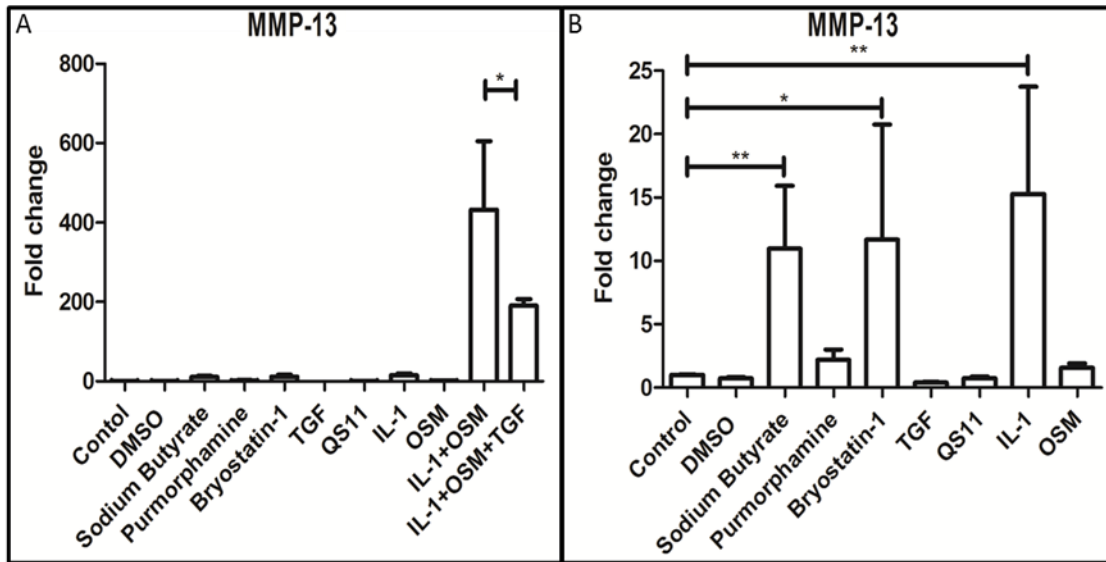


Figure 3.5 **MMP-13 expression at 24 hours after treatment with various activating compounds.** SW1353 cells were stimulated for 24 hours with SB (1mM), QS11 (2.5 μ M), Pur (0.5 μ M), TGF β (0.15 μ M), Bro-1 (20nM), IL-1 (0.5ng/ml), OSM (10ng/ml) or DMSO as a vehicle control. qPCR was then performed on the isolated mRNA to measure MMP-13 expression. A) Data shown for all conditions B) Data from the same experiment with IL-1+OSM and IL-1+OSM+TGF β excluded to aid the visualisation of smaller fold changes. Data are presented as fold change relative to control (mean \pm SD, n=5-6). Statistics calculated using unpaired Student's t-test, where * p < 0.05; ** p < 0.01.

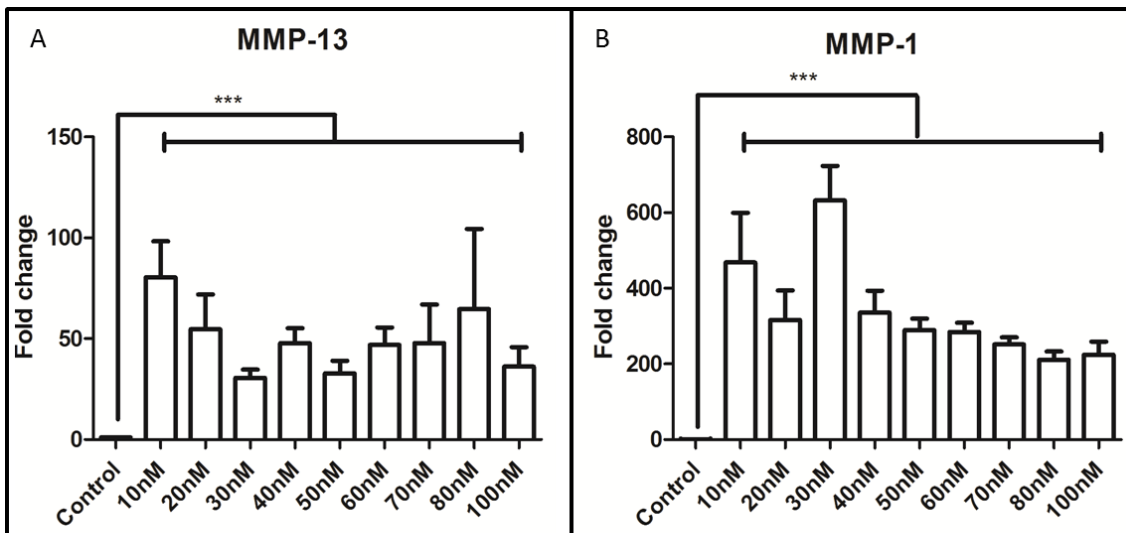


Figure 3.6 **MMP-1/13 expression after 6 hours of Bryostatatin-1 treatment.** SW1353 cells were stimulated with Bro-1 for 6 hours at concentrations ranging from 10-100nM. qPCR was then performed on the isolated mRNA to measure A) MMP-13 expression B) MMP-1 expression. Data are presented as fold change relative to control (mean \pm SD, n=4-6) except 80nM where N=2. Statistics calculated using unpaired Student's t-test, where *** p < 0.001.

3.2.4 Protective effect of TGF β

I initially wanted to confirm that TGF β -mediated repression of MMP-1/-13 in SW1353 cells treated with IL-1+OSM. Preliminary experiments looked at the effects of OSM, IL-1 and TGF β on MMP-1/-13 over a range of time scales (Fig 3.7 and 3.8). These determined that it took IL-1+OSM at least 3 hours to have a significant effect on MMP-1/-13 expression (Fig 3.7 and 3.8). TGF β appeared to have little or no effect on MMP-1/-13 expression prior to 24 hours. However, at 24 hours it appeared to repress the effect of IL-1+OSM (Fig 3.7 and 3.8). Initial studies also showed that the fold change expression of MMP-13 could vary markedly between experiments with fold changes around 150 (Fig 3.7A) being closer to 3000 in the repeat experiment (Fig 3.7B). The fold change variability was reduced for MMP-1, despite being between 80 (Fig 3.8A) and 300 fold (Fig 3.8B). This was a result of low basal levels of MMP-13, meaning that control samples had a high CT value. This means even marginal differences in either control or treated samples could equate to large variations in fold change. This was less of an issue for MMP-1 as its basal expression was higher. I also confirmed that OSM and TGF β alone had no noticeable effect on MMP-1/-13 expression and that the effect of IL-1 alone was also reduced, when compared to IL-1+OSM. Therefore I could exclude TGF β and OSM alone from future experiments. In order to generate significant robust data I looked at the time when repression seemed the most potent and matched previous experimental data, 24 hours (Hui et al. 2000).

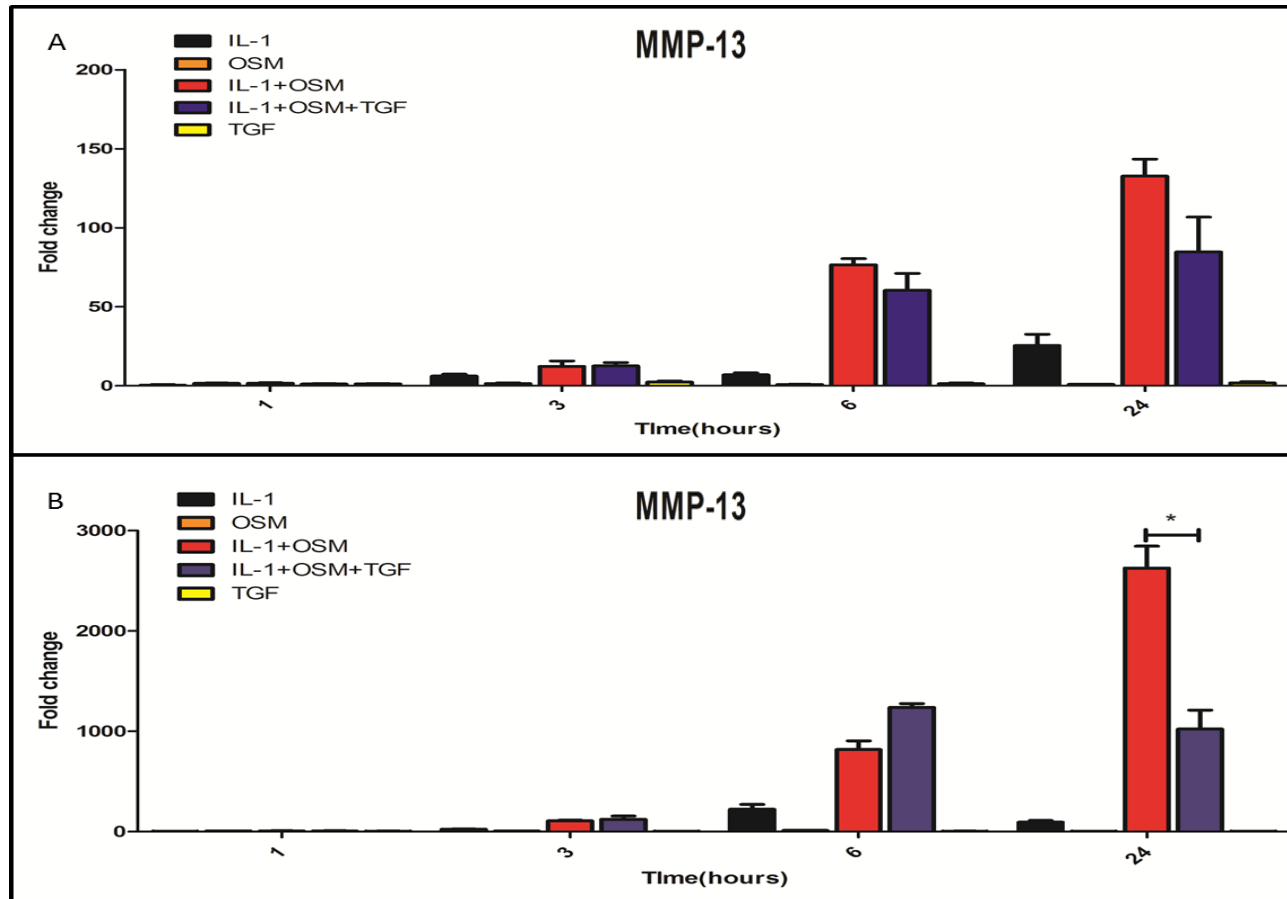


Figure 3.7 **Time course of MMP-13 expression across a range of stimulations.** SW1353 cells stimulated with varying combinations of IL-1 (0.5ng/ml), OSM (10ng/ml) and TGF β (0.15ng/ml) for 1, 3, 6 and 24 hours. qPCR was then performed on the isolated mRNA to measure MMP-13 expression. A) and B) Show the expression across two independent experiments. Data are presented as fold change relative to control (mean \pm SD, n=3-4). Statistics calculated using unpaired Student's t-test, where* p < 0.05.

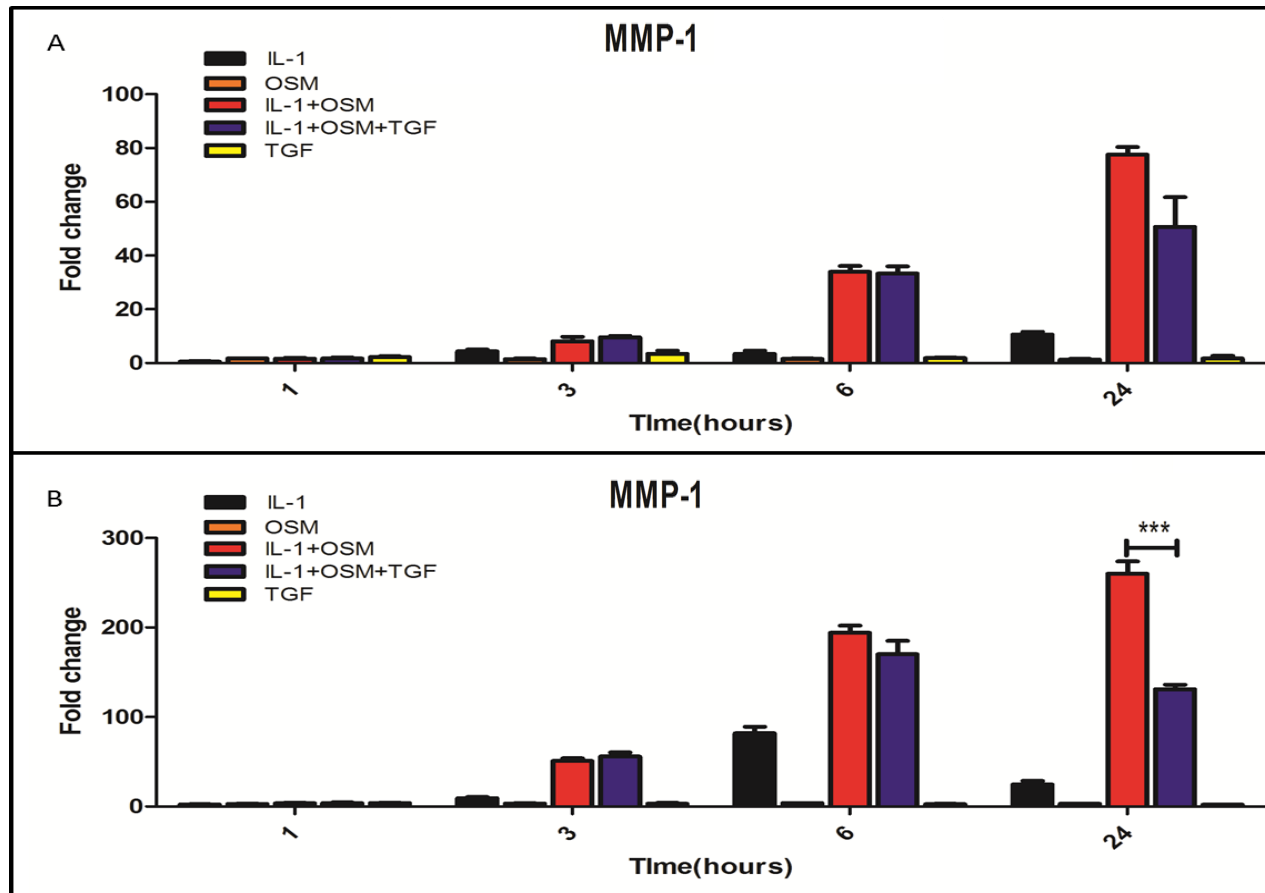


Figure 3.8 **Time course of MMP-1 expression across a range of stimulations.** SW1353 cells were stimulated with varying combinations of IL-1 (0.5ng/ml), OSM (10ng/ml) and TGF β (0.15ng/ml) for 1, 3, 6 and 24 hours. qPCR was then performed on the isolated mRNA to measure MMP-1 expression. A) and B) Show the expression across two independent experiments. Data are presented as fold change relative to control (mean \pm SD, n=3-4). Statistics calculated using unpaired Student's t-test, where*** p < 0.001

Increasing the n number allowed me to confirm that there was a significant down regulation of MMP-1/-13 in IL-1+OSM+TGF β treated cells, when compared to IL-1+OSM alone (Fig 3.9A and 3.10A). As in the first two experiments (Fig 3.7 and 3.8) fold changes varied considerably. To address this I used percentage of repression to provide a robust way of examining the effect of TGF β , by calculating the $\Delta\Delta$ CT values relative to the IL-1+OSM samples, rather than the control. This allowed pooling of samples from multiple experiments to calculate the average amount of repression mediated by TGF β . Pooling data this way showed highly significant repression for both MMP-1/-13 (Fig 3.9B and 3.10B).

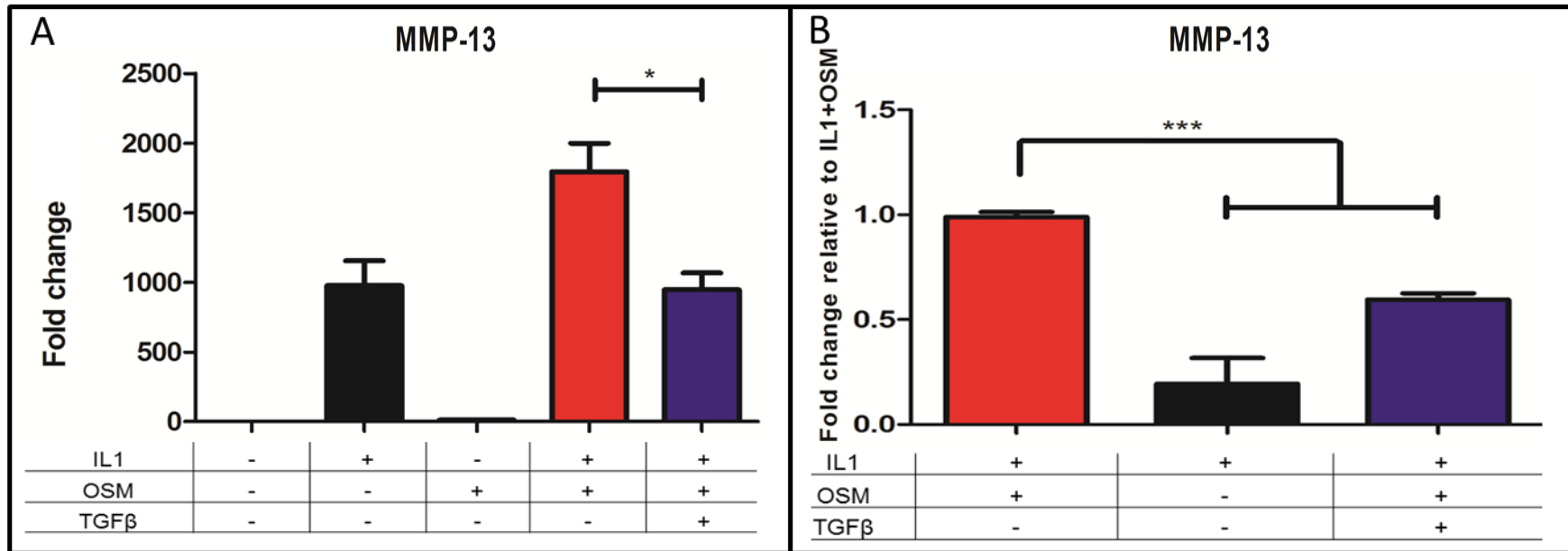


Figure 3.9 **Effect of TGFβ on IL-1+OSM induced MMP-13 expression.** SW1353 cells were stimulated with IL-1 (0.5ng/ml), OSM (10ng/ml) and IL-1+OSM±TGFβ (0.15ng/ml) for 24 hours. qPCR was then performed on the isolated mRNA to measure MMP-13 expression. Data are presented as fold change relative to control (A) or IL-1+OSM (B) (mean ± SEM). A) A lone experiment, n=5-6. Representative of 4 independent experiments on separate SW1353 cell populations. B) Data pooled from 4 independent experiments at 24 hours, n=14. Statistics calculated using unpaired Student's t-test, where * p < 0.05; *** p < 0.001

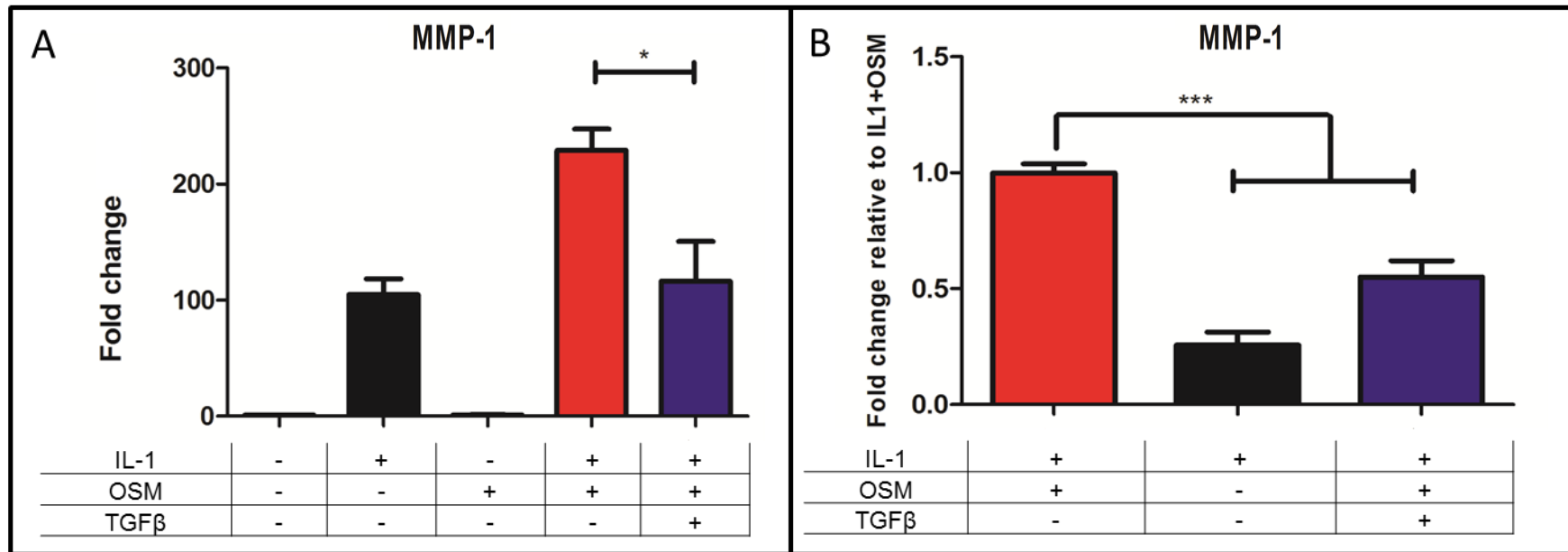


Figure 3.10 **Effect of TGFβ on IL-1+OSM induced MMP-1 expression.** SW1353 cells were stimulated with IL-1 (0.5ng/ml), OSM (10ng/ml) and IL-1+OSM±TGFβ (0.15ng/ml) for 24 hours. qPCR was then performed on the isolated mRNA to measure MMP-1 expression. Data are presented as fold change relative to control (A) or IL-1+OSM (B) (mean ± SEM). A) A single experiment, n=4-6. Representative of 3 independent experiments on separate SW1353 cell populations. B) Data pooled from 3 independent experiments at 24 hours, n=10-13. Statistics calculated using unpaired Student's t-test, where * p < 0.05; *** p < 0.001

3.2.5 Bioinformatic validation of TGF β selection

Publically available microarray data provided an opportunity to look at mRNA expression data from SRT/ort mice, a model of spontaneous OA development (Poulet et al. 2012). Cartilage was taken from the mice at 8, 16 and 40 weeks (Poulet et al. 2012). I took the genes with significant enrichment and using gene set enrichment analysis (GSEA) identified the most significantly enriched KEGG pathways. At 8 and 16 weeks there were no significantly upregulated KEGG pathways, whilst at 40 weeks there were 7 positively regulated and 22 negatively regulated. Exploring these pathways identified a potential role for IL-1, OSM and TGF β in OA development. Looking in more depth at the specific pathway “KEGG_CYTOKINE_CYTOKINE_RECEPTOR_INTERACTION” (Fig 3.11), it contained 17 core enriched receptors some of which have a role in inflammatory signalling. IL-1 (IL1A and IL1B), OSM (OSMR) and TGF β (ACVRL1) receptors were all shown to have increased expression in these older mice (Fig 3.11).

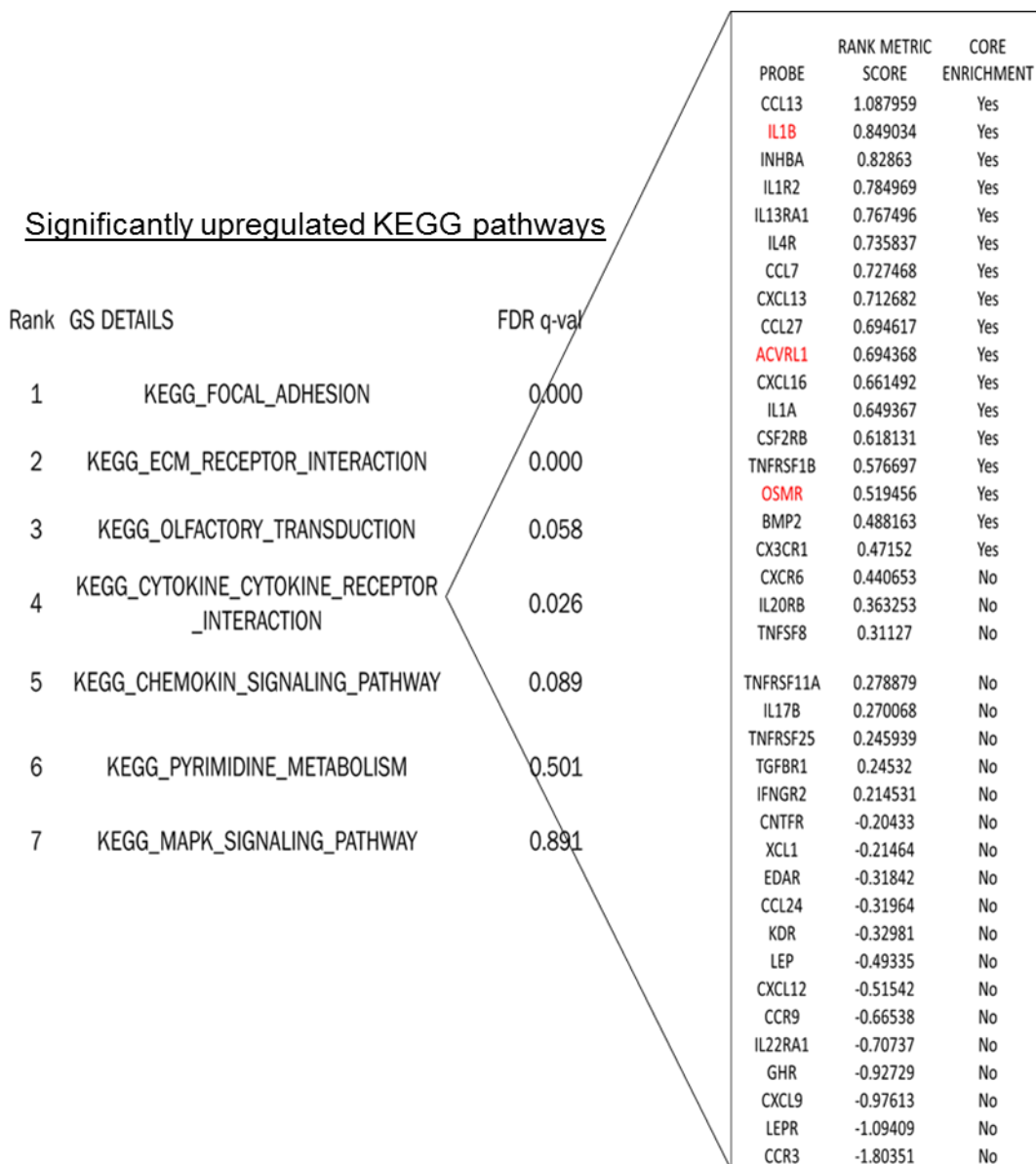


Figure 3.11 **Key KEGG processes in Srt/ort mice.** Data presented are publically available Affymetrix microarray data. Articular cartilage was extracted from STR/ort and CBA mice at 8, 18 and 40 weeks. The differentially expressed genes, from the STR/ort mice, were run using GSEA to determine their importance in KEGG process. Based on significant enrichment scores only 40 weeks had any enriched KEGG pathways. The 7 positively regulated pathways are shown here, the specific pathway “KEGG_CYTOKINE_CYTOKINE_RECEPTOR_INERACTION” has been expanded to visualise the genes that have led to its enrichment. Core enriched genes are a subset of genes that contributes most to the enrichment result, of these the IL-1, OSM and TGFβ (ACVRL1) receptors are highlighted in red. FDR is the false discovery rate and is the estimated probability that a gene set represents a false positive finding. An FDR of 0.1 represents a 1% chance the result is a false positive.

3.3 Discussion

Bioinformatic analysis confirmed the importance of inflammation in OA development and also highlighted how important the interactions between inflammatory genes are. As a result I looked at the effect all five pathways had on MMP-13 expression. My initial aim was to build a computational model for all five pathways and then assess how they interacted with each other to modulate MMP-13, or more widely inflammation-driven OA development. However, it became clear that this was overly ambitious and instead I used the data I to choose one pathway to progress with further.

3.3.1 Activating compounds

The limitation of the live/dead assay is that it requires manual selection of the image and cell counting, leaving both open to human error. However, this approach also allowed close examination of the changes between concentrations. The only viable alternative was a Toxilight assay which I found to be variable with decreased sensitivity to the live/dead assay.

One concern of altering the concentration was that activation of the pathways themselves may have led to cell death, so altering the concentration would only serve to prevent their activation. It is also possible that the activating compounds must be at a toxic concentration in order to activate their respective pathways. However, if either of these situations were correct they would not be an ideal pathway for further study.

QS11, despite not being toxic, had a variable effect on MMP-13, possibly because the concentration was sufficient to initiate signalling in some cells but not all. Bro-1 led to a significant increase in MMP-1/-13 expression at 6 hours despite having little effect at 24 hours. This finding was intriguing as PKC signalling effects MMP-1 in a more robust manner than MMP-13. This was difficult to explain as no work performed by our group or others has shown this phenomenon. It also highlighted that 24 hours may not be the optimal time point for all the compounds. However, 24 hours was chosen because it was a significant period of time for slow acting pathways to have an effect but not so long that you would lose an early effect.

Neither SB nor Pur had a prominent effect on MMP-13 expression. Whether this is due to the activating compounds used, the time point, or that Notch/IHH signalling does not have a strong effect in SW1353 cells, is unclear. The subsequent work into Bro-1 demonstrated that in order to fully comprehend the action of all the different activators I would need to examine more conditions. Further studies into all of these pathways would undoubtedly have its uses but time was a limiting factor and exploring all of them would have been impossible.

3.3.2 TGF β selection

The TGF β -mediated increase in cell viability was unsurprising given the role of TGF β in maintaining chondrocyte homeostasis and preventing hypertrophy (Blom et al. 2004; Blaney Davidson et al. 2007). Regardless, to see such a pronounced effect in cell culture at only 24 hours was interesting. It also led me back to work done previously by our group that showed TGF β can inhibit pro-inflammatory responses, whether this be IL-1+OSM or OSM+TNF α (Hui et al. 2003; Hui et al. 2000). This work showed that TGF β could block collagen release, and that this effect was most likely mediated by reducing the effect pro-inflammatory stimuli had on MMP-1/-13 expression (Hui et al. 2000). This reduction in MMP-1/-13 expression was shown in bovine cartilage by Northern blot (a semi quantitative technique) (Hui et al. 2000). qPCR as a quantitative technique allowed me to more accurately show the levels of repression mediated by TGF β . This improved level of quantification was useful for model construction.

At this point TGF β or PKC signalling seemed the most reasonable pathways to progress with, both showing interesting effects on MMP-13 expression that could be built upon. TGF β was chosen because exploring the microarray data from STR/ort mice identified it had a role in the development of spontaneous OA. This led to research also carried out on the STR/ort mice by Blaney Davidson et al. (2009). They showed that, with age, TGF β signalling moved from its previously protective effects towards damaging effects in cartilage. This is mediated through a move from ALK5 receptor signalling towards ALK1 signalling. How the protective effect of TGF β against pro-inflammatory stimuli changed with age has not previously been explored. Losing the potent

protective effect against cell death I have seen, as well as potentially altering the protective effect of TGF β against inflammation with age, could conceivably be key in OA development. Looking at mRNA expression in these mice allowed me to validate the role of ALK1. I found that not only ALK1 but also IL-1 and OSM receptors have core enrichment at 40 weeks in these mice. The KEGG pathway that was present represented cytokine receptor interactions suggesting there is increased signalling through these receptors in these mice. This was not seen in the younger mice, suggesting that this increased signalling may be one of the factors that drive OA development. I also had access to two computational models; a model of age-related changes in molecular pathways which included a TGF β signalling component (W. Hui et al. 2014) and a model of IL-1+OSM signalling (Proctor et al. 2014). These provided a framework on which to base the direction of the work, expanding and combining these models to better understand the effects of TGF β on inflammation with age.

3.3.3 Summary

- Through this chapter I explored 5 different biological pathways (Notch, IHH, PKC, Wnt/ β -catenin and TGF β) that may be important in OA development by examining their effect on cell viability and MMP-13 expression at 24 hours.
- Notch activation with SB initially induced cell death but this was elevated by reducing the concentration. Notch activation was able to induce increased MMP-13 expression at 24 hours.
- Neither WNT/ β -catenin or IHH activation had a significant effect on MMP-13 expression.
- Activating PKC significantly upregulated MMP-1/-13 at 6 hours. This upregulation was still seen at 24 hours, for MMP-13, but was greatly reduced.
- PKC activation-mediated MMP-1 upregulation more robustly than MMP-13, at 24 hours.
- TGF β was the only pathway that could protect against cell death in SW1353 cells.
- TGF β represses the IL-1+OSM-driven upregulation of MMP-1/-13 mRNA at 24 hours.
- Bioinformatic analysis demonstrated the importance of inflammation in OA. It also showed increased IL-1, OSM and TGF β receptor activation in end stage OA for SRT/ort mice.

Chapter 4. Exploring the TGF β signalling pathway

4.1 Synopsis

The previous chapter identified the need to focus on one pathway to study using a computational approach. It showed how the first step in building a model is to find out what is already known about the pathway and then ensure you have a model that can match previous data. Once this has been established you can identify an area to explore. I chose TGF β as I matched SW1353 data to what was seen previously but also located an unexplored area; looking at how the effect of TGF β on a pro-inflammatory stimulus changes with age. Before continuing with the construction of the model, I wanted to examine the pathway closer. Throughout this chapter I will present the current literature around the role of TGF β in OA. I will then expand on this experimentally, by exploring the time scale by which TGF β mediates its effect on IL-1+OSM-driven MMP-1/-13 expression. I will then identify the importance of the ALK5 receptor in this repression. It is worth noting that the TGF β pathway is incredibly complex and it was not possible to explore all aspects of the pathway in one model.

4.2 Introduction

4.2.1 TGF β

Originally discovered in 1978 as a growth factor in rat kidney fibroblasts, that could lead to malignant transformation of cells, TGF β was called sarcoma growth factor (SGF) (de Larco and Todaro 1978). It later became apparent that SGF was comprised of two separate factors, which were renamed transforming growth factor (TGF) α and β (Roberts et al. 1981). TGF β was then examined further discovering that it could inhibit cell growth (Roberts et al. 1985). The same group subsequently showed it could also lead to growth and proliferation of chondrocytes, demonstrating the opposing roles of TGF β (Roberts et al. 1986).

The complex nature of OA is highlighted by TGF β , a growth factor with a lot of therapeutic potential due to its pleiotropic role in disease progression. It has varying effects depending on not only the type of tissue but the age and environment surrounding the tissue. There are three TGF β isoforms: TGF β 1, 2 and 3, all of which are identical in almost all biological properties (Panoulas et

al. 2009). All three isoforms of TGF β are expressed in chondrocytes during differentiation. TGF β 1 and 2 have continuous expression in healthy adult chondrocytes, Baugé et al. (2014) highlighting the role they have in maintaining homeostasis. Despite this, chondrocytes can still secrete all three isoforms under the right stimuli (Villiger and Lotz 1992). All isoforms appear to have a role in the development of OA, with removal of TGF β signalling via the TGF β receptor type 2 (TGFBR2) receptor having both positive and negative effects on OA development (Scharstuhl, Glansbeek, et al. 2002). Equine cartilage has shown that TGF β 1 is the most abundant isoform in cartilage and all three isoforms are decreased with age. Mice deficient in any isoform have embryonic lethality. For example TGF β 1-deficiency resulting in a diffuse and lethal inflammation in mice (Dunker and Kriegelstein 2000). This inflammatory phenotype is particularly relevant as TGF β 1 has been shown to oppose the effects of inflammatory mediators; our group demonstrating this for IL-1+OSM and TNF- α (Hui et al. 2003; Hui et al. 2000; W. Hui et al. 2014). I chose TGF β 1 because of its prominent role in protecting against inflammation and in particular how this might change with age (Hui et al. 2000). It was also chosen as a result of the research done previously by the group which provided me with a wealth of information from which to plan experiments. It is also the best characterised in the literature and has a prominent role in the development of OA (Fang et al. 2016).

4.2.2 TGF β activation

TGF β is secreted into the synovial joint in an inactive form and must first be activated in order to have an effect. Directly after synthesis TGF β binds to latency associated peptide (LAP) to create a complex that can then interact with its binding partner latent TGF β binding protein-1 (LTBP1). This creates a latent form of TGF β that can be secreted into the various tissues (Pedrozo et al. 1998). In this form it cannot bind to any TGF β receptor, so in order to have an effect it must be activated by a two-step process; first removing it from LTBP1, then cleaving LAP to form the active TGF β . Both of these events can be mediated by plasmin, F-spondin or MMP-2/-9 (Yu and Stamenkovic 2000; Attur et al. 2009), as well natural detergents such as lysophosphatidylethanolamine

(LPE) and lysophosphatidylcholine (LPC). Both LPC and LPE can release TGF β from LTBP1 but cannot directly remove LAP, instead they promote the activation of proteases to form active TGF β (Gay et al. 2004). Many other proteins and substances have been linked to TGF β indicating that the activation of the TGF β pathway is complex and not yet fully understood.

4.2.3 TGF β signalling

Once activated TGF β can signal through the SMAD-dependent (canonical) or SMAD-independent (non-canonical) pathways. The non-canonical pathways, active TGF β interacts with a number of other important biochemical pathways. Using a variety of MAP kinases it can interact with ERK (Hartsough and Mulder 1995), p38 kinase (A. Nakao et al. 1997), or Rho-like GTPase (Bhowmick et al. 2001) signalling pathways, amongst many others, which potentially could help to contribute to the development of OA. An example of this is its interaction with Wnt/ β -Catenin. Dong et al, (2005) showed that TGF β could inhibit all of the Wnt proteins. However, the most important interaction is with β -Catenin, regulating its ability to cause chondrocyte differentiation, with TGF β removal resulting in excess differentiation (Dong et al. 2005).

4.2.3.1 Canonical pathway

The canonical TGF β pathway is important to study as it can have either catabolic or anabolic effects depending on which of its receptors it activates (Fig 1.6). TGF β can signal through two receptors in cartilage; either Activin A Receptor Like Type 1 (ACVRL1 or ALK1) or TGF β receptor 1 (ALK5). Which of these receptors it binds to leads to different downstream effects. ALK1 is the preferential binding partner, but TGF β predominantly signals through ALK5 due to its abundance (van der Kraan et al. 2012). ALK5 binding leads to SMAD2/3 phosphorylation, which in turn blocks terminal differentiation, chondrocyte hypertrophy and also stimulates the production of matrix components (Blaney Davidson et al. 2009) (Fig 4.1). Problems arise if the balance is switched towards ALK1 signalling which causes increased SMAD1/5/8 phosphorylation. This has the exact opposite effect of ALK5 signalling leading to chondrocyte hypertrophy, terminal differentiation and matrix breakdown by MMPs such as

MMP-13 (Blaney Davidson et al., 2009). As mentioned in chapter 3, this change in ALK1/ALK5 has been shown to correspond with the development of spontaneous OA in the STR/ort mouse model (Blaney Davidson et al. 2009) but these results have also been seen in guinea pigs (Zhao et al. 2016).

In order to have an effect, phosphorylated SMAD2/3 and 1/5/8 must bind to SMAD4, also known as the co-SMAD (Massaous and Hata 1997). SMAD4 is constantly shuttling between the cytoplasm and nucleus, both in unstimulated and ligand-stimulated cells (Bernhard Schmierer et al. 2008). Once bound SMAD4 can translocate the phosphorylated SMADs to the nucleus (Massaous and Hata 1997). When in the nucleus the SMADs are released from SMAD4 and function as transcription factors to mediate their effects. The inhibitor I-SMADs 6/7 regulate TGF β signalling at two levels, targeting the receptors to stop signalling but also competing with SMAD4 to reduce the impact of SMAD signalling (Atsuhito Nakao et al. 1997; Imamura 1997). SMAD7 is a major regulator for SMAD2/3 signalling but it does have a smaller role in regulating SMAD1/5/8 (Hayashi et al. 1997). It binds to activated TGF β receptors preventing them from phosphorylating SMAD proteins (Hayashi et al. 1997). It also has a key role in TGF β receptor ubiquitination and destruction via interactions with the Smurf proteins (Kavsak et al. 2000). Smurf 2 can bind to SMAD7 to shuttle the receptors to the cytoplasm. Once there the Smurf-SMAD7 complex can target the receptor for destruction (Kavsak et al. 2000). SMAD6 is the primary regulator of SMAD1/5/8 signalling (Imamura 1997). SMAD6 competes with SMAD4 for interaction with receptor activated SMADs. For example binding to phospho-SMAD1 creates a SMAD1 - 6 complex that can no longer be shuttled to the nucleus (Hata et al. 1998). The activity of both I-SMADs is regulated at many levels. TGF β induces the expression of SMAD7 (Atsuhito Nakao et al. 1997), whilst BMP signalling seems to induce SMAD6 (Afrakhte et al. 1998). SMAD7 is also present in the nucleus but moves to the cytoplasm in response to TGF β signalling (Itoh et al. 1998). Both I-SMADs can also be induced by other signals that effect TGF β signalling such as IL-1 (Bitzer et al. 2000).

TGF beta receptor 2 (TGFBR2) is required to mediate TGFβs effect; two TGFBR2 molecules form a homodimer that forms a complex with TGFβ and either of its type 1 receptors (Bierie and Moses 2006). This complex can be comprised of TGFBR2 homodimers, TGFβ and a homodimer of ALK5 leading to SMAD2/3 phosphorylation, or the heterodimer of ALK5/ALK1 which leads to SMAD1/5/8 phosphorylation (M. J. Goumans et al. 2003). ALK1 cannot mediate its effect without ALK5 (M. J. Goumans et al. 2003). Endoglin may also play a role in mediating ALK1 signalling by facilitating its binding to TGFBR2; although it is not yet clear to what extent it is required (Finsson et al. 2010). Which type 1 receptor TGFβ is signalling through can be determined by gene specific expression patterns. Goumans et al. (2002) showed that plasminogen activator inhibitor-1 (PAI1) is a downstream target of ALK5 and that inhibitor of DNA Binding 1 (ID1) is downstream of ALK1; both can be upregulated by TGFβ. During TGFβ treatment, when ALK1 was removed, there was no change in ID1 expression whilst, when ALK5 was removed, PAI1 was unchanged. Constitutively active forms of ALK1 and ALK5 also upregulated ID1 and PAI1 exclusively (Goumans et al. 2002). ALK1 signalling inhibits downstream ALK5 signalling; meaning that when ALK1 starts to become the dominant receptor SMAD2/3 phosphorylation becomes less abundant, whereas ALK5 downstream signalling has no direct effect on SMAD1/5/8 phosphorylation (M. J. Goumans et al. 2003).

Figure 4.1 summarises TGFβ signalling through both type 1 receptors. The pluripotent effect of TGFβ here is interesting as the joint produces a large amount of it in response to damage, or in the event of inflammation, due to its protective effect mentioned earlier. If the tissue has changed to ALK1 signalling then this previously beneficial response will now lead to even greater damage. High levels of TGFβ are seen in osteoarthritic joints (Schlaak et al. 1996), and this could be a major source of damage if TGFβ is signalling through ALK1. Identifying the causes of this change from ALK5 to ALK1 signalling could potentially be of great benefit as a therapeutic target, as reversing this change would not only prevent damage but restore a previously protective pathway.

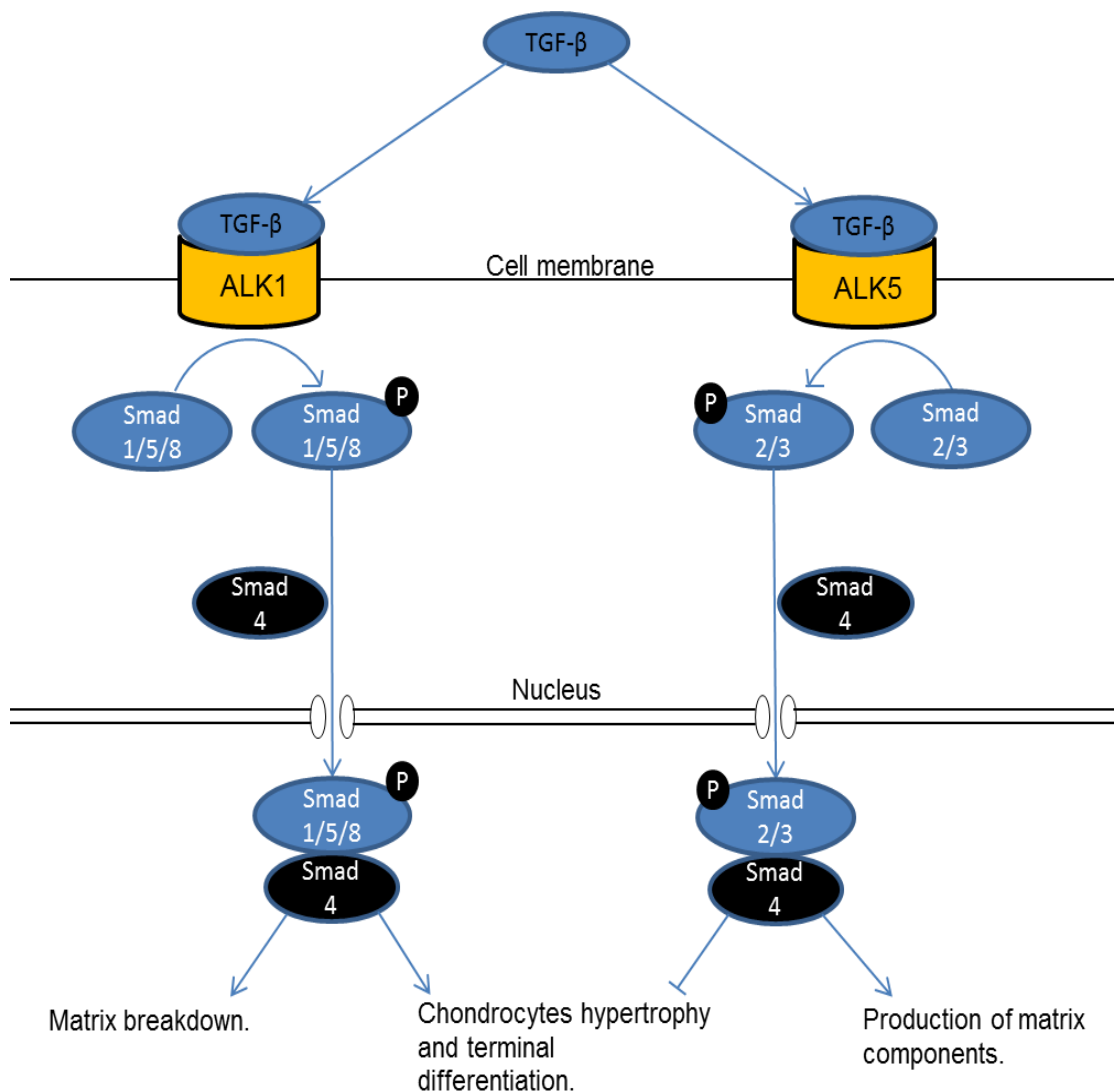


Figure 4.1 An overview of TGFβ signalling pathway in chondrocytes. Depending on which of the two type I receptors TGFβ binds to determines the downstream effect. Binding to ALK1 starts a series of reactions that result in matrix breakdown, chondrocyte hypertrophy and terminal differentiation. Conversely, binding to ALK5 produces the opposite effect. Both ALK1 and ALK5 are in dimers with ALK5 but this has been omitted for simplicity.

4.2.4 TGFβ and cartilage

It has been demonstrated that TGFβ is required for normal cartilage development and is crucial for maintaining articular chondrocyte homeostasis in synovial joints (Blaney Davidson et al. 2007). Cartilage maintenance, as discussed in chapter 1.1.2.3, is mediated by many biological pathways. Figure 4.2 highlights the central role of TGFβ in cartilage maintenance. Loss of TGFβ

signalling in cartilage induces chondrocyte hypertrophy, ultimately resulting in cartilage degeneration (Hiramatsu et al. 2011). Furthermore, in mice, when tissue is aged TGF β has the opposite effect on cartilage development (Blaney Davidson et al. 2009) (Fig 4.1). High levels of TGF β in the synovial fluid of OA patients indicated it may also affect synovial fibroblasts (Blom et al. 2004). Further studies have confirmed this, with constitutively active TGF β injections into the synovial fluid leading to synovial fibrosis whilst also increasing production of pro-inflammatory cytokines such as IL-1 and TNF- α (Scanzello and Goldring 2012).

TGF β has a potent anti-inflammatory effect and has been shown to protect against the synergistic effects of OSM with pro-inflammatory cytokines. It can reduce collagen release by both TNF- α + OSM and IL-1+OSM (Hui et al. 2003; Hui et al. 2000). In the case of IL-1+OSM, TGF β reduced collagen release by $\geq 80\%$. This effect was most likely mediated by reducing the downstream effects of IL-1 and OSM on MMP-1/-13 mRNA production (Hui et al. 2000). Both MMP-1/-13 mRNA was significantly downregulated at 24, 48 and 72 hours. How TGF β leads to this reduction is currently unknown. TGF β can also increase expression of TIMPs and PAI1, both of which have been reported to target cartilage destructive enzymes to reduce damage (Campbell et al. 1994; Blaney Davidson et al. 2007). Whether or not the protective effect of TGF β against inflammatory stimuli remains in aged organisms is yet to be examined. However, I hypothesised that this effect will either be removed or reversed with TGF β , leading to increased damage by further upregulation of MMP-13 and possibly MMP-1.

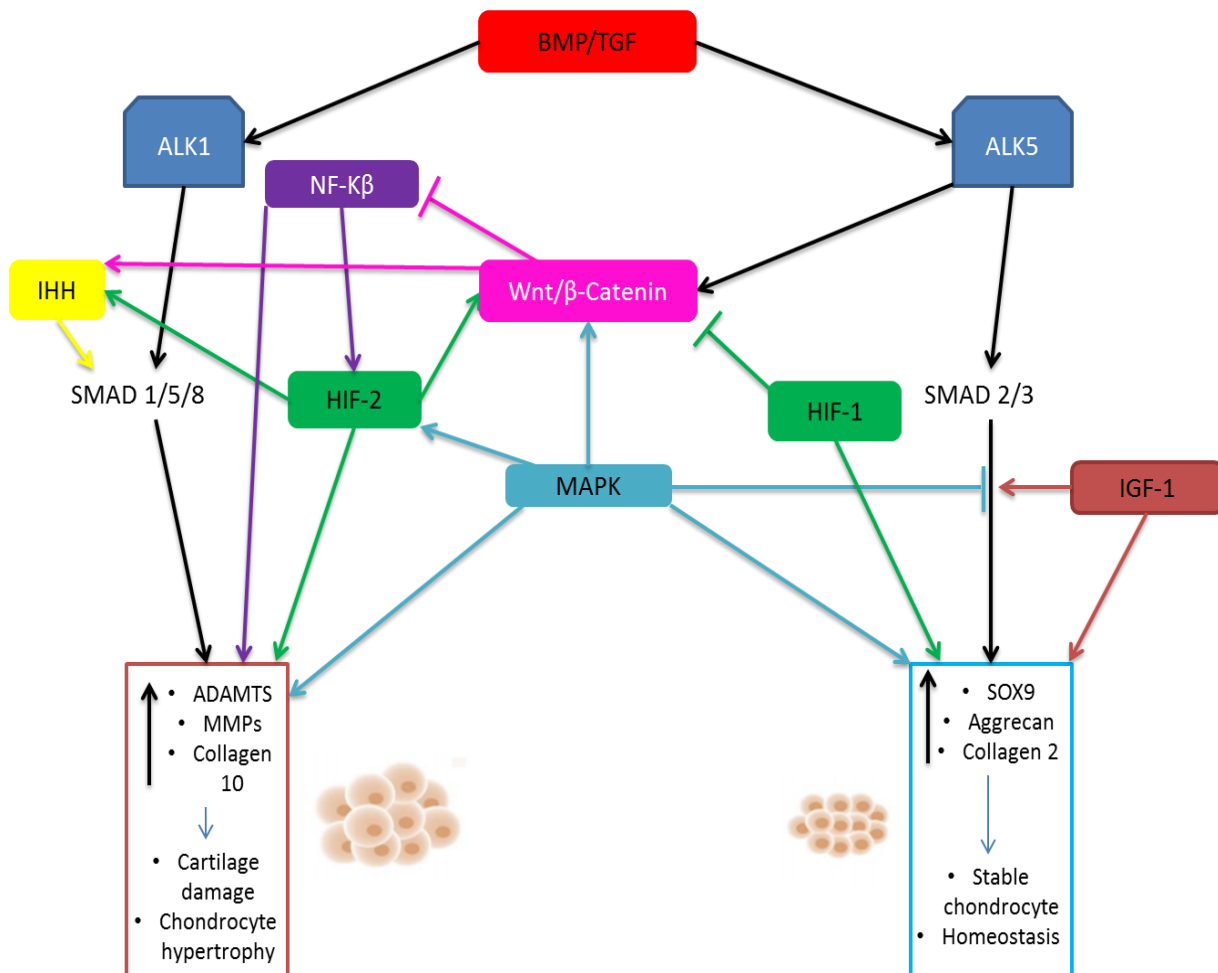


Figure 4.2 **Interaction of cartilage maintenance pathways.** Adapted from Mariani et al. (2014) it shows a schematic overview of how multiple pathways interact with TGFβ to maintain cartilage homeostasis.

4.2.5 TGFβ and bone

TGFβ has a relatively minor role in bone compared to cartilage but despite this proper maintenance of its expression is vital for bone health. TGFβ is released by osteoclasts when they degrade old or damaged bone, allowing it to direct mesenchymal stem cells (MSC) to the resorption site. MSCs can then form osteoblasts leading to new bone synthesis as well as inactivating TGFβ (G. Zhen and X. Cao 2014). This process is summarised in Figure 4.3. As TGFβ has a relatively minor role, excess TGFβ in bone is easier to characterise than in cartilage as it appears to only have negative effects (G. Zhen and X. Cao 2014). TGFβ is regularly found to be upregulated in OA bone, from both animal and human tissues. Osteoblast cells that constitutively expressed active TGFβ in transgenic mice lead to abnormal subchondral bone structure and eventually

degradation of cartilage (Tang et al. 2009). The increased levels of TGF β result in increased bone thickness which reduces the bones ability to react to mechanical loading (G. Zhen et al. 2013). Subchondral bone also begins to form osteophytes which lead directly to pain in patients and cartilage destruction (van Beuningen et al. 2000).

4.2.6 Changing role of TGF β with age

Age has been suggested as the major driving factor for conversion of ALK5 to ALK1 signalling. ALK5 levels decrease with age whilst ALK1 levels stay relatively constant (Blaney Davidson et al. 2009). This emphasises how dysregulation can occur in an ageing system (Blaney Davidson et al. 2009). How exactly ageing leads to increased ALK5 degradation is unknown. What is known is that SMAD7 targets ALK5 for ubiquitination by Smurf 1 and 2 proteins followed by proteolytic destruction (Yan et al. 2009). It may be that as TGF β signalling is persistently stimulated over a person's life, ALK5 is slowly depleted until ALK1 becomes the most dominant type 1 receptor. It appears ALK1 is not targeted in this same manner since its signalling is predominantly regulated by SMAD6 (König et al. 2005). This change can also be mediated by crosstalk with other pathways. Wnt signalling, for example, has been shown to affect the expression of a number of proteins downstream that can skew TGF β signalling towards the catabolic ALK1 pathway (Martijn H. van den Bosch et al. 2014). As shown earlier, Wnt signalling can also be affected by non-canonical TGF β signalling, indicating a level of crosstalk between these pathways and highlighting the complexity of TGF β .

4.2.6.1 Pro-inflammatory interactions with TGF β signalling

Particularly interesting is how this change in the ALK5/ALK1 ratio affects the ability of TGF β to protect against the damaging effect of inflammation, in particular the pro-inflammatory stimulus IL-1 and OSM. Looking at the pathway suggests that it is an ALK5-dependent effect, due primarily to the reduction shown in MMP-13 when TGF β was present, compared to IL-1+OSM alone. This is unlikely to be an ALK1-mediated effect as it can lead to an upregulation of MMP-13 independently. It has been demonstrated previously that TGF β can protect against the damaging effect of IL-1 in murine models (Scharstuhl, van

Beuningen, et al. 2002; Kuruvilla et al. 1991). Our group have shown that this effect also extends to IL-1+OSM but how this effect is mediated is not currently understood (Hui et al. 2000).

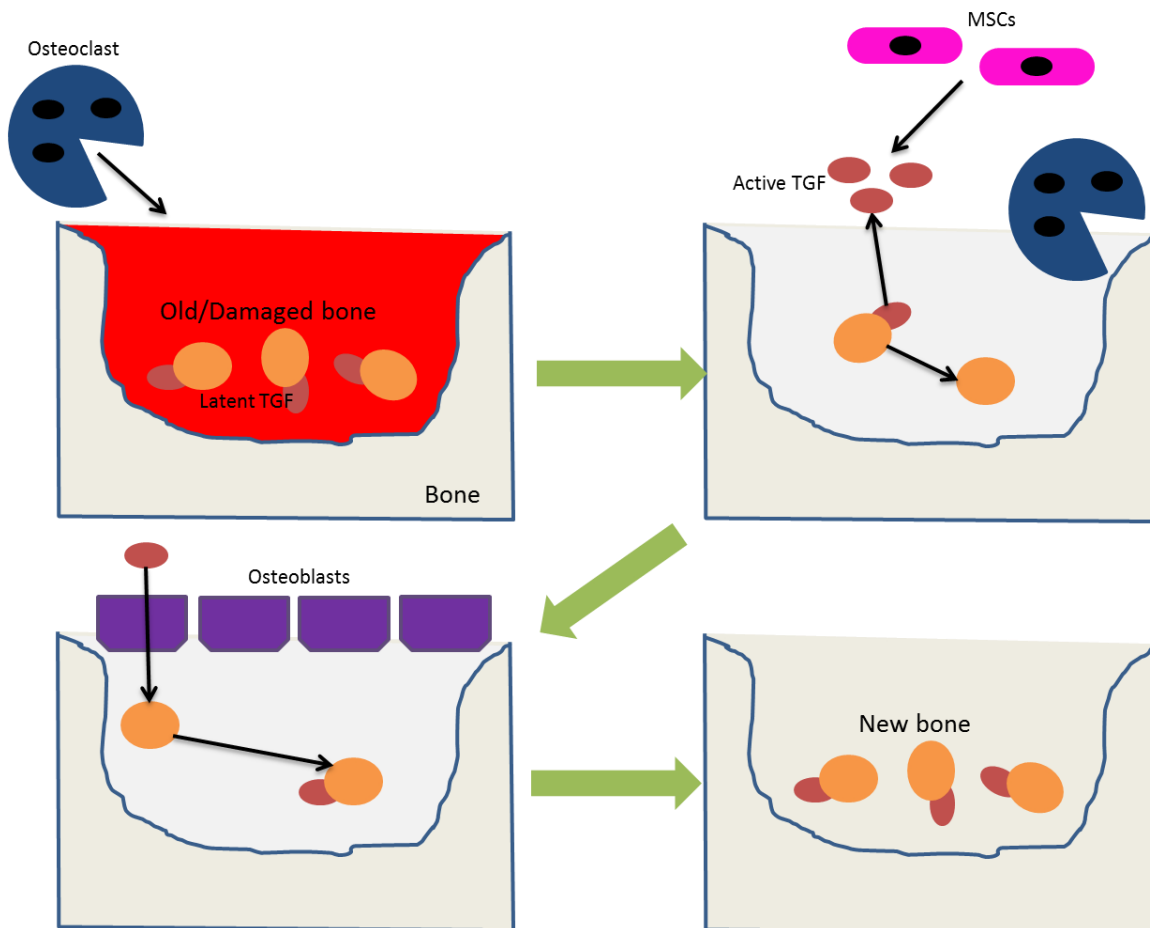


Figure 4.3 **The role of TGFβ in new bone formation.** TGFβ is released and becomes activated by osteoclasts during the removal of old or damaged bone. TGFβ can then recruit mesenchymal stem cells (MSC) to the site. MSCs can then differentiate into osteoblasts and form new bone. TGFβ is inactivated during new bone formation. Adapted from (G. Zhen and X. Cao 2014)

4.2.7 Importance of TGF β in OA

Given the role of TGF β in almost all facets of cartilage biology, it is unsurprising that there is a large body of evidence showing changes in the TGF β pathway culminate in a diseased phenotype. Multiple genetic studies have highlighted this, such as a genetic variant in asporin (ASPN) resulting in an extra aspartic acid which has been shown across several studies to correlate with a susceptibility to OA in Asian, Spanish and Caucasian populations (Shen et al. 2014). This change causes asporin to be a stronger regulator of TGF β signalling, with a reduction in signalling leading to a higher OA risk (Kizawa et al. 2005). Another study has shown a polymorphism in the TGF β signal region (T29 to C), or a mutation in TGF β by Camurati–Engelmann disease, can increase OA prevalence by increasing TGF β activity (Kinoshita et al. 2000). In addition, a single nucleotide change in the TGF β downstream target Smad3 has also been linked to the incidence of hip and knee OA in a European patient cohort (Valdes et al. 2010).

Microarray studies have consistently shown the importance of TGF β in OA, with its continued functionality being important in preventing OA. They have also identified how specific changes can be the cause of OA. Olex et al. (2014) induced OA in mice then looked at OA development as a whole across a range of time points (2, 4, 8 and 16 weeks post induction). They identified TGF β as one of the key pathways at all the time points except week 8. Although they could not identify if it was being up or down regulated in their study, they showed it was important in OA development. They did this by identifying clusters essential for biological functions that changed during OA, and TGF β was central for a high proportion of these clusters. The importance of TGF β is something shown by many microarray studies. Finnsen et al. (2012) reviewed the importance of TGF β in OA and created a table that incorporates many large screen OA studies. Table 4.1 summarises the relevant points which makes it clear how components of the TGF β pathway can be central in OA development. Olex et al. (2014) explained how TGF β signalling changes is not obvious, as some studies show a downregulation of TGF β whilst others show it is upregulated. This discrepancy in TGF β could be a result of many things such as

the age of the tissue, if it is an inflammatory driven OA, an injury driven OA or a variety of other reasons. From table 4.1 what is also obvious is that, when present, ALK5 is downregulated. ALK1 can be up or down regulated, but it is always the case that the ALK1/ALK5 ratio is increased (Finnsen et al. 2012). SMAD2 is also always downregulated and SMAD3 is also altered but not as clearly (Finnsen et al. 2012). ALK1 becoming dominant indicates that the move of TGF β from SMAD2/3 to SMAD1/5/8 clearly plays a role in development of many OA phenotypes. Unfortunately, SMAD1/5/8 was not explored and so not present in the table.

More targeted studies can also highlight how important TGF β is for OA. Two studies looking specifically at the role of clock genes BMAL1 and NR1D1 in OA development did microarrays to identify the most important pathways (M. Dudek et al. 2016; Akagi et al. 2017). In both cases TGF β was identified as one of the most significant upstream regulators. M. Dudek et al. (2016) showed that ALK1 expression was cyclic through the day and altering BMAL1 could result in a change in ALK1/ALK5 ratio, resulting in a significant downregulation of SMAD2 phosphorylation. This suggests that TGF β is once again having a negative effect on OA progression by moving from signalling through ALK5 to primarily ALK1 signalling.

Targeting TGF β to treat OA is a promising avenue but it is complicated because of the varying roles it can have in OA development. Lee et al. (2001) used gene therapy to produce fibroblasts expressing active TGF β , then injected these into the knee joints of rabbits with induced cartilage damage. They showed that after 4-6 weeks the cartilage had been repaired in these mice (Lee et al. 2001). They later showed that radiation treated versions of the same fibroblasts injected into mice could still repair the cartilage (Song et al. 2004): the advantage being the injected fibroblasts die rapidly so do not linger and result in any negative changes later. Blocking of TGF β (either directly or indirectly by overexpressing Smad7) significantly attenuated TGF β induced synovial fibrosis in murine experimental OA models, whilst Blaney Davidson et al. (2006), demonstrated that they could reverse cartilage damage caused by IL-1 with the addition of a constitutively active form of TGF β (Blaney Davidson et al. 2006)). However, in

order to avoid synovial fibrosis they needed to co-express a constitutively active form of Smad7. This despite alleviating synovial fibrosis, unfortunately failed to reduce osteophyte formation in the surrounding bone tissues. Nevertheless, these studies showed that with a better understanding of its function, TGF β could serve well as a therapeutic target in the future, helping to reverse cartilage destruction in OA patients. Conversely, Chen et al. (2015) argued that inhibition of TGF β rather than activation should be considered for treatment. They looked at blocking TGF β due to studies that showed it was upregulated in OA (Pombo-Suarez et al. 2009). To do this they made conditional knockout TGFBR2 mice. Mice deficient in TGFBR2 are embryonic lethal, but their mice could have the deletion induced later in development. They found that mice deficient in TGFBR2 were protected from degradation in the knee, delaying OA development after DMM surgery by up to 6 weeks (Chen et al. 2015). To further confirm this they used inhibitors of TGFBR2 in wild type mice and found a similar result. The same group later used these mice to confirm TGF β was low in cartilage of wild type mice pre DMM surgery. TGF β then increased during the early stages of OA, with phosphorylated SMAD2/3 levels following the same pattern (Fang et al. 2017). They argue that previous studies have proven TGF β is required for the development of joints, and if TGFBR2 or SMAD3 is removed early, the mice develop OA phenotypes. Despite this TGFBR2 removal in adult cartilage protects against cartilage damage, possibly because TGF β is required for joint development but no longer essential once formed (Fang et al. 2017). Alternatively, they suggest TGF β may work in a dose-dependent manner, as above or below a certain threshold it will lead to damage (Fang et al. 2017). They argue all their data confirm that inhibition of TGF β should be used for treatment. Taken in context with the other studies that show the positive effects of overexpressing TGF β , I would argue that neither blocking nor activating TGF β will provide the answer. Instead a better understanding of the pathway will allow us to assess what changes occur in TGF β signalling during cartilage degradation. Therapeutic targets may then arise from normalising the TGF β response to what it was before the onset of OA.

Component	Model	Alteration
TGFβ1	Human OA Human OA Human OA Human OA Mouse OA (papain) Rabbit ACLT/PCLT	↓TGFβ1 protein (proteomics) ↓TGFβ1 protein (IHC) ↑TGFβ1 mRNA (qPCR) and protein (IHC) ↑TGFβ1 mRNA (microarray and qPCR) ↑ TGFβ1 protein (IHC and ELISA) ↓TGFβ1 mRNA (RT-PCR)
ALK5	Human OA Mouse Aging Mouse OA (STR/Ort) Mouse OA (DMM) Rat OA (PM/PST)	ALK5 mRNA correlates with COL2 + AGG mRNA expression (qPCR) ↓ ALK5 protein (IHC) ↓ ALK5 protein (IHC) ↓ ALK5 protein (IHC) ↓ ALK5 protein (IHC)
ALK1	Human OA Mouse OA (STR/Ort) Mouse OA (DMM) Mouse Ageing Rat OA (MT)	ALK1 mRNA correlates with MMP-13 mRNA expression (qPCR) ↓ ALK1 protein (IHC); ↑ALK1/ALK5 ratio ↓ ALK1 protein (IHC); ↑ALK1/ALK5 ratio ↓ALK1 protein (IHC); ↑ALK1/ALK5 ratio ↑ALK1 protein (IHC); ↑ALK1/ALK5 ratio
SMAD2	Mouse OA (STR/Ort) Mouse OA (CIA) Mouse aging	↓ phospho-Smad2 (IHC) ↓ phospho-Smad2 (IHC) ↓ phospho-Smad2 (IHC)
SMAD3	Human OA Human OA Mouse aging	Smad3 missense mutation a risk factor for OA Smad3 intronic SNP a risk factor for OA ↑ Smad3 protein (IHC)

Table 4.1 How TGFβ signalling components are altered during OA development. Looking across multiple animal and human studies with a range of different techniques, shows how the expression of TGFβ1, ALK1/5 and SMAD2/3 change as OA develops. Abbreviations are as follows; IHC, immunohistochemistry; ACLT, anterior cruciate ligament transection; PCLT, posterior cruciate ligament transection; MT, meniscal tear; DMM, destabilization of the medial meniscus; CIA, collagenase-induced arthritis; PM/PST, partial meniscectomy/post-surgical training; SNP, single nucleotide polymorphism. Data taken from (Finsson et al. 2012)

4.2.8 TGF β specific modelling

Expanding on already developed models can be beneficial for increasing understanding of a system. Knowledge of TGF β signalling has been improved greatly by this concept. Vilar et al. (2006) developed a concise model to represent the TGF β signalling pathway. This model highlighted that receptors were not simply transducers of signals but key modulators of a downstream TGF β response; their “constitutive-to-induced degradation ratio” being key for matching observed signalling responses (Vilar et al. 2006). Shortly after B. Schmierer et al. (2008) created two models, retention only (RO) and an alternative retention/enhanced complex import (ROCI) model. Attempting to match both of these models to their experimental data provided insight into the importance of SMAD-phosphorylation and nucleocytoplasmic dynamics. The RO could not fit their four datasets, whereas the ROCI model could be altered to replicate them all. This highlighted the importance of correct SMAD-dynamics (B. Schmierer et al. 2008). Zi et al. (2011) realised the importance of both component dynamics (receptors and SMADs) and so created a more comprehensive model that took elements from both models as well as including TGF β depletion and ligand dynamics. This model better matched the switch like behaviour of TGF β over longer time scales that previous models could not replicate. It also showed how signalling changed with varying concentration/volumes of TGF β present, concluding that receptors react to molecule numbers rather than absolute concentrations (Zi et al. 2011). Wegner et al. (2012) expanded on elements of all these previous models to include more detailed negative and positive feedback mechanisms. SMAD7 and SMURF2 have the largest effect on dynamics (Wegner et al. 2012). TGF β is known to signal through two type 1 receptors to cause the downstream phosphorylation of either SMAD2/3 or SMAD1/5/8. The previous models had only looked at SMAD2 dynamics until Nicklas and Saiz (2013) created a model that examined both SMAD2/3 and 1/5/8 signalling. They wanted to examine how TGF β can have distinctly different results across multiple cell lines. They succeeded in matching experimental data from human keratinocyte (HaCaT), bovine aortic endothelial (BAEC) and mouse mesenchymal (C2C12) cell lines to the same model. The model demonstrated how concentrations of the species in

the model could explain the differing response across cell lines under identical experimental conditions, without the pathway structure changing (Nicklas and Saiz 2013). This is particularly interesting for ageing as it demonstrates that although the TGF β response has changed, the pathway may be identical and the changes in receptors/ligands may be resulting in the altered response. Therefore if we can better understand how they are changing, restoring the pathway to its original response may be possible.

4.2.9 Chapter aims

- Expand on the work from the previous chapter to look at TGF β -mediated repression in detail across 4 time points: 6, 12, 24 and 48 hours.
- Determine the importance of ALK5 in TGF β -mediated protection against IL-1+OSM-driven MMP-1/-13 expression.

4.3 Results

4.3.1 TGF β -mediated repression is robust.

In the previous chapter the concentration of TGF β was 0.15ng/ml. However, the literature examined suggested a higher concentration was generally used.

Having data that reflected the literature was important in model construction, so the concentration was increased accordingly. Screening a range of concentrations showed that repression was robust, as significant repression of both MMP-1/-13 was seen at 24 hours irrespective of the concentration (Fig 4.4). After the screen I continued with the concentration 10ng/ml as this is more commonly seen in the literature.

After changing the concentration I looked at the effect TGF β had on IL-1+OSM treatment across four time points. MMP-1/-13 followed a similar pattern for IL-1+OSM treatment, with expression increasing between 6 to 24 hours, then decreasing at 48 hours (Fig 4.5A and 4.6A). One noticeable difference was MMP-13 had a sharp increase between 12 and 24 hours, whilst MMP-1 was relatively constant across the two time points (Fig 4.5A and 4.6A).

In order to accurately determine the percentage of repression mediated by TGF β I repeated all of the individual time points (6, 12, 24 and 48) across a multitude of experiments. I then pooled all of these results (Fig 4.5B and 4.6B). The pattern seen was similar for MMP-1/-13, taking an excess of 12 hours for TGF β to have an effect. Significant repression was seen at 24 hours and for MMP-13 this repression was increased by 48 hours (Fig 4.5B). However, this was not seen for MMP-1 with repression still highly significant but similar to that at 24 hours (Fig 4.6B).

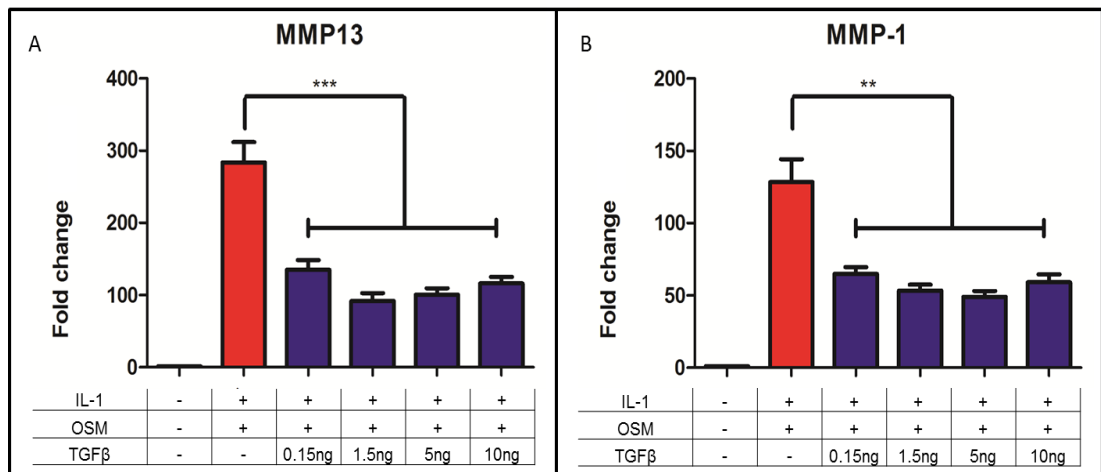


Figure 4.4 **Various concentrations of TGFβ repress IL-1+OSM-induced MMP expression at 24 hours.** SW1353 cells were stimulated for 24 hours with IL-1 (0.5ng/ml) +OSM (10ng/ml) ±TGFβ at concentrations ranging from 0.15ng to 10ng. qPCR was performed on the isolated mRNA to measure A) MMP-13 expression B) MMP-1 expression. Data are presented as mean fold change relative to control ± SEM, N = 5-6. Statistics calculated using unpaired Student's t-test, where ** p < 0.01; *** p < 0.001.

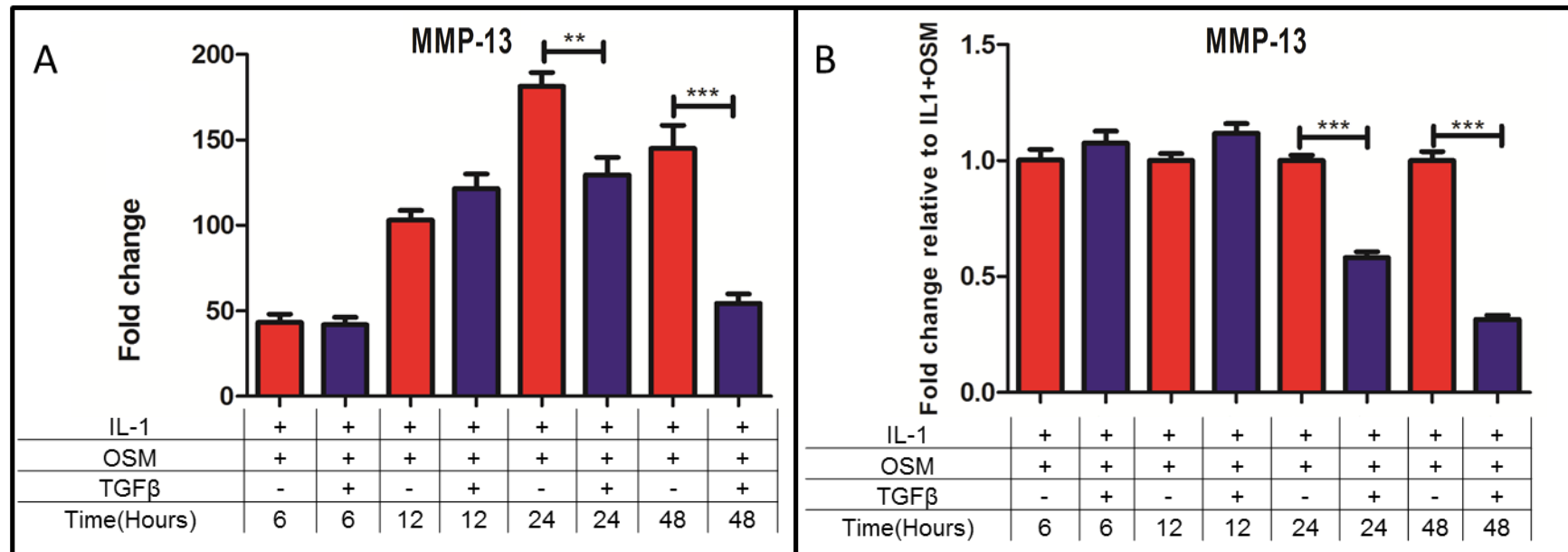


Figure 4.5 **Effect of TGFβ on IL-1+OSM induced MMP-13 expression.** SW1353 cells were stimulated with IL-1 (0.5ng/ml), OSM (10ng/ml) and IL-1+OSM±TGFβ (0.15ng/ml (B) (10ng/ml (A and B))). qPCR was then performed on the isolated mRNA to measure MMP-13 expression. Data are presented as fold change relative to control (A) or IL-1+OSM (B) (mean ± SEM). A) A single experiment showing cells treated for 6, 12, 24 and 48 hours with IL-1+OSM±TGFβ, n=5-6. B) Pooled data from experiments at 6, 12, 24 and 48 hours in cells stimulated with IL-1+OSM±TGFβ treatment. At 6h n=35 from 7 experiments; 12h n=39-45, across 7 experiments; 24h n= 42-48, across 10 experiments and 48h n=47 across 7 experiments. Statistics calculated using unpaired Student's t-test, where ** p < 0.01; *** p < 0.001

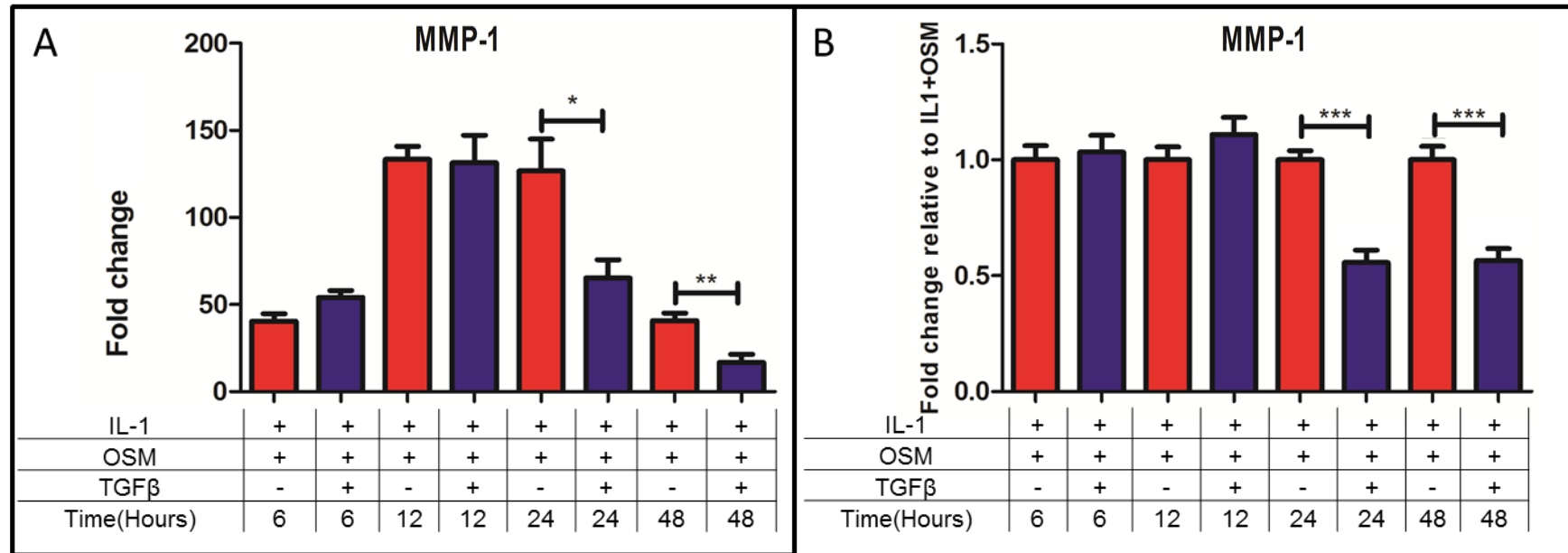


Figure 4.6 **Effect of TGFβ on IL-1+OSM induced MMP-1 expression.** SW1353 cells were stimulated with IL-1 (0.5ng/ml), OSM (10ng/ml) and IL-1+OSM±TGFβ (0.15ng/ml (B) or 10ng/ml (A and B)). qPCR was then performed on the isolated mRNA to measure MMP-1 expression. Data are presented as fold change relative to control (A) or IL-1+OSM (B) (mean ± SEM). A) A lone experiment showing cells treated for 6, 12, 24 and 48 hours with IL-1+OSM±TGFβ, n=4-6. B) Pooled data from experiments at 6, 12, 24 and 48 hours in cells stimulated with IL-1+OSM±TGFβ treatment. At 6h n=28-31 from 5 experiments; 12h n=33-38 from 6 experiments; 24h n=20-21 from 5 experiments and 48h n=27-28 from 5 experiments. Statistics calculated using unpaired Student's t-test, where * p < 0.05; ** p < 0.01; *** p < 0.001

4.3.2 Importance of ALK5 in protection

The literature suggested ALK5 may have an important role in TGF β -mediated repression of IL-1+OSM-mediated MMP-1/-13 expression. Therefore I measured the basal level of expression of ALK1 and ALK5 in SW1353 cells. I used the universal probe library. Therefore, it was necessary to test primer efficiency before comparing the basal expression. This was done as described in chapter 2.1.8 briefly, samples were diluted and the CT values of ALK5/ALK1 were measured relative to the dilution; from this I could ascertain how accurate the primers were at determining quantity and alter CT accordingly. Comparing the altered CTs showed the expression of ALK5 was approximately 19 fold higher than ALK1 (Fig 4.7A). Comparing the expression of PAI1 (downstream of ALK5) and ID1 (downstream of ALK1) after 2 hours TGF β treatment, showed that PAI1 was significantly upregulated (Fig 4.7B) whilst ID1 mRNA remained constant (Fig 4.7C). All of these data suggested that SW1353 cells signal almost exclusively through ALK5 (Fig 4.7).

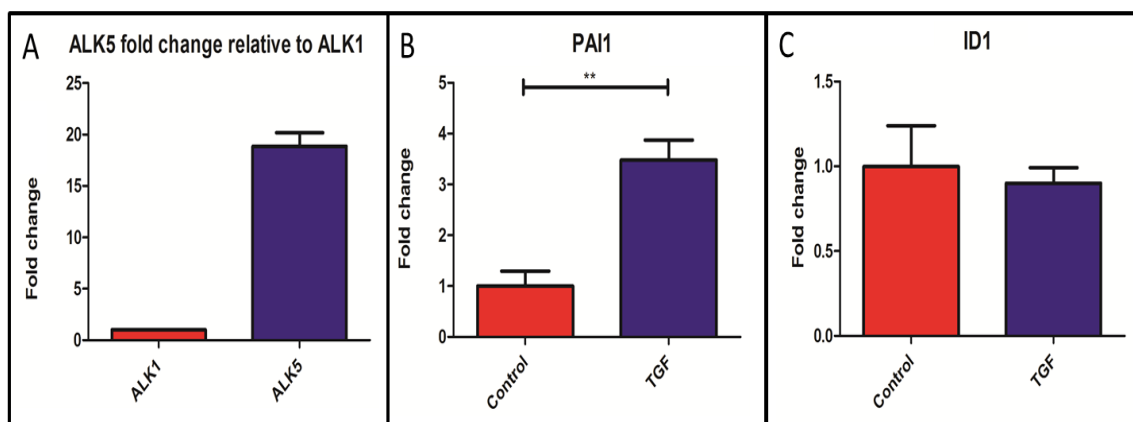


Figure 4.7 **Level of ALK5 mRNA relative to ALK1 leading to downstream expression of TGF β specific genes after 2h treatment.** A) SW1353 cells were serum starved overnight then harvested without stimulation. qPCR was then performed on the isolated mRNA to measure expression of ALK1 and ALK5. The data are presented as fold change relative to ALK1 \pm SEM, N=10. B and C) SW1353 cells were stimulated for 2 hours with TGF β (10ng/ml). qPCR was performed on the isolated mRNA to measure A) PAI1 expression B) ID1 expression. Data are presented as mean fold change relative to control \pm SEM, N = 4-6. Statistics calculated using unpaired Student's t-test, where ** p < 0.01.

As ALK5 appeared to be the dominant receptor, I explored how removing it from the system would affect TGF β -mediated repression of MMP-13. ALK5 siRNA (siALK5) significantly reduced ALK5 expression at both the mRNA and protein levels (Fig 4.8A and B). At the mRNA level there was approximately 95% less ALK5 mRNA at 100 and 50nM (Fig 4.8A), whilst no significant change was seen with a non-targeting siRNA (siCON). This reflected in the protein where no ALK5 signal could be seen in samples treated with 50nM siALK5 (Fig 4.8B). This reduction in ALK5 does not seem to affect ALK1 protein expression (Fig 4.8B). Non-targeting siRNA transfection resulted in repression similar to that seen previously (Fig 4.5, Fig 4.9), while siRNA against ALK5 completely removed the protective effect that TGF β had on the IL-1+OSM stimulus (Fig 4.9). It is worth noting that removing ALK5 did not result in a significant increase of MMP-13 in IL-1+OSM+TGF β samples.

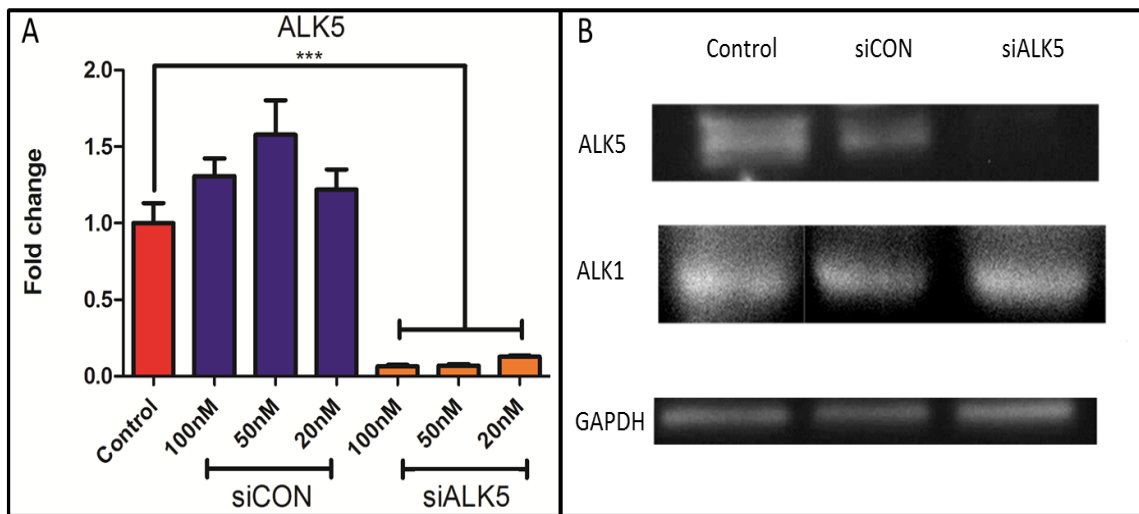


Figure 4.8 Potency of ALK5 siRNA on SW1353 cells. SW1353 cells were harvested following 24 hour treatment with a non-targeting siRNA (siCON) or a siRNA specific to ALK5 (siALK5), at concentrations ranging from 20nM to 100nM (B = 50nM). A) qPCR was then performed on the isolated mRNA to measure expression of ALK5. Data are presented as mean ALK-5 fold change relative to control \pm SEM, N=5-6 Statistics calculated using unpaired Student's t-test, where *** $p < 0.001$. B) Whole cell lysates were run on SDS page gels and then Western blots for ALK1, ALK5 and GAPDH were performed. Data are representative of N=2 independent experiments on separate SW1353 cell populations.

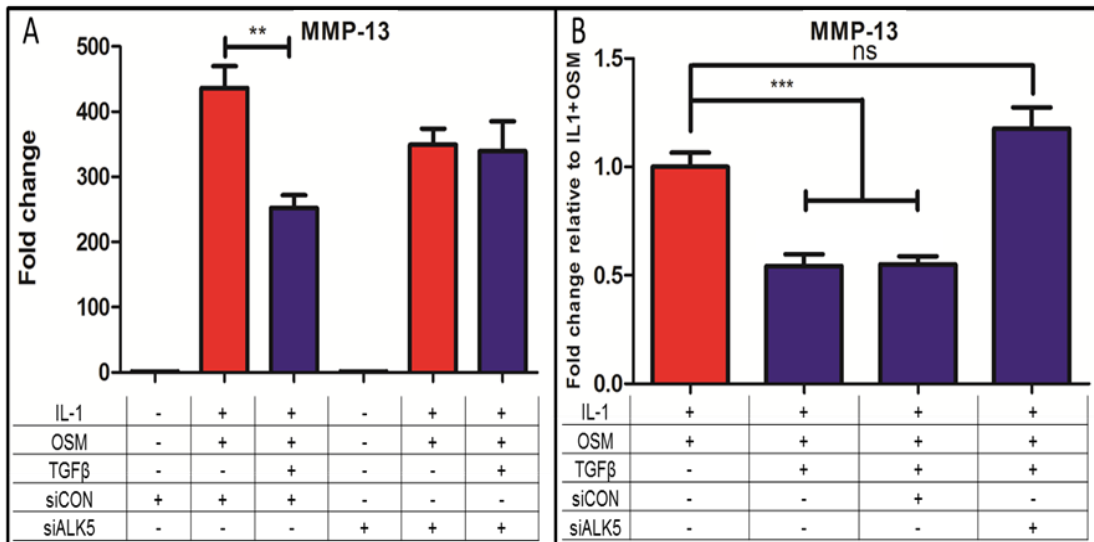


Figure 4.9 Effect of ALK5 silencing on TGFβ-mediated MMP-13 repression at 24h. SW1353 cells were stimulated for 24 hours with IL-1 (0.5ng/ml) +OSM (10ng/ml) ±TGFβ (10ng/ml), following 24 hour treatment with serum free media or 50nM of a non-targeting siRNA (siCON) or a siRNA specific to ALK5 (siALK5). qPCR was then performed on the isolated mRNA to measure expression of MMP-13. Data are presented as mean fold change relative to control (A) or IL-1+OSM (B) ± SEM A) A lone experiment at 24 hours, N=5-6. Representative of N=6 independent experiments on separate SW1353 cell populations. B) Pooled data from multiple experiments, N= 32-34, across 6 experiment, except for IL-1+OSM+TGFβ with neither siRNA where N= 18 across 3 experiments. Statistics calculated using unpaired Student's t-test, where ** p < 0.01; *** p < 0.001.

Exploring how ALK5 removal affected MMP-1 was more problematic than looking at MMP-13, as for some unidentified reason the siRNA transfection procedure appeared to affect MMP-1 expression (Fig 4.10). Figure 4.10 shows MMP-1/-13 gene expression across the same experiment. MMP-13 showed significant repression in both the control and siCON samples that was lost in siALK5 treated samples (Fig 4.10A). MMP-1 showed repression in the control samples as expected (Fig 4.10B) but not in either siCON or siALK5 samples, where there appeared to be a significant increase in MMP-1 expression when TGFβ was present (Fig 4.10B). This was also seen in two other experiments (data not shown).

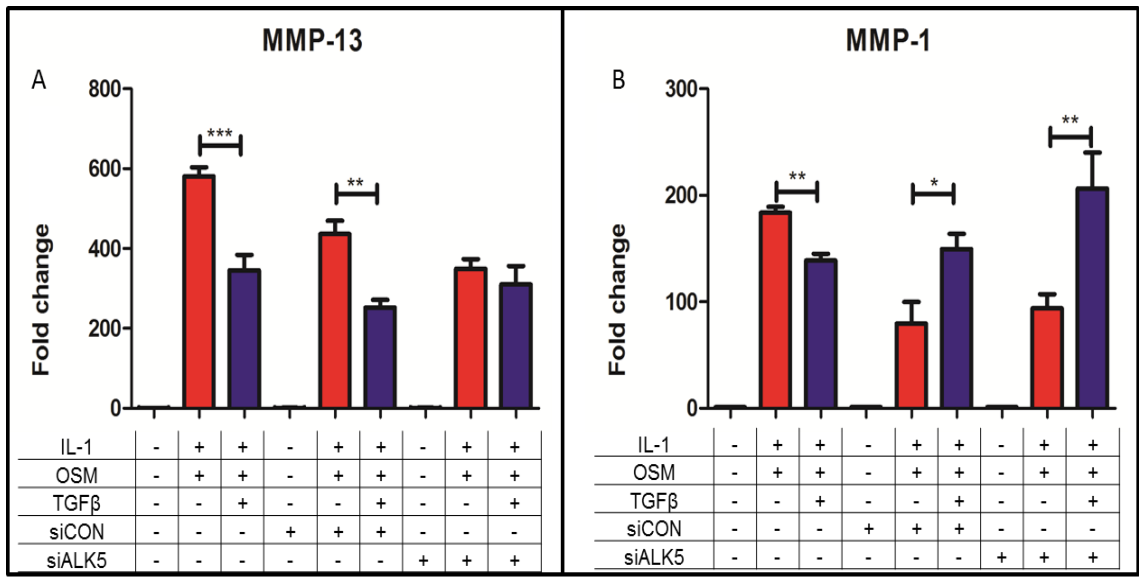


Figure 4.10 Effect of siRNA transfection on TGFβ-mediated MMP repression. SW1353 cells were stimulated for 24 hours with IL-1 (0.5ng/ml) +OSM (10ng/ml) ±TGFβ (10ng/ml), following 24 hour treatment with serum free media or 50nM of a non-targeting siRNA (siCON) or a siRNA specific to ALK5 (siALK5). qPCR was then performed on the isolated mRNA to measure A) MMP-13 expression B) MMP-1 expression. Data are presented as mean fold change relative to control ± SEM. N=5-6, representative of N=3 independent experiments on separate SW1353 cell populations. Statistics calculated using unpaired Student's t-test, where * p < 0.05; ** p < 0.01; *** p < 0.001.

4.4 Discussion

To build a model of TGF β I required a detailed understanding of how TGF β mediates its effect on IL-1+OSM over a period of time. TGF β needs 12 hours to mediate a repressive effect suggesting *de novo* synthesis is required, as the time delay provides sufficient time for the relevant protein, or proteins, to be transcribed and activated accordingly. The relevant protein, or proteins, are then present at 24 hours resulting in a robust repression across a range of concentrations (0.15ng – 10ng), with this repression being increased at 48 hours. Studies have demonstrated the protective effect of TGF β on chondrocytes is mediated through ALK5 (van Caam et al. 2015), and these effects may be lost as ALK1 becomes dominant.

Comparing their basal expression showed that ALK5 mRNA was 19 fold higher than that of ALK1, which is representative of what is normally found in young tissues (Blaney Davidson et al. 2009). It is documented that mRNA does not always correspond to protein expression (Vogel and Marcotte 2012) and downstream effects. It was not possible to compare the relative levels of ALK1 and ALK5 expression using a semi-quantitative approach such as Western blot. Instead I examined two proteins directly downstream of ALK1 (ID1) or ALK5 (PAI1) at two hours. This time point was chosen as it has been used to compare expression in cartilage tissue previously (Madej et al. 2013), and is a time when both genes can be upregulated depending on receptor composition. PAI1 showed increased expression whilst ID1 was unchanged confirming that TGF β is signalling through ALK5.

This did not confirm that ALK5 was responsible for the repressive effect of TGF β against IL-1+OSM, as TGF β activates a range of different responses through non-canonical pathways (Zhang 2009). Removing ALK5 from the system allowed me to verify its role in TGF β -mediated repression of MMP-13. This could not be verified for MMP-1 as siCON altered the effect of TGF β on IL-1+OSM. Off-target effects are known to occur during transfection (Baum et al. 2010). Non-targeting siRNAs are designed as negative controls as they undergo the same transfection protocols but should not target any genes. The siRNA used (ON-TARGET plus) is designed to minimise off-target effects, but in

the case of MMP-1 the effects seen appear to be a result of off-target effects. To explore the effect of ALK5 silencing on MMP-1 an alternative system would need to be used. I considered using a clustered regularly interspaced short palindromic repeats (CRISPR)-cas9 system to remove ALK5 without the off target effects. Unfortunately, the reagents to remove ALK5 were not commercially available so the primers for the system would have had to be designed, which can be a very time consuming process. Since I have a system that can remove ALK5 and appears to have no off target effects for MMP-13, I progressed without MMP-1. Another reason for this decision was the repression patterns of MMP-1/-13 at 24 and 48 hours. MMP-13 had greater repression at 48 hours in the IL-1+OSM+TGF β treatment than 24 hours, whilst MMP-1 has similar levels of repression at both 24 and 48 hours. This means that the model would have needed increased complexity to explain how both genes could be repressed, but in subtly different ways. Reducing complexity where possible is important for model design and as both are MMPs and MMP-13 is regarded as the most important in OA development I decided to progress with MMP-13, with the scope to return to MMP-1.

4.4.1 Pro-inflammatory interactions with TGF β signalling

Although this work showed ALK5 was required for TGF β -mediated repression, it was not clear how ALK5 enabled these effects. There are numerous interactions between these three factors (TGF β , IL-1 and OSM) that could be responsible for the effect that is seen. TGF β induction of JunB is mediated by the ALK5 pathway; once transcribed it has been shown to interact with c-Jun, an important component of the activator protein 1 (AP1) complex that controls upregulation of both MMP-1 and -13 (Ponticos et al. 2009). JunB upregulation may cause competitive inhibition of the AP1 complex that limits the production of these key matrix-degrading enzymes. There are also reports that Smad3 can bind to, and inhibit the AP1 sites directly leaving fewer sites available for the activated AP1 complex to bind to and induce expression of the MMPs (Zhang et al. 1998). Chen et al. (2012) showed Smad3 helped to maintain the balance of cartilage synthesis by inducing Collagen II expression whilst repressing Runx-2 inducible MMP-13 expression. They suggest this effect was through the actions of Histone deacetylase 4 (HDAC4), which is known to bind to and repress the

MMP-13 promoter (E. Shimizu et al. 2010). This protective effect has been questioned by other reports claiming the opposite is true and HDAC4 is responsible for an increase in MMP-13 (Lu et al. 2014; Queirolo et al. 2016). The protective effect may also be a result of upregulation of proteins such as TIMPs, which counteract the effects of MMP-1/-13 (Leivonen et al. 2013). It is also possible that TGF β could interact with the receptors that mediate the IL-1 and OSM response.

4.4.2 Age-related changes to pro-inflammatory TGF β interactions

Cartilage in older mice has a reduced ability to repair after treatment with IL-1 and changes in TGF β signalling appear to have a key role in this change (Davidson et al. 2005). If we assume, based on the evidence, that the protective effect against pro-inflammatory stimuli shown by TGF β is mediated entirely by an ALK5-dependent response, then what happens when it signals through ALK1 could potentially be very interesting. When signalling through ALK1, TGF β has been shown to upregulate MMP-13 (Blaney Davidson et al. 2009). The addition of a pro-inflammatory stimuli, such as IL-1 + OSM, could result in an even greater increase in MMP-13 and conceivably MMP-1. It has been shown that IL-1+OSM represents a good model of pro-inflammatory stimulus (Chan et al. 2017). Signalling through ALK1 has also been demonstrated to increase the phosphorylation of p38 (C. G. Chen et al. 2012), which is important in IL-1+OSM, AP1-driven, MMP-1 and -13 upregulation (Proctor et al. 2014). Both these findings suggest an increase in matrix-degrading proteins, which would be very damaging in a patient. TGF β would be released, intended to reduce the inflammatory response, but instead would only serve to exacerbate the situation by increasing matrix degradation. It is also possible that the change in signalling would then result in an upregulation of Smad6, a primary regulator of ALK1 signalling (König et al. 2005), which could then start to target ALK1 for destruction by one of the Smurf proteins (as Smad7 may do for ALK5). It is also worth noting that ALK1 requires ALK5 in order to have an effect, so the reduction in ALK5 protein may also affect its ability to signal (M. J. Goumans et al. 2003). The change from ALK5 to ALK1 signalling as well as the actions of the Smurfs proteins could potentially contribute to what could be an intriguing but complex interaction between TGF β , IL-1 and OSM.

4.4.3 Summary

- TGF β represses the IL-1+OSM-driven upregulation of MMP-1/-13 mRNA, post 12 hours. This repression is robust by 24 hours and increased at 48 hours for MMP-13. For MMP-1 the repression is robust at 24 and 48 hours but is at a similar level.
- TGF β must bind to ALK5 receptors to repress IL-1+OSM-driven upregulation of MMP-13 mRNA.

Chapter 5. Modelling the changing effects of TGF β on pro-inflammatory stimuli with age.

5.1 Introduction

The data presented throughout chapters 3 and 4 demonstrated why I chose TGF β as the pathway to design and build a computational model around. The TGF β -mediated repression of IL-1+OSM-driven MMP-13 expression data, presented in both chapters, was key to this decision, as well as the data that I will base model construction upon throughout this chapter. In order to better understand the interaction TGF β has with IL-1+OSM, I will modify and combine two previous models (Proctor et al. 2014; Wang Hui et al. 2014) looking at how TGF β mediates its effect and how it changes with age.

The signalling cascades for both IL-1 and OSM are complex and include a lot of cross talk. Their synergistic upregulation of MMP-13 seems to be mainly caused by their effect on activator protein 1 (AP-1). IL-1 binds to the IL-1 receptor (IL-1R) and by a series of downstream regulators leads to phosphorylation of c-Jun; this, in turn, binds to c-Fos forming a transcriptionally active part of AP-1 (Chambers et al. 2013). This heterodimer has a high affinity for the promoter regions of the MMPs (Chambers et al. 2013). Regardless, c-Fos mRNA has a short half-life and as IL-1 only slightly increases its transcription, the majority of c-Jun forms homodimers which have a much lower affinity for DNA promoter regions (Sen and Packer 1996). Previous studies suggest that p38 can phosphorylate c-Fos resulting in increased transcription (Tanos et al. 2005). OSM signals primarily through the JAK/STAT pathway which can stimulate p38-mediated phosphorylation of c-Fos (Tanos et al. 2005). The resulting c-Fos/c-Jun heterodimers may result in changes of AP-1 composition that could explain the synergistic effect both cytokines have on MMP-13 expression (Proctor et al. 2014). I have demonstrated that the protective effect of TGF β requires the ALK5 receptor but how is unknown. My initial hypothesis, based on literature and work done previously by our group, was that JunB was leading to competitive inhibition of the AP-1 complex that mediated the repression.

In this chapter I will design and test a model that expands on how TGF β could mediate this repression through ALK5, and how this might change as it moves

towards ALK1. I will build upon a section of a model presented by Wang Hui et al. (2014) which explored age-related changes such as increased levels of oxidative stress, apoptosis, MMP-13 and a decrease in chondrocyte autophagy. Part of the simulation looked at the change in ALK1/ALK5 receptors over 30 months in a mouse model and the downstream effects of these changes i.e. increasing MMP-13. The model looked at both the deterministic and stochastic elements of the pathway, matching them to immunohistochemistry data taken from mice between 3-30 months (Wang Hui et al. 2014). I will take this section of the model and combine it with another model (Proctor et al. (2014) which showed the effect of IL-1+OSM treatment on cartilage cell cultures.

5.1.1 ODE modelling for TGF β signalling.

I will be using an ODE system to model TGF β because my network, although relatively large for an ODE model, will not require excess computing power for any tasks. Using ODE will allow me to generate a detailed understanding of the system that can be altered to match generated data and also make future predictions. As it is also the most commonly used system for TGF β studies it will give me a wealth of information to draw on. Careful planning of models before starting is important for structure and parameters (Hasdemir et al. 2015). Therefore having previous models assisted with this design. A PN model would be unfavourable as the intricate details would be difficult to design. Boolean networks are difficult to represent time accurately and also do not allow for deterministic simulation, both of which will be important for matching the model to experimental data. Finally LP and ABM are both in their infancy for examining these types of systems. Therefore, using either system would require substantially more effort for no reward.

Mass action kinetics will be used for the model, as it is the most used rate law for mathematical and biological studies that some argue requires no justification (Voit et al. 2015). In this case my justification is that the two models that the majority of my network is based on are built using mass action equations, which proves it can be implemented for this type of study. Although they could be adapted, mass action also allows me to switch with ease between deterministic and stochastic simulations, allowing me a deeper understanding of the model

interactions. Other functions do not allow this, as they are either unsuitable for stochastic simulation or must be modified to accommodate it, which then makes them unsuitable for deterministic. Mass action kinetics works from the principle that the reaction rate is proportional to the probability that reactants will collide (Voit et al. 2015). It takes into account the concentration of reactants, the power of their molecularity and how many are involved in the reaction (Voit et al. 2015).

Advances in computing power have also allowed complex modelling that would have previously been impossible. This has led to an increase in the number of biologists using computational modelling to unravel complex systems. As a result there has been a number of modelling tools designed to facilitate their move into an area that was once exclusively for mathematics and physics researchers. Most approaches have associated programmes, Boolean using CellNetAnalyzer for example (Klamt et al. 2007). However, ODE modelling has been the most used and has resulted in a number of programmes being made available, including but not limited to simbiology, SBTOOLBOX (both Matlab plugins) (MATLAB vR2016a, The MathWorks Inc., Natick, MA) and COPASI (S. Hoops et al. 2006). My model has been built in COPASI as it contains many tools including pre-set or custom functions; the input of events; deterministic, stochastic and hybrid simulations as well as a multitude of analysis tools such as: sensitivity analyses, parameter estimations and parameter scans amongst others. It is also well maintained and constantly being improved upon. Finally, I believe it has the most user friendly interface.

5.1.2 Chapter aims

- Alter and combine two previous computational models to create a model that represents IL-1+OSM+TGF β signalling, whilst still matching the profiles seen by the original models.
- Match the model simulation output to data created in the previous chapters.
- Test the model by showing its ability to match novel experimental data, without modification. Then alter the structure if it cannot.
- Use the model to explore how TGF β will affect IL-1+OSM-driven MMP-13 expression with age, as ALK1 becomes the dominant receptor.

5.2 Model construction

In order to create my model I first had to alter the previously published models separately to make them compatible. In order to ease the computational burden I also reduced complexity where possible, removing or altering any interactions that were not necessary for what I was studying. Combining both models in their original forms would have resulted in a very large model, which would have been difficult to parameterise and simulate.

5.2.1 IL-1+OSM

The original IL-1+OSM model was presented in three sections, OSM, pro-MMP activation and IL-1 (Proctor et al. 2014) all of which can be seen in appendix 5.1. As I was only looking at MMP-13 mRNA and had no interest, at that time, in its transition to an active MMP, I removed the pro-MMP activation component completely. The remaining two sections were simplified but still fit the same profiles. To achieve this some approximations were made: Three proteins were originally present in the model: DUSP16, MKP1 and PP4. As these were upregulated by the same source and only relevant for blocking, I replaced all three of these species with one “block” species. This blocked all three reactions that the original proteins did. However, each reaction was blocked at a different rate, in order to have the same effect that the original proteins would have had. The receptor profile for IL-1 was changed to include an internalisation step that replaced the need for IRAK and TRAF6. The phosphorylation and subsequent nuclear translocation of STAT3 was altered so that it could be represented by a single reaction. Finally any mRNAs that were produced, other than MMP-13, were removed. The resulting model is represented in Figure 5.1.

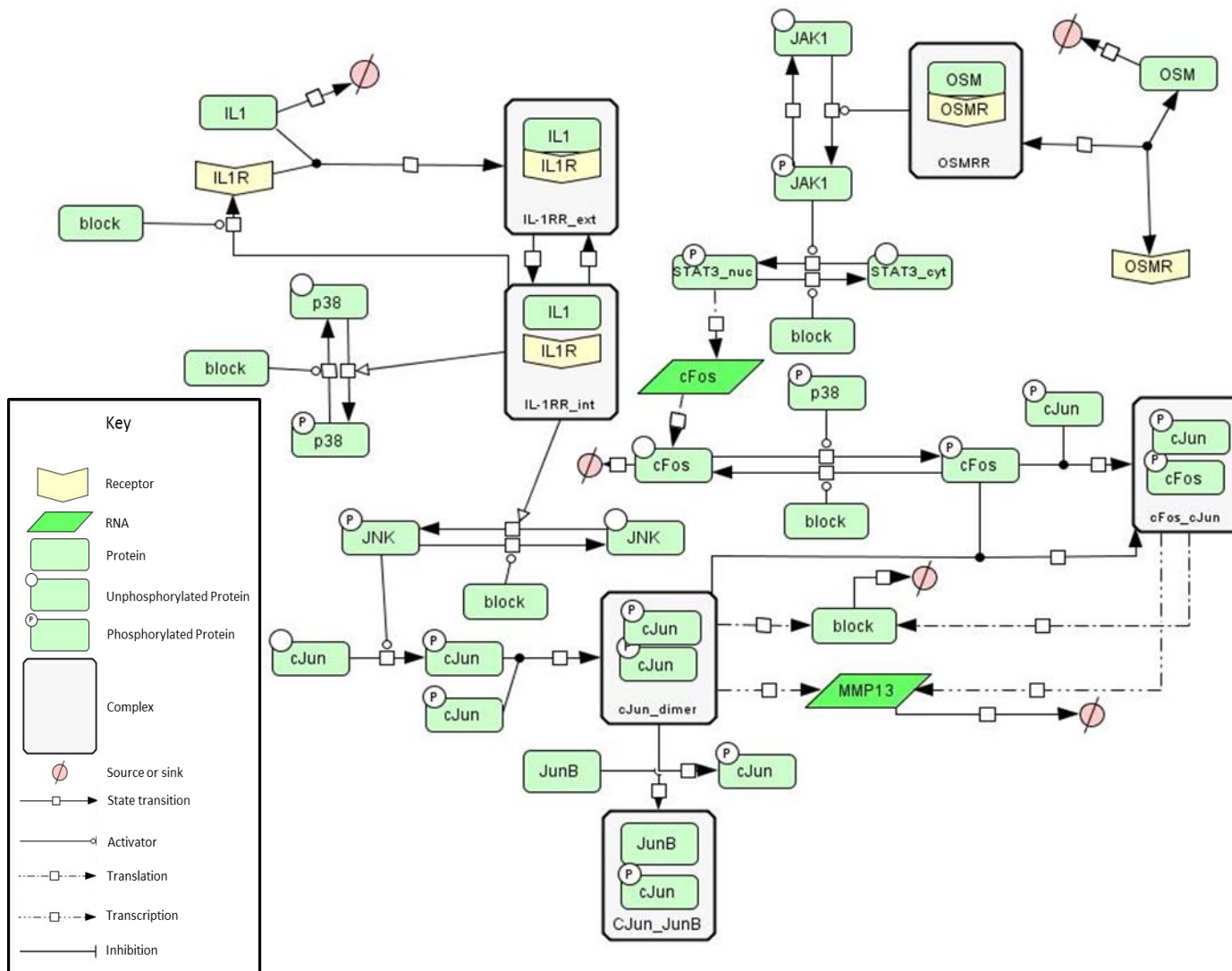


Figure 5.1 **Network diagram showing species and reactions involved in the IL-1+OSM response.** Schematic representation of the simplified IL-1+OSM signalling section of my newly developed model. CellDesigner was used to create the schematic.

5.2.2 TGFβ

The TGFβ section of the model is based on the TGFβ section, described in Wang Hui et al. (2014), which can be seen in appendix 5.2. It had only minor alterations in comparison to the IL-1+OSM section. This was for two reasons:

1. It was a smaller model.
2. It was the pathway being explored so required more detail.

The biggest change was the removal of the SOX9, aggrecan and collagen component from the original model as I had no interest in their expression at this time. MMP2 was completely removed as it had no effect on the model in this form. The role of active RUNX2 was also altered, no longer inducing the production of pro-MMP-13 but instead producing MMP-13 mRNA. This change was reasonable as RUNX2 induced upregulation of MMP-13 has been shown to be at the mRNA level (Ijiri et al. 2005).

The original models had not been created to be combined and as a result they did not share any interactions. Therefore, I performed a literature search to identify some ways IL-1, OSM and TGFβ may interact. I then altered my version of the model to facilitate TGFβ and IL-1+OSM interactions. The first alteration was JunB production through SMAD2 (which represents SMAD2/3 as explained in chapter 2.3.3) signalling because there is a substantial body of evidence showing that it is a direct downstream target of SMAD3 (Ponticos et al. 2009; Gervasi et al. 2012) and works to antagonise rapid gene transcription (Mauviel et al. 1996; Verrecchia et al. 2001; Selvamurugan et al. 2004). Studies have shown it can displace c-Fos in the AP-1 complex and bind to c-Jun (Ponticos et al. 2009; Mauviel et al. 1996). It has also been demonstrated to limit the effects of IL-1, in particular its effect on MMP synthesis (Emi Shimizu et al. 2010). Finally it has been shown to repress gene expression in epithelial–mesenchymal transition in cancer due to upregulation by TGFβ. This demonstrates TGFβ can produce significantly high JunB expression to limit gene transcription (Gervasi et al. 2012). SMAD1 signalling could also now lead to an increase in p38 phosphorylation, as shown in C. G. Chen et al. (2012). Figure 5.2 shows the complete TGFβ section of my model.

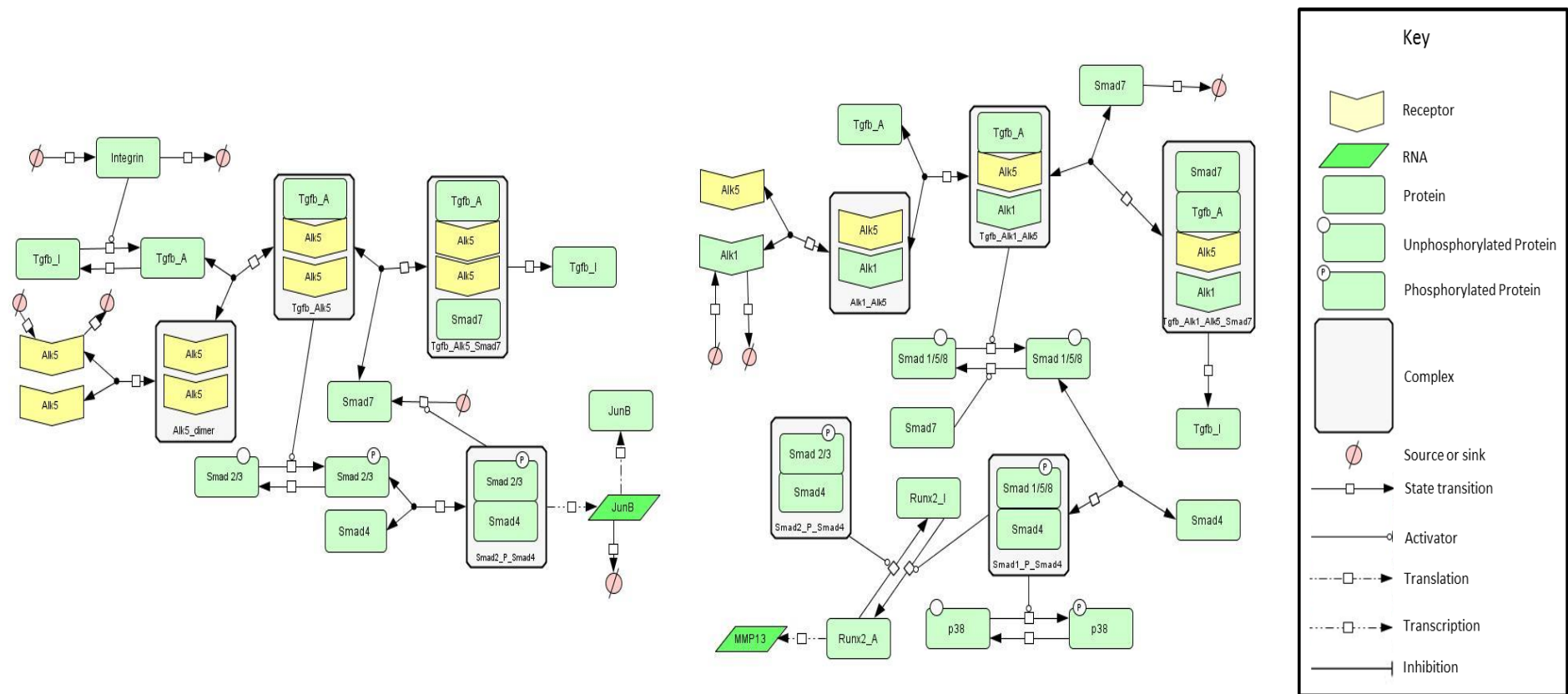


Figure 5.2 **Network diagram showing all the species and reactions involved in the TGFβ pathway.** Schematic representation of the modified TGFβ section in my newly developed model. CellDesigner was used to create the schematic.

5.3 Model parameterisation

After altering the structure of the two model components, I combined them together to form my complete model (Fig 5.3). The original parameters from both models were also incorporated and the parameters for the newly added reactions were assigned default values. With this model I attempted to match the simulation output to the data that were generated in chapters 3 and 4.

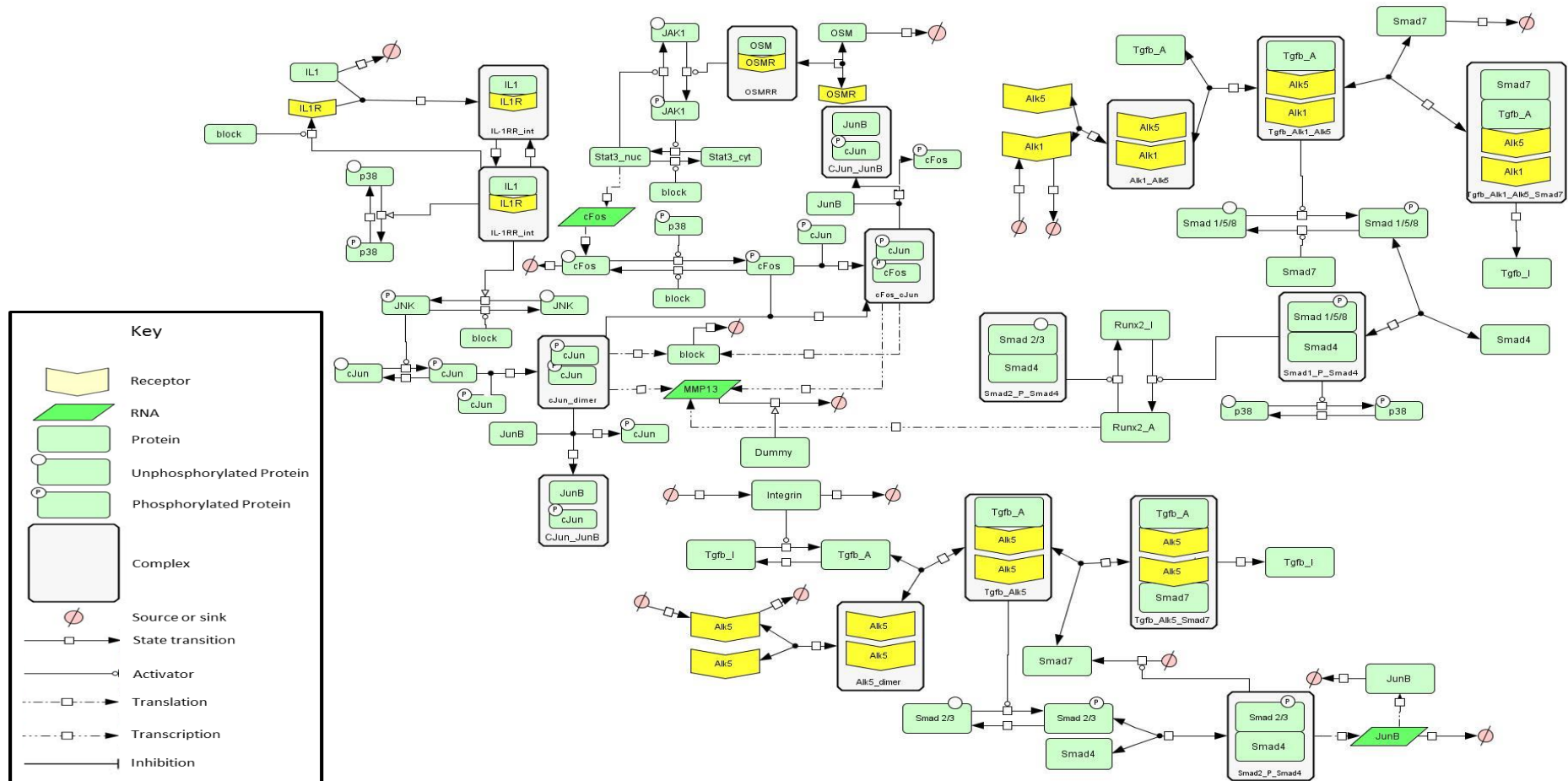


Figure 5.3 **Network diagram showing species and reactions involved in the IL-1+OSM+TGFβ model.** Schematic representation of my complete model. Detailing all interactions between the IL-1, OSM and TGFβ signalling pathways. The “block” species is involved in multiple reaction but represents one species upregulated by cJun_dimers or cFos_cJun and provides a negative feedback for multiple reactions but at different rates. CellDesigner was used to create the schematic.

5.3.1 Model fit with hypothesised AP-1 competitive inhibition.

Initially in the model, TGF β only interacted with the IL-1+OSM response via the JunB protein which was being synthesised by phospho-SMAD2 upon addition of TGF β . This in turn provided competitive inhibition to the formation of AP-1 components (c-Jun homodimers and c-Jun/c-Fos heterodimers) (Fig 5.3). I attempted to match this structure to the time course data generated in chapter 3 and 4 using parameter estimations (Fig 5.4). The complete model appeared to fit these data (Fig 5.4) but when the model was compared with and without TGF β , the addition of TGF β had no effect (Fig 5.5). The parameter estimations had matched the data by changing IL-1+OSM signalling rather than by the involvement of TGF β signalling.

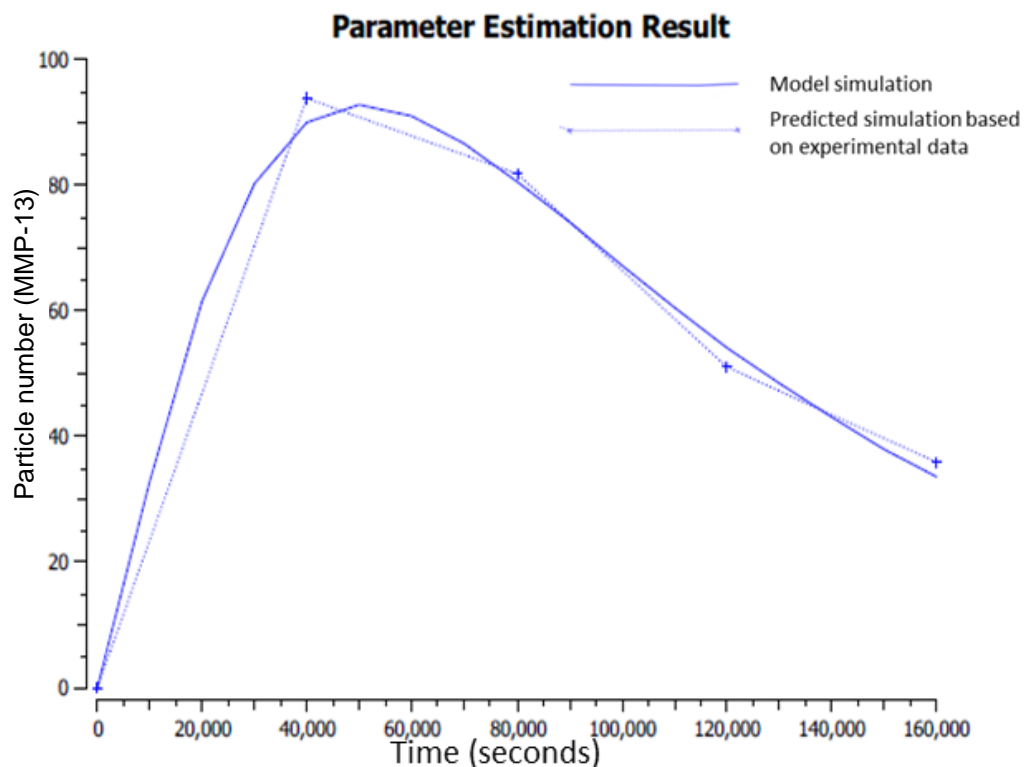


Figure 5.4 **Fitting the model using only AP-1 competitive inhibition.** Results of parameter estimation ran using COPASI, which allowed alterations to all the reactions from the model presented in Fig 5.3. The genetic algorithm was used to match MMP-13 mRNA simulation data, during IL-1+OSM+TGF β treatment, to that generated in SW1353 cells. The cross marks represent what the particle number should be at the given time point in order to match the level of repression seen in SW1353 cells. The solid line shows the model output whilst the dashed line shows the simulation COPASI aimed for based on the experimental data. The genetic algorithm was executed for 1000 generations with a population size of 20, followed by Hooke and Jeeves with an iteration limit of 50.

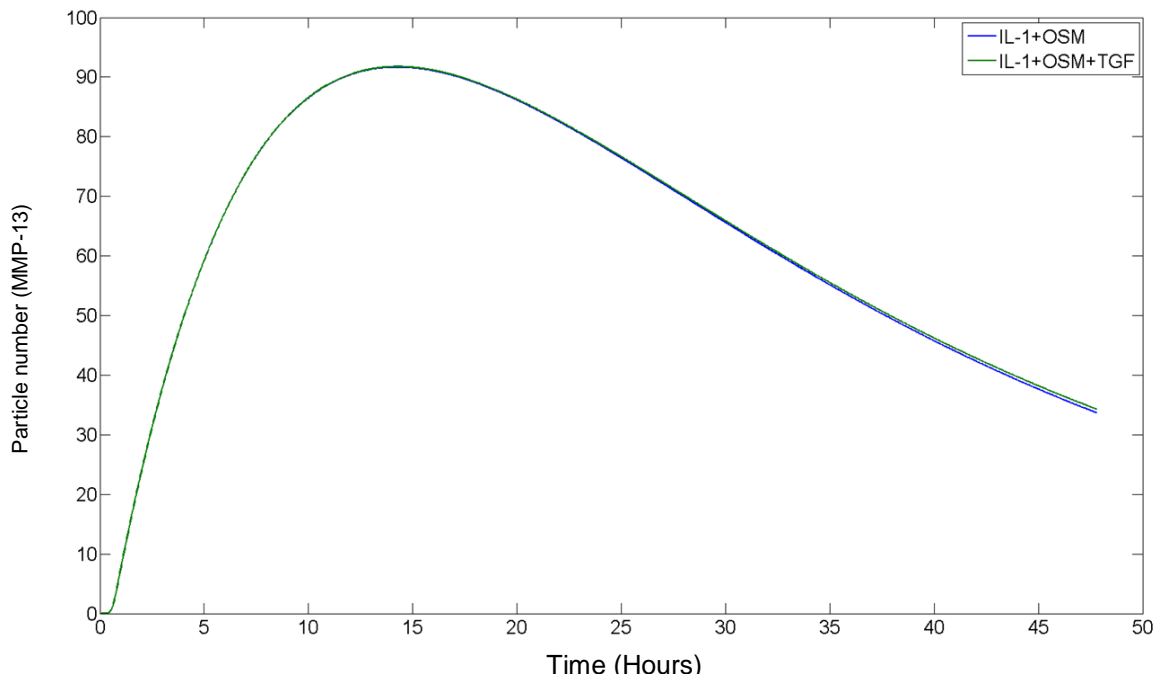


Figure 5.5 Effect of TGFβ over 48 hour simulation. Deterministic simulation results showing the effect of IL1+OSM±TGFβ treatment on the fully parameterised model presented in Fig 5.3, over a simulation time of 48 hours. An active form of TGFβ is present in the model to replicate experimental conditions. Curves show how the particle numbers of MMP-13 mRNA change over the simulation. Simulations were run using COPASI.

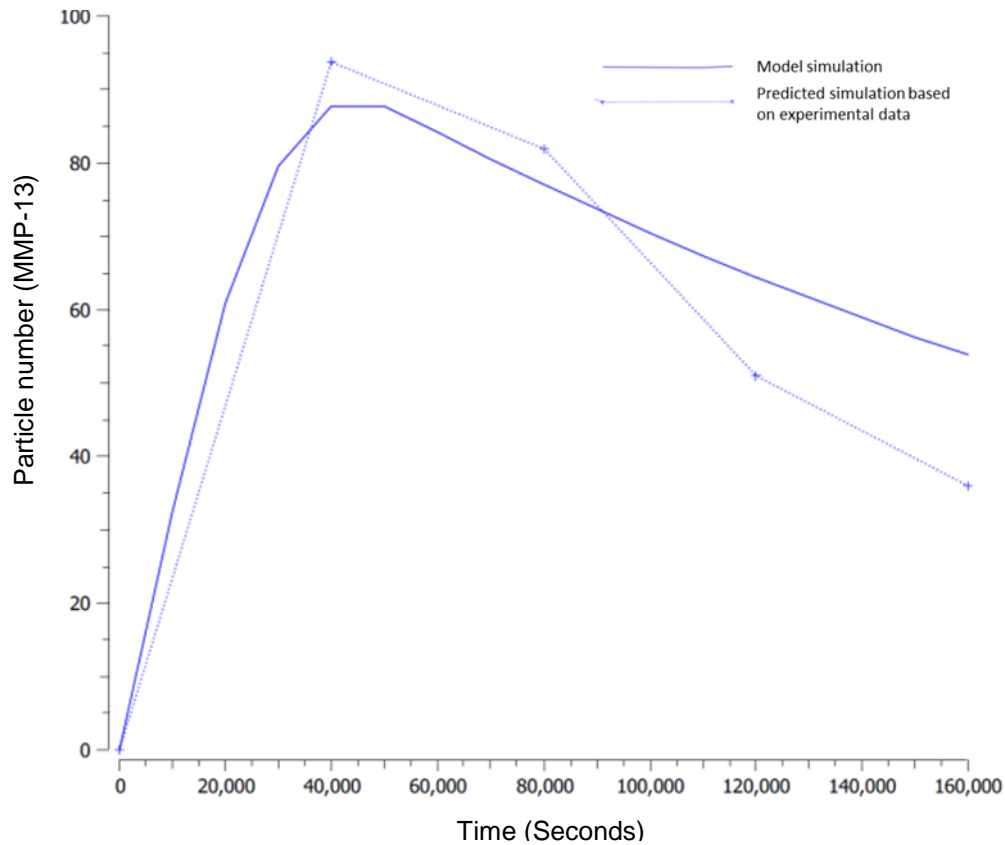


Figure 5.6 **Parameter estimation based on experimental data.** Results of a parameter estimation run using COPASI for the model presented in Fig 5.3, which allowed alterations to the reactions affected by TGF β addition but not IL-1+OSM. The genetic algorithm was used to match MMP-13 mRNA simulation data, during IL-1+OSM+TGF β treatment, to that generated in SW1353 cells. The cross marks represent what the particle number should be at the given time point in order to match the level of repression seen in SW1353 cells. The solid line shows the model output whilst the dashed line shows the simulation based on the experimental data. The genetic algorithm was executed for 1000 generations with a population size of 20, followed by Hooke and Jeeves with an iteration limit of 50.

5.3.2 Model fit with only mRNA degradation

I hypothesised that the extra repression seen at 48 hours may be a result of TGF β stimulation being able to increase the degradation of MMP-13 mRNA. I was unsure what may mediate this but I incorporated it into the model structure using a dummy species, upregulated by SMAD2, which could degrade MMP-13 mRNA. It was upregulated by SMAD2, as I showed previously that repression cannot occur without ALK5. The updated model can be seen in Figure 5.7. Figure 5.8 is a vastly simplified schematic, which focuses on the receptor interactions that mediate IL-1, OSM and TGF β effects.

As I had tried to fit the model with only JunB I wanted to check if the model could fit the data with only this newly added component active (Fig 5.9A), before combining both interactions. I found it could match the pattern of repression seen in the experimental data at the early and late time points (Fig 5.9B). However, when I altered the levels of active TGF β in the model it had a substantial effect on the repression (Fig 5.9C). This was contrary to what was seen in the experimental data, where a change in TGF β concentration had little effect on repression (Fig 5.9D)

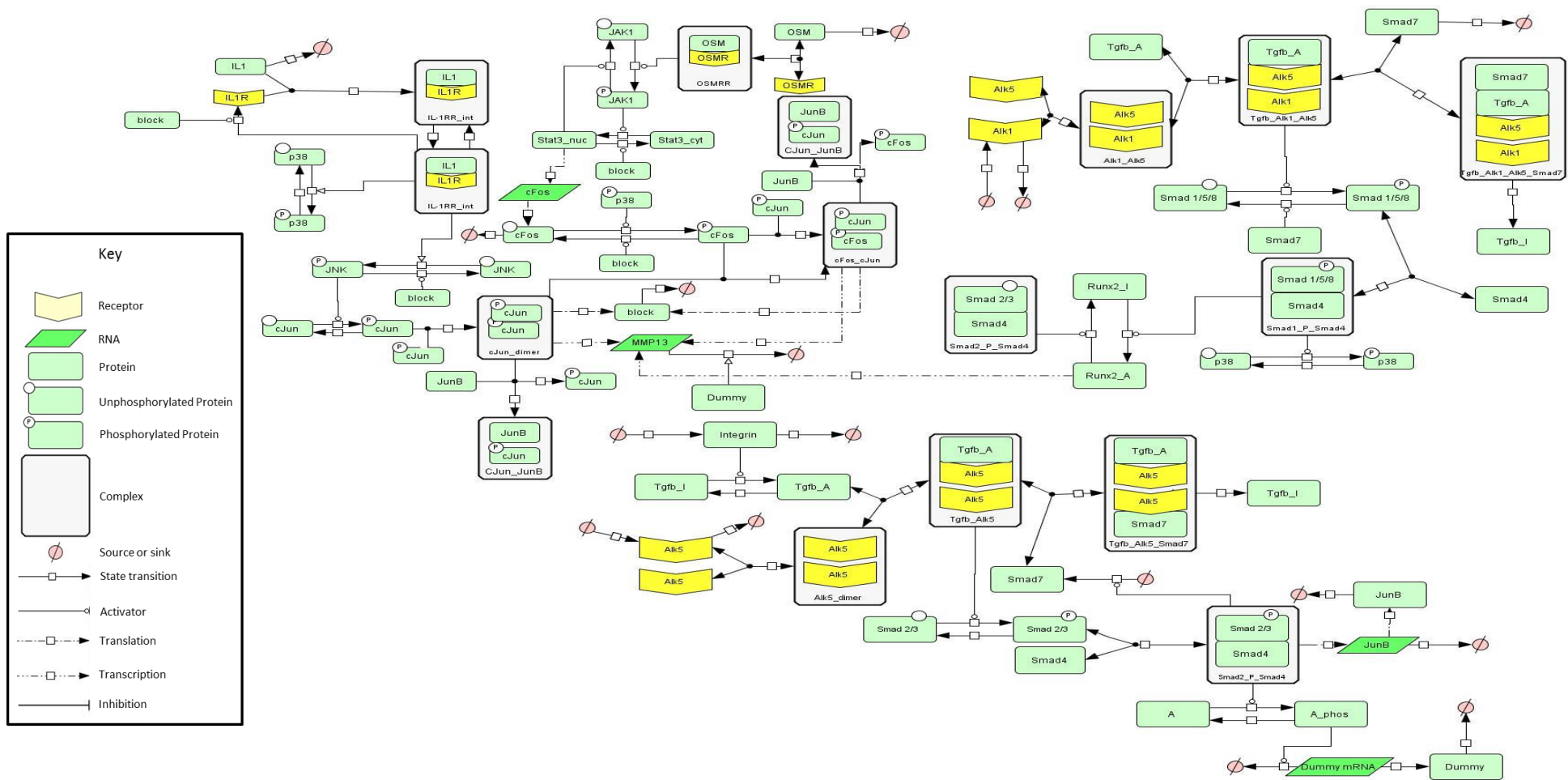


Figure 5.7 **Network diagram showing all species and reactions involved in the IL-1+OSM+TGFβ model.** Schematic representation of the complete model. Detailing all interactions between the IL-1, OSM and TGFβ signalling pathways. Though similar to Figure 5.3, the dummy species has now been added that can degrade MMP-13 mRNA. CellDesigner was used to create the schematic. The “block” species is involved in multiple reaction but represents one species upregulated by cJun_dimers or cFos_cJun and provides a negative feedback for multiple reactions but at

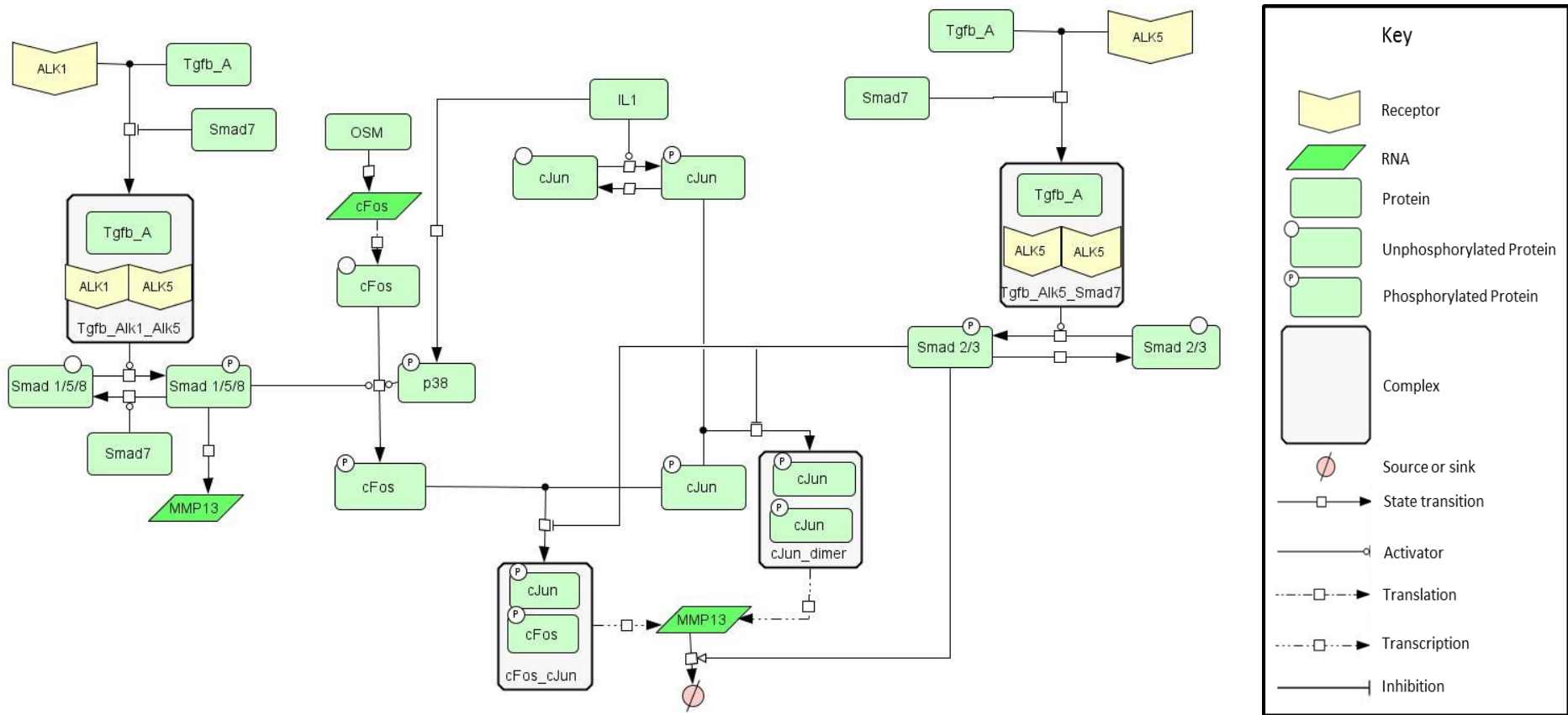


Figure 5.8 **A simplified network diagram showing the key interactions between the IL-1, OSM and TGFβ components.** Schematic representation showing a simplified version of the model presented in Figure 5.7. The focus is specifically on the key reactions that mediate the interactions between IL-1, OSM and TGFβ. CellDesigner was used to create the schematic.

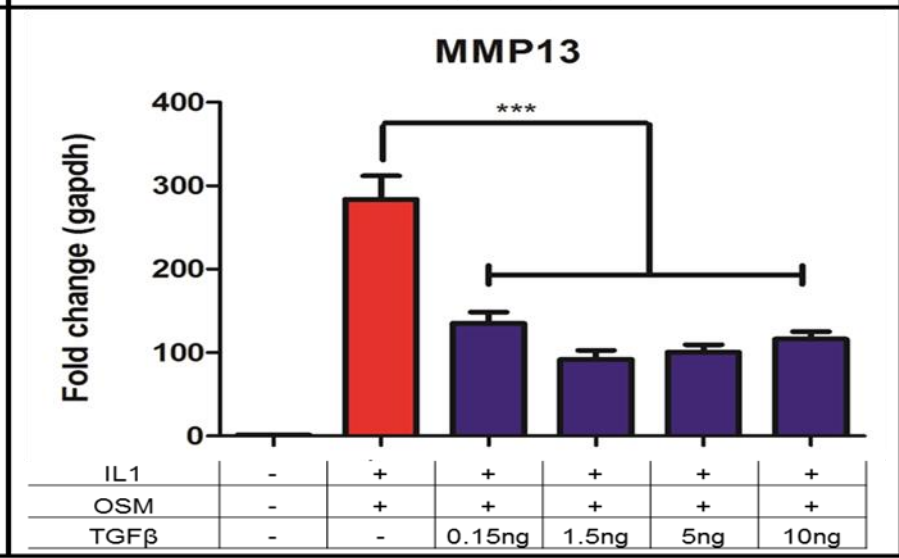
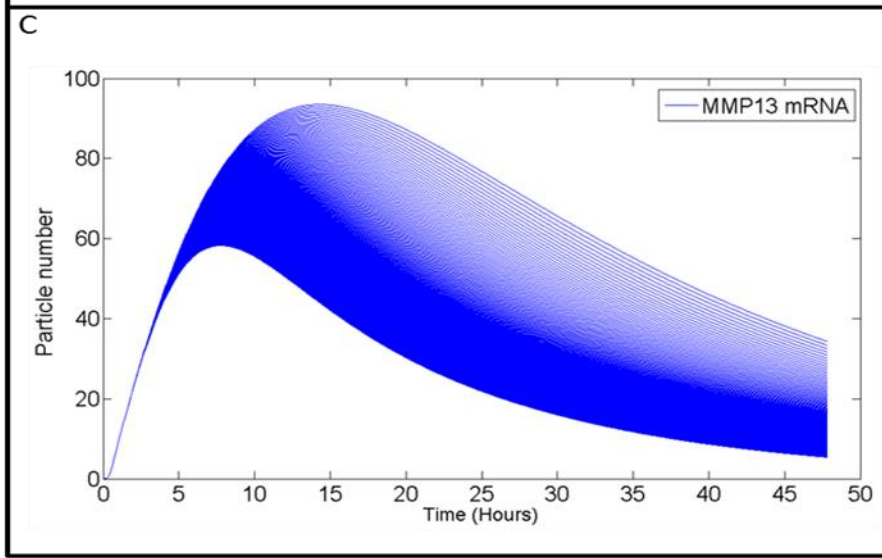
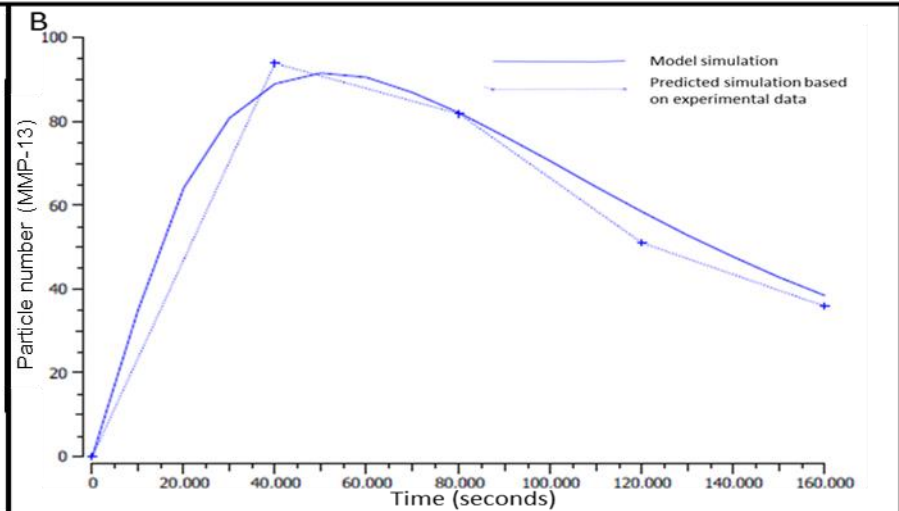
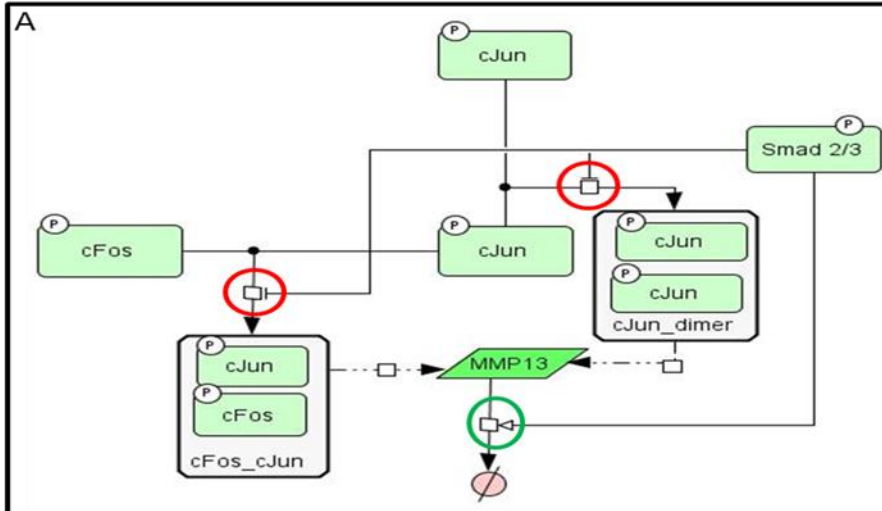


Figure 5.9 **Using MMP-13 mRNA degradation to fit the model.** A) Schematic representation of a section of the model presented in Fig 5.8 highlighting the interactions between AP-1 components (upregulated by IL-1+OSM) and SMAD2 (phosphorylated by TGF β). The green circles show the active components whilst the red curve shows inactive component (during this simulation). B) Results of a parameter estimation ran using COPASI for the model presented in Fig 5.7 using the components active in A. Alterations to the reactions affected by TGF β addition are allowed but not for IL-1+OSM. The genetic algorithm was used to match MMP-13 mRNA simulation data, during IL-1+OSM+TGF β treatment, to that generated in SW1353 cells. The cross marks represent what the particle number should be at the given time point in order to match the level of repression seen in SW1353 cells. The solid line shows the model output whilst the dashed line shows the simulation based on the experimental data. The genetic algorithm was executed for 1000 generations with a population size of 20, followed by Hooke and Jeeves with an iteration limit of 50. C) Simulation results from a deterministic parameter scan (post parameter estimation in B) changing the concentration of active TGF β in the model by 1000 fold. Run using COPASI over a 48 hour simulation shows how the change affects MMP13 mRNA expression. D) Data are first presented in chapter 4 (Fig 4.4). qPCR data for SW1353 cells treated for 24 hours with IL-1+OSM or IL-1+OSM+TGF β at concentrations ranging from 0.15ng to 10ng. *** $p < 0.001$.

5.3.3 Model fit with both AP-1 inhibition and mRNA degradation

Running the parameter estimations, with both AP-1 complex inhibition and the mRNA degradation components active (Fig 5.10A) allowed me to match the simulation data to experimental data (Fig 5.10B). When both of these components were active, changing the concentration of TGF β had only a minor effect on the simulation output (Fig 5.10C). This was in stark contrast to the effect seen when only mRNA degradation was active (Fig 5.9) and was a better match to the experimental data (Fig 5.10C and D). Figure 5.11A shows the model output when simulated with or without TGF β present. These simulation data were representative of the original time course data generated in chapter 4. There was little difference between IL1+OSM \pm TGF β simulations at 6 and 12 hours, whereas at 24 hours TGF β results in 37% repression increasing to 73% by 48 hours (Fig 5.11A). This closely mirrored the 42% repression, increasing to 69% at 48 hours, that was seen in SW1353 cells (Fig 5.11B).

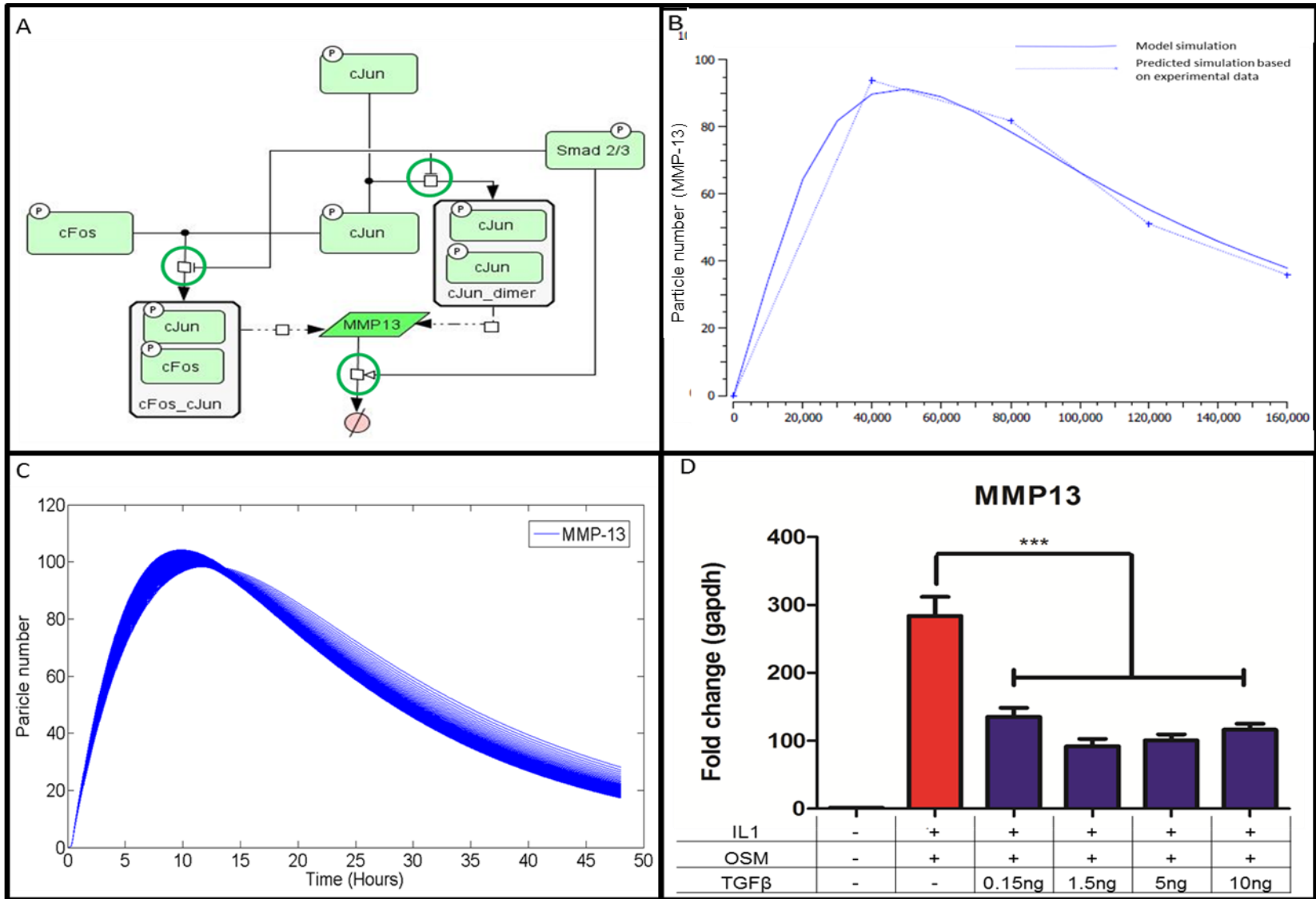


Figure 5.10 **Fitting the complete model to experimental data.** A) Schematic representation of a section of the model highlighting the interactions between AP-1 components (upregulated by IL-1+OSM) and SMAD2 (phosphorylated by TGF β). The green circles show the active components whilst the red shows inactive component (during this simulation). B) Results of a parameter estimation ran using COPASI for the model presented in Fig 5.7 using the components active in A. Alterations to the reactions affected by TGF β addition are allowed but not for IL-1+OSM. The genetic algorithm was used to match MMP-13 mRNA simulation data, during IL-1+OSM+TGF β treatment, to that generated in SW1353 cells. The cross marks represent what the particle number should be at the given time point in order to match the level of repression seen in SW1353 cells. The solid line shows the model output whilst the dashed line shows the simulation based on the experimental data. The genetic algorithm was executed for 1000 generations with a population size of 20, followed by Hooke and Jeeves with an iteration limit of 50. C) Simulation results from a deterministic parameter scan (post parameter estimation) changing the concentration of active TGF β in the model by 1000 fold. Ran using COPASI over a 48 hour simulation time, it shows how the change affects MMP13 mRNA over 48 hours. D) Data were first presented in Fig 4.4. qPCR data for SW1353 cells treated for 24 with IL-1+OSM \pm TGF β at concentrations ranging from 0.15ng to 10ng. *** $p < 0.001$ vs IL-1+OSM.

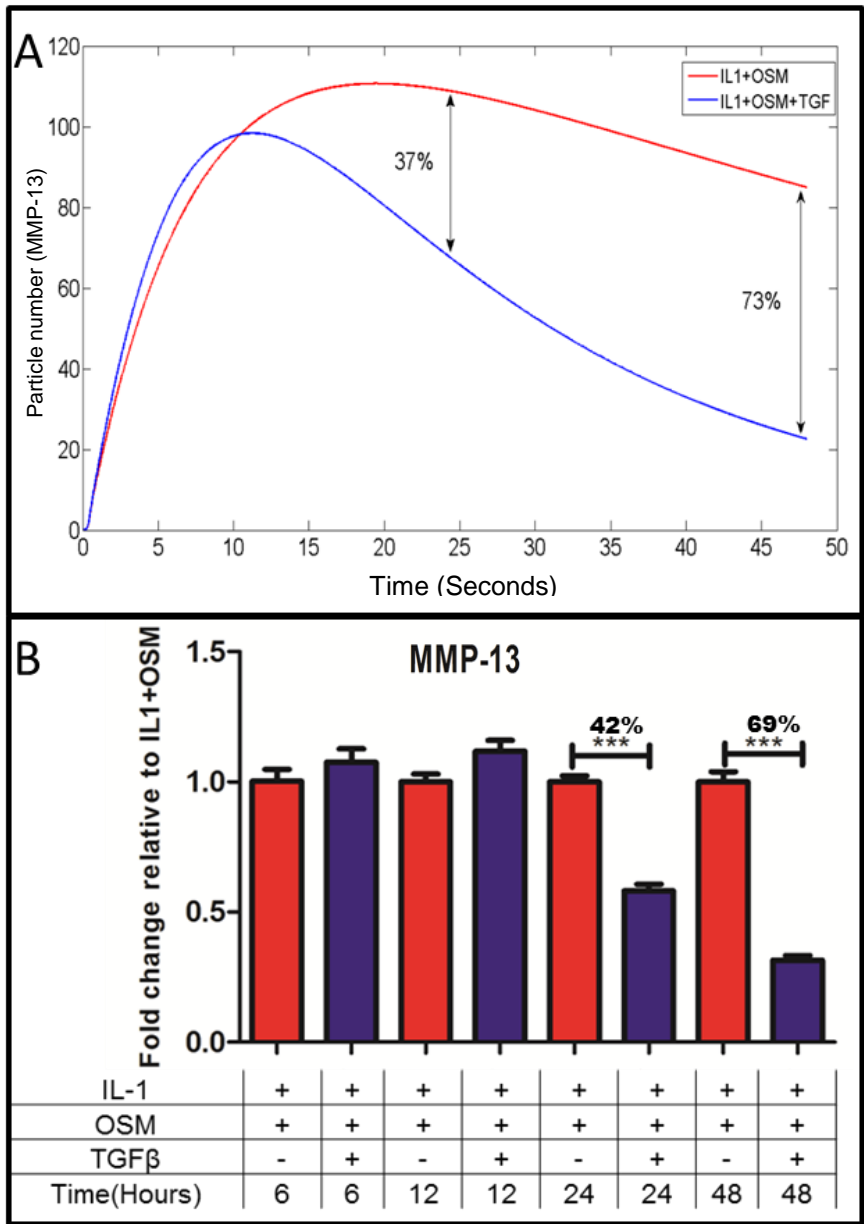


Figure 5.11 **Complete model run for 48 hours ± TGFβ**. A) Deterministic simulation results showing the effect of IL1+OSM±TGFβ treatment on the fully parameterised model presented in Fig 5.7, over a simulation time of 48 hours. An active form of TGFβ is present in the model to replicate experimental conditions. Curves show how the particle numbers of MMP-13 mRNA change over the simulation. The black arrows show the percentage of repression seen at 24 and 48 hours, caused by TGFβ addition. Simulations were run using COPASI. B) Data are first present in Figure 4.5. Shows the average expression of MMP-13 at 6, 12, 24 and 48 hours in cells treated with IL1+OSM ±TGFβ. *** p < 0.001. The percentages represent the amount of repression mediated by TGFβ at the given time point.

As both AP-1 complex inhibition and mRNA degradation were necessary for the model to fit the data, I looked at the effect that removing either one had on the complete model. Removing AP-1 complex inhibition, via JunB, resulted in a higher peak at 12 hours. Removing mRNA degradation, via the dummy species, resulted in the repression at 24 and 48 hours being reduced. This suggested JunB limits the initial peak of MMP-13 expression, whilst increased mRNA degradation was responsible for mediating the high levels of repression seen at the later time points (Fig 5.12).

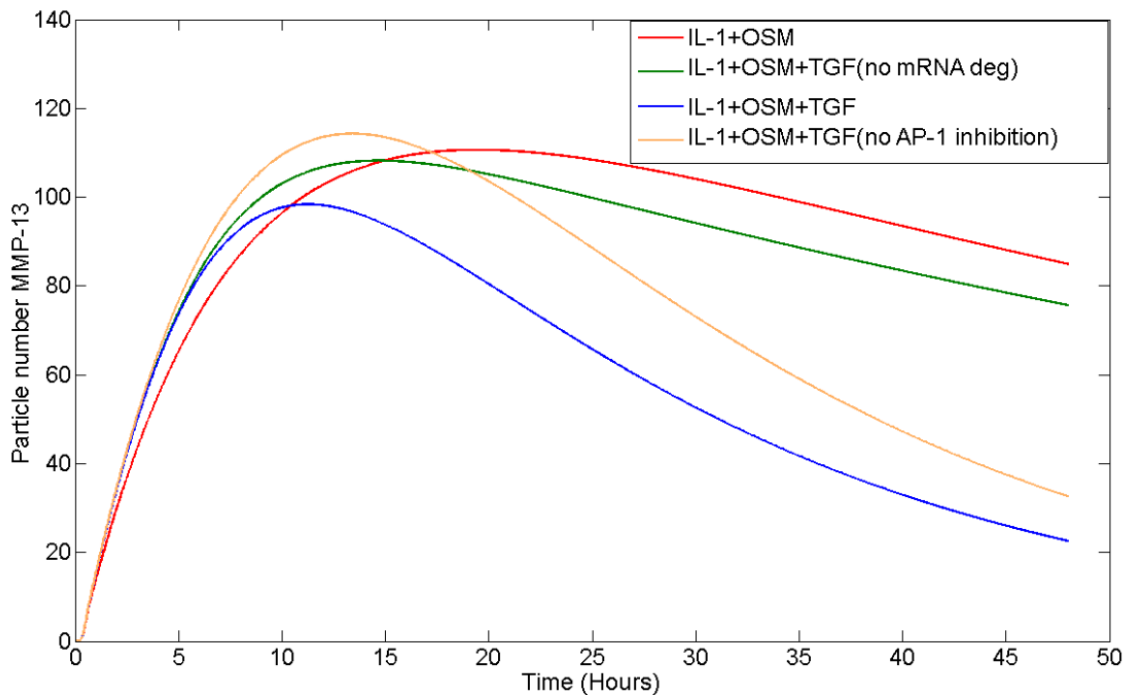
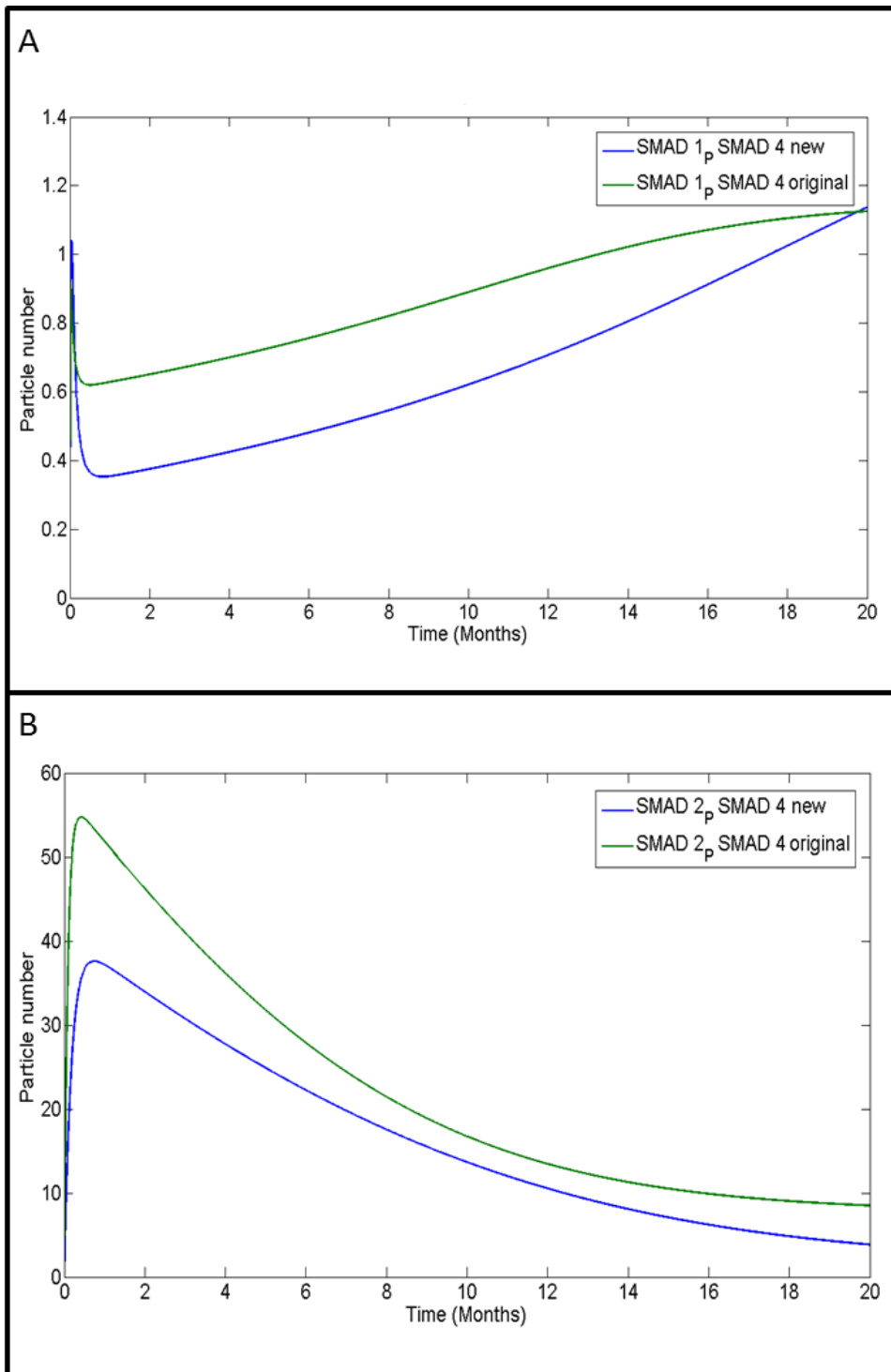


Figure 5.12 **Effects of mRNA degradation and AP-1 complex inhibition in the complete model.** Deterministic simulation results showing the effect of IL1+OSM±TGFβ treatment on altered versions of the fully parameterised model presented in Fig 5.7, over a simulation time of 48 hours treatment. An active form of TGFβ is present in the model to replicate experimental conditions. Curves show how the particle numbers of MMP-13 mRNA change over the simulation. The red curve shows the complete model simulated with IL-1+OSM. All other curves show IL1+OSM+TGFβ simulations with: the complete model (red curve); mRNA degradation removed (green curve); AP-1 complex inhibition removed (yellow curve). Simulations were run using COPASI

5.4 Model comparison

The completed model could now replicate the data from chapter 4. However, I wanted to compare this parameterised model to the original IL-1, OSM and TGF β models in order to confirm that the output had not been dramatically altered. In the original model presented in Wang Hui et al. (2014) the TGF β component was designed to look at the effect simulation with an inactive form of TGF β had over a 20 month period. Comparing this 20 month simulation in my model and the original model showed an almost identical pattern (Fig 5.13).



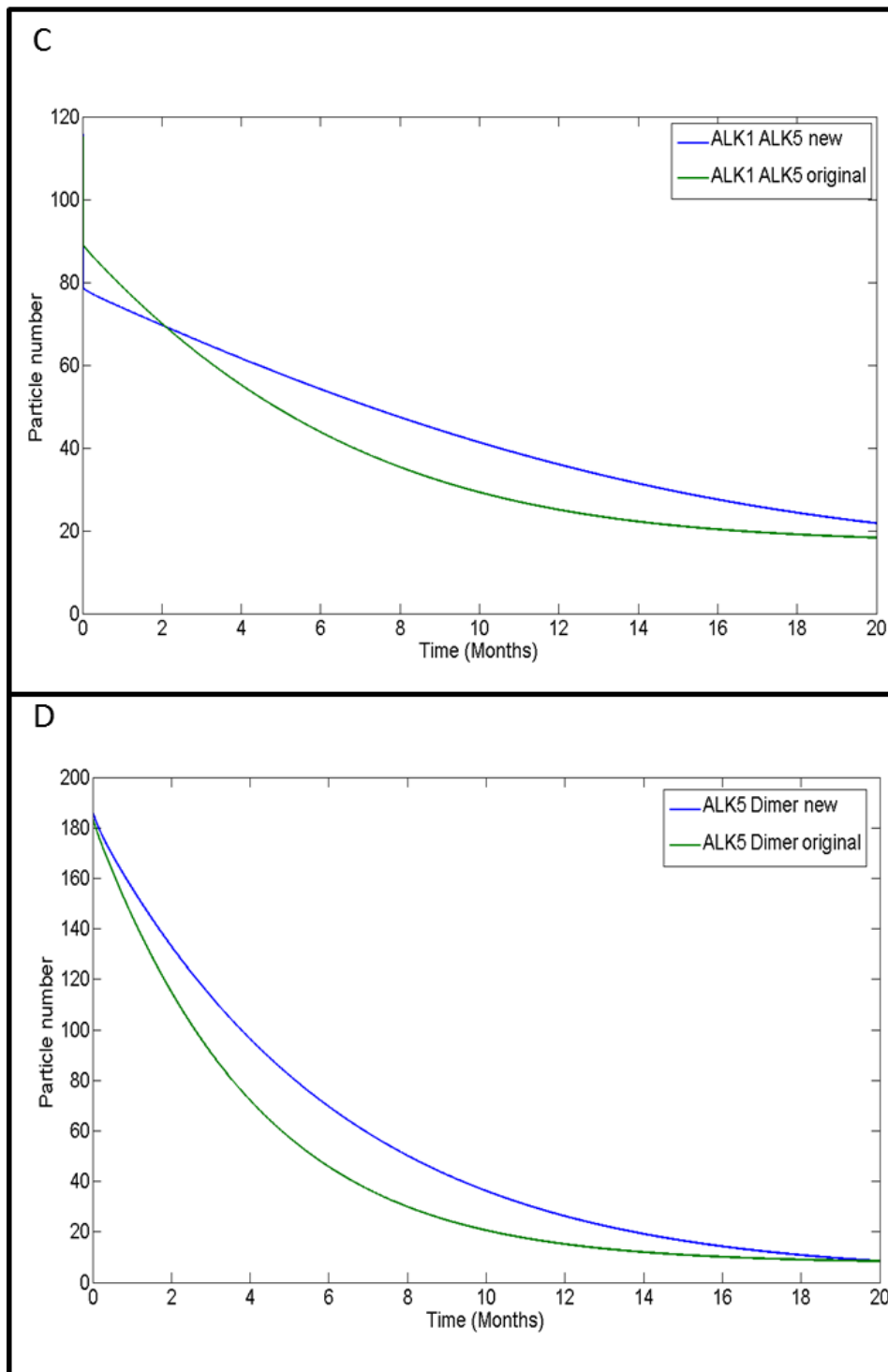
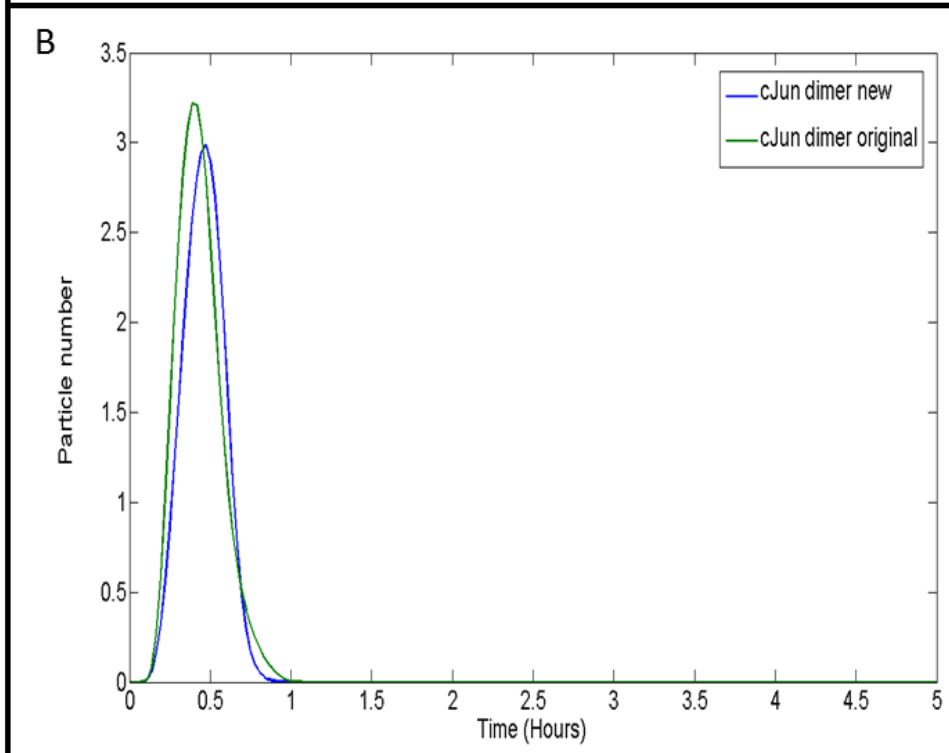
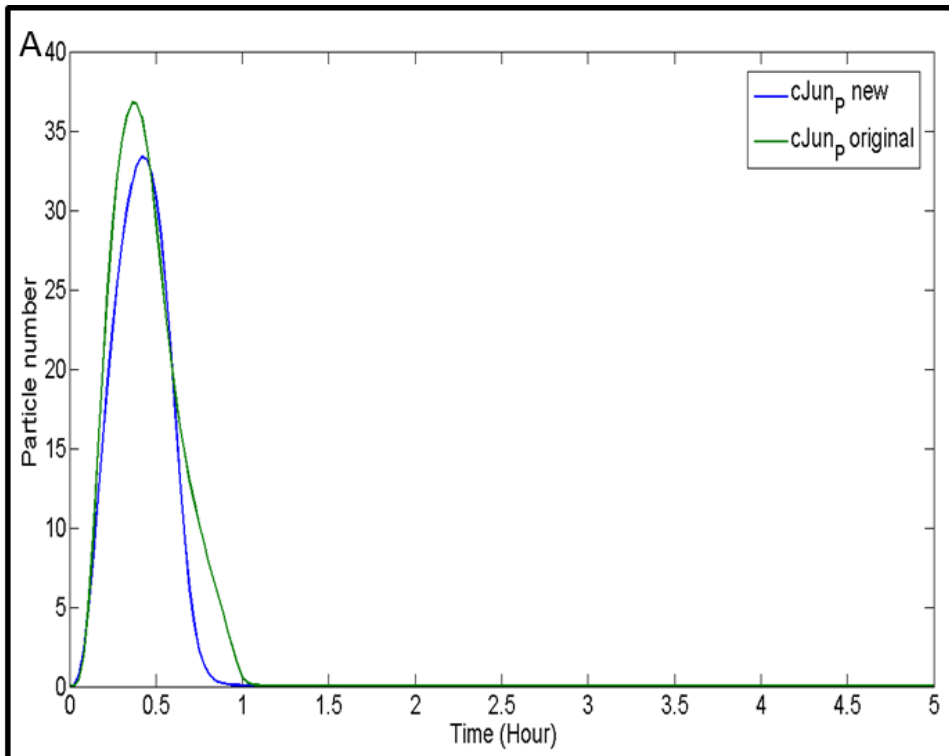


Figure 5.13 **Comparison of SMAD signalling and TGF β receptor expression in response to active TGF β treatment.** Simulation results showing the effect of inactive TGF β on the profiles of SMAD signalling and TGF β receptor expression. Using a simulated time period of 20 months, both the original TGF β model component presented in Wang Hui et al. (2014) (green) and my new integrated model presented in Fig 5.7 (blue) were simulated deterministically using COPASI. Curves show the amount in particle numbers of A) Phosphorylated SMAD1 bound to SMAD4. B) Phosphorylated SMAD2 bound to SMAD4. C) ALK1 ALK5 heterodimers. D) ALK5 homodimers.

The structure of the IL-1+OSM component from my model had multiple alterations from the original presented in Proctor et al. (2014). Despite this, it could still match the profiles for the AP-1 components that were seen in the original model. Figure 5.14 shows that both of the models showed similar AP-1 component patterns at 5 hours. The biggest difference was seen in c-Fos phosphorylation (Fig 5.14C), where my model showed a slightly higher peak and a longer response. The difference was not significant enough to cause a concern as they did still have a very similar pattern. Also, the profile of c-Jun/c-Fos dimerisation, which proceeds c-Fos phosphorylation, had a near identical profile. c-Jun/c-Fos heterodimerisation was the only AP-1 component that took longer than 5 hours to completely leave the system. Comparison of the two models at 48 hours showed that c-Jun/c-Fos dimers persisted in the model for the same amount of time, with an analogous rate of decay (Fig 5.15).



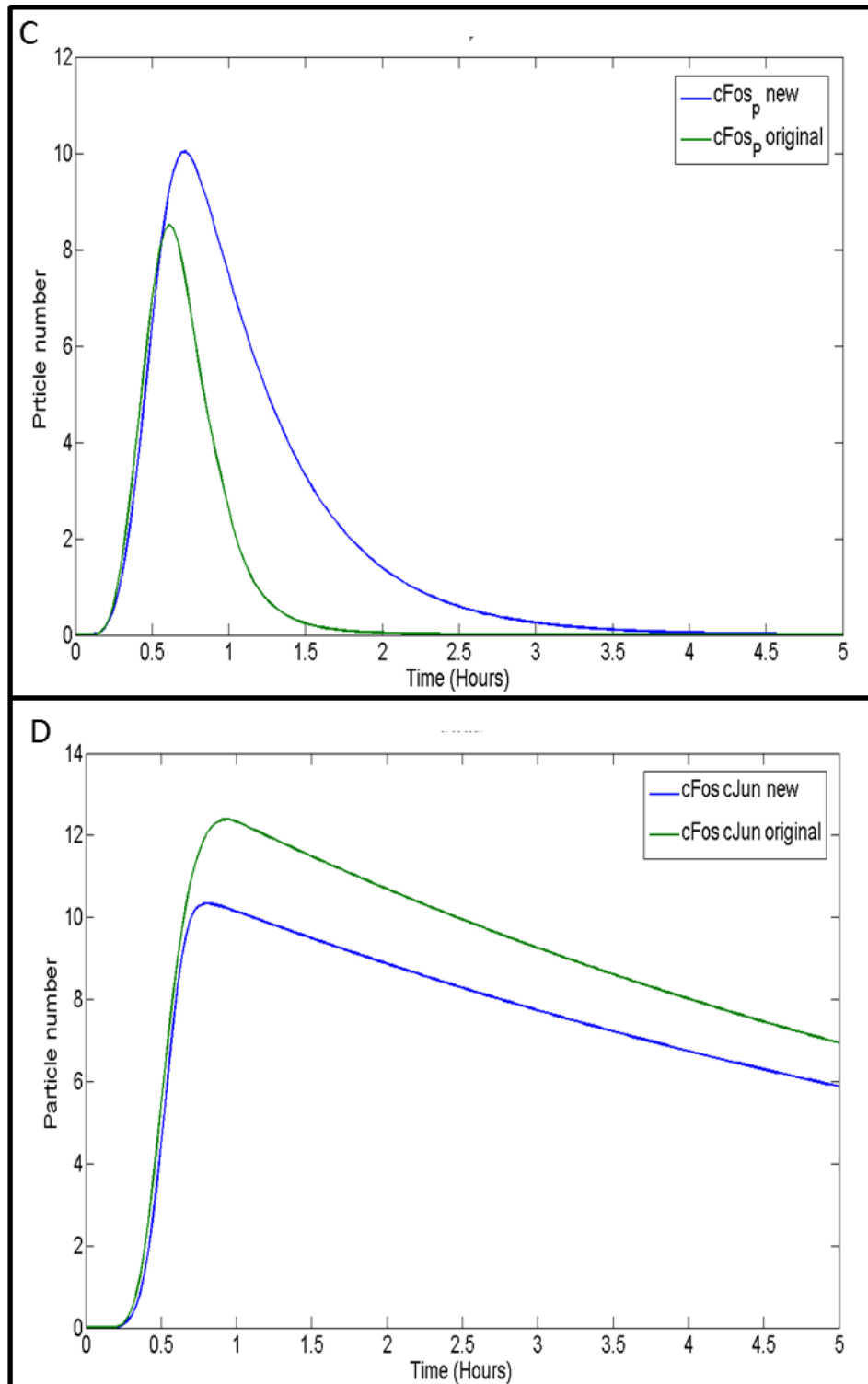


Figure 5.14 Comparison of AP-1 component profiles after IL-1+OSM simulation. Simulation results showing the effect of IL-1+OSM treatment on the profile of AP-1 components, using a simulated time period of 5 hours. Both the original IL1+OSM model described in Proctor et al. (2014) (green) and my new integrated model presented in Fig 5.7 (blue), were simulated deterministically using COPASI. Curves show the level of A) c-Jun phosphorylation. B) c-Jun homodimer formation. C) c-Fos phosphorylation. D) c-Fos/c-Jun heterodimer formation.

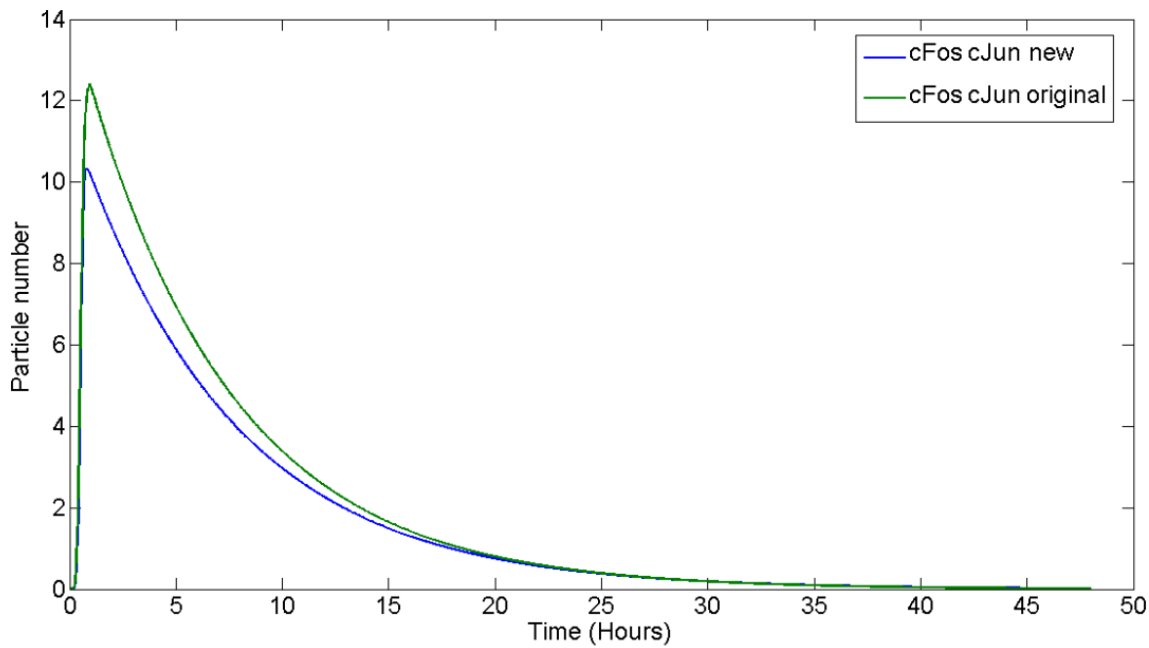


Figure 5.15 **Comparing the formation of c-Fos/c-Jun Heterodimers during a 48 hour simulation.** Simulation results showing the effect of IL-1+OSM treatment on the formation of c-Fos/c-Jun heterodimers, using a simulated time period of 48 hours. Both the original IL1+OSM model described in Proctor et al. (2014) (green) and my new integrated model presented in Fig 5.7 (blue) were simulated deterministically using COPASI.

5.5 Model testing and predictions

It is argued that most model structures, whether correct or not, can fit given data with enough time and effort. As I had created a model that fit to the experimental data generated previously, I needed to confirm it could make correct predictions. Testing model predictions provides a lot more confidence in the model structure if they match. However, if the predictions are not correct then the model structure needs to be altered.

5.5.1 TGF β -mediated repression after 6 hour exposure to cells.

Treating SW1353 cells with TGF β for 6 hours prior to IL-1+OSM stimulation was sufficient to mediate repression of MMP-13, even if TGF β was no longer present (Fig 5.16A). However, no repression was seen 6 hours after IL-1+OSM treatment. When the cells had been pre-treated with TGF β repression was seen by 12 hours of IL-1+OSM treatment, which was not seen without pre-treat (Fig 5.16A). Once established, repression of MMP-13 mRNA could be seen up to at least 48 hours after stimulation, even if TGF β was removed (Fig 5.16A). Unlike the previous data, the pre-treatment experiments were done in parallel with the modelling. My complete model (Fig 5.7) was run with TGF β present for 6 hours prior to IL-1+OSM stimulation, via an event. This, without alteration, produced a similar pattern of repression to the experimental data. This provided confidence that the model could make accurate predictions about the effects of TGF β on a pro-inflammatory stimulus (Fig 5.16B).

5.5.2 Importance of new protein synthesis

The model includes *de novo* synthesis of the dummy species and JunB, which are required for TGF β to mediate its effect. Emetine blocks new protein synthesis by binding to the 40S subunit of the ribosome. I pre-treated the cells with emetine to see if once emetine was removed treatment with IL-1+OSM could still mediate its full effect. By pre-treating with a combination TGF β and emetine, I hoped to remove the protective effect of TGF β . However, even after it was removed from the cells emetine continued to have an effect, preventing new protein synthesis. This resulted in a substantial reduction in MMP-13 expression in IL-1+OSM treated cells at 24 hours (Fig 5.17). This was probably

a result of IL-1+OSM no longer being able to induce c-Fos synthesis. IL-1+OSM±TGFβ still resulted in a significant upregulation of MMP-13 expression at 24 hours after emetine pre-treatment, but this was most likely an IL-1-mediated response (Fig 5.17B). Emetine pre-treatment led to an upregulation of MMP-13 by itself and also caused some cell death. This experiment was also repeated with cycloheximide and Actinomycin D but this resulted in complete cell death (data not shown).

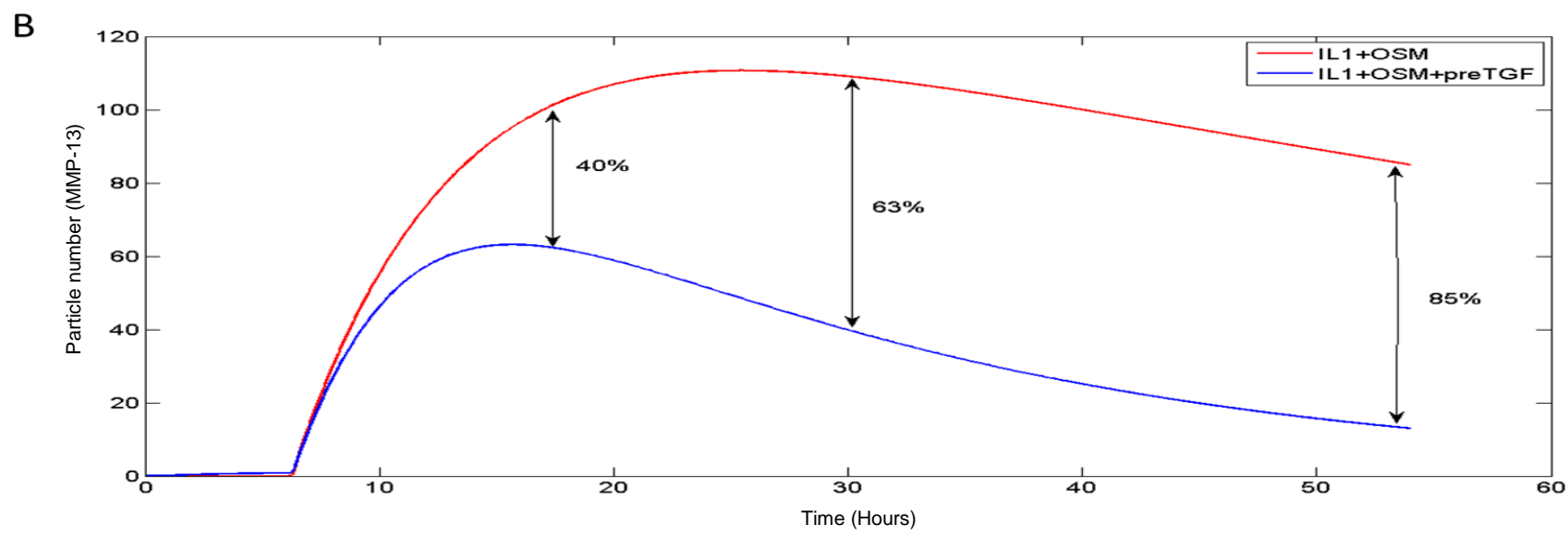
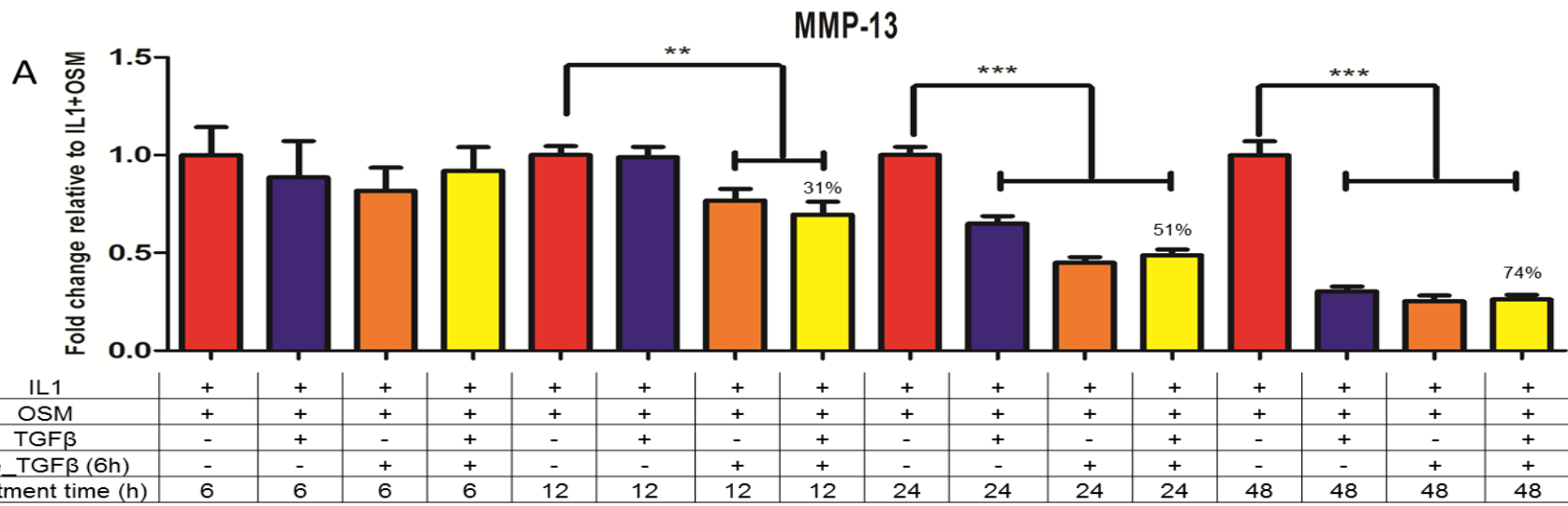


Figure 5.16 6 hour pre-treatment with TGFβ was enough to mediate repression of IL-1 and OSM effects. A) Pooled data from SW1353 cells stimulated with IL-1 (0.5ng/ml), OSM (10ng/ml) and TGFβ (10ng/ml) for 6, 12, 24 or 48 hours, following 6 hours pre-treatment with serum free media or TGFβ (10ng/ml). qPCR was then performed on the isolated mRNA to measure MMP-13 expression. Data are presented as fold change relative to IL-1+OSM (mean ± SEM). Percentages represent the percentage of repression in IL-1+OSM+TGFβ treated samples, relative to IL-1+OSM alone at the relevant time point. n=14-19 across 3 experiments on separate cell populations. Statistics calculated using unpaired student t-test, where * p < 0.05; ** p < 0.01; *** p < 0.001 B) Deterministic simulation results showing the effect of IL1+OSM±TGFβ treatment on the fully parameterised model presented in Fig 5.7, over a simulation time of 54 hours. An event triggers IL-1 and OSM stimulation 6 hours after TGFβ (red) or unstimulated (blue) pre-treat. An active form of TGFβ is present in the model to replicate experimental conditions. Curves show how the particle numbers of MMP-13 mRNA change over the simulation. The black arrows show the percentages of repression seen at 18, 30 and 54 hours, caused by the presence of TGFβ. Simulations were run using COPASI.

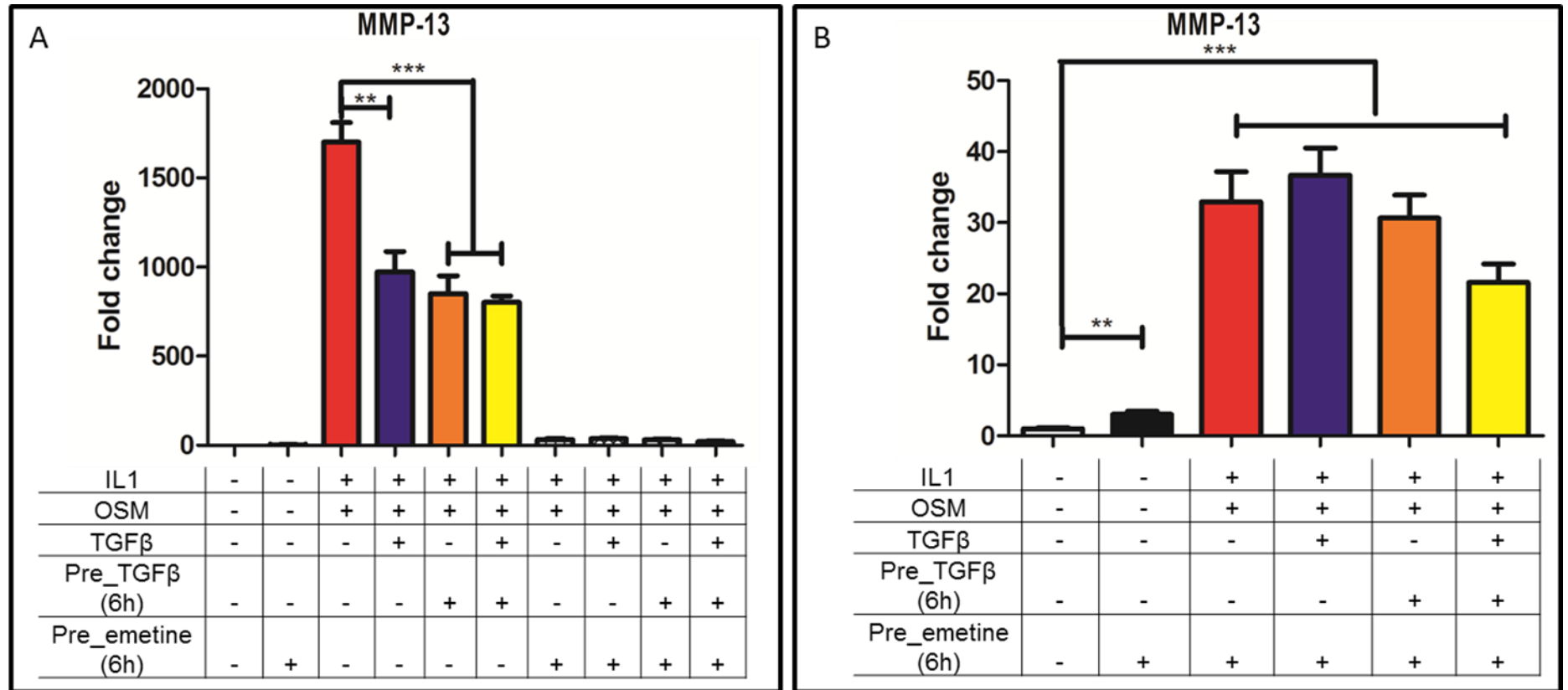


Figure 5.17 **The effect of 6 hour emetine pre-treatment IL-1+OSM+TGFβ signalling.** SW1353 cells stimulated with IL-1 (0.5ng/ml), OSM (10ng/ml) and TGFβ (10ng/ml) for 24 hours, following 6 hours pre-treatment with TGFβ (10ng/ml), emetine (10μM/ml) or serum free media. qPCR was then performed on the isolated mRNA to measure MMP-13 expression. Data are presented as fold change relative to control (mean ± SEM, n=4-6). Statistics calculated using unpaired student t-test, where * p < 0.05; ** p < 0.01; *** p < 0.001. A) Data shown for all conditions B) Data from the same experiment with the serum free media pre-treat excluded to aid the visualisation of smaller fold changes.

5.5.3 Increased signalling through ALK1 with age alters the TGF response to a pro-inflammatory stimulus.

The decreased abundance of ALK5 with age, combined with ALK1 remaining relatively constant, alters the ratio of ALK1/ALK5. This results in ALK5 homodimers which are abundant in young organisms becoming less prevalent with age, whilst ALK5/ALK1 heterodimers levels decrease at a much lower rate. The computational model was set up to simulate this change over a representative 20 months (Fig 5.18A). Initially ALK5 homodimer are abundant but they decrease and after 8 months ALK1/ALK5 heterodimer start to become the dominant receptor; this coincides with a gradual increase in MMP-13 mRNA (Fig 5.18A). 3 events were triggered across the 20 months which introduced an IL-1+OSM stimulation. The first event was at 4 months, the second at 8 months and the third at 19 months. It is important to note that IL-1+OSM would leave the system quickly after the events.

I used this to examine how an ageing system reacts to a pro-inflammatory stimulus (IL-1+OSM). Early in the system (~4 months), I saw that the pro-inflammatory stimulus was greatly reduced and MMP-13 mRNA levels returned to zero very quickly (Fig 5.18B). As the ratio began to change at ~8 months, I still saw the repression of MMP-13 mRNA but it was reduced. However, MMP-13 mRNA returned to basal level of expression much faster than with IL-1+OSM alone (Fig 5.18C). By ~19 months, when ALK1 had been the dominant receptor for a number of months, MMP13 mRNA has a higher basal level prior to the simulation, than for the previous two simulations. IL-1+OSM produced a potent increase in MMP-13 mRNA at 19 months but there was still some repression mediated by TGF β (Fig 5.18D). However, because of the higher basal level of MMP-13, this response appeared almost as strong as IL-1+OSM alone. The increased MMP-13 also took much longer to return to basal expression than when ALK5 was dominant (Fig 5.18D). When MMP-13 returns to basal expression after the 19 month simulation, it was also higher than before stimulation (Fig 5.18A and D). Table 5.1 shows that the repression seen decreases at a linear rate across the 20 month simulation, with peak MMP-13 mRNA levels increasing by ~2.5-3.5% each month, when compared to the previous month.

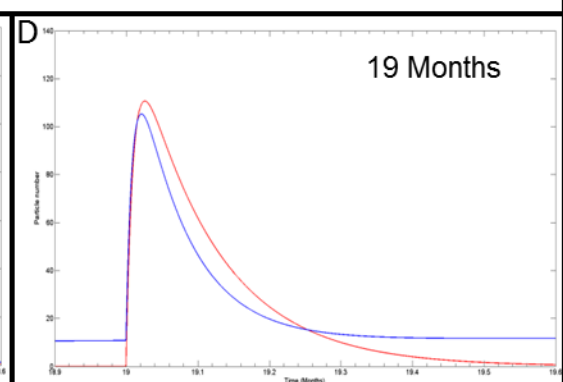
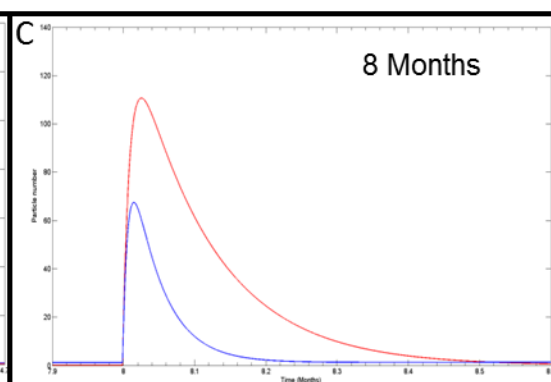
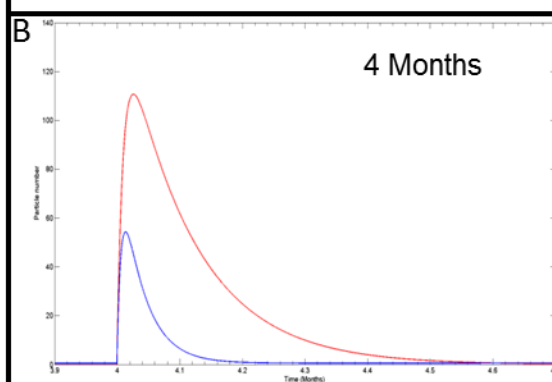
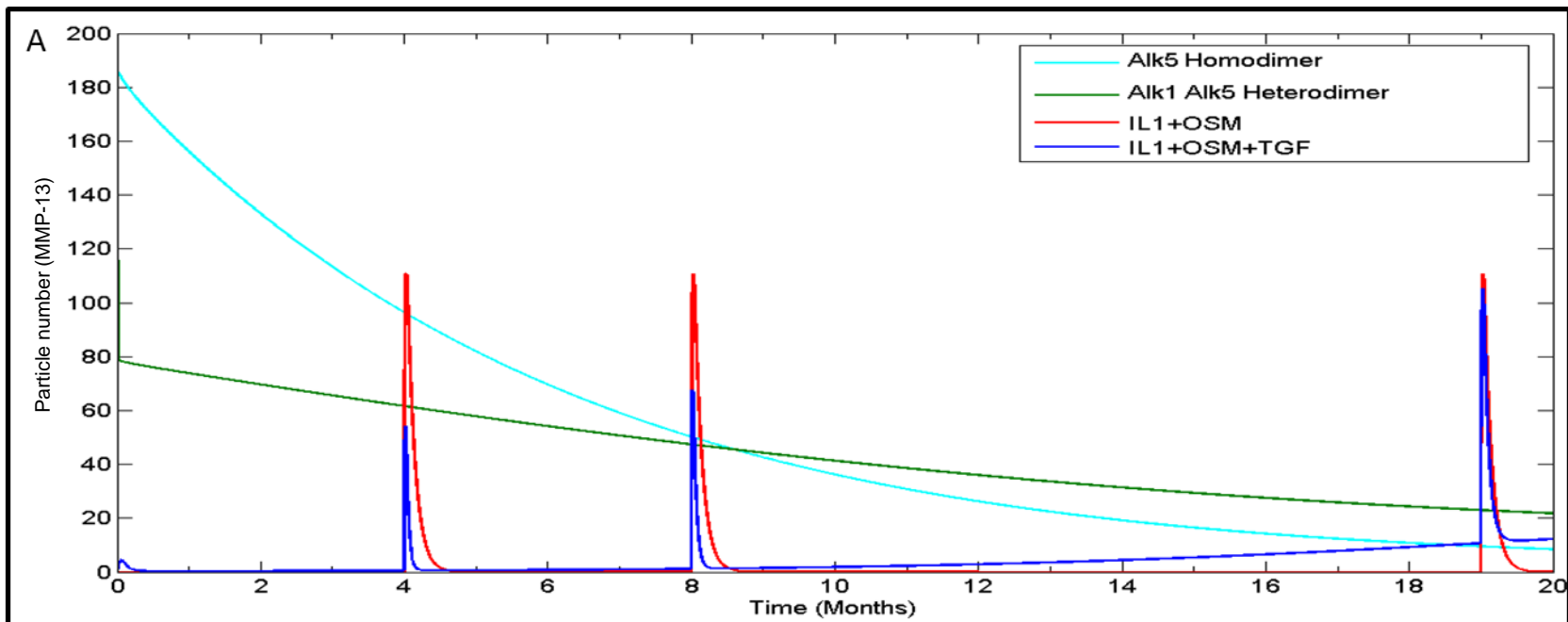


Figure 5.18 Changing responses of TGFβ to a pro-inflammatory stimulus over 20 months. Deterministic simulation results for the model presented in Figure 5.7 ran for 20 months simulation time, using COPASI. The simulation was run with an inactive form of TGFβ present to also allow for the activation and deactivation of the growth factor. IL-1+OSM were triggered using events at three time points at which the ALK5/ALK1 ratio had changed. A) Shows the fully 20 month simulation B, C and D) Highlight the time marginally before, during and after the change in MMP-13 mRNA expression following the events (B=~4 months, C=~8 months and D=~19 months). The light blue and green lines show the respective changes in the ALK5 homodimers and ALK1 ALK5 heterodimers over 20 months. The dark blue line shows the expression of MMP-13 mRNA across the simulation, whilst the red line shows MMP-13 mRNA expression in the model with TGFβ removed.

Month IL-1+OSM was introduced to the simulation, as an event.	Percentage of MMP-13 mRNA repression mediated by TGFβ upon IL-1+OSM addition.	Change in repression since previous month.
1	67.85%	
2	65.18%	2.67
3	62.20%	2.98
4	59.06%	3.14
5	55.76%	3.30
6	52.33%	3.43
7	48.79%	3.54
8	45.14%	3.65
9	41.49%	3.65
10	37.76%	3.73
11	34.02%	3.74
12	30.28%	3.73
13	26.62%	3.66
14	22.93%	3.69
15	19.32%	3.60
16	15.82%	3.50
17	12.38%	3.45
18	9.19%	3.19
19	5.95%	3.24

Table 5.1 Change in TGFβ-mediated repression of IL-1+OSM-driven MMP-13 expression, with age. This data expands on figure 5.18 by showing the percentage of MMP-13 mRNA repression that TGFβ mediates when an IL-1+OSM event is introduced to a 20 month simulation. The simulation was run as in figure 5.18 but an IL-1+OSM event was triggered every month. The percentage of repression was calculated by comparing the peak expression of MMP-13 mRNA at each month when TGFβ was or was not present.

5.6 Discussion

TGF β appears to be affecting the system by both competitive AP-1 inhibition and MMP-13 mRNA degradation, without both of which it cannot produce its effect in order to fit the experimental data. Some alternatives to the degradation of MMP-13 mRNA were explored during the development. For example I looked at the effect of SMADs 2/3 also being able to bind to AP-1 components, as well as TGF β affecting the receptors for IL-1+OSM. I also designed a version of the model which included an MMP-13 gene, which c-Fos/c-Jun dimers bound too to increase repression, with TGF β preventing this binding. However, fitting these versions of the model to experimental data indicated none of them would have been capable of matching the experimental data. MMP-13 mRNA instability on the other hand improved the fit of the model significantly so I progressed with that in the model. It is worth noting that I did significantly more work fitting the MMP-13 mRNA instability version of the model but this was a result of it showing more promise initially than the other versions of the model.

There are a number of potential candidates mediated by TGF β . The primary candidate for AP-1 competitive inhibition is JunB, for the reasons given previously. However, there is also evidence that Smad2/3 can interact directly to antagonise AP-1 complex binding, in particular to c-Fos and c-Jun (Zhang et al. 1998). JunD is also a promising candidate along with the TIMPs which are all strongly induced by TGF β (Hall et al. 2003). How TGF β leads to MMP-13 mRNA degradation does not have as clear a candidate but there are a number of ways it could potentially be mediated. Both Vinculin and far upstream element (FUSE) have been shown to bind to the 3' UTR of MMP-13, which in turn leads to the decay of MMP-13 mRNA (Clark et al. 2008). NAD-dependent deacetylase sirtuin-2 (Sirt2) has also been shown to suppress MMP-13, possibly as a result of TGF β (Lin et al. 2013). Reports have also suggested that HDAC4 can repress MMP-13 (Cao et al. 2014) by binding to the MMP-13 promoter (E. Shimizu et al. 2010), preventing further transcripts being produced. This is not directly increasing degradation but creates a situation where with no new production, mRNA leaves the system giving an impression of degradation. This protective effect has been questioned by other reports claiming the opposite is true and HDAC4 is responsible for an increase in MMP-13 (Lu et al. 2014;

Queirolo et al. 2016). There is potential for degradation to be mediated by miRNAs as they have been shown on multiple occasions to mediate an effect by increasing mRNA degradation. A number of these have been linked to IL-1, TGF β and MMP-13 such as; miR-145, miR-483, miR146a, miR-140 and miR127-5p (Li et al. 2015). Determining how TGF β mediates both AP-1 complex inhibition and mRNA degradation, is a difficult question to answer but both are needed in the model to replicate experimental results. Future work into how specifically they are mediated may identify specific therapeutic targets to help reduce cartilage damage with age and OA progression.

5.6.1 Importance of *de novo* synthesis

The initial delay in TGF β -mediated repression of IL-1+OSM-driven MMP-13 expression (around 12 hours) led me to hypothesise that *de novo* synthesis may be required in order for TGF β to have an effect. For this reason it was included in the model and was required for the model to fit the data.

Demonstrating that TGF β could mediate repression after 6 hours pre-treatment, even when TGF β was subsequently removed from the system, further indicated that *de novo* synthesis may be required. This initial delay may be a result of the time for new proteins to be transcribed, but once the proteins were present then removal of TGF β would have no effect as further protein synthesis is not required. I hypothesised that blocking new protein synthesis would prevent TGF β from repressing IL-1+OSM-driven MMP-13 upregulation. However, OSM leads to the synthesis of c-Fos (Tanos et al. 2005) and this may be key in the synergistic increase of MMP-13 driven by IL-1+OSM (Proctor et al. 2014). Blocking proteins synthesis by TGF β without affecting the IL-1+OSM response was not possible, thus I cannot confirm that *de novo* synthesis was required for TGF β to have an effect. Although it does further validate the importance of *de novo* synthesis in IL-1+OSM synergy.

5.6.2 Potential effect of ALK1 dominance

ALK1 is known to lead to the upregulation of MMP-13 (Blaney Davidson et al. 2009) and has also been reported to increase phosphorylation of c-Fos through p38 (C. G. Chen et al. 2012). I expected that, when it was the dominant receptor, an inflammatory stimulus would lead to an even greater increase of

MMP-13 than when TGF β is not present, due to the effect of p38 and the higher basal levels of MMP-13. The model suggests that this is inaccurate and although repression was greatly reduced when ALK1 is dominant (compared to when ALK5 was dominant), there still appeared to be some measure of repression. This may be because ALK1 stimulates MMP-13 upregulation through a different mechanism to IL-1+OSM. ALK1 is believed to upregulate MMP-13 via SMAD1, which can activate Runx2 and this in turn leads to an increase in MMP-13 (Ijiri et al. 2005), whereas, IL-1+OSM mediate their effect through AP-1 components (Chambers et al. 2013). As a result the remaining ALK5 dimers can still provide some repression as ALK1 has little direct effect. I hypothesised there may be a switch in repression when the effect of TGF β on MMP-13 expression becomes markedly less. However, it appeared this change happened at a linear rate across the 20 month simulation.

Despite this, I did find when ALK1 receptor, is the dominant receptor the increase in MMP-13 from IL-1+OSM treatment took longer to leave the system and return to basal expression (compared to when ALK5 was dominant). As the basal expression is already high, this will lead to a longer and more pronounced response that could result in damage to already weakened tissue. Therefore, inflammation could still potentially lead to more damage in older organisms than their younger counterparts, as basal levels of MMP-13 will be higher and any inflammatory response may be prolonged.

TGF β is stored in a latent form in the synovial fluid (Pedrozo et al. 1998) and is constantly being activated in the joint (Gay et al. 2004). This release and activation is increased when under load or during exposure to inflammation (Lee et al. 2005; Albro et al. 2012). There are no reports of this changing with age, but if TGF β is now dysregulated in these older organisms, the release of TGF β could result in increased inflammatory damage. Whether inflammation is general, or a result of injury, it could become more damaging than in younger counterparts. Identifying how the TGF β response has changed with age may provide therapeutic targets to help limit this damage in aged individuals, averting cartilage damage and OA development or progression.

5. 7 Summary

- The IL-1+OSM and TGF β models were adapted from previous published models. Despite being changed for purpose, both sections of my model could still replicate the important profiles from the original models.
- The model requires both AP-1 complex inhibition and MMP-13 mRNA degradation, in order to match the experimental data accurately.
- TGF β can mediate repression of IL-1+OSM-driven MMP-13 expression after 6 hours pre-treatment, even if it is then removed from the system. This was simultaneously shown in the model simulations and the experimental data.
- Using the model to explore how TGF β will affect IL-1+OSM, when ALK1 becomes dominant, suggests there will not be an increase in MMP-13 expression (compared to IL-1+OSM alone) but instead a prolonged inflammatory response.

Chapter 6. Exploring the effects of ALK1 over-express in SW1353 cells

6.1 Introduction

In the previous chapter my computational model suggested that, as an individual aged, ALK1 dominance would reduce the inhibitory effect TGF β has on IL-1+OSM-mediated MMP-13 expression. However, it would not result in a greater increase in MMP-13 expression than IL-1+OSM alone, which was contrary to our original hypothesis. In order to confirm these model predictions I looked to create an experimental model of ALK1 over-expression. This was attempted in three ways: (i) stable over-expression with a plasmid, and transient over-expression using (ii) lentivirus or (iii) adenovirus.

6.1.1

Stable transfection of cells, although initially time consuming, has the advantage of reproducible results, which is not always the case with transient over-expression. Theoretically, any cells which survive the stable transfection protocol must have taken up the plasmid of interest and hence over-express the gene of interest. Once established, the stable cell line can then be treated as a wild-type cell line allowing for multiple experiments to be performed quickly in cells with a consistent level of (over) expression (Chambers et al. 2015). Stable over-expression of the protein of interest also has the advantage that any post-translational modifications or necessary subcellular translocation of the proteins required for functionality should have sufficient time to occur during cell growth (Chambers et al. 2015).

The time taken to create the stable cell line, however, can become very prominent if there are mistakes with the plasmid or if expression does not provide the expected results. Transient expression allows for a significantly quicker method of over-expressing the gene of interest and looking at its effect (Vorburger and Hunt 2002; Federici et al. 2009). The level of over-expression with transient transfection is not constant and although this can be a problem, it means higher levels of expression are also possible (Vorburger and Hunt 2002; Federici et al. 2009).

6.1.1 Aims

- To develop a method that facilitates over-expression of ALK1 to a sufficient level for it to become the dominant receptor.

6.2 Stable over-expression of ALK1

To attempt to mimic the changes seen in type I TGF β receptors in an ageing model (both in mice and computationally), I sought to create SW1353 cells that stably over-expressed a plasmid containing the ALK1 gene. Physiologically, ALK5 is also reduced so it was not an ideal representation. However, as ALK1 is the preferential binding partner of TGF β , if there is sufficient over-expression it should signal through ALK1. siRNA against ALK5 also allowed me to reduce the levels of ALK5 to better represent what is happening with age.

6.2.1 First attempt at stably over-expressing ALK1.

I initially used two plasmids to make stable cell lines: the original plasmid (mEmerald-ALK1-N-13) and one with an induced stop codon (STOP-ALK1-N-13). mEmerald-ALK1-N-13 expressed ALK1 but also had a fluorophore attached called mEmerald. Due to the size of the mEmerald protein (239 amino acids), I was concerned it may interfere with the activity of ALK1 (503 amino acids). In order to address this, I used site direct mutagenesis (SDM) to induce a stop codon in the linker sequence upstream of mEmerald but downstream of the complete ALK1 sequence (Table 6.1). This new plasmid was named STOP-ALK1-N-13. When using the SDM technique it is feasible that the primers will not anneal due to their nonhomologous sequences, so it was important to check there was a product. Figure 6.1 shows the SDM products ran next to the original mEmerald-ALK1-N-13 plasmid. The bright band ran at approximately the same molecular mass as mEmerald-ALK1-N-13, suggesting that the process had been successful. It ran slightly lower because it is single stranded until transfected into bacteria. Conversely, mEmerald-ALK1-N-13 is a double stranded circular plasmid which caused the two bands seen in the mEmerald-ALK1-N-13 lane (Fig 6.1). The second band in the STOP-ALK1-N-13 lane was the excess primer from SDM (Fig 6.1). The STOP-ALK1-N-13 was then sent for sequencing, where it was confirmed that the mutation was as predicted (data not shown).

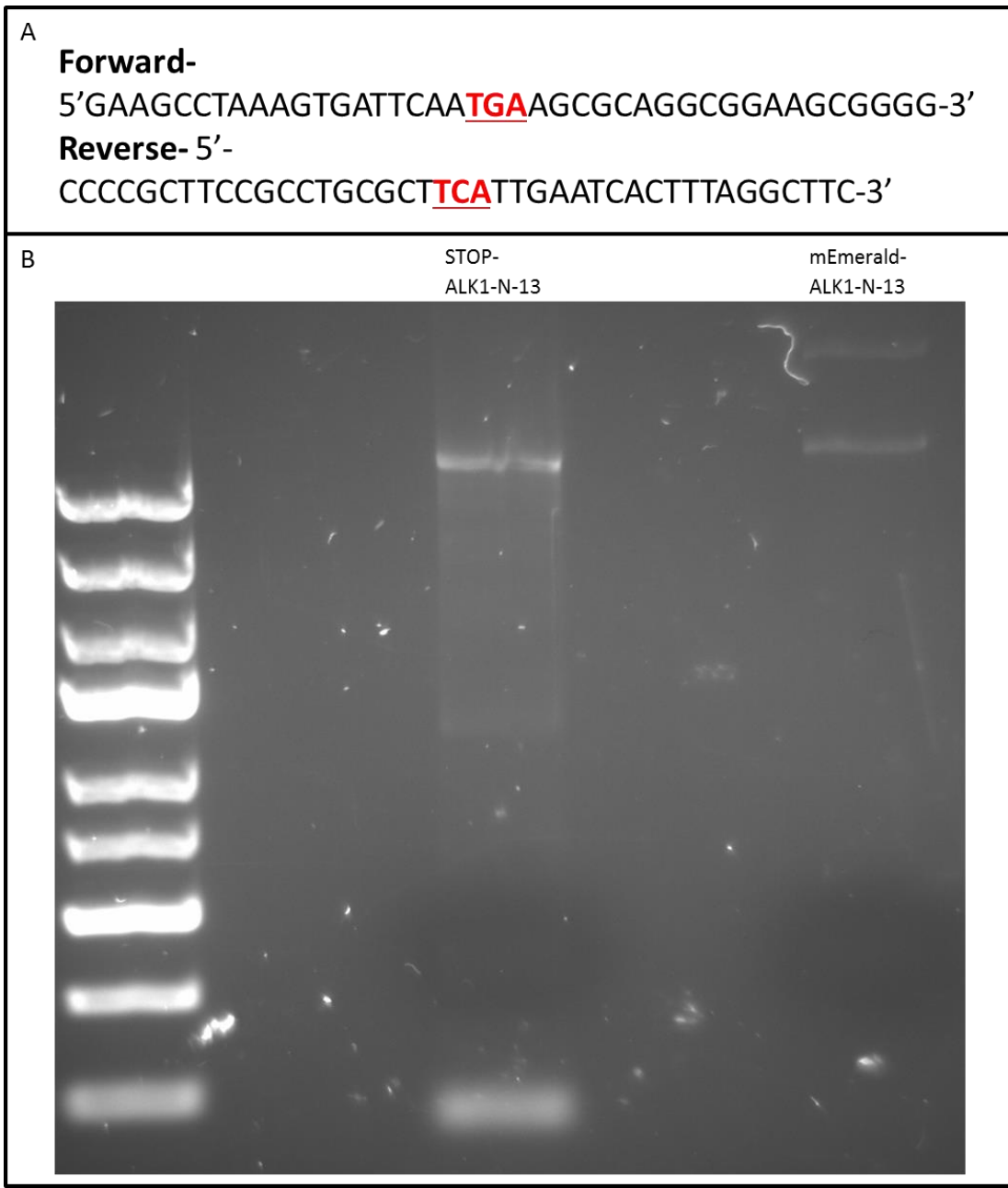


Figure 6.1 **Confirmation of site directed mutagenesis products.** SDM was performed on the mEmerald-ALK1-N-13 plasmid using the primers in A. A) The primers used for SDM the red nucleotides highlight the nucleotides that differ from the normal plasmid sequence. B) An ethidium bromide gel was run containing the product of the SDM (STOP-ALK1-N-13) as well as the original plasmid mEmerald-ALK1-N-13.

ATGGTGAGC - mEmerald Sequence
 ATGACCTTG - Human ALK1 Sequence
 AGCGCAGGC - Linker between mEmerald
 and ALK1
 GGC - Altered sequence
 TGA - Stop codon

Section of the original plasmid (mEmerald-ALK1-N-13).	CTGCGGATCAAGAAGACACTACAAAAAATTAGCAACA GTCCAGAGAAGCCTAAAGTGATTCAA GGCAGCGCAGGCGGAAGCGGGGATCCACCGGTTCGC CACCATGGTGAGCAAGGGCGAG
Section of the plasmid after site directed mutagenesis.(STOP-ALK1-N-13)	CTGCGGATCAAGAAGACACTACAAAAAATTAGCAACA GTCCAGAGAAGCCTAAAGTGATTCAA TGAAGCGCAGGCGGAAGCGGGGATCCACCGGTTCGC CACCATGGTGAGCAAGGGCGAG

Table 6.1 **Stop codon introduction into the mEmerald-ALK1-N-13 plasmid.**

A small section from the sequence of the SMD and mEmerald-ALK1-N-13 plasmids, showing where the linker sequence joins the sequences for ALK1 and mEmerald. Site directed mutagenesis was used to introduce a stop codon into the linker sequence, preventing mEmerald from being transcribed.

I created two stable cell lines in parallel, using the mEmerald-ALK1-N-13 and STOP-ALK1-N-13 plasmids. If the stable protocol worked the cells should be able to survive in the antibiotic G418, which would normally kill SW1353 cells. Both cell lines survived so I assumed they had been transfected successfully. Figure 6.2A shows the expression of ALK5 and ALK1 in both of the cell lines. ALK5 expression is unaffected in either cell line but ALK1 also appears to be unaffected. As the receptor should have been localised to the cell membrane, I attempted membrane specific extraction in an attempt to visualise increased ALK1 expression. Again there appeared to be no change in ALK1 concentration (Fig 6.2B). Looking at the mEmerald-ALK1-N-13 cell line for mEmerald expression (Fig 6.3) showed that although there was some green fluorescence this was only negligible. This suggested that ALK1 was being over-expressed but not to a sufficiently high level to visualise, by Western blots.

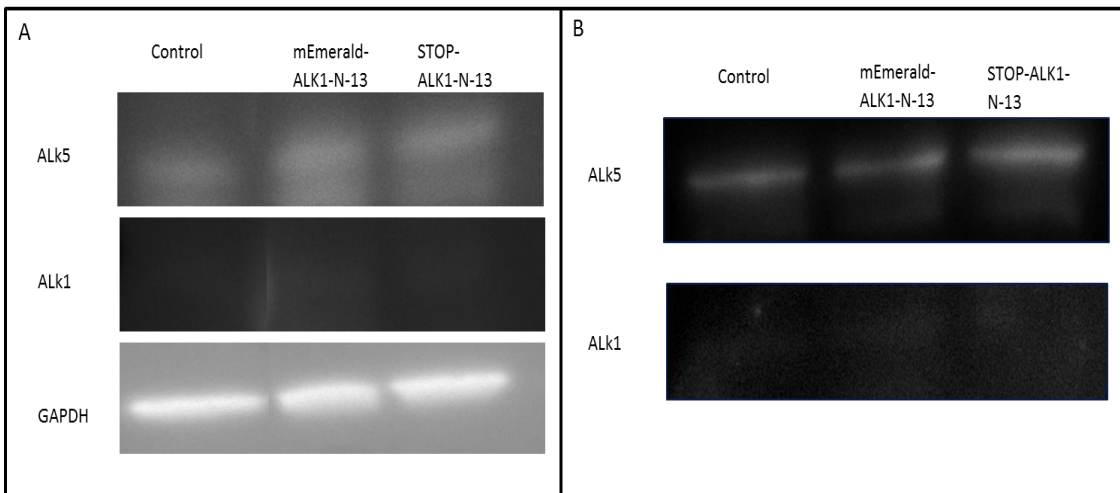


Figure 6.2 **TGF β type I receptors in stable cell lines.** ALK1 over-expressing SW1353 cell lines (mEmerald-ALK1-N-13 and STOP-ALK1-N-13) were grown to confluency in G418. Control cells were also grown to confluency in serum containing medium but without G418. The cells were then lysed and A) whole cell lysis was performed on 1 million cells. B) Membrane specific lysis was performed on 1 million cells. The samples were then run on 12% SDS-PAGE gel and western blots were undertaken for ALK5, ALK1 and GAPDH. A) Is representative of 3 experiments on separate SW1353 cell populations. B) Is representative of a single experiment.

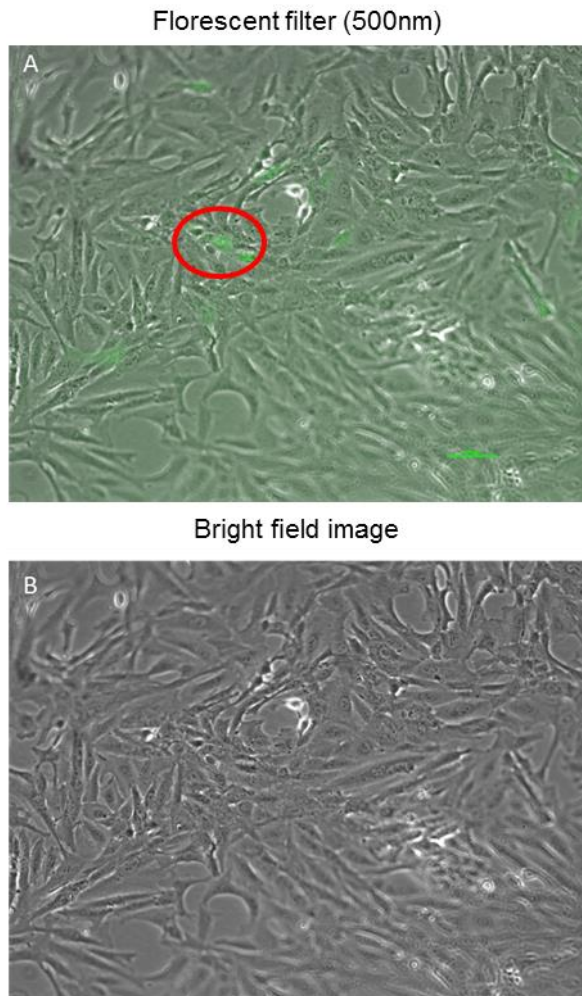


Figure 6.3 **Live-cell plasmid expression.** SW1353 cells stably over-expressing the mEmerald-ALK1-N-13 plasmid were live imaged whilst in G418 serum-containing medium. A) With a fluorescent filter at 500nm which is optimum for visualising the mEmerald fluorophore. Bright green cells show where ALK1 with mEmerald attached is being expressed (the red circle highlights an example of this). B) The same section of cells imaged without any filter.

6.2.2 Creation of the pcDNA3.1 ALK1 HIS plasmid.

There were two possible reasons why the initial stable cell lines had negligible expression. First, plasmids were not linearised prior to transfection which is known to reduce transfection efficiency. Secondly, the plasmids may not have had a satisfactory promoter sequence. Since the plasmid sequence was not publically available, it was not possible to confirm or deny this. In order to address the second problem I used in-fusion cloning to remove the ALK1 gene and move it to a different plasmid, pcDNA3.1+, which had been used previously by our group with success. I also added a His tag to the protein in order to increase the ease of detection. Forward and reverse primers (Fig 6.4A) allowed me to remove the ALK1 gene with overhangs. These overhangs could be cut with restriction enzymes to give sticky ends (Fig 6.4B), which were homologous to cuts in the pcDNA3.1+ plasmid. Figure 6.5 shows the DNA fragments created at two different cycle temperatures during replication. Both 64 and 72 degrees resulted in fragments being created at the correct molecular weight (1566kb). It also shows the pcDNA3.1+ plasmid being linearised by both *BamHI* and *XbaI*. When both restriction enzymes were combined the plasmid still only had one band, suggesting that as predicted they only removed one section of the plasmid rather than cutting it into multiple fractions.

The in-fusion kit then allowed the ALK1 product and the linearised plasmid to be combined to create a new plasmid (pcDNA3.1_ALK1_HIS). This plasmid was then transfected into bacteria. These cells were left to grow on antibiotic containing agar plates, with only the cells that took up the plasmid being able to survive. This however does not mean that the plasmid contained ALK1 as the plasmid may have re-annealed without incorporating it into its sequence, so I ran a colony PCR on a selection of the bacteria colonies using the primers in Figure 6.4. Only two colonies appeared to contain the ALK1 gene (Fig 6.6): Both of these were subject to a Mini-prep, then sequenced, and were found to contain the sequence I was expecting. One of these colonies did have the expected sequence and was amplified using a Maxi-prep to produce large quantities of pcDNA3.1_ALK1_HIS.

A	Overhang	Kosac	Forward primer
5'	TACCGAGCTCGGATC	-GCCACC-	ATGACCTGGGCTCCCCAGGAAA 3'
	Overhang	Stop	His
5'	AAACGGGCCCTCTAG	-TCA-	ATGGTGGTGGTGATGATG - TTGAATCACTTTAGGCTTCTCTGGACTGTTGC 3'
B	Overhangs.		
	TACCGAGCTCG -3'		5'- CTAGAGGGCCCGTTT
	ATGGCTCGAGCCTAG -5'		3'- TCCCGGGCAAA

Figure 6.4 **ALK1 specific primers.** A) Primers designed to flank the ALK1 gene in the mEmerald-ALK1-N-13 plasmid. They also contain a Stop codon, Kozak site, His tag and overhangs designed to be cut by BamHI and XbaI. B) The expected overhangs when products made using the primers in A are cut with BamHI and XbaI.

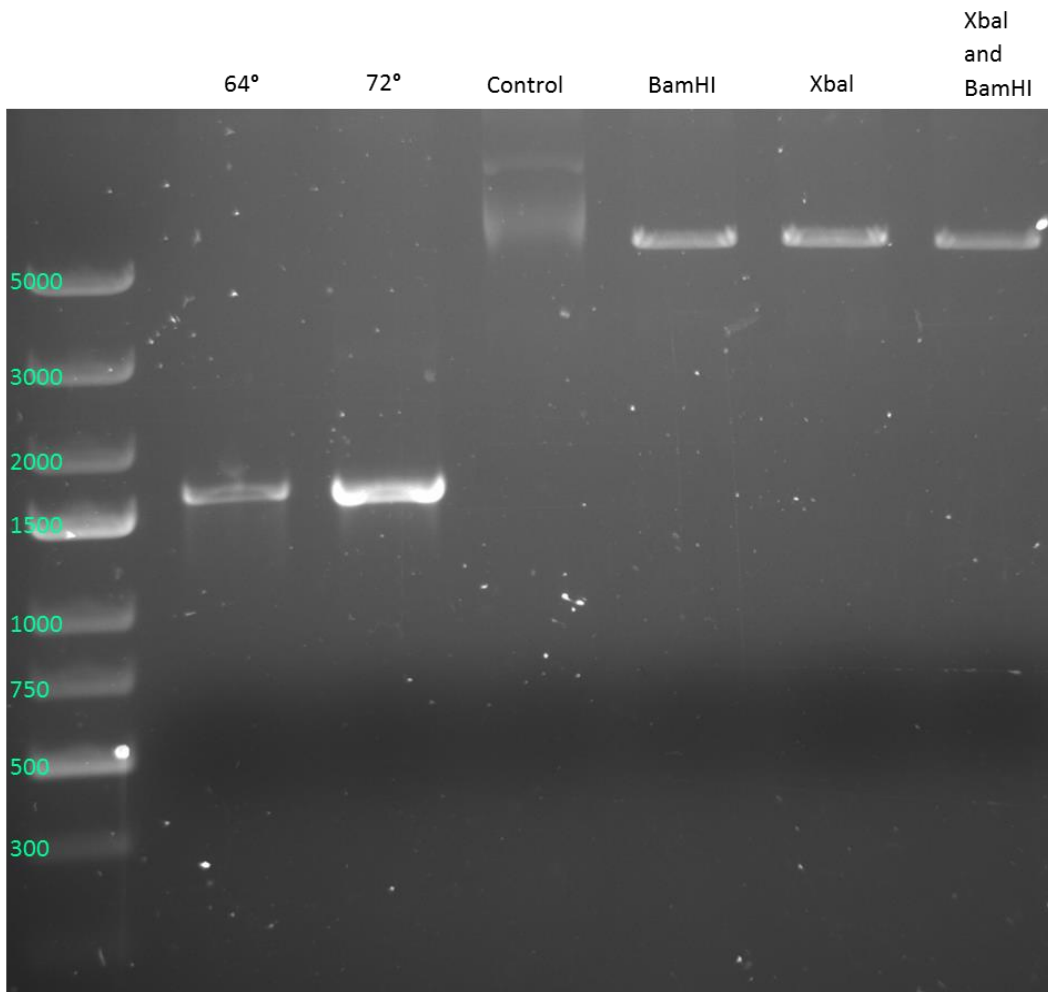


Figure 6.5 **Linearisation of pcDNA3.1+ allows incorporation of ALK1 containing fragments.** ALK1 fragments for in-fusion cloning were generated by cycling the mEmerald-ALK1-N-13 plasmid at 64 and 72° containing the primers in Figure 6.4A and the mEmerald-ALK1-N-13 plasmid. The pcDNA3.1+ plasmid was also linearisation by treatment with *XbaI* and *BamHI* individually or combined for 4 hours at 37°. An ethidium bromide gel was run using the products of these reactions; the pcDNA3.1+ plasmid was also run as a control (Size 5428bp).

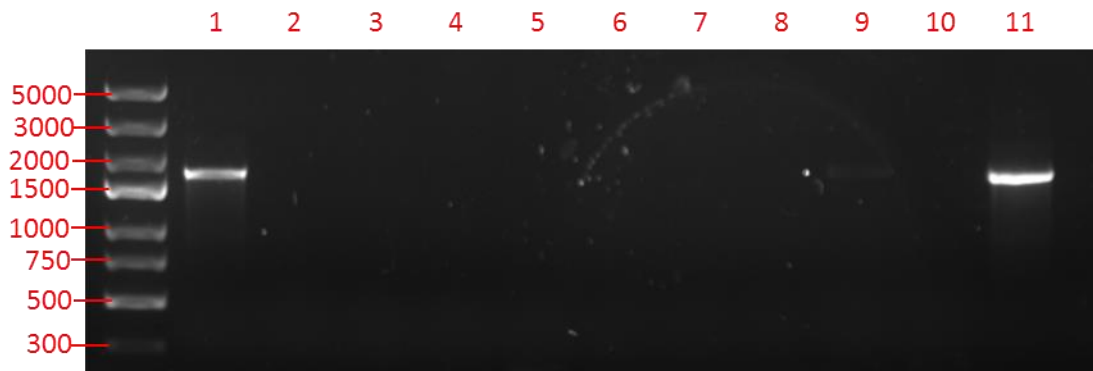


Figure 6.6 **Colony PCR reveals the colonies that have incorporated the ALK1 expressing plasmid.** In-fusion cloning was used to transfected bacteria with the plasmid pcDNA3.1_ALK1_HIS. Colonies that survived in kanamycin (50mg/ml) containing agar plates were subject to colony PCR. An ethidium bromide gel was run with colony PCR products from 11 colonies. The primers used are shown in Figure 6.4 and would only replicate DNA if ALK1 was present. Any product meant ALK1 had successfully incorporated in to the plasmid. This was seen for lanes 1 and 11.

6.2.3 Second attempt at stably over-expressing ALK1.

STOP-ALK1-N-13 and pcDNA3.1_ALK1_HIS were both linearised for the second attempt at creating a stable cell line. Figure 6.7 shows pcDNA3.1_ALK1_HIS linearisation by *MfeI* and *PvuI* respectively. STOP-ALK1-N-13 was linearised in the same way by the same restriction enzymes (data not shown). These linearised forms of the plasmids were used to transfect SW1353 cells and left until the cells could survive in G418 containing media. Unlike the previous cell line, both plasmids led to an increase of ALK1 protein expression (Fig 6.7), with neither of them affecting ALK5 expression and only pcDNA3.1_ALK1_HIS being able to express HIS as expected. This was true in both whole cell lysates and membrane specific blots (Fig 6.8). To assess if this increase in ALK1 protein expression led to downstream changes I looked at the expression of ID1 and PAI1. Previous 2 hour treatment with TGF β (chapter 4) led to no increase in ID1 (Fig 4.7). However, in both stable cell lines the same treatment resulted in a significant upregulation of ID1 (Fig 6.9A and C), whilst

also retaining the effect on PAI1 (Fig 6.9B and D). It has been reported that the ALK1 receptor cannot work without the ALK5 receptor present. To further explore this I silenced ALK5 using siALK5 to test if ID1 could still be increased. When ALK5 was silenced TGF β stimulation failed to induce PAI1 or ID-1 expression (Fig 6.9), indicating that ALK5 was required for ALK1 to function. pcDNA3.1_ALK1_HIS and STOP-ALK1-N-13 cell lines behaved in the same way (Fig 6.9), and as pcDNA3.1_ALK1_HIS had the His tag to aid detection I used it for all future experiments.

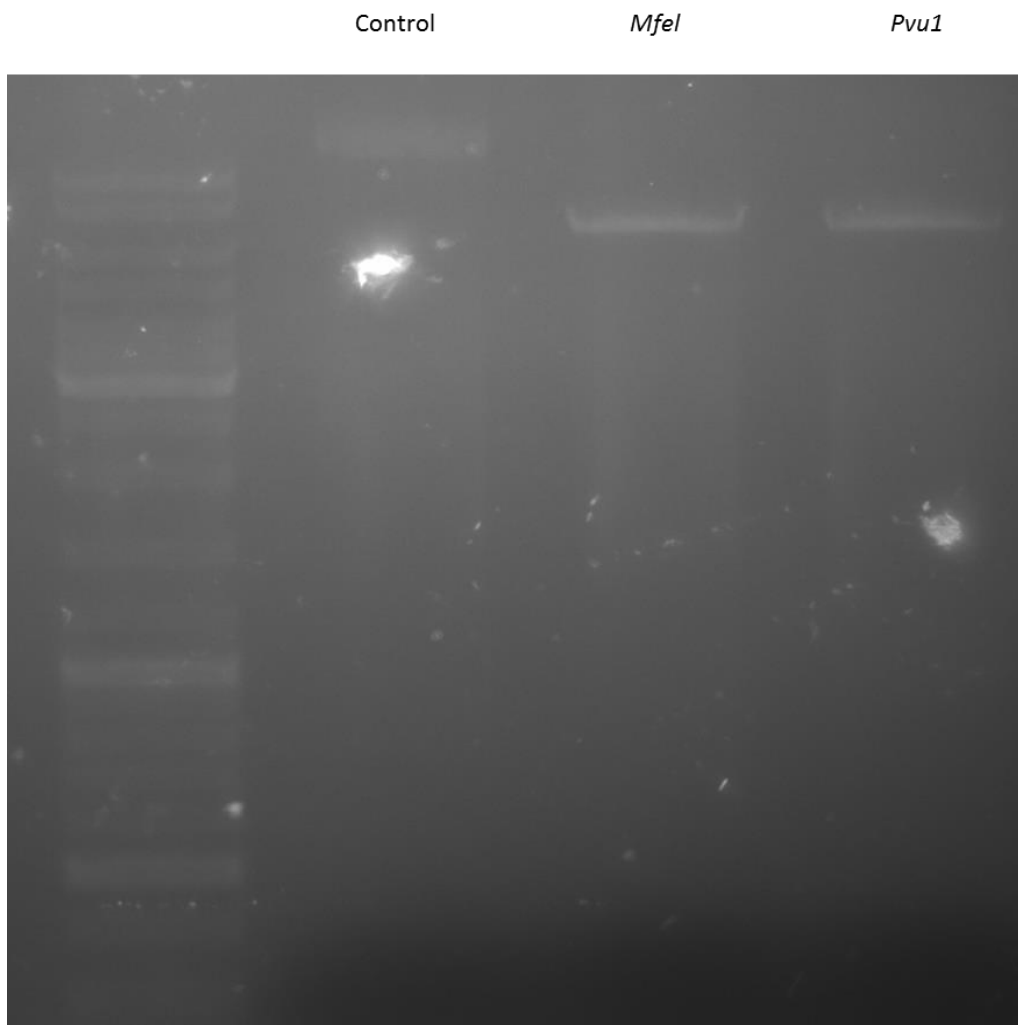


Figure 6.7 **Linearisation of pcDNA3.1_ALK1_HIS plasmid.** The pcDNA3.1_ALK1_HIS Plasmid was linearised by treatment with *MfeI* or *PvuI* for 4 hours at 37°. PCR clean-up was then used to purify the resulting products and they were run on an ethidium bromide gel to show linearisation. Uncut pcDNA3.1_ALK1_HIS plasmid was run as a control.

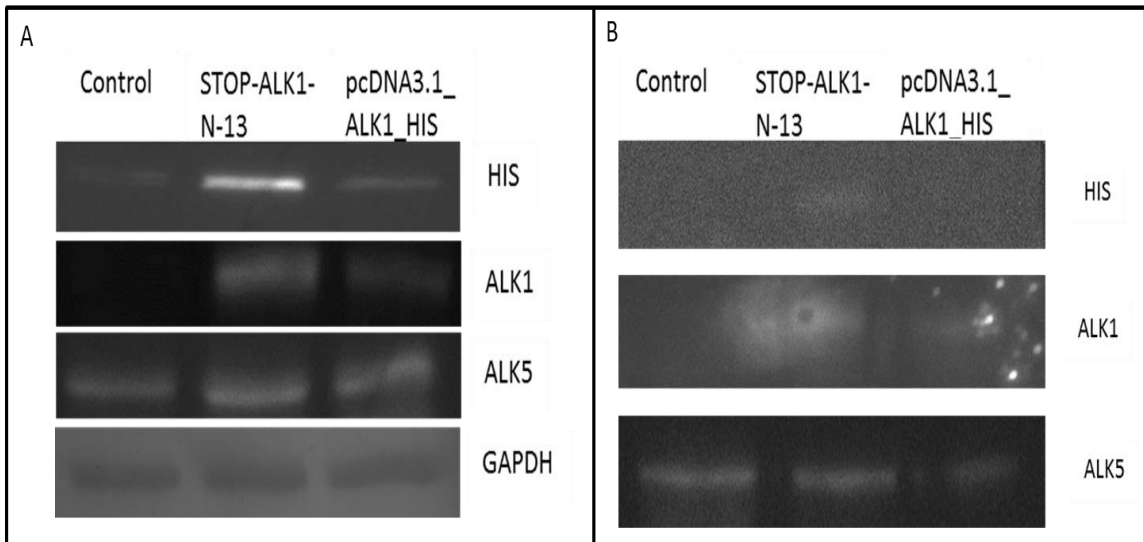


Figure 6.8 TGFβ type 1 receptor composition after second stable transfection. ALK1 overexpressing SW1353 cell lines (STOP-ALK1-N-13 and pcDNA3.1-ALK1_HIS) were grown to confluency in G418. Control cells were also grown to confluency in serum containing media without G418. The cells were then lysed and A) whole cell lysis was performed on 1 million cells. B) Membrane specific lysis was performed on 1 million cells. The samples were then run on 12% SDS-PAGE gel and western blots were undertaken for ALK5, ALK1, HIS tag and GAPDH. Blots are representative of 2 experiments on separate SW1353 cell populations.

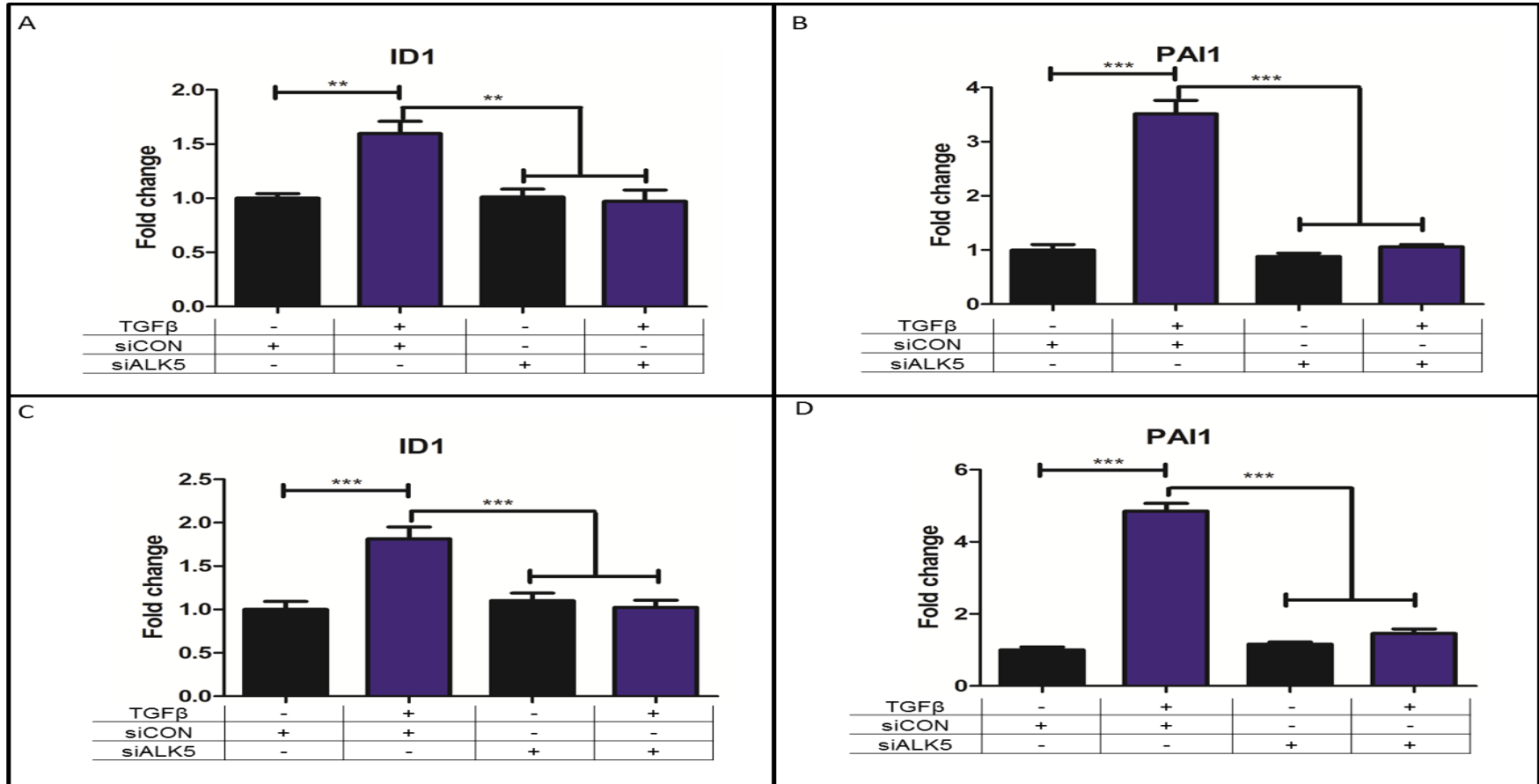


Figure 6.9 **Effect of ALK5 removal on ALK1 over-expressing SW1353 cells.** SW1353 cells stably over-expressing A and B) pcDNA3.1_ALK1_HIS or C and D) STOP-ALK1-N-13 plasmid were treated for 2 hours with TGFβ (10ng/ml) after 24h pre-treatment with 50nM of either siCON or siALK5. qPCR was then performed on the isolated mRNA to measure A) and C) ID1 expression B) and D) PAI1 expression. Data are presented as fold change relative to control (mean ± SD, n=5-6). Statistics calculated using unpaired Student's t-test, where ** p < 0.01; *** p < 0.001.

With a better understanding of how the stable cell lines were signalling, I wanted to look at what effect it would have on the TGF β -mediated repression of IL-1+OSM-driven MMP-13 expression. Comparing the stable cell lines directly to regular SW1353 cells (Fig 6.10A) showed that the ALK1 over-expression had no effect on the ability of TGF β to repress IL1+ OSM driven MMP-13 upregulation. Significant reduction can still be seen, which was around the same level as in wild type SW1353 cells (Fig 6.10A). Silencing ALK5 had the same effect as seen in chapter 4, with ALK5 depletion resulting in a loss of TGF β -mediated repression (Fig 6.10B). TGF β alone also had no significant effect on MMP-13 expression (Fig 6.10).

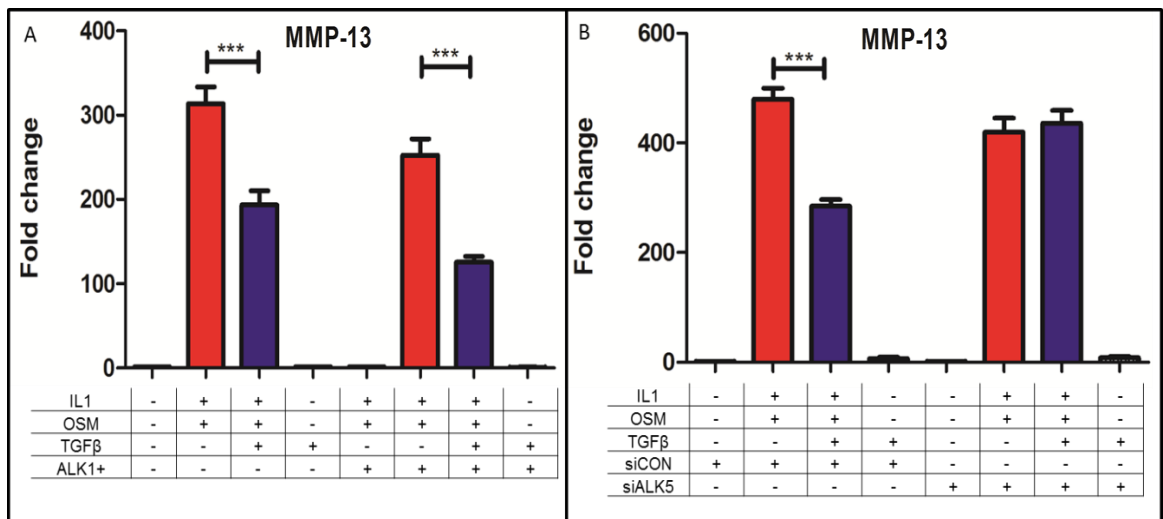


Figure 6.10 TGF β -mediated repression in ALK1 over-expressing SW1353 cells. SW1353 cells with or without the pcDNA3.1_ALK1_HIS plasmid stably overexpressed were treated for 24 hours with IL1 (0.5ng/ml), OSM (10ng/ml) and TGF β (10ng/ml). qPCR was then performed on the isolated mRNA to measure MMP-13 expression. A) Expression in the stable cell line (ALK1+) compared to wild type SW1353 cells. B) Expression in the stable cell line when pre-treated with 50nM siCON or siALK5 for 24h. Data are presented as fold change relative to control (mean \pm SD, n=5-6). Statistics calculated using unpaired Student's t-test, where; *** p < 0.001

I aimed to find a concentration at which siALK5 would decrease ALK5 levels but not alter ALK1 function, allowing signalling to switch from ALK5 toward ALK1. I first used the concentrations: 50, 40, 30, 20 and 10nM (Fig 6.11A and B). However, these all produced results identical to Figure 6.9. For this reason a lower concentration of siALK5 was used.

ID1 expression was increased with TGF β treatment but this effect was lost after pre-treatment with 10 and 5nM siALK5 (Fig 6.11C). However, at 2.5 and 1nM siALK5 pre-treatment TGF β led to a significantly increase in ID1 expression (Fig 6.11C). At both 2.5 and 1nM there was no significant difference between pre-treatment with siCON or siALK5 on the increase in ID1 expression after TGF β treatment (Fig 6.11C). PAI1 expression was significantly increased regardless of pre-treatment (Fig 6.11D). However, siALK5 pre-treatment at 2.5 and 1nM did reduce the extent to which PAI1 was increased, as the fold change was significantly less than pre-treatment with the siCON (Fig 6.11D). At 2.5nM siALK5, it appeared that signalling through ALK5 was reduced but ALK1 was still able to propagate a signal. For this reason I repeated Figure 6.10 with siALK5 at 2.5nM. The effect was that TGF β -mediated repression was retained with no difference to treatment with non-targeting siRNA (Fig 6.12). MMP-13 expression was also unaffected by TGF β treatment (Fig 6.12).

All of these results suggested that, although ALK1 was being over-expressed, ALK5 was still the dominant receptor. If ALK1 was the dominant receptor then TGF β should be able to increase MMP-13 mRNA. To look at this I treated cells with TGF β for 24 - 144 hours (Fig 6.13), but saw no significant increase at any of these time points. From this I concluded that ALK1 over-expression by this method was not sufficient to remove ALK5 dominance of the canonical pathway.

It is worth noting that stable cell lines cannot be maintained indefinitely and freeze thawing can result in the over-expression being lost. During these experiments one cell line became too old and a second was made. Figure 6.14 compares the older cell line to the new one, demonstrating that the process can be accurately repeated.

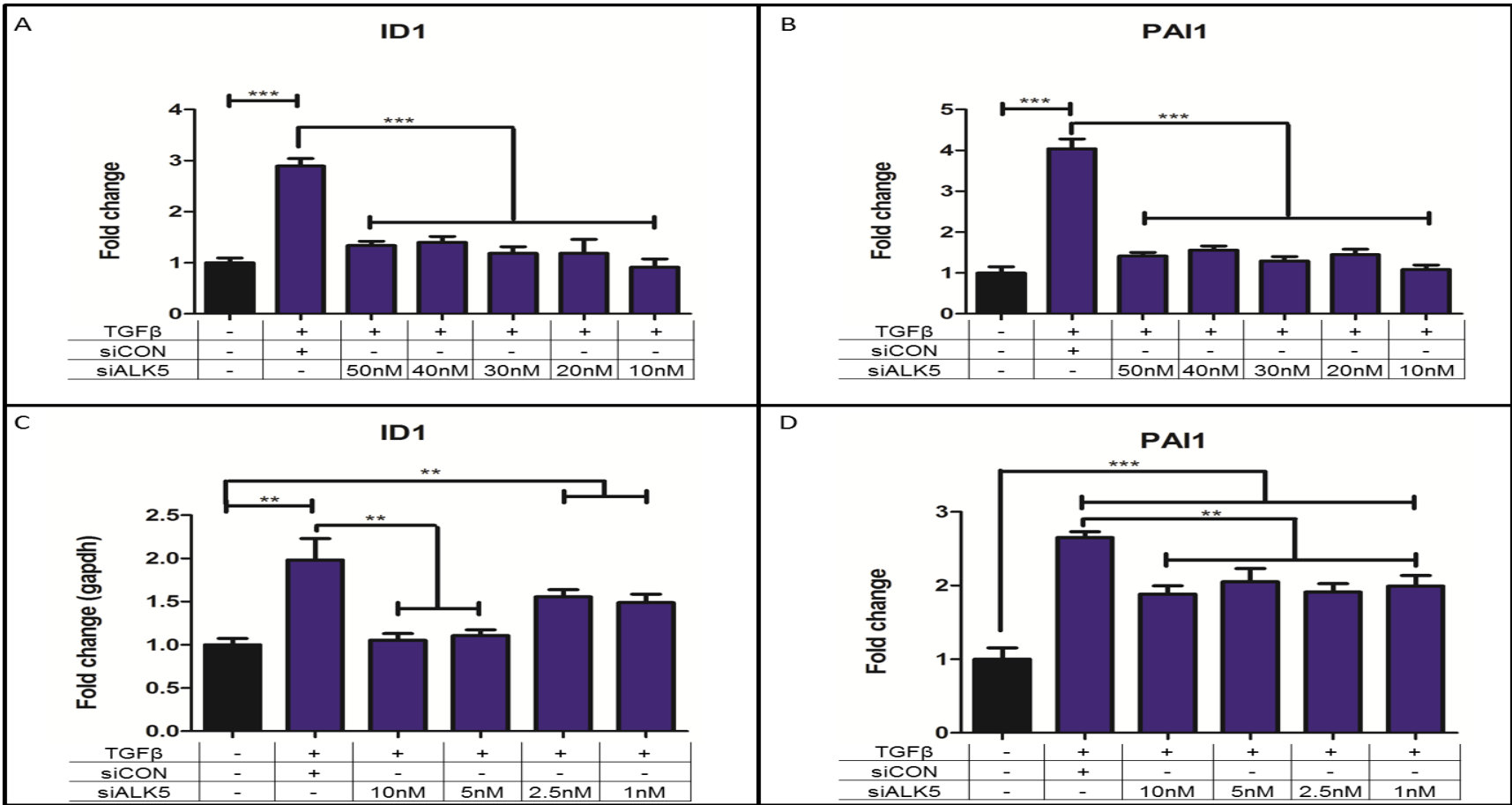


Figure 6.11 **Effect of varying siALK5 concentrations on TGFβ-mediated response.** SW1353 cells stably over-expressing the pcDNA3.1_ALK1_HIS plasmid were treated for 2 hours with TGFβ (10ng/ml), after a 24h pre-treatment with 50nM of either siCON or varying concentrations of siALK5. qPCR was then performed on the isolated mRNA to measure A) and C) ID1 expression B) and D) PAI1 expression. Data are presented as fold change relative to control (mean ± SD, n=4-6). Statistics calculated using unpaired Student's t-test, where ** p < 0.01; *** p < 0.001. Data presented are representative of 2 experiments on separate cell populations

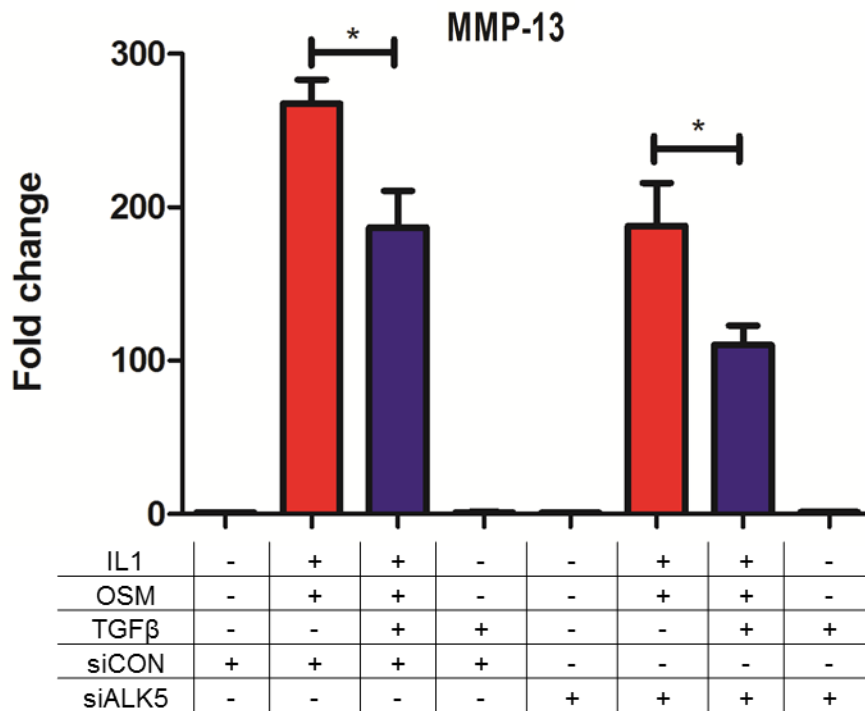


Figure 6.12 How reduced ALK5 affects TGFβ-mediated repression in ALK1 over-expressing SW1353 cells. SW1353 cells stably over-expressing the pcDNA3.1_ALK1_HIS plasmid were treated for 24 hours with IL1 (0.5ng/ml), OSM (10ng/ml) and TGFβ (10ng/ml), after pre-treatment with 2.5nM siCON or siALK5 for 24h. qPCR was then performed on the isolated mRNA to measure MMP-13 expression. Data are presented as fold change relative to control (mean ± SD, n=5-6). Statistics calculated using unpaired Student's t-test, where; * p < 0.05. Representative of 2 experiments on separate SW1353 cell populations.

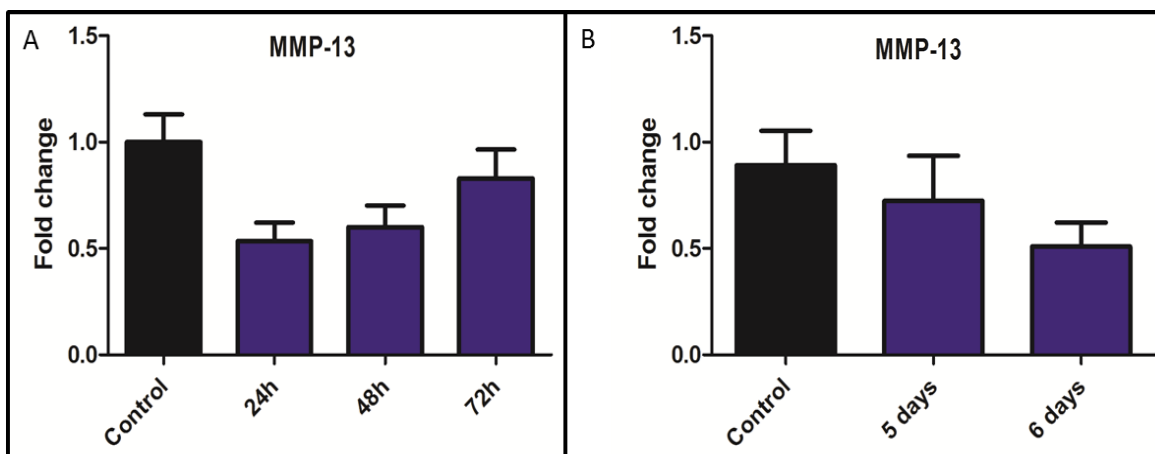


Figure 6.13 MMP-13 expression after TGFβ treatment in ALK1 over-expressing SW1353 cells. SW1353 cells stably over-expressing the pcDNA3.1_ALK1_HIS plasmid were treated for A) 24, 48 and 72 B) 5 and 6 days with TGFβ (10ng/ml). qPCR was then performed on the isolated mRNA to measure MMP-13 expression. Data are presented as fold change relative to control (mean ± SD, n=5-6). If the treatment took longer than 3 days TGFβ was replenished, by removing medium and immediately replacing it with fresh TGFβ-containing medium.

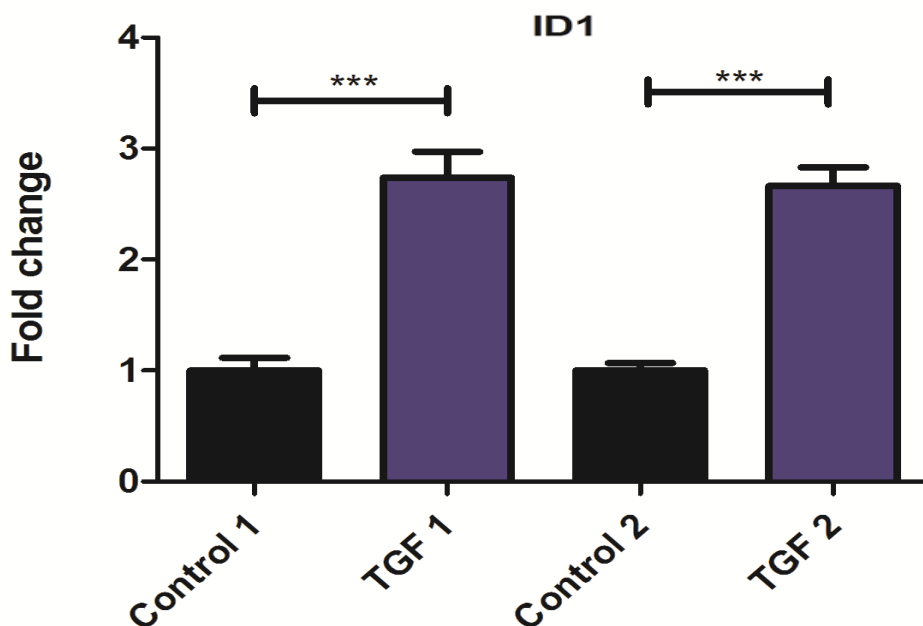


Figure 6.14 **Comparison of the first and second pcDNA3.1_ALK1_HIS stable SW1353 cells.** SW1353 cells stably over-expressing the pcDNA3.1_ALK1_HIS plasmid were treated for 2 hours with TGF β (10ng/ml). 1 was the original stable cell line and 2 was created when 1 was beginning to stop dividing. qPCR was then performed on the isolated mRNA to measure ID-1 expression. Data are presented as fold change relative to control (mean \pm SD, n=5-6). Statistics calculated using unpaired Student's t-test, where *** $p < 0.001$.

6.2.4 Adenoviral transduction

It appeared that over-expressing ALK1 in SW1353 cells was possible but the stable cell line did not provide sufficient expression to make it the dominant receptor. I aimed to find another system that may be able to provide increased ALK1 expression. Adenoviral transduction was a system that had provided robust and repeatable over-expression in many previous studies (Thrasher et al. 2006; Vorburger and Hunt 2002). An adenovirus that over-expresses ALK1 (adALK1) was kindly gifted to us by Peter Van Der Kraan (Radboud, Nijmegen, Netherlands).

adALK1 had never been tested on SW1353 cells so I attempted to find an MOI at which it may have an affect on the TGF β response. Figure 6.15 shows the effect of pre-treatment of adALK1 at 10,100 and 500 multiplicity of infection

(MOI) for 48 hours followed by 2 hour TGF β treatment. The first time I did this experiment (Fig 6.15A and B) TGF β increased PAI1 at all MOIs. TGF β treatment had no effect on ID1 expression at all MOIs, except for an MOI of 500, when it appeared to increase ID1 expression significantly (Fig 6.15A). Conversely, when the experiment was repeated, adALK1 not only failed to increase ID1 expression with TGF β treatment at any MOI (Fig 6.15C), but led to a significant decrease in ID1 expression at 0, 10 and 100 MOI and had no effect at 500MOI (Fig 6.15C). Again pre-treatment with adALK1 did not appear to effect PAI1 expression, as it was significantly upregulated after 2 hours TGF β treatment at all MOIs (Fig 6.15D).

I next examined whether adALK1 pre-treatment for 24 or 48 hours could upregulate ALK1 to a sufficient level to induce MMP-13 expression after 24 TGF β treatments. At 24 hour pre-treatment MOI of 100 resulted in a significant increase of MMP-13 mRNA, compared to control (Fig 6.16A). However TGF β addition led to no further increase (Fig 6.16A). At an MOI of 500 there was no change in MMP-13 mRNA expression (Fig 6.16A). When cell were pr –treated with adALK1 for 48 hours at an MOI of 100 it resulted in a significant increase in MMP-13 mRNA (Fig 6.16A). Addition of TGF β appeared to reverse this effect (Fig 16A). Again at an MOI of 500 there was no change in MMP-13 mRNA expression (Fig 6.16A).

There was a highly significant increase in ALK1 mRNA after adALK1 pre-treatment (Fig 6.16B) but as this was leading to confusing downstream effects, I wondered what effect the increase in ALK1 mRNA was having on protein expression. Figure 6.17 shows the protein expression of ALK1 after adALK1 transduction at 10, 100 and 500 MOI. Both ALK1 and ALK5 appear unaffected by the treatment. I concluded that although the adenovirus was affecting ALK1 mRNA, there was no evidence that this was going to have a more pronounced effect on ALK1 signalling than the stable cell line.

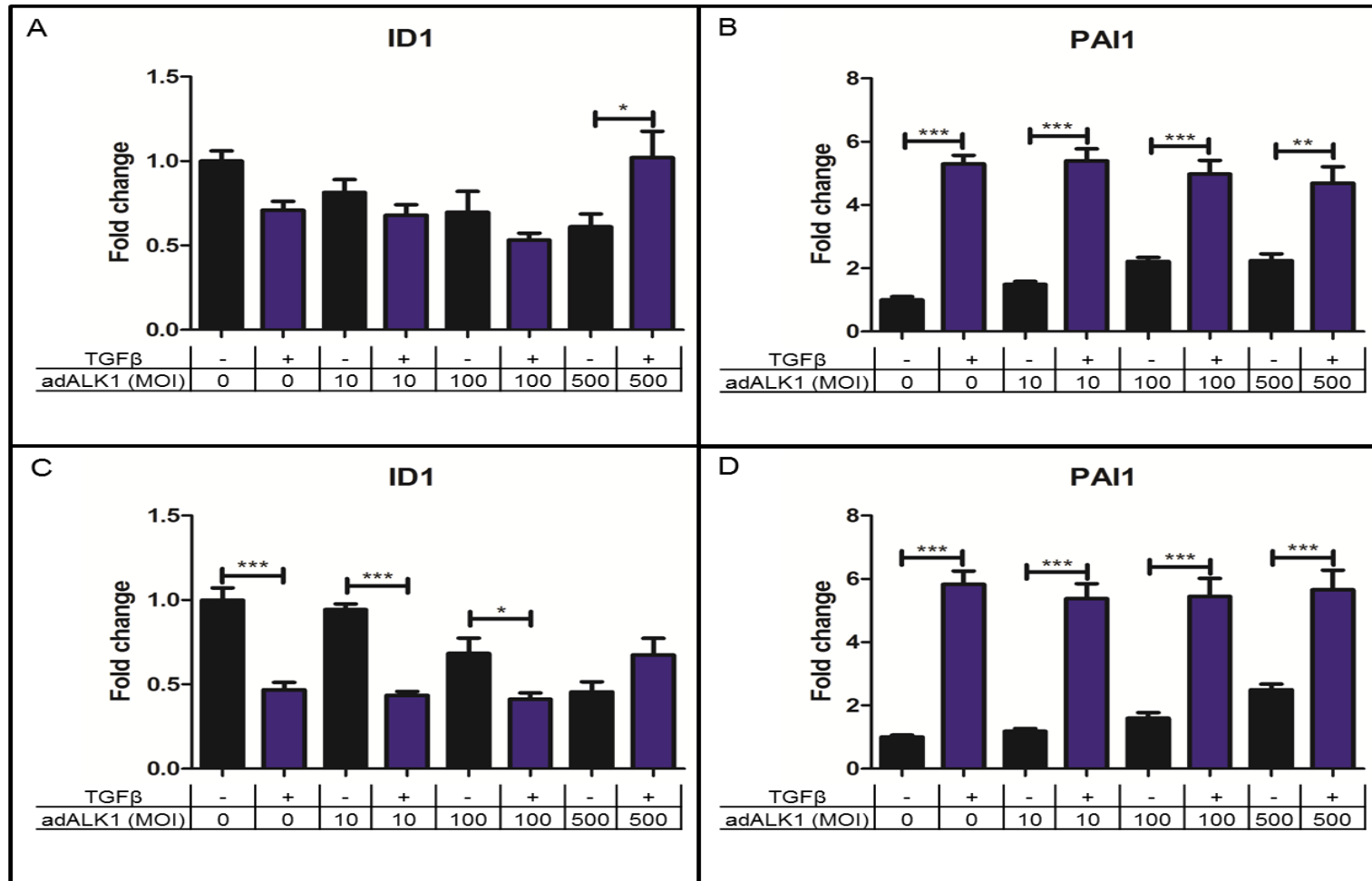


Figure 6.15 **Effect of ALK1 adenoviral transduction on TGFβ-mediated response at 2 hours.** SW1353 cells were treated for 2 hours with TGFβ (10ng/ml), after 48 hour pre-treatment of adALK1 at varying MOIs. qPCR was then performed on the isolated mRNA to measure ID1 expression (A and C) or PAI1 expression (B and D). Data are presented as fold change relative to control (mean ± SD, n=5-6). Statistics calculated using unpaired Student's t-test, where * p < 0.05; ** p < 0.01; *** p < 0.001.

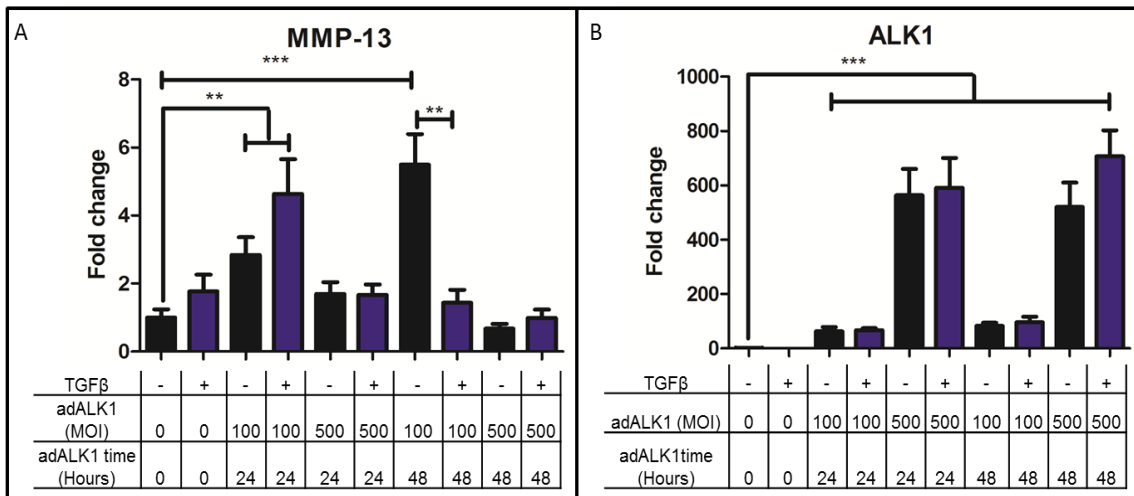


Figure 6.16 Effect of ALK1 adenoviral transduction on ALK1 and MMP-13 expression. SW1353 cells were treated for 24 hours with TGFβ (10ng/ml) after a 24 or 48 hour pre-treatment of adALK1 at varying MOIs. qPCR was then performed on the isolated mRNA to measure A) MMP-13 expression B) ALK1 expression. Data are presented as fold change relative to control (mean ± SD, n=5-6). Statistics calculated using unpaired Student's t-test, where ** p < 0.01; *** p < 0.001.

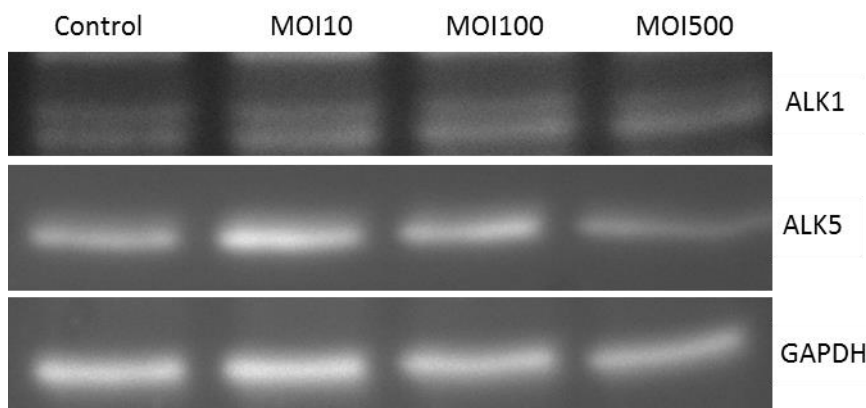


Figure 6.17 Protein expression after ALK1 adenoviral transduction. SW1353 cells were treated for 48 hours with adALK1 at 10, 100 or 500 MOI. Whole cell lysis was performed and the samples were then run on 12% SDS-PAGE gel. Western blots were then undertaken for ALK5, ALK1 and GAPDH. Blots are representative of 2 experiments on separate SW1353 cell populations.

6.2.5 Lentiviral transduction

Commercially available lentivirus that over-expressed ALK1 (lenALK1) provided another possible technique that may allow higher levels of ALK1 expression. Previous work done by our group suggested different lentiviruses lead to peak expression at 24 hours whilst other studies take 48, so my initial experiment incorporated both of these time scales. Due to previous experience with the adenovirus I also looked at protein prior to mRNA. Figure 6.18 shows ALK1 expression after 24 and 48 hour treatment with 1, 5, 10 or 100 MOI of lenALK1. After 48 hours MOI of 1 and 5 appear to have the strongest effect on ALK1 expression. However, there does appear to be some level of increased expression in all lanes (Fig 6.18). At 48 hours 5, 10, 50 and 100 MOI lenALK1 led to a significant increase in ALK1 mRNA expression (Fig 6.19).

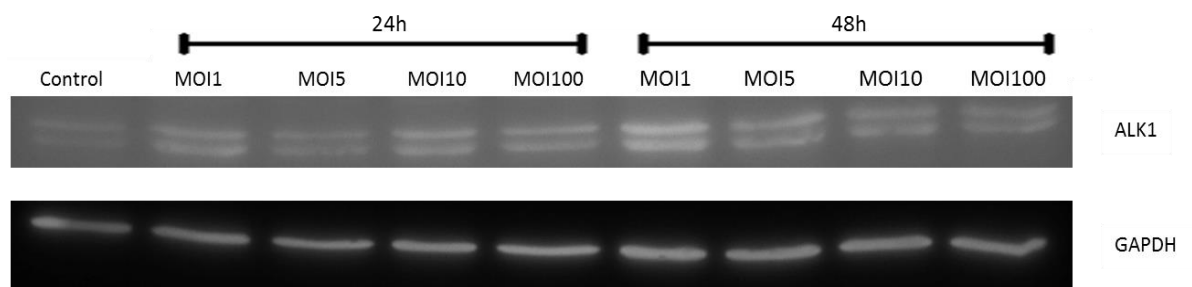


Figure 6.18 **Protein expression after ALK1 lentiviral transduction.** SW1353 cells were treated for 24 or 48 hours with lenALK1 at 1, 5, 10, 100 MOI. Whole cell lysis was performed and the samples were then run on 12% SDS-PAGE gel. Western blots were then undertaken for ALK5, ALK1 and GAPDH.

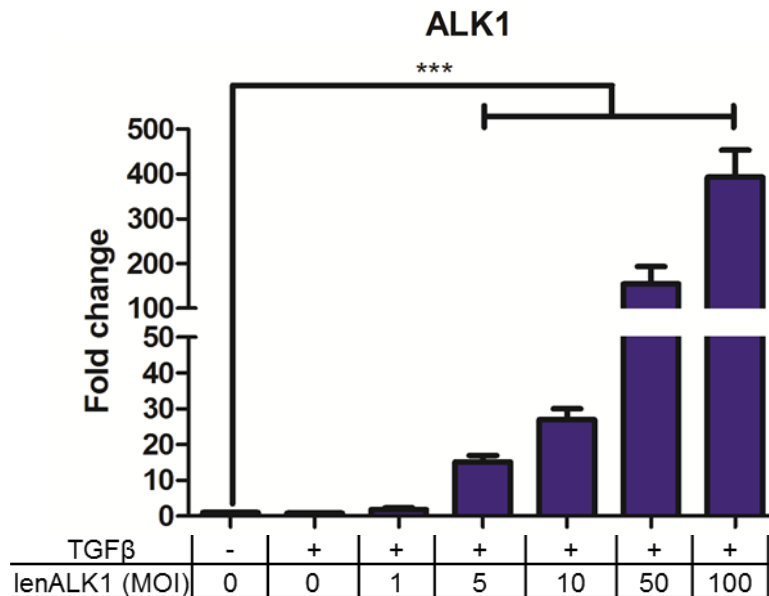


Figure 6.19 ALK1 mRNA expression after ALK1 lentiviral transduction. SW1353 cells were treated for 2 hours with TGFβ (10ng/ml), after 48 hours pre-treatment with lenALK1 at various MOIs. qPCR was then performed on the isolated mRNA to measure ALK1 expression. Data are presented as fold change relative to control (mean ± SD, n=5-6). Statistics calculated using unpaired Student's t-test, where *** p < 0.001.

I moved on to look at how the increase in ALK1 mRNA and protein affected the expression of PAI1 and ID1 after 2 hour TGFβ treatment. PAI1 was no longer significantly increased by TGFβ in the lenALK1-treated cells (Fig 6.20A).

Intriguingly, ID1 expression was unaffected by lenALK1 treatment suggesting that the cells were signalling through neither ALK1 nor ALK5 (Fig 6.20B). I explored if lack of signalling continued after prolonged TGFβ or could lenALK1 lead to the upregulation of MMP-13. Based on the protein and mRNA data I used an MOI of 5. At three days lenALK1 did not alter the effect of TGFβ on MMP-13 (Fig 6.21A). The empty lentiviral control (lenCON) behaved the same as lenALK1 (Fig 6.21A). Based on this, I looked at 3 days combining lenALK1 with siALK5: this time lenALK1 managed to significantly upregulate MMP-13 in the control and siCON cells when treated with TGFβ (Fig 6.21B). However, when treated with siALK5, TGFβ failed to upregulate MMP-13 higher than the untreated cells (Fig 6.21B). This may have been because siALK5+lenALK1 increased MMP-13 significantly with or without TGFβ, when compared to siCON cells (Fig 6.21B). I also ran both of these experiments at 6 days and found that MMP-13 mRNA was not significantly affected by any treatment (Fig 6.22).

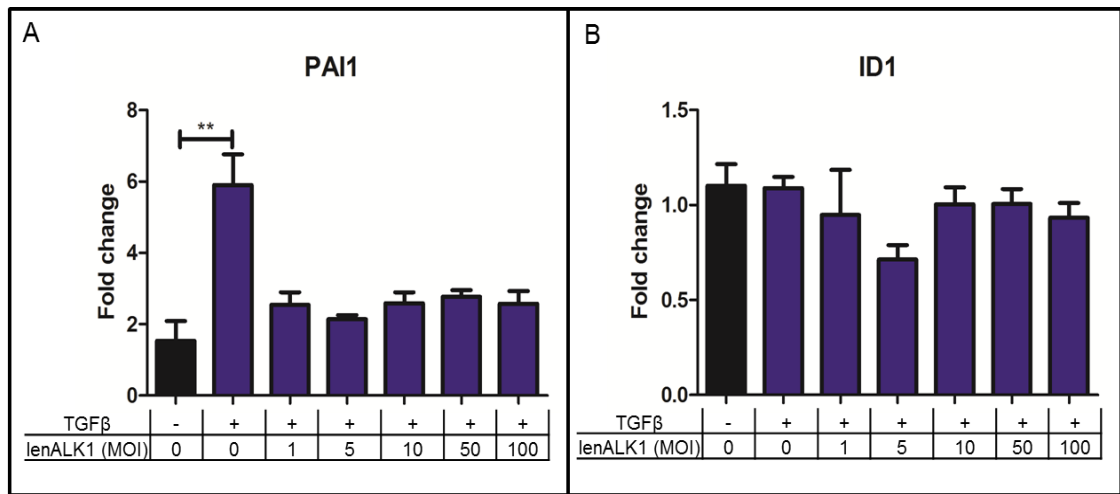


Figure 6.20 **Effect of ALK1 lentiviral transduction on TGFβ-mediated response, at 2 hours.** SW1353 cells were treated for 2 hours with TGFβ (10ng/ml), after 48 hours pre-treat with lenALK1 at various MOIs. qPCR was then performed on the isolated mRNA to measure A) PAI1 expression B) ID1 expression. Data are presented as fold change relative to control (mean ± SD, n=5-6). Statistics calculated using unpaired Student's t-test, where ** p < 0.01.

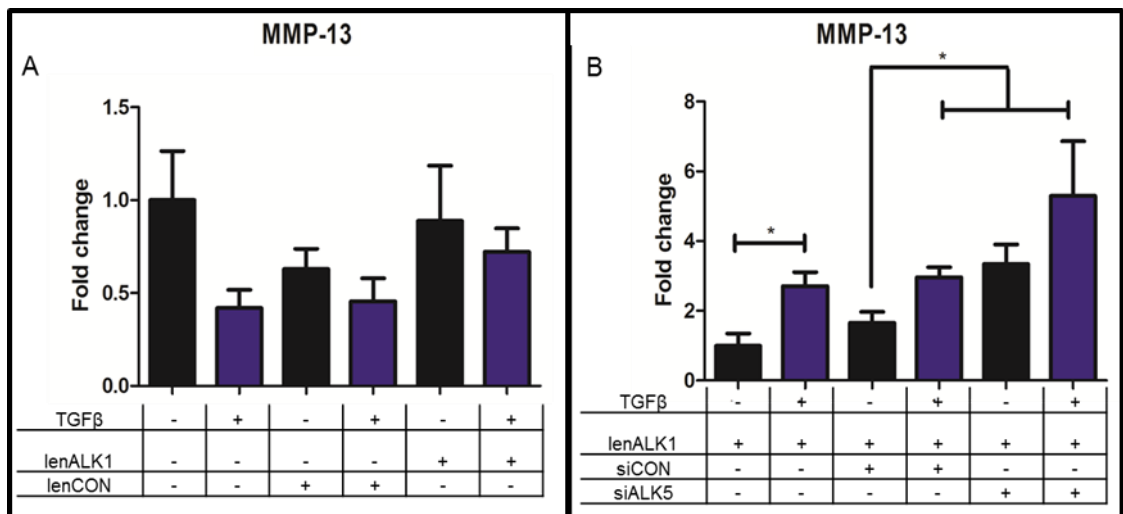


Figure 6.21 **Effect of ALK1 lentiviral transduction on TGFβ-mediated MMP-13 expression, at 72 hours.** SW1353 cells were treated for 72 hours with TGFβ (10ng/ml) after A) 48 hours pre-treat with lenALK1 or lenCON at an MOI of 5 and B) 48 hours pre-treat with lenALK1 at an MOI of 5, followed by 24 hours siCON or siALK5 (2.5nM) treatment. qPCR was then performed on the isolated mRNA to measure MMP-13 expression. Data are presented as fold change relative to control (mean ± SD, n=5-6). Statistics calculated using unpaired Student's t-test, where *p < 0.05.

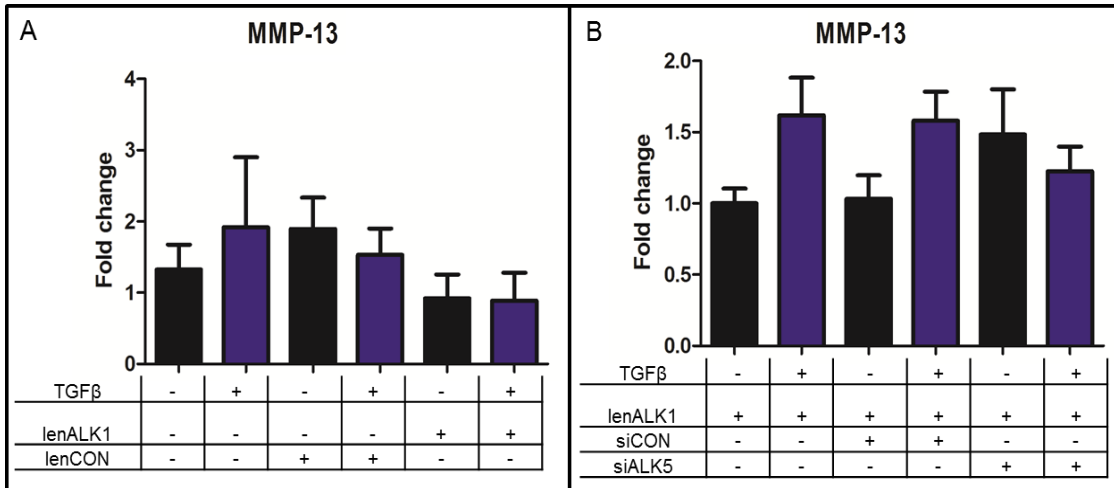


Figure 6. 22 **Effect of ALK1 lentiviral transduction on TGFβ-mediated MMP-13 expression at 6 days.** SW1353 cells were treated for 6 days with TGFβ (10ng/ml) treatment A) after 48 hour pre-treatment of either lenALK1 or lenCON (5 MOI). B) After 48 hour pre-treatment of lenALK1 (5 MOI) followed by 24 hours siCON or siALK5 (2.5nM). qPCR was then performed on the isolated mRNA to measure MMP-13 expression. Data are presented as fold change relative to control (mean ± SD, n=5-6). If the treatment took longer than 3 days TGFβ was replenished.

6.3 Discussion

Over-expressing ALK1, although problematic, was accomplished. However, over-expressing to a sufficient level for ALK1 to become the dominant TGF β receptor has not been possible and the reason(s) for this are unclear. My data replicate the well-established dogma that ALK5 is needed for ALK1 signalling (M. J. Goumans et al. 2003) but also highlight the delicate balance between the two receptors. The stable cell line allowed adequate ALK1 production to increase ID1 expression, indicating an increase in SMAD 1/5/8 signalling which has been shown to inhibit SMAD 2/3 signalling (M. J. Goumans et al. 2003). It would therefore be expected that as this ALK1 response becomes prominent the ALK5 response would be inhibited (M. J. Goumans et al. 2003). This should result in ALK1 dominance and a subsequent increase in MMP-13 expression with TGF β treatment (Blaney Davidson et al. 2009). Even a reduction in ALK5 levels in these cells, which did downregulate the ALK5 response, appears insufficient to allow ALK1 dominance. This suggests that when ALK1 becomes dominant in ageing it may be at a specific ALK1/ALK5 ratio. How tightly regulated this system is may further indicate the importance of ALK5 and why disease starts to develop when ALK1 is dominant.

6.3.1 Functionality of ALK1

Even when a high level of ALK1 protein has been achieved, ALK1 must be transported to the cell surface in order to mediate an effect (Mitchell et al. 2010). I initially created a cell line that stably expressed ALK1 since incorporation into the genome means that all protein folding and post-translational modifications are possible. This should allow ALK1 to be incorporated into the membrane and function correctly. All cells should also have similar levels of expression, hence there will be similar levels of expression between experiments (Chambers et al. 2015). This was seen with the stable cell line with a functional ALK1 over-expression having repeatable results. Unfortunately, this expression was not sufficient for TGF β to induce MMP-13 expression, which is an established consequence of ALK1 signalling (Blaney Davidson et al. 2009). As a result, transient transfection was attempted as it has the potential to induce much higher fold change expression (Vorburger and Hunt 2002; Federici et al. 2009). In the case of adenovirus this was seen at

the mRNA level but did not reflect in the protein or downstream response to TGF β . Lentivirus has also not shown an immediately obvious ALK1 response. However, I have not fully explored transient expression at this point so cannot make any firm conclusions.

It is possible that despite being over-expressed ALK1 failed to have a pronounced effect because of an inability to signal. Endoglin has been shown to have important implications in ALK1 signalling, and strengthens the interactions between the type I and type II receptors to allow increased signalling (Finnson et al. 2010). Low expression of endoglin in SW1353 cell may prevent this increased level of ALK1 from having its full effect, as there is insufficient endoglin to interact with all the newly formed receptors. Barksby et al. (2006) performed RNA microarray on SW1353 cells, looking at the control samples from this study showed the basal expression of many genes in SW1353 cells. Examining this data allowed me to confirm that endoglin is expressed and to a sufficient level for it to be measured by RNA microarray. It is impossible to infer from this data the relative protein level expression of endoglin in SW1353 cells or how this compares to other cells types. Over-expressing endoglin at the same time as ALK1 may allow for increased SMAD 1/5/8 signalling but I am unaware of any studies which have shown this yet. It is also possible that low levels of TGFBR2 could result in this effect (Bierie and Moses 2006). If TGFBR2 was responsible a similar effect should be seen in ALK5 signalling, yet ALK5 signalling through PAI1 is abundant. The Barksby et al. (2006) data also indicate there is basal expression of TGFBR2 to a sufficient level for it to be measured by RNA microarray.

6.3.2 Were SW1353 cells the correct cell type?

Basal expression of ALK5 and ALK1 in SW1353 cells, as shown in chapter 4, appears heavily biased towards ALK5. Overcoming this discrepancy is difficult as the cells appear incapable of producing high levels of ALK1 protein despite increased mRNA expression. Why protein cannot be produced is unclear, but it could be the result of many factors such as; insufficient translational machinery, a high level of ALK1 degradation, or the formation of inclusion bodies. These are aggregates regularly formed from over-expressed protein that has been incorrectly folded or transcriptionally modified (Wingfield et al. 2001). The high

levels of ALK1 protein may result in the system not being able to correctly modify the protein so instead it forms these aggregates that cannot function (Thomas and Baneyx 1996). The cells inability to translate high levels of mRNA may be why I can only detect increased ALK1 protein when there is a modest mRNA increase. This results in insufficient ALK1 to overcome ALK5 dominance.

This research seems to suggest that SW1353 cells are not an ideal cell type to study ALK1 over-expression. Finnsen et al. (2010) over-expressed ALK1 in the chondrocyte cell line C28/I2. Similarly to SW1353 cells, the basal expression of ALK1 could not be detected by western blot. However, despite this, their over-expression was sufficient to mediate an effect. Using these cells may provide a system where I could more easily manipulate the ALK1/ALK5 ratio. Primary human chondrocytes may also allow me to better manipulate the ALK1/ALK5 ratio, in a cell type that is the closest to *in vivo* human studies. However, tissues from late stage OA or older patients would most likely have an altered ALK1/ALK5 ratio already, so would undoubtedly present their own challenges (van der Kraan 2014). Human tissues are also a lot less readily available than cell lines and this could hinder the progression of a study solely reliant on them.

6.3.3 Future work

Despite the limited success currently seen with transient expression I would still like to perform further tests on both the adeno and lenti-virus. The adenovirus has only been tested at MOIs higher than those successful for the lentivirus and this was an oversight. Therefore I would like to repeat the experiments at a lower MOI to test if a smaller increase in ALK1 mRNA can result in upregulation of protein. For the lentivirus, I would like to repeat the 3 day experiment as it currently has some results that are difficult to explain. I would also like to try and uncover why both ID-1 and PAI-1 expression was not affected by TGF β at two hours after lentiviral pre-treatment treatment.

6.4 Summary

- Throughout this chapter I altered an ALK1 containing plasmid to create two new plasmids. Using these and the original plasmid I created a SW1353 cell line that stably over-expressed ALK1. Testing this cell line showed that although it could signal through ALK1, it was not the dominant receptor. Transient over-expression also failed to mediate ALK1 dominance.
- Although transient expression has not yet resulted in ALK1 being over-expressed to a level that it is dominant, future work is needed to determine if it possible in SW1353 cells.
- ALK5 is required for ALK1 to function. ALK5 dominance is tightly regulated; the ALK1/ALK5 ratio that favours ALK1 is most likely very specific.
- The problems encountered in over-expressing ALK1 may be specific to SW1353 cells, suggesting future work may be more successful in a different cell type.

Chapter 7: Model predictions and theoretical interventions

7.1 Introduction

The construction of a computational model has the advantage that it can be used to make predictions. For example, Passos et al. (2010) expanded on a previously developed model of p53 dynamics (Proctor and Gray 2008) to show that a small proportion of cells could avoid cell cycle arrest. They then later confirmed this experimentally (Passos et al. 2010). Similarly Dolan et al. (2015) created an integrated model by combining two previous published models Passos et al. (2010) and Dolan et al. (2013). Using the combined model they predicted the effect of low dose irradiation on cellular senescence. When they tested the model predictions experimentally they found it matched the general pattern that was observed, but some effects were smaller than predicted (Dolan et al. 2015). This demonstrated that although model predictions may not always be 100% accurate they can lead to the discovery of novel behaviours that otherwise may have gone unnoticed. In this chapter I will use the model created in chapter 5 to make predictions that could be tested in future studies. It is important to note the simulations were run with an inactive form of TGF β present to allow for the activation and deactivation of the growth factor, across the 20 month simulations.

7.1.1 Theoretical therapeutic interventions

Mathematical models can also provide a mechanism for testing potential interventions to limit disease progression. This allows you to test theoretical treatments that may yet not be possible and help to identify how worthwhile their development would be. For example, Tian and Kreeger (2014) created a mass action model that they used to look at antibody treatment of the Insulin-like growth factor 1 (IGF) pathway in ovarian cancer. It suggested that blocking IGF1–IGF1R binding would have a more pronounced effect on proliferation than neutralising IGF directly. Proctor and Gartland (2016) used a model to look at treatments that could reverse age-related bone loss. They demonstrated that not just the treatment but also the timing of its addition could have significant effects on its function, thus providing predictions for future studies.

1D11 is an antibody that targets TGF β , leading to its degradation. It has been demonstrated that injection of this antibody into the subchondral bone can

attenuate surgically induced OA progression in mice and rats (Gehua Zhen et al. 2013). A reduction was shown in the number of MMP-13 positive cells and cartilage damage was reduced (Gehua Zhen et al. 2013). They claimed that TGF β signalling had not been reduced in cartilage so the intervention would not affect normal cartilage homeostasis (Gehua Zhen et al. 2013). However, incorporating this antibody into my model may allow me to examine how it would affect the increase in MMP-13 caused by a shift in the ALK1/ALK5 ratio with age.

7.1.2 Alterations to the model

The original model present by Wang Hui et al. (2014), from which the TGF β portion of my model is based upon, partially focused on how the change in TGF β type I receptors affected RUNX2 driven MMP-13 mRNA expression. The model was made so that SMAD1 could activate RUNX2 whilst SMAD2 was required to deactivate it, meaning RUNX2 was incapable of becoming inactive without TGF β (or ALK5) present. In my model I was also only interested in how the interactions of TGF β and RUNX2 change as the TGF β type I receptors change, so I left this section unaltered. However, it is a simplification and RUNX2 can be inactivated by other mechanisms, independent of TGF β (Jonason et al. 2009). The inclusion of another mechanism for RUNX2 deactivation is required to model the attenuation of TGF β signalling.

7.1.3 Chapter aims

- Use the model to test theoretical therapeutic interventions which may help to reduce the negative changes associated with TGF β in age e.g. increased MMP-13 mRNA or reduced protection against pro-inflammatory stimuli.
- Explore the model to examine the stochastic behaviours between IL-1, OSM and TGF β .

7.2 Results

7.2.1 Therapeutic interventions.

As mentioned in the introduction, the original model assumption that RUNX2 cannot be inactivated without TGF β may be an issue when exploring therapeutic interventions. To address this I added a reaction that allowed RUNX2 to transition from an active to inactive state without a stimulus, whilst still requiring active SMAD1 for activation. Figure 7.1 shows that this small change had little effect on the overall model predictions across 20 months.

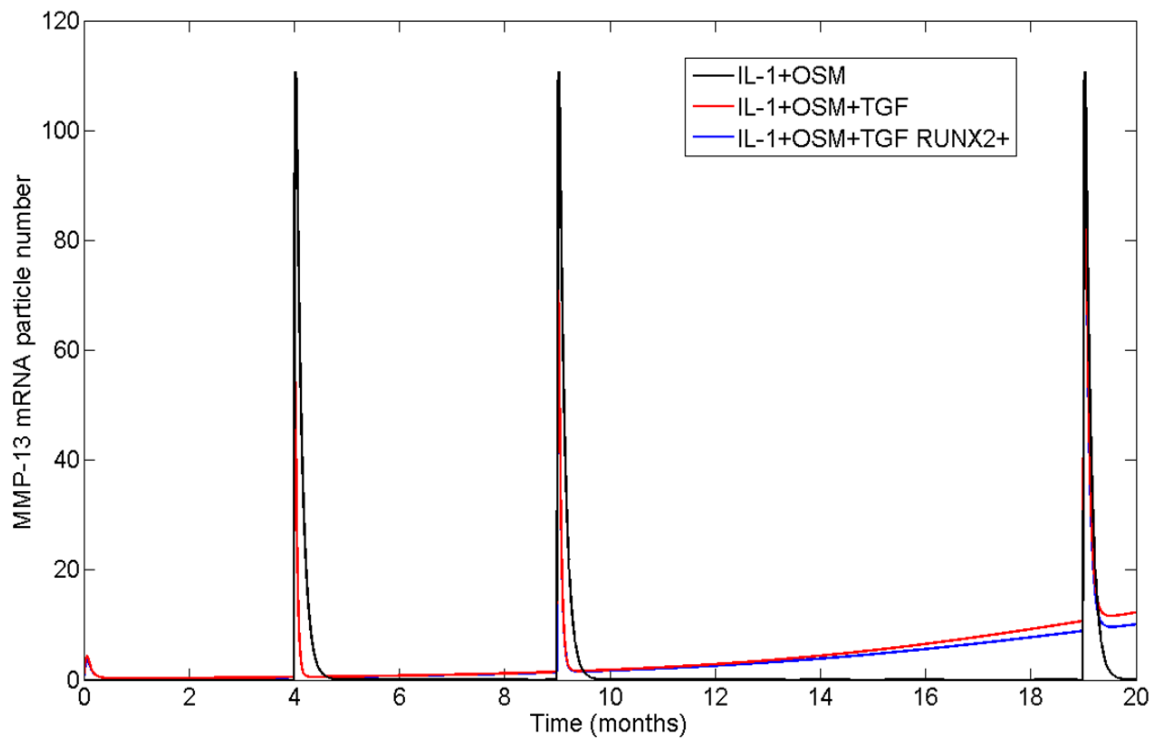


Figure 7.1 **Effects of an additional RUNX2 inactivation reaction, on my complete model.** Deterministic simulation results for my complete model, presented in chapter 5, showing the change in MMP-13 mRNA across 20 months simulation time. IL-1+OSM were triggered using events at ~4, ~9 and ~19 months. RUNX2+ represents an extra reaction added to the model, which allows RUNX2 to move from its active form to its inactive form without SMAD2 involvement. The simulations were run using COPASI.

7.2.1.1 Anti-TGF β treatment

In order to look at how the 1D11 antibody may interact with the system that I have created, I made a species “Anti-TGF”, which could bind to TGF β and degrade it in both its inactive and active forms (see appendix 7.1). The model also included degradation of anti-TGF so that it would gradually decay and leave the system. Leaving the system took Anti-TGF ~34 hours, the same length of time it was reported as taking to leave murine models by Xie et al. (2016) (see appendix 7.2 and 7.3). I wanted to look at how addition of Anti-TGF affected TGF β signalling across 20 months and how these changes may affect the interaction between TGF β and pro-inflammatory stimuli. The simulations began without Anti-TGF but it was introduced at ~6 months as an event. ~6 months was chosen as the time point as ALK1 becomes the dominant receptor after ~8 months. Therefore, I wanted to treat with Anti-TGF when ALK5 was beginning to lose dominance but when MMP-13 mRNA levels had not started to increase. I found that when Anti-TGF was first introduced at ~6 months the effects varied depending on how many subsequent times the antibody was added (Fig 7.2A). Focusing on the baseline expression of MMP-13 mRNA, rather than the 3 pro-inflammatory events (IL-1+OSM) at ~4, 9 and 19 months, a single introduction of Anti-TGF (at ~6 months) moved TGF β signalling towards an ALK1 response. This led to an initial increase in MMP-13 mRNA that continued until 20 months (Fig 7.2A). A second addition ~ 24 days later, also resulted in an initial increase in MMP-13 mRNA but this reached a plateau and decreased gradually towards 20 months (Fig 7.2A). A third simulated intervention, after another ~24 days was required to completely nullify the upregulation of MMP-13 mRNA across the entire 20 months (Fig 7.2A). Looking at the model output suggests this is because removing some, but not all, of the TGF β in the system drives it to signal through the receptor it has the highest affinity for, namely ALK1. So although both SMAD1 and SMAD2 have reduced phosphorylation, SMAD1 is not reduced by the same magnitude and this leads to activation of RUNX2.

Addition of Anti-TGF led to an increase of MMP-13 mRNA at both the ~9 and 19 month pro-inflammatory events, compared to IL-1+OSM+TGF β (Fig 7.2B and C). Also only when Anti-TGF was added to the system at three intervals ~24

days apart (starting at ~6 months), did the treatments not lead to larger increases of MMP-13 mRNA than IL-1+OSM alone, at both ~9 and 19 months (Fig 7.2B and C). Figure 7.3 shows three treatments with different time intervals (~1 days, ~6 days, ~12 days, or ~24 days) between the first, second and third Anti-TGF addition. The simulations suggested that treatments were more effective with longer intervals between Anti-TGF additions (Fig 7.3).

In both Figure 7.2 and 7.3 the ~6 month Anti-TGF treatment meant that the pro-inflammatory events (IL-1+OSM) at ~9 and ~19 months had a more pronounced effect than they would have without treatment. Therefore, I examined whether the treatment could still be effective later in the simulation, when ALK1 had become the dominant receptor. Treating with Anti-TGF at ~15 months, again focusing on baseline MMP-13 mRNA rather than the 3 pro-inflammatory events at ~4, 9 and 19 months, suggested a single induction of Anti-TGF led to a significant increase in MMP-13 mRNA (Fig 7.4A). The result is MMP-13 mRNA reaching higher levels than it would without treatment. A second and third induction of Anti-TGF, with a gap of ~24 days between each addition, was sufficient to alleviate the effect on MMP-13 mRNA, with the three treatments having a marginally stronger effect (Fig 7.4A).

After two or three Anti-TGF treatments (at ~15 months) the pro-inflammatory event at ~19 month had approximately the same effect as IL-1+OSM alone (no TGF β in the simulation), but had a more pronounced effect with only one Anti-TGF treatment (Fig 7.4B). The delay in the Anti-TGF treatments has a different effect at this later time point than the earlier one. Every ~day is still the least effective resulting in an increase in MMP-13 mRNA and a stronger pro-inflammatory response at ~19 months, than the other delays (Fig 7.5). However the ~6 days and ~12 days delays are both sufficient to mediate a constant reduction in MMP-13 mRNA (Fig 7.5). Leaving the delay to ~24 day reduces MMP-13 mRNA eventually but there is slight peak at ~16 months where MMP-13 mRNA increases (Fig 7.5). This increase is only minor but suggests the smaller delays are better when giving the treatment at a later time point.

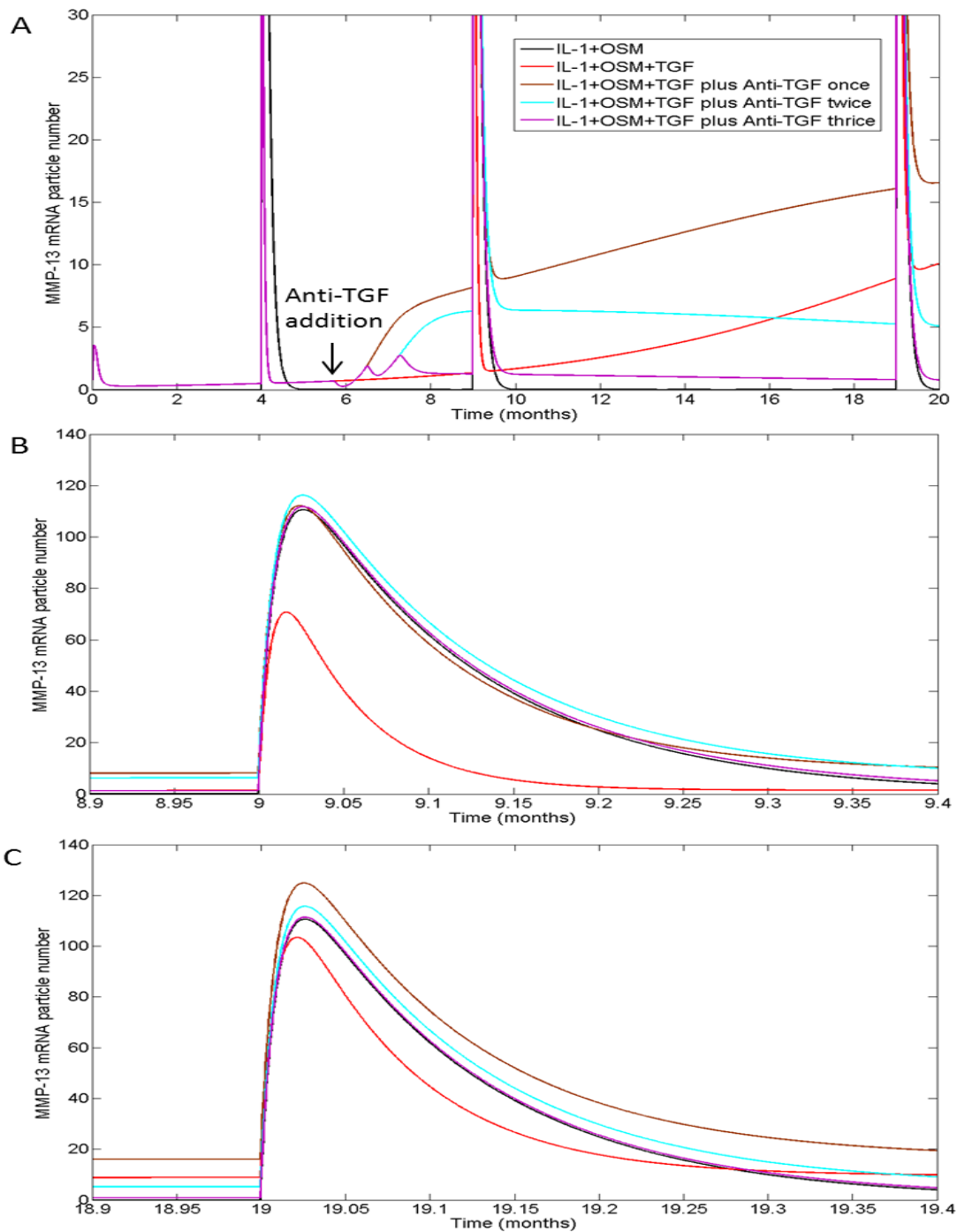


Figure 7.2 The effects of Anti-TGF treatment, starting at 6 months, on MMP-13 mRNA expression. A) Deterministic simulation results for my complete model, presented in chapter 5, with an extra reaction to allow RUNX2 inactivation. The data show the change in MMP-13 mRNA across a 20 months simulation time. IL-1+OSM were triggered using events at ~4, ~9 and ~19 months. The model also contained the species “Anti-TGF” which targeted and degraded both active and inactive TGF β . Anti-TGF concentration was at zero when the simulation started but at ~6 months Anti-TGF was added to the system, using an event. Anti-TGF was added either once, twice or thrice with a ~24 days interval between each addition. B, C) Highlights the time marginally before, during and after the change in MMP-13 mRNA expression following the IL-1+OSM events (B=~9 months and C=~19 months).

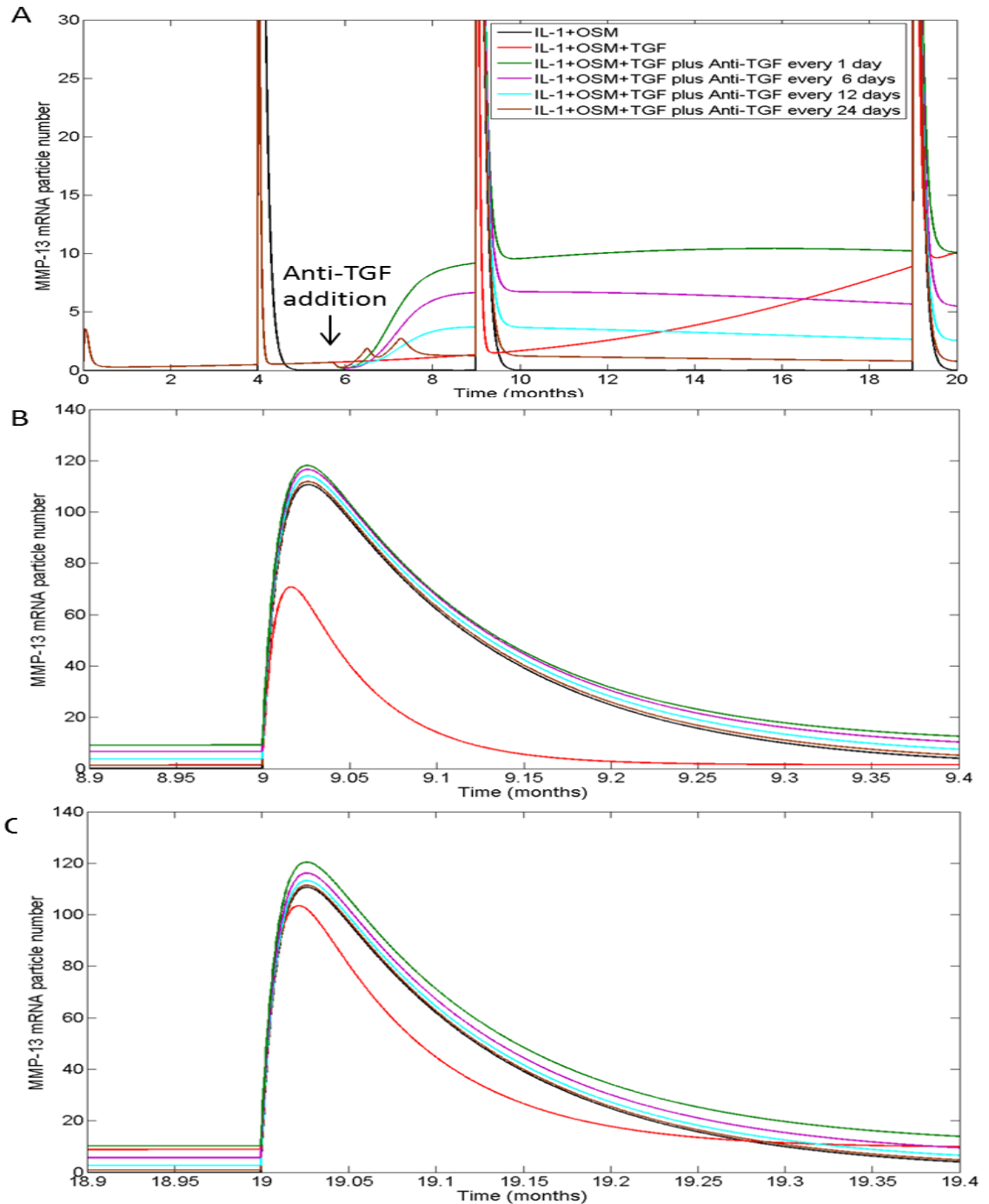


Figure 7.3 The effect of time delays on Anti-TGF treatment, starting at 6 months.
 A) Deterministic simulation results for my complete model, presented in chapter 5, with an extra reaction to allow RUNX2 inactivation. The data show the change in MMP-13 mRNA across a 20 months simulation time. IL-1+OSM were triggered using events at ~ 4 , ~ 9 and ~ 19 months. The model also contained the species “Anti-TGF” which targeted and degraded both active and inactive TGF β . Anti-TGF concentration was at zero when the simulation started but at ~ 6 months Anti-TGF was added to the system, using an event. Anti-TGF was added three times to the model with a ~ 24 days, ~ 12 days, ~ 6 days or ~ 1 day interval between each addition. B, C) Highlight the time marginally before, during and after the change in MMP-13 mRNA expression following the IL-1+OSM events (B= ~ 9 months and C= ~ 19 months).

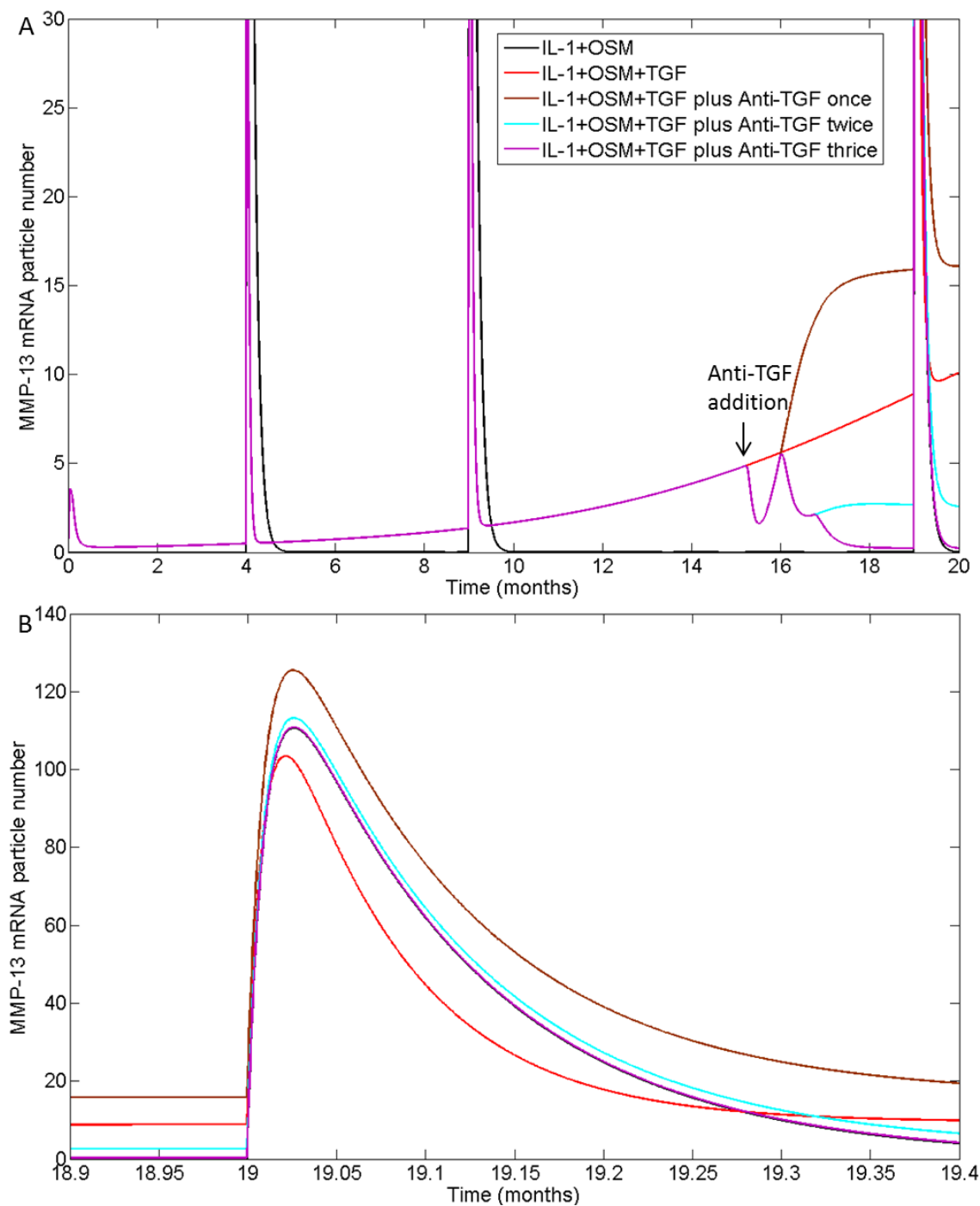


Figure 7.4 The effects of Anti-TGF treatment, at 15 months, on MMP-13 mRNA expression. A) Deterministic simulation results for my complete model, presented in chapter 5, with an extra reaction to allow RUNX2 inactivation. The data show the change in MMP-13 mRNA across a 20 months simulation time. IL-1+OSM were triggered using events at ~4, ~9 and ~19 months. The model also contained the species “Anti-TGF” which targeted and degraded both active and inactive TGF β . Anti-TGF concentration was at zero when the simulation started but at ~15 months Anti-TGF was added to the system, using an event. Anti-TGF was added either once, twice or thrice with a ~24 days interval between each addition. B) Highlights the time marginally before, during and after the change in MMP-13 mRNA expression following the IL-1+OSM event at ~19 month.

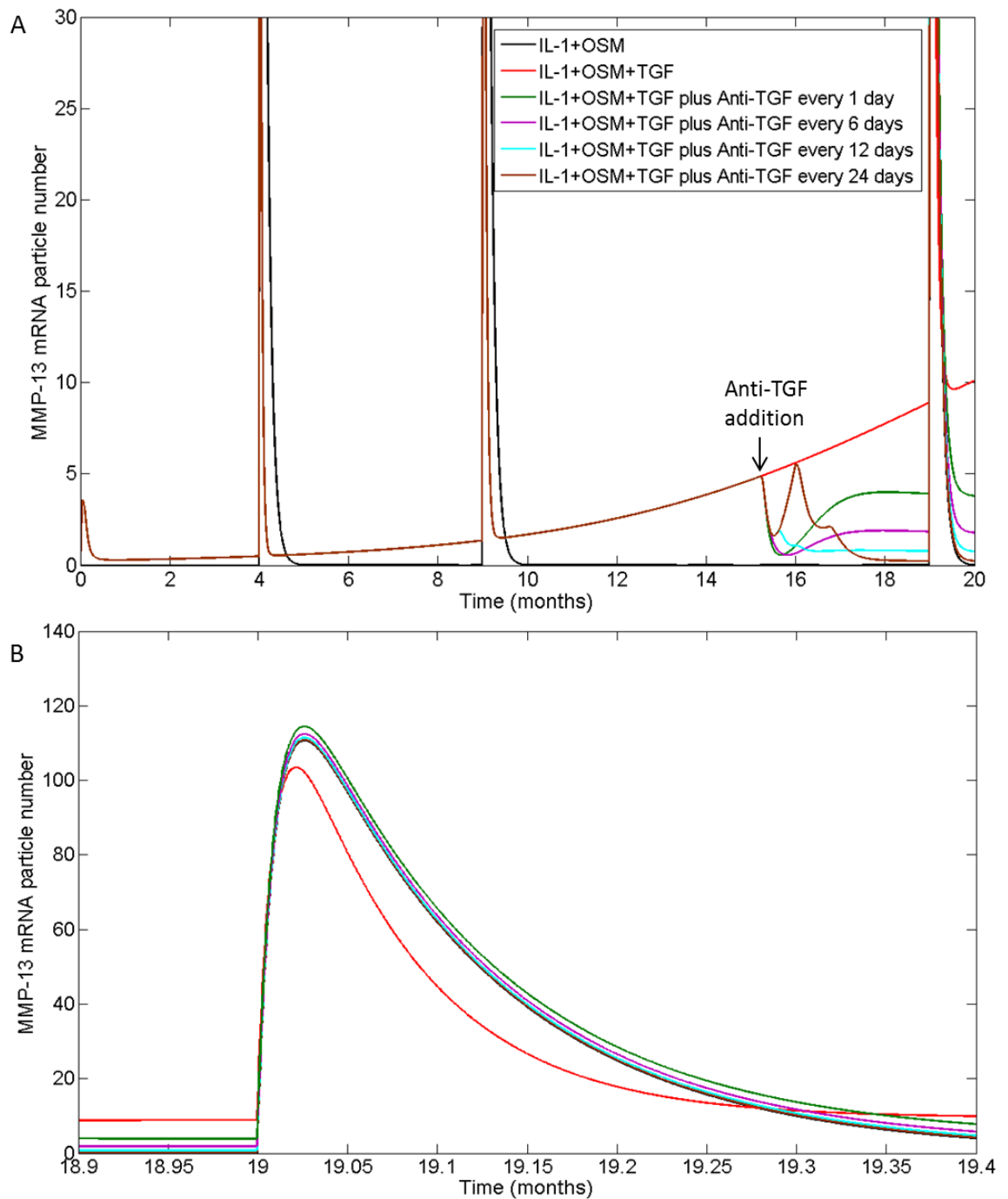


Figure 7.5 The effect of time delays on Anti-TGF treatment, starting at 15 months. A) Deterministic simulation results for my complete model, presented in chapter 5, with an extra reaction to allow RUNX2 inactivation. The data show the change in MMP-13 mRNA across a 20 months simulation time. IL-1+OSM were triggered using events at ~4, ~9 and ~19 months. The model also contained the species “Anti-TGF” which targeted and degraded both active and inactive TGF β . Anti-TGF concentration was at zero when the simulation started but at ~15 months Anti-TGF was added to the system, using an event. Anti-TGF was added three times to the model with a 24 days, ~12 days, ~6 days or ~1 day interval between each addition. B) Highlight the time marginally before, during and after the change in MMP-13 mRNA expression following the IL-1+OSM event at ~19 month.

7.2.1.2 Anti-ALK1 treatment

Although I am unaware of an antibody that targets ALK1, I used the model to test how targeting ALK1 would affect the system. To simulate this I made ALK1 the target of Anti-TGF, and changed the species name to “Anti-ALK1”. I treated with Anti-ALK1 at two different time points to see how they compared, ~6 and ~15 months (Fig 7.6). The model showed that multiple treatments of Anti-ALK1 did not affect the results, regardless of the time delay between treatments (data not shown). Therefore, I only gave one treatment in the future experiments. The ~6 month treatment with Anti-ALK1 reduced basal expression of MMP-13 mRNA throughout the simulation, but in the later time points there was still a steady increase. It also marginally increased the repression of the pro-inflammatory stimuli by TGF β at ~19 months (Fig 7.6). On the other hand, the late (~15 month) Anti-ALK1 treatment resulted in a larger reduction of MMP-13 mRNA after 15 months, whilst also increasing the repression seen by TGF β on the pro-inflammatory stimulus at ~19 months (Fig 7.6). It is worth noting that addition of Anti-ALK1 at both ~6 and ~15 months had no further effects. Although MMP-13 mRNA was marginally lower when the second treatment was added, it then followed the same pattern as a single treatment at ~15 months (data not shown).

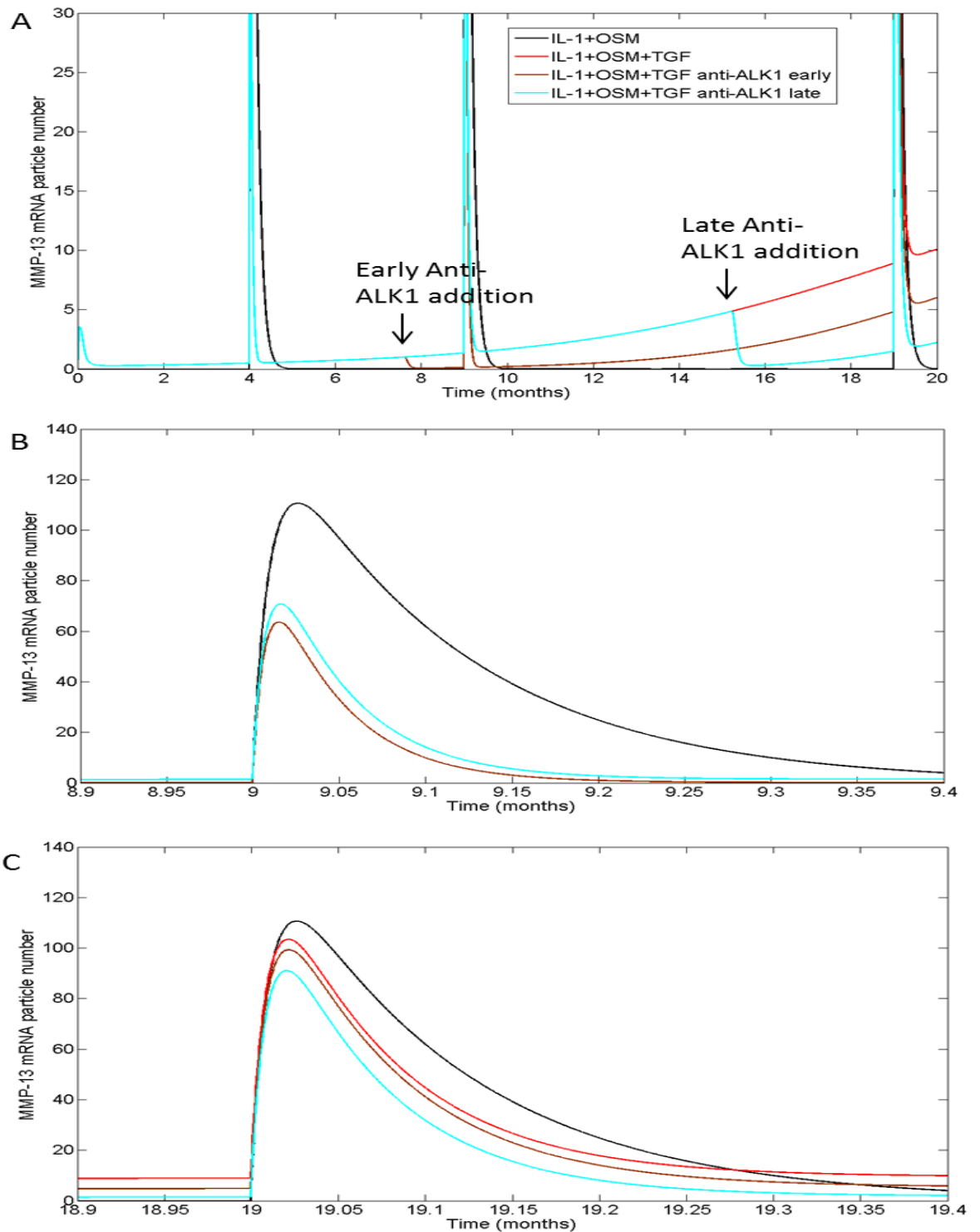


Figure 7.6 The effects of Anti-ALK1 treatment, at 6 or 15 months, on MMP-13 mRNA expression. A) Deterministic simulation results for my complete model, presented in chapter 5, with an extra reaction to allow RUNX2 inactivation. The data show the change in MMP-13 mRNA across a 20 months simulation time. IL-1+OSM were triggered using events at ~4, ~9 and ~19 months. The model also contained the species “Anti-ALK1” which targeted the ALK1 receptor for degradation. Anti-ALK1 concentration was at zero when the simulation started but at either ~6 months (early) or ~15 months (late) Anti-ALK1 was added to the system, using an event. B, C) Highlighted the time marginally before, during and after the change in MMP-13 mRNA expression following the IL-1+OSM events (B=~9 months and C=~19 months).

7.2.1.3 Pro-ALK5 treatment

Simulating the effects of removing ALK5 with an antibody in the same way as ALK1, exacerbated the negative effects of TGF β , resulting in increased MMP-13 mRNA both at basal and during pro-inflammatory stimuli (data not shown). However, overexpression of ALK5 had positive effects (Fig 7.7). Currently I am unaware of any treatments that would allow overexpression of ALK5 in patients. In the model I created an event that increased the levels of ALK5 in the system. I found that if this increased expression was early in the model it reduced the level of MMP-13 mRNA at the later time points. There was also an increase in TGF β -mediated repression of the pro-inflammatory stimuli at both ~9 and ~19 months (Fig 7.7). Increasing ALK5 levels at the later time point (~15 months) led to a marginally greater reduction in MMP-13 mRNA at >15 months, when compared to the early treatment. It also restored the TGF β -mediated repression of the pro-inflammatory stimulus at ~19 months to a level comparable with ~9 months (Fig 7.7). When both treatments were added their effects were combined resulting in MMP-13 mRNA levels never increasing and TGF β -mediated repression of the pro-inflammatory stimulus remaining relatively constant through the simulation (Fig 7.8).

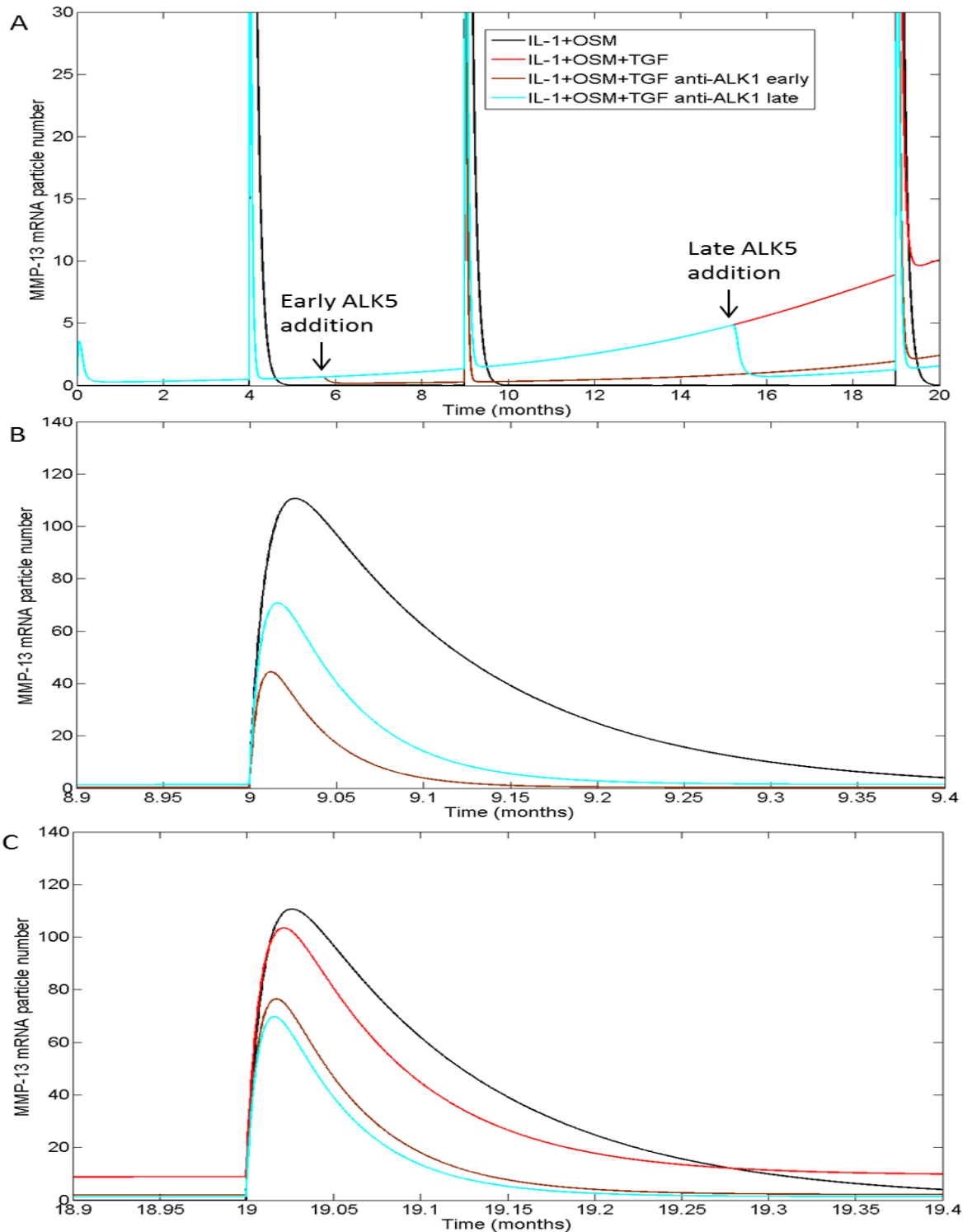


Figure 7.7 The effects of ALK5 addition, at 6 or 15 months, on MMP-13 mRNA expression. A) Deterministic simulation results for my complete model, presented in chapter 5, with an extra reaction to allow RUNX2 inactivation. The data show the change in MMP-13 mRNA across a 20 months simulation time. IL-1+OSM were triggered using events at ~4, ~9 and ~19 months. ALK5 level was restored to its initial level of 500 particle number, using an event, at either ~6 months (early) or ~15 months (late). B, C) Highlighted the time marginally before, during and after the change in MMP-13 mRNA expression following the IL-1+OSM events (B~9 months and C~19 months).

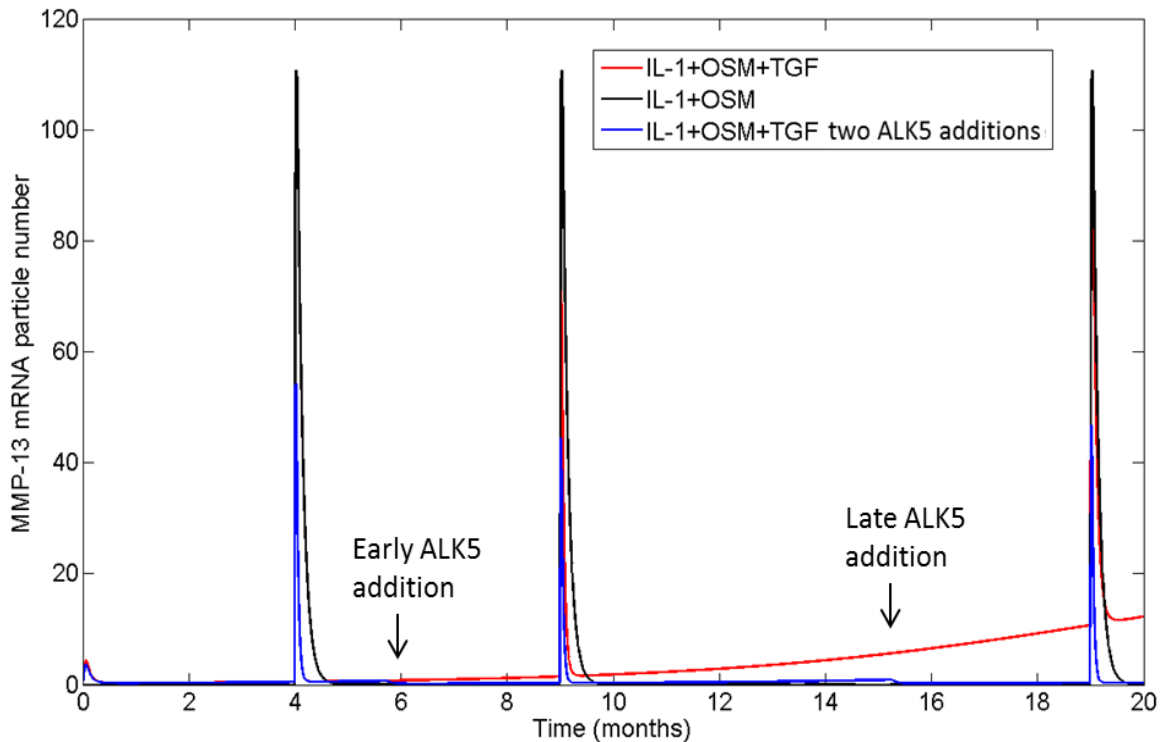


Figure 7.8 **The effects of ALK5 addition, at 6 and 15 months, on MMP-13 mRNA expression.** A) Deterministic simulation results for my complete model, presented in chapter 5, with an extra reaction to allow RUNX2 inactivation. The data show the change in MMP-13 mRNA across a 20 months simulation time. IL-1+OSM were triggered using events at ~4, ~9 and ~19 months. ALK5 level was restored to its initial level of 500 particle number, using events, at ~6 months (early intervention) and ~15 months (late intervention).

7.2.1.4 Altering SMAD levels

SMAD4 is required for SMAD1 and SMAD2 to have their downstream effect. So I looked at how altering the expression in the model, via an event, would effect TGF β signalling. Either increasing or decreasing SMAD4 levels had only minor effects at the early time points, unless it was completely removed which stopped signalling completely (data not shown). At a later time point, ~15 months increasing SMAD4 led to a reduction of MMP-13 mRNA, whilst decreasing SMAD4 led to a more potent increase in MMP-13 mRNA (Fig 7.9). This suggests that SMAD4 levels are important for propagating SMAD2 signalling when ALK1 starts to become dominant, with a loss in SMAD4 still allowing SMAD1 signalling but preventing SMAD2 from opposing its effects. I also altered the levels of SMAD7 in the same way as SMAD4 but seen only minor changes in behaviour (data not shown).

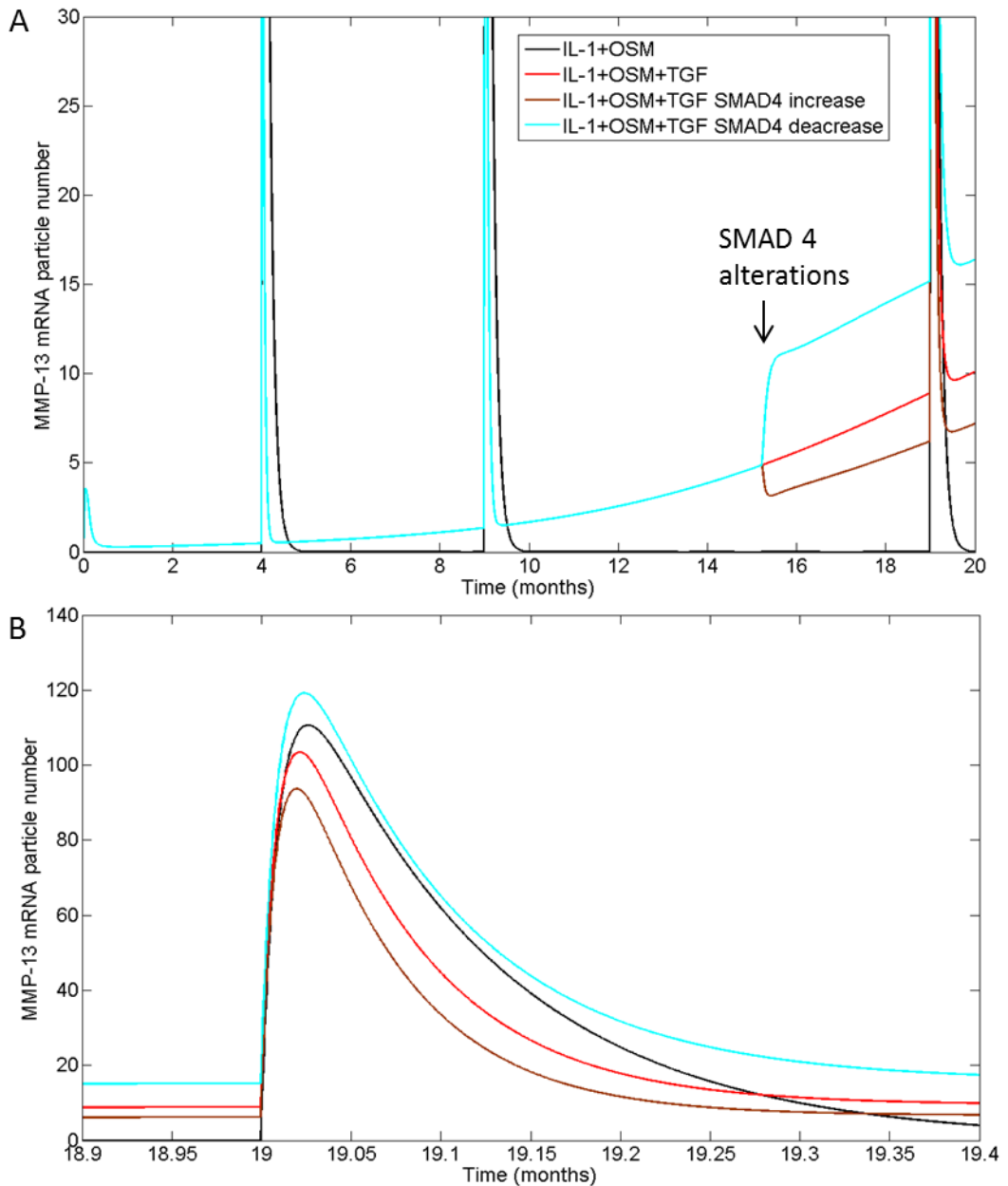


Figure 7.9 The effects of altered SMAD4 expression, at 15 months, on MMP-13 mRNA expression. A) Deterministic simulation results for my complete model, presented in chapter 5, with an extra reaction to allow RUNX2 inactivation. The data show the change in MMP-13 mRNA across a 20 months simulation time. IL-1+OSM were triggered using events at ~4, ~9 and ~19 months. SMAD4 concentration was either increased to 1000 particle number or decreased to 400 particle number at ~15 months. B, C) Highlight the time marginally before, during and after the change in MMP-13 mRNA expression following the IL-1+OSM events (B=~9 months and C=~19 months).

7.2.2 TGF β reduces the impact of an inflammatory response whilst increasing stability.

The stochastic nature of inflammatory responses means that the effects can have a large variability. So in addition to examining the effects of interventions on MMP-13 mRNA expression, I decided to inspect the effect of stochasticity on the TGF β -mediated repression of IL-1+OSM. Stochastic simulation provides information not just on just the pattern of expression but also how variable that response is. The amount of MMP-13 mRNA that was generated during IL-1+OSM stimulation was very variable in the model (Fig 7.10) and when TGF β was added to this system the first 12 hours of simulation had a similar level of variability. However, post 12 hours there was a reduction in not only the average level of MMP-13 mRNA but also the variability (Fig 7.10A). When the system was stimulated with IL-1+OSM treatment, after 6 hours pre-treatment with TGF β , this reduced variability was even more pronounced (Fig 7.10B).

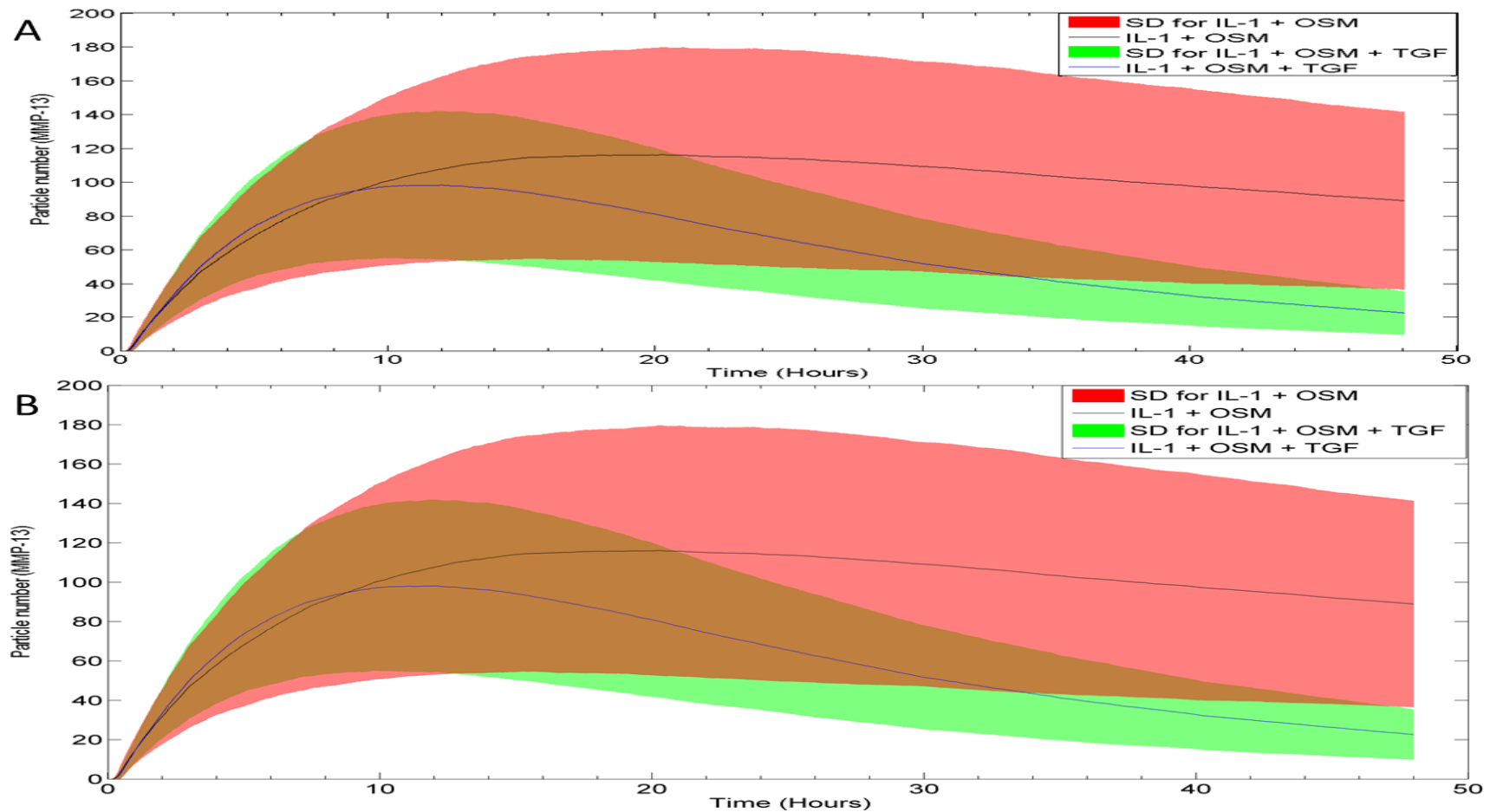


Figure 7.10 **Average behaviour of 100 stochastic model runs showing inherent variation in the system.** Stochastic simulation results showing the average behaviour \pm the standard deviations of 100 stochastic runs of the complete (presented in chapter 5) A) Model run over a simulation time of 48 hours. The model was run with IL-1+OSM \pm TGF β B) Model run over a simulation time of 54 hours. An event triggers IL-1 and OSM stimulation 6 hours after TGF β pre-treatment. An active form of TGF β was used in all simulations. Curves show how the particle numbers of MMP-13 mRNA change over the simulation. The coloured shading shows the variation at each time point. Simulations were run using COPASI.

7.3 Discussion.

It is important to note that the model I have created only looks at the changing role of TGF β with age, in the context of inflammatory damage. So any predictions made do not encompass the effect interventions would have on other key TGF β -mediated processes; for example how Anti-TGF would affect normal cartilage homeostasis. Despite this, the interventions I have looked at have shown some exciting behaviours and they may provide direction for future studies.

7.3.1 Incomplete removal of TGF β favours ALK1 signalling.

The model is unable to regenerate TGF β , if it is removed from the system (justified in chapter 2). Physiologically this is not accurate as *in vivo* latent TGF β is continually released (Pedrozo et al. 1998). However, the model does suggest that when targeting TGF β in cartilage it is important to completely remove TGF β from the system, as at lower levels it will signal through ALK1. The model suggests that under normal conditions there is an abundance of TGF β molecules over type I receptors and as there is significantly more ALK5, it becomes the dominant receptor. ALK1 is the preferential binding partner of TGF β (van der Kraan et al. 2012) so when TGF β is in low abundance it tries to signal predominantly through that receptor. As there is now more receptors than TGF β molecules this results in ALK5 signalling being affected more by the reduction in TGF β . If correct, this prediction could have implication in TGF β targeting therapies as attempting to remove TGF β to elevate joint damage may result in increased damaged.

7.3.2 Similarities between all theoretic interventions.

Unsurprisingly targeting ALK1 for degradation or overexpressing ALK5 had positive effects, with either treatment reducing baseline MMP-13 mRNA expression and restoring the protective effect of TGF β on IL-1+OSM-driven MMP-13 mRNA expression. However, what was evident is that the time at which the interference took place was important in the effect. Finding the most effective time to target TGF β may be key in developing therapeutics that will help it regain the protective functions that it has in younger animals. It appears that therapeutics will be most effective if they can be prescribed just as the ALK1 receptor is starting to become dominant. The model also suggested that attempting to overexpress ALK5 will be a more promising treatment than targeting ALK1. This is based on the effects of overexpressing ALK5 being more prolonged and combining treatments could theoretically reverse all effects on MMP-13 mRNA. Interestingly although targeting ALK1, ALK5 or TGF β directly had strong effects, targeting SMAD4 had comparatively minor effects and targeting SMAD7 had negligible effects to the system.

The model also predicted that targeting TGF β itself will require more than one treatment. The reason for this in the model is that TGF β is bound to receptors so cannot be targeted for degradation, when the receptors are recycled it is released and can then bind to new receptors. What was evident is that the intervals between Anti-TGF treatments had to be significant to see any effect. Therefore, a larger dose may not be sufficient to mediate the optimum effects.

7.3.3 Stabilising the inflammatory response.

Stochastic simulations predicted that TGF β adds stability to a pro-inflammatory response. Throughout this thesis I have looked at the negative effects of inflammation in OA development. However, when functioning correctly inflammation is an important biological response that helps to eliminate causes of cell injury, degrade necrotic cells and the damaged parts of tissues, as well as initiating repair (Rock and Kono 2008). Therefore inflammatory responses are normally beneficial but they can become chronic and lead to damage, and as a result must be tightly regulated (Martel-Pelletier et al. 2008).

In cartilage MMP-13 is upregulated in response to inflammation and has important roles in maintaining healthy cartilage, as well as degrading damaged cartilage components to allow repair and maintenance to the system (Masaki Inada et al. 2004). It is when this becomes dysregulated that we start to see disease. The variability of the IL-1+OSM response can lead to damage, with high levels of MMP-13 leading to degradation of cartilage that could cause early onset of cartilage damage (Goldring and Otero 2011). Conversely, not enough upregulation of MMP-13 could result in the body not being able to properly turn over tissues. Therefore, a uniform response is a key way of controlling damage during an inflammatory response and TGF β may add the stability that allows the body to regulate this response. A loss of this with age could also contribute to an incoherent system and OA development.

7.3.4 Summary

- Targeting TGF β for degradation protected against an increase in baseline MMP-13 mRNA with age but removed any protective effect against pro-inflammatory stimuli.
- Targeting ALK1 for degradation or increasing ALK5 concentration protected against MMP-13 mRNA with age and restored the protective effect against pro-inflammatory stimuli.
- SMAD4 had only minor effects on MMP-13 mRNA expression and SMAD7 had no effects.
- At what time interval interventions were added to the system, as well as their quantity was important for their effects. Anti-TGF, was also effected by the time delay between each intervention.
- TGF β provides stability to a pro-inflammatory response, reducing variability to make the increase in MMP-13 mRNA more uniform.

7.4 Future work

Designing experiments to validate the prediction that TGF β provides stability to pro-inflammatory stimuli could allow me to explore how a change in that effect may occur with age. I would also like to expand the model, in order to make more accurate predictions, by including TGF β turnover into the model. This would also allow me to factor in daily loading, which has been suggested to increase TGF β signalling (Gehua Zhen and Xu Cao 2014). Both of these changes may provide a more accurate prediction of how TGF β attenuation would affect the system. It would also be interesting to include other roles of TGF β in cartilage homeostasis: for example terminal differentiation of chondrocytes. Then I would explore how process such as this could be affected by therapeutic intervention.

Chapter 8. Bioinformatic analysis provides insight into OA as a whole.

8.1 Introduction

Large scale bioinformatic studies have been used to better understand disease progression by identifying the common events that lead to a diseased phenotype. In cancer studies, collecting and analysing data sets from multiple sources has resulted in common transcriptional profiles being identified (Daniel R. Rhodes et al. 2004). In chapter 3 I first introduced a cytoscape network that was representative of human OA. This highlighted the role of inflammation in human OA and led to me focus my attention on two cytokine pathways (IL-1 and OSM) and their interaction with the TGF β signalling pathway. However, we know that there are multiple pathways involved in the initiation and progression of OA and that there will be considerable crosstalk between them. Therefore I used bioinformatics tools to explore the OA network to identify processes that may drive OA, and more specifically the genes involved in these process. The network also allowed me to give my model context in a global environment.

PhenomeScape is a cytoscape plugin that can identify sub-networks from a main network, whilst also providing functional processes of these sub-networks. The programme also identifies which genes are up- and down-regulated in these sub-networks, and can link individual genes to specific phenotypes (Soul et al. 2016). To identify these sub-networks a separate gene list relative to your disease of interest must be overlaid. For this I used publically available microarray data specifically for human knee OA (S. L. Dunn et al. 2016). This data is available at ArrayExpress with the identifier E-MTAB-4304.

By overlaying the genes from my model to the network I aimed to demonstrate how dysregulation of the IL-1+OSM+TGF β pathways can lead to changes in genes important in other pathways. In addition, the analysis will reveal how components of my model interact with other genes and pathways. This information could be used to suggest future extensions to the model

8.1.1 Chapter aims

- Use a cytoscape network representation of human OA to explore sub-networks to locate genes important in OA development. Identify specific phenotypes linked to these genes that may be responsible for disease progression.

- Explore the network around my model genes to identify how my model network interacts with other genes and pathways. Use these to show how the model genes fit into OA development as a whole.

8.2 Results

PhenomeScape has a built in network for human genes that allows you to run your data against known gene interactions. However, as I had already created a network specific for OA I used it as the major network (Fig 8.1). This network is the same as that presented in chapter 3, but prior to gene clustering. I then ran the knee specific OA data, from S. L. Dunn et al. (2016), over my created network.

8.2.1 Knee osteoarthritis sub-networks

The desired phenotypes have to be specified before PhenomeScape can be run; I selected any that related to “cartilage”, “osteoarthritis”, “cytokines”, “inflammation”, “signaling” and “chondrocyte”. PhenomeScape was then run overlaying the knee OA data (S. L. Dunn et al. 2016). This determined 10 sub-networks shown combined in Figure 8.2, and individually in Figures 8.3-8.12. Table 8.1 shows all of the phenotypes that were connected to genes, as well as their identifiers. The sub-networks represent ten processes:

- Cell adhesion
- Cellular response to insulin
- Cell surface receptor signalling pathway
- Membrane invagination
- Negative regulation of neural precursor cell proliferation
- Negative regulation of neuron apoptotic process
- Response to organic cyclic compound
- Extracellular matrix organisation
- Positive regulation of angiogenesis
- Osteoclast differentiation

The programme suggests all of these processes are altered in my complete OA network and the knee OA data. The network also shows the gene changes that justified these predictions, with downregulated genes shown in green and the upregulated in red. Many of the phenotypes link the different sub-networks genes: for example Hif-1A linked to Plasminogen Activator Urokinase Receptor (PLAUR) via “abnormal cytokine level” (Fig 8.2).

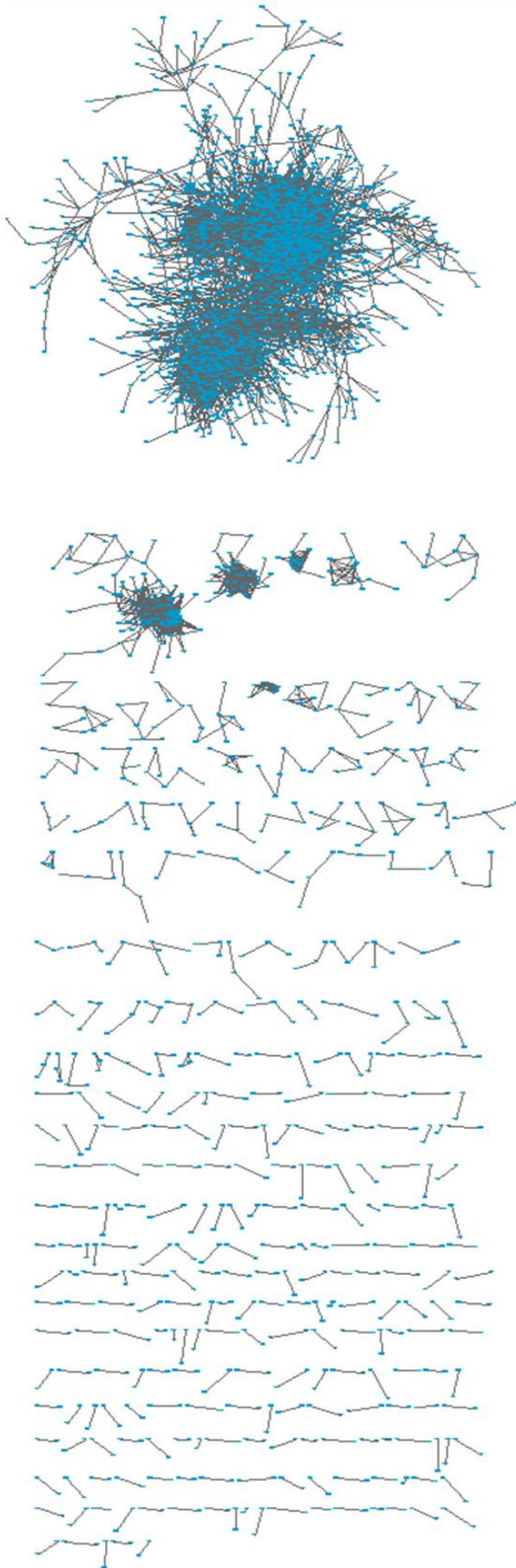


Figure 8.1 **Complete gene network, representative of human OA.** Affymetrix microarray data from 50 knee OA patients were collected from the GEO database, normalised, and the genes combined. ARACNE then inferred the interactions between these genes providing mutual information (MI) values. These gene interactions formed a network that could be visualised using Cytoscape. The nodes (blue dots) represent differentially expressed genes and the edges are connections based on MI values. The specific MI values can only be viewed in cytoscape.

Identifier	Phenotype
HP:0002758	Osteoarthritis
HP:0002815	Abnormality of the knees
HP:0003088	Premature osteoarthritis
HP:0100593	Calcification of cartilage
MP:0000164	abnormal cartilage development
MP:0000165	abnormal long bone hypertrophic chondrocyte zone
MP:0000167	decreased chondrocyte number
MP:0000166	abnormal chondrocyte morphology
MP:0003120	abnormal tracheal cartilage morphology
MP:0003408	increased width of hypertrophic chondrocyte zone
MP:0006433	abnormal articular cartilage morphology
MP:0008713	abnormal cytokine level
ZP:0000057	abnormal(ly) decreased size Meckel's cartilage
ZP:0000064	abnormal(ly) decreased size ceratohyal cartilage
ZP:0000066	abnormal(ly) absent ceratobranchial cartilage
ZP:0000126	abnormal(ly) malformed Meckel's cartilage
ZP:0000269	abnormal(ly) morphology Meckel's cartilage
ZP:0000906	abnormal(ly) aplastic Meckel's cartilage
ZP:0000921	abnormal(ly) morphology ceratohyal cartilage
ZP:0000925	abnormal(ly) aplastic ceratohyal cartilage
ZP:0001067	abnormal(ly) aplastic ceratobranchial cartilage
ZP:0001977	abnormal(ly) hypoplastic ceratohyal cartilage
ZP:0001979	abnormal(ly) split ethmoid cartilage
ZP:0002100	abnormal(ly) morphology cranial cartilage
ZP:0003107	abnormal(ly) malformed palatoquadrate cartilage
ZP:0004231	abnormal(ly) hypoplastic cranial cartilage
ZP:0004534	abnormal(ly) morphology pectoral fin cartilage
ZP:0008344	abnormal(ly) decreased process quality collagen fibril organization
ZP:0008484	abnormal(ly) absent ethmoid cartilage
ZP:0009520	abnormal(ly) premature chondrocyte hypertrophy
ZP:0009549	abnormal(ly) increased width ceratobranchial cartilage

Table 8.1 **Table of PhenomeScape phenotypes, with identifying numbers.** PhenomeScape matches gene expression with associated phenotypes. This table shows the phenotypes relevant for my data, along with their identifiers. HP refers to Human Phenotype Ontology; MP refers to Mammalian Phenotype Ontology; ZP refers to zebrafish phenotypes. Inclusion of zebrafish and mammalian phenotypes was justified in chapter 2.2.7

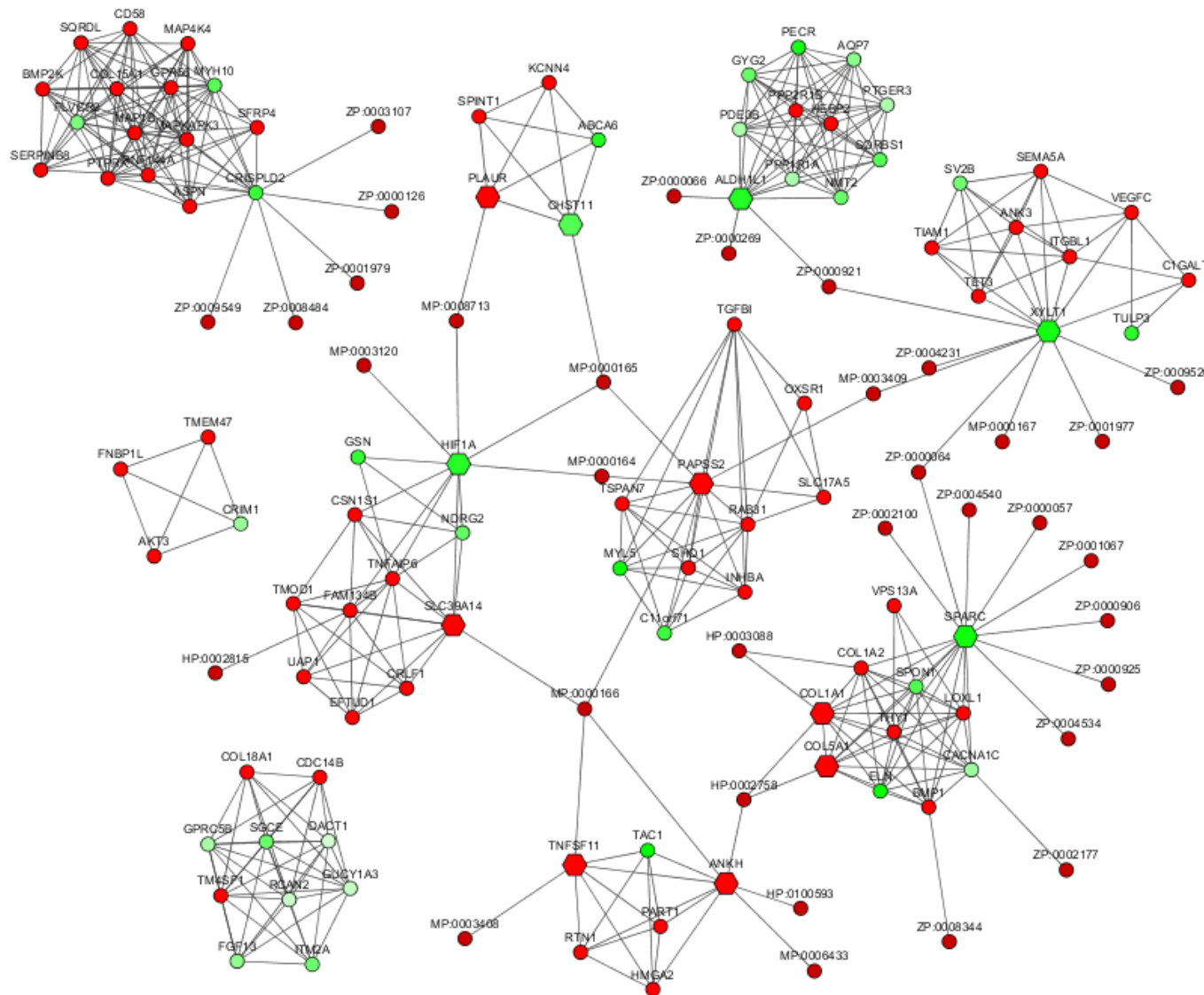


Figure 8.2 Knee OA specific sub-networks identified with PhenomeScape. Phenotypes were selected in PhenomeScape that are relevant for Osteoarthritis. These phenotypes are then linked to the input data (knee samples from (S. L. Dunn et al. 2016)) to determine phenotype-gene associations. After which both the expression data and the phenotypes are used to calculate activity scores with the proteins in the original network I compared them to (Fig 8.1). The high scoring groups are identified as sub-networks. These Sub-networks have been combined showing how they interact with each other. Green represents downregulated genes, whilst red shows upregulated, compared to the control. Table 8.1 shows all of the phenotype identifiers present in this Figure.

Cell adhesion

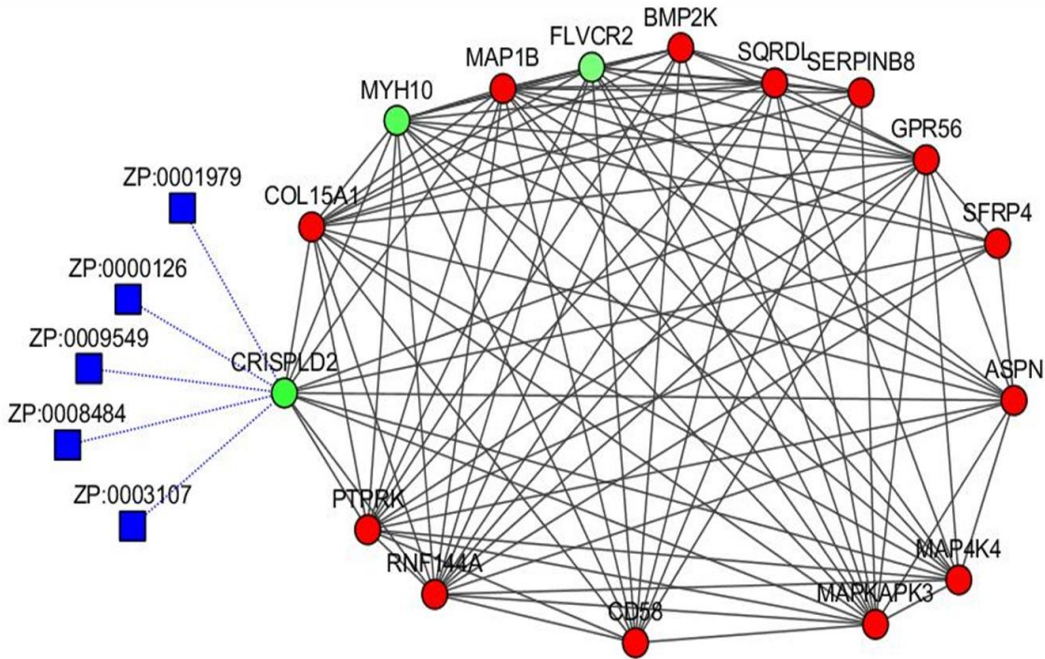


Figure 8.3 **PhenomeScape sub-network; Cell adhesion.** Individual sub-network, from Figure 8.2.

Cellular response to insulin

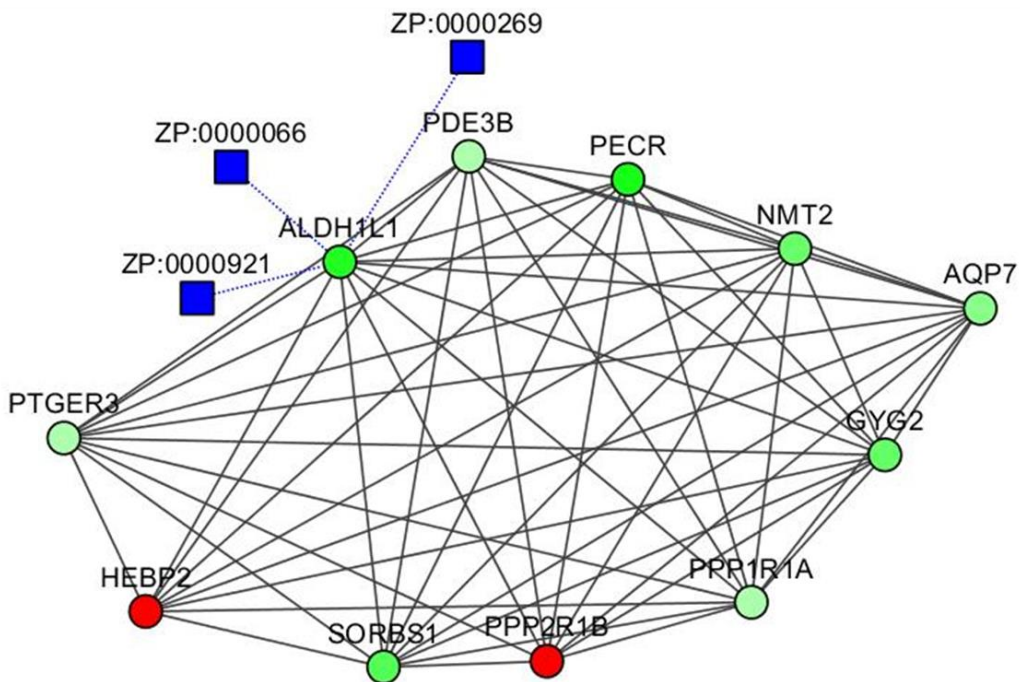


Figure 8.4 **PhenomeScape sub-network; Cellular response to insulin.** Individual sub-network, from Figure 8.2.

Cell surface receptor signalling pathway

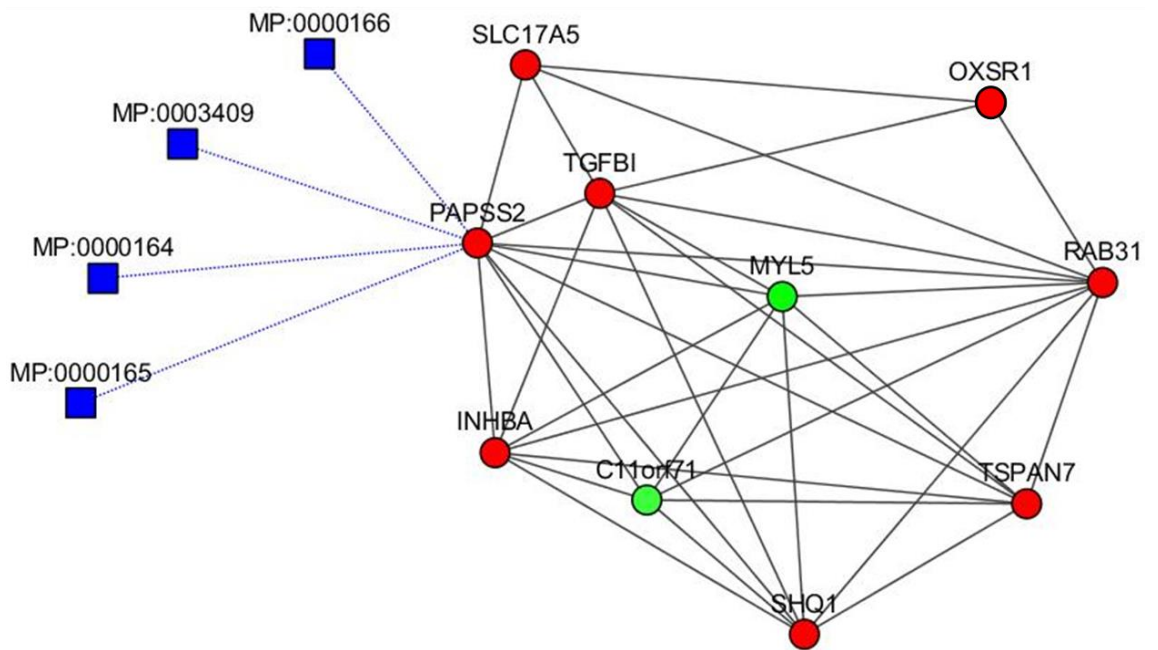


Figure 8.5 **PhenomeScope sub-network; Cell surface receptor signalling pathway.** Individual sub-network, from Figure 8.2.

Membrane invagination

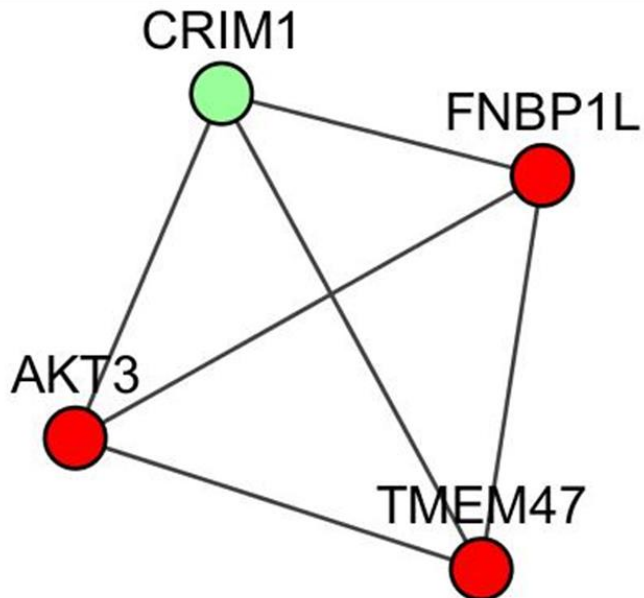


Figure 8.6 **PhenomeScope sub-network; Membrane invagination.** Individual sub-network, from Figure 8.2.

Negative regulation of neural precursor cell proliferation

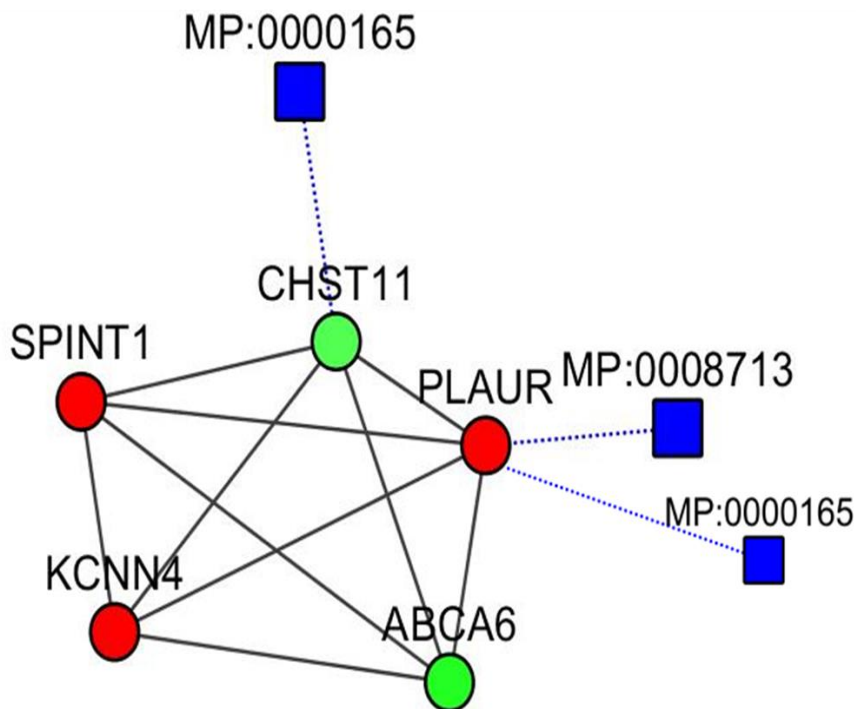


Figure 8.7 **PhenomeScape sub-network; Negative regulation of neural precursor cell proliferation.** Individual sub-network, from Figure 8.2.

Negative regulation of neuron apoptotic process

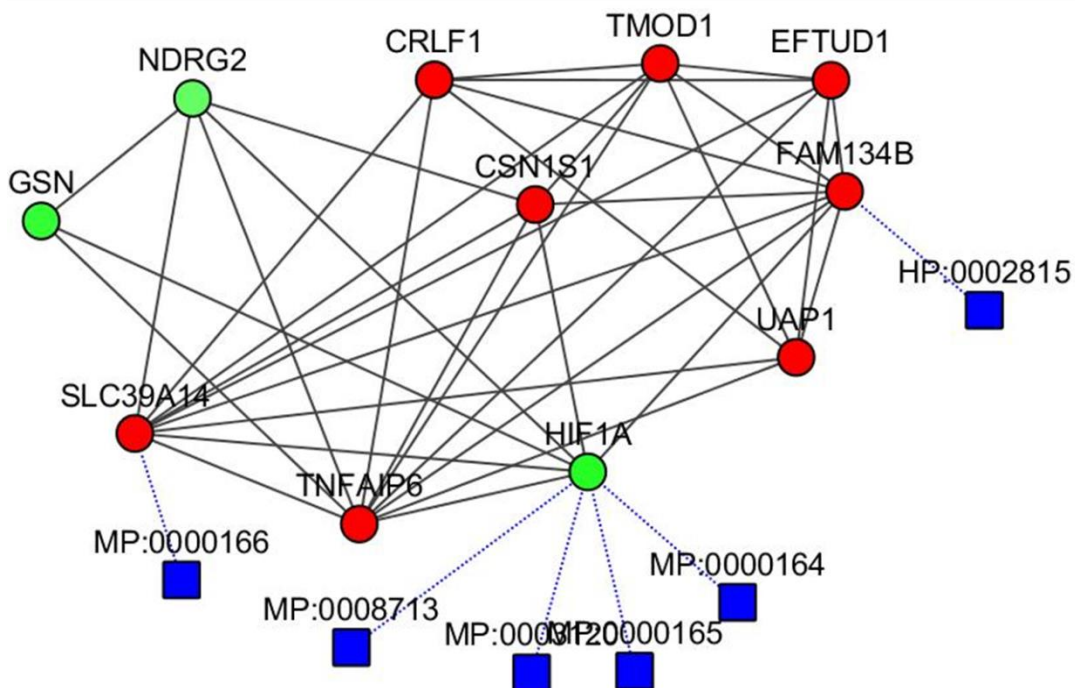


Figure 8.8 **PhenomeScape sub-network; Negative regulation of neuron apoptotic process.** Individual sub-network, from Figure 8.2.

Response to organic cyclic compound

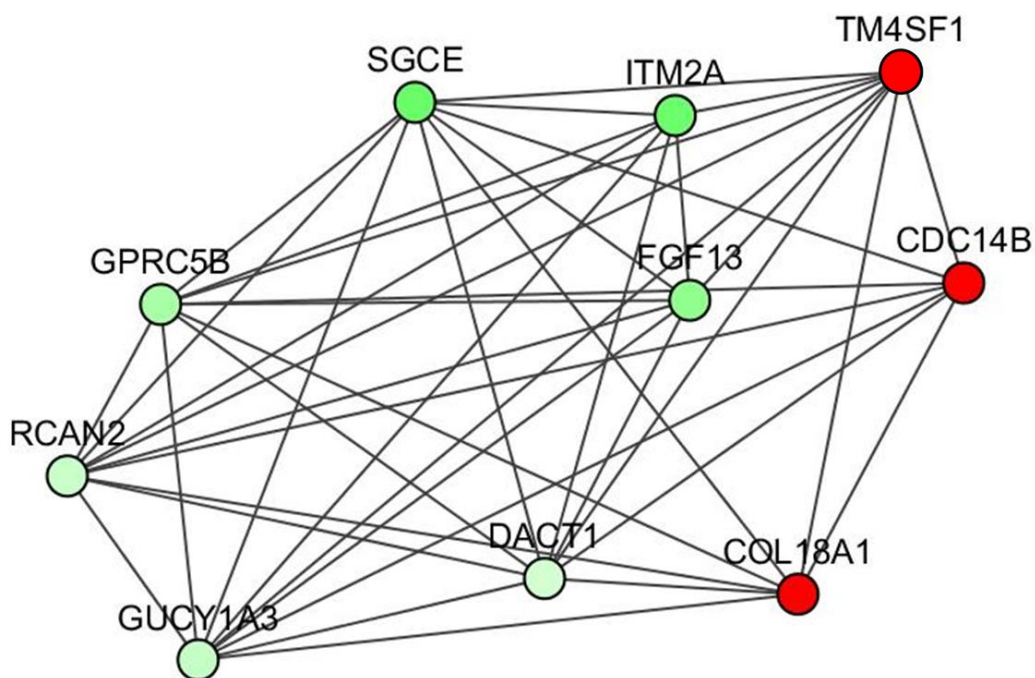


Figure 8.9 **PhenomeScape sub-network; Response to organic cyclic compound.** Individual sub-network, from Figure 8.2.

Extracellular matrix organisation

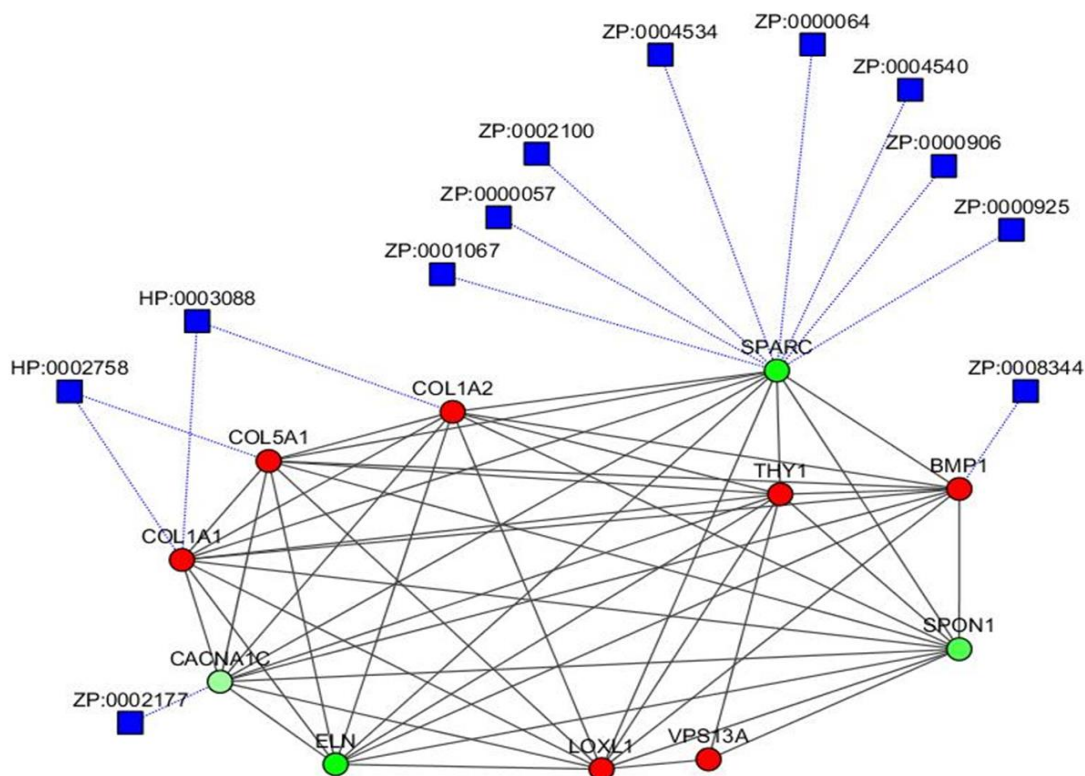


Figure 8.10 **PhenomeScape sub-network; Extracellular matrix organisation.** Individual sub-network, from Figure 8.2.

Positive regulation of angiogenesis

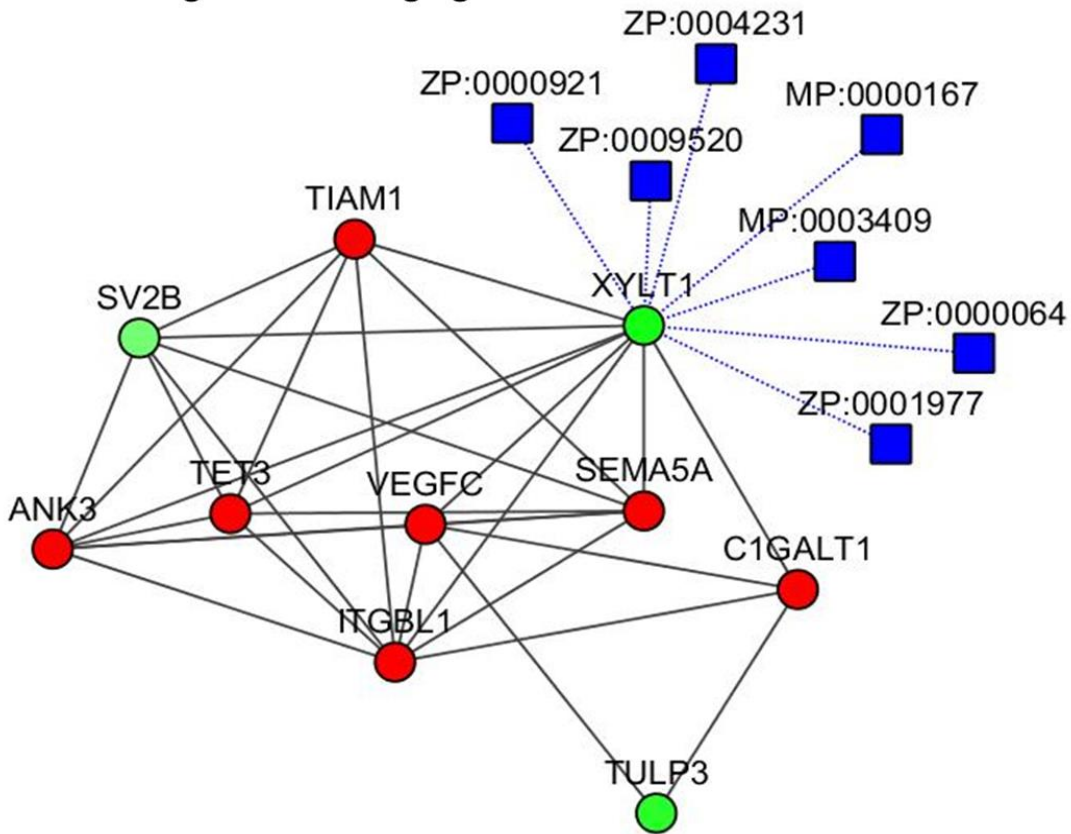


Figure 8.11 **PhenomeScape sub-network; Positive regulation of angiogenesis.** Individual sub-network, from Figure 8.2.

Osteoclast differentiation

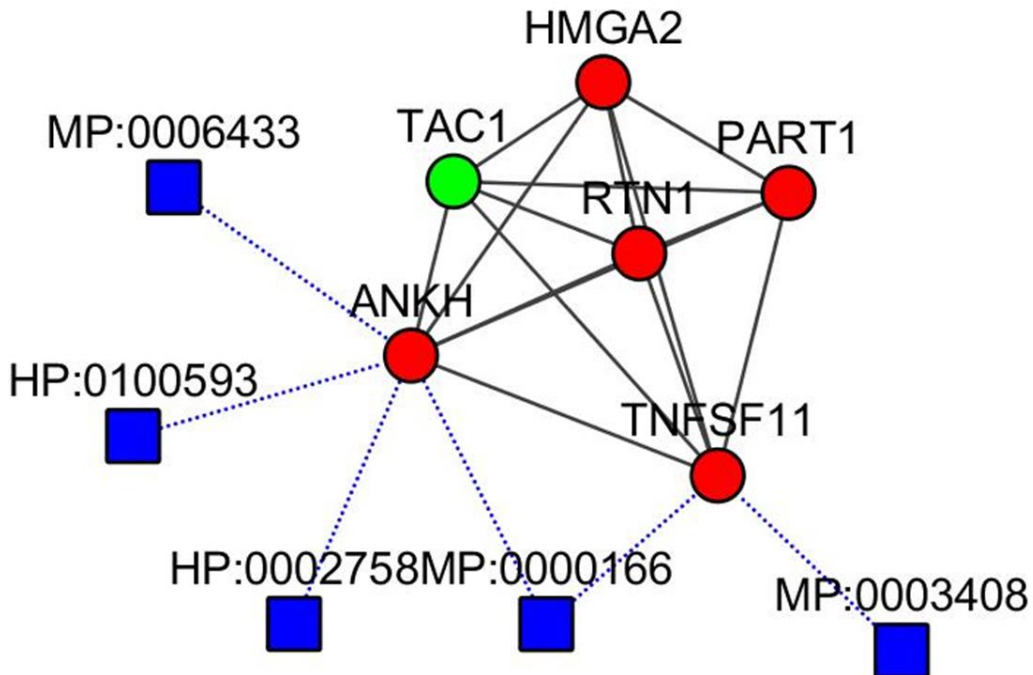


Figure 8.12 **PhenomeScape sub-network; Osteoclast differentiation.** Individual sub-network, from Figure 8.2.

8.2.2 Bioinformatic analysis highlights the importance of inflammation in OA.

As previously mentioned in chapter 3, the OA network (Fig 8.1) was clustered to better represent interacting genes. I made a list of all the genes present in my model (presented in chapter 5), and then overlaid these genes to the clustered network. This provided insight into how the model fits in with other processes that are important in OA development. For example both SMAD1 and TGFBR1 were located in the “inflammatory response in plasma membrane” cluster (shown in chapter 3, Figure 3.1). Figure 8.13 shows all the model genes that were linked to genes in the network, as well as the genes that directly interact with them. Both TGFBR1 and SMAD1 were located in the large cluster “Inflammatory response in plasma membrane” highlighting the importance of TGF β in OA associated inflammation. Furthermore, both c-Fos (FOS) and JunB (JUNB) also had links to genes in the network.

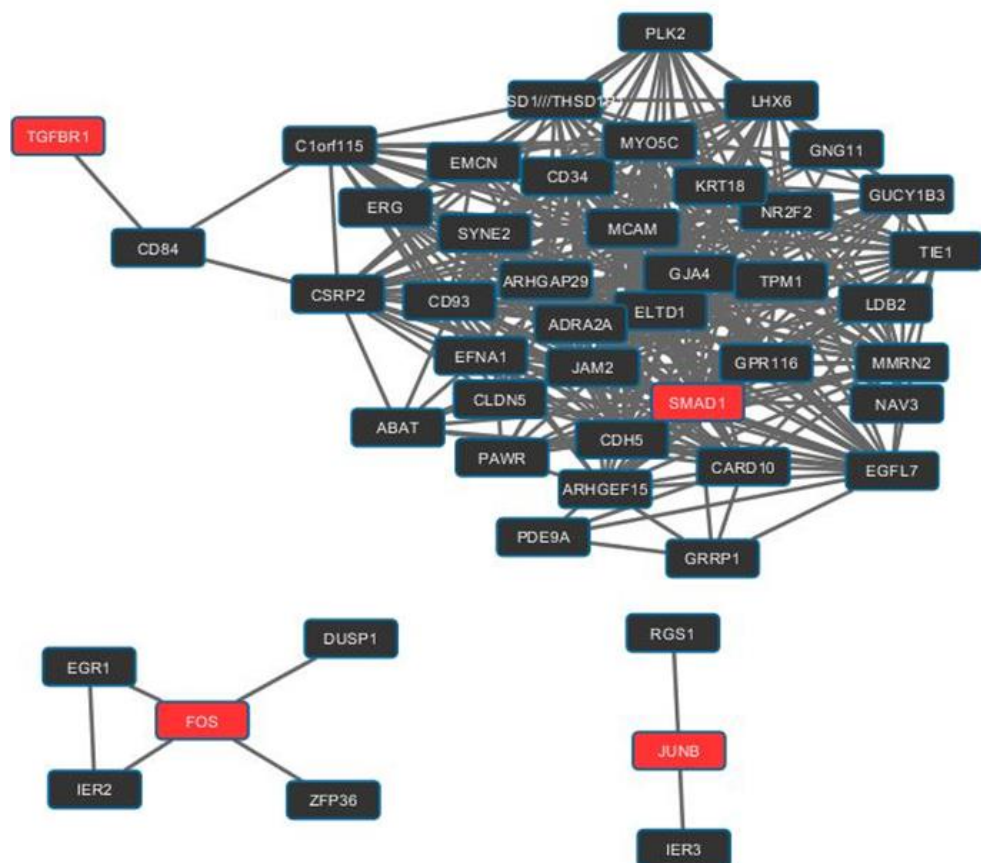


Figure 8.13 Overlaying model genes to the complete OA network.

Overlaying the genes for my model to a clustered version of the network presented in Figure 8.1 highlighted the genes that were present. 4 genes were shown to be present (red) SMAD 1, ALK5 (TGFBR1), c-Fos (FOS) and JunB (JUNB). These were extracted along with all the genes that directly interacted with them (black), to create these sub-networks.

8.3 Discussion

Using PhenomeScape I found 10 knee OA specific sub-networks. Analysing these sub-networks provided some insight into the processes and genes important in the development of knee OA. The “Positive regulation of angiogenesis” and “Extracellular matrix organisation” subnetworks suggest increased blood flow and tissue remodelling, which could suggest growth of the tissues. Angiogenesis has also been shown to contribute to structural damage and pain in OA (Andia and Maffulli 2013). It does this by facilitating both endochondral ossification and the recruitment of inflammatory mediators (Suri and Walsh 2012; Gravallesse et al. 2003).

The “Negative regulation of neural precursor cell proliferation” sub-network suggests that there is not tissue growth, as precursor cells are important for this process (Kim et al. 2010). This is in contrast to the two networks mentioned previously and highlights how systems can become dysregulated in OA. Precursor cells are also important in cartilage repair, so negative regulation could contribute to OA development (Hiraki et al. 2001). However, this process refers specifically to neural precursor cells, which to my knowledge have not been linked to OA.

The “Cellular response to insulin” sub-network is interesting as diabetes has recently been linked to an increased risk of OA development (Louati et al. 2015). Exploring the genes in this sub-network may help provide a functional understanding of how altered insulin signalling can lead to OA development. Further to this, one gene in particular Aldehyde Dehydrogenase 1 Family Member L1 (ALDH1L1) was linked to three abnormal cartilage phenotypes. This suggests ALDH1L1 may be changing cartilage morphology when insulin signalling is altered. ALDH1L1 was also shown to be upregulated in a porcine cartilage model of OA (Schlichting et al. 2014). Understanding how ALDH1L1 is leading to altered cartilage, as well as how the other genes in the sub-network are affecting OA development, may help us understand the role of diabetes.

8.3.1 Individual genes identified from PhenomeScape.

Many of the individual genes highlighted by the PhenomeScape analysis coincide with current literature surrounding OA. For example Hif-1A downregulation is linked to four phenotypes, three of which are related to altered cartilage and chondrocyte morphology. This is unsurprising given the role Hif-1A plays in cartilage homeostasis (as mentioned in detail in chapter 1). Future studies into the genes in the sub-networks may help identify changes that can lead to OA progression. The following genes have been chosen as examples of interesting genes that would benefit from further study.

8.3.1.1 PAPSS2

3'-Phosphoadenosine 5'-Phosphosulfate Synthase 2 (PAPSS2) is found in the "Cell surface receptor signalling pathway" sub-network and provides a phenotype link between four other sub-networks. This suggests it may have a role in the development of phenotypes, which could also be driven by other genes. This either means that all the genes linked to that phenotype need to be dysregulated for it to develop, or that the phenotype can develop because of a change in any of the linked genes. PAPSS2 expression is crucial for proper sulfation of cartilage matrix (Ramaswamy et al. 2012), with mutations in PAPSS2 leading to a susceptibility to OA (Ikeda et al. 2001). PAPSS2 upregulation is normally beneficial for cartilage (Ramaswamy et al. 2012), so its increased expression linking to abnormal chondrocyte morphology and cartilage development is surprising. Further work would be needed to determine if it had an altered role in OA tissue or if its upregulation is an attempt to prevent cartilage degradation.

PAPSS2 is upregulated by SOX9 and SMAD3 in cartilage (Chavez et al. 2017). Therefore, its upregulation in the network may suggest that TGF β is still signalling through SMAD3, or SOX9 is being stabilised in another way. The Transforming Growth Factor Beta Induce (TGF β I) gene is linked to PAPSS2 and is upregulated by non-canonical TGF β signalling (Lin et al. 2010). As

TGF β 1 is also upregulated, this further suggests TGF β signalling is affecting genes in the “Cell surface signalling receptor” sub-network.

8.3.1.2 SPARC

The Secreted Protein Acidic and Cysteine Rich (SPARC) gene is linked to eight phenotypes all of which are related to abnormal cartilage; this indicates that it may be important in the development of OA. In these samples SPARC is downregulated (Nakamura et al. 1996), but is upregulated by TGF β in cartilage. SPARC is also linked to BMP1 which can activate TGF β (Ge and Greenspan 2006). However, BMP1 can also activate BMP 2/4 (Ge and Greenspan 2006; Vadon-Le Goff et al. 2015), which are associated with SMAD 1/3/5 signalling (Wu et al. 2016). Therefore I hypothesise that these changes may be a result of TGF β signalling changing from signalling primarily through ALK5, to signalling through ALK1. Changes in signalling may then result in the increased BMP1 and decreased SPARC expression (as seen in this data). This change could then contribute to the abnormal cartilage development in OA. An important caveat is that SPARC has been previously shown to be upregulated in both porcine and human OA samples (Sieker et al. 2017; Nakamura et al. 1996).

8.3.1.3 XYLT1

The cartilage repair process requires the synthesis of proteoglycan. Xylosyltransferase 1 (XYLT1) is a key enzyme that transfers the first sugar residue to the proteoglycan core protein, initiating GAG synthesis (McCoy et al. 2012). XYLT1 expression is decreased in the samples and this is linked to phenotypes which relate to abnormal cartilage and chondrocytes. This may suggest it is no longer initiating GAG synthesis, which in turn results in the abnormal cartilage. Alternatively, abnormal chondrocytes could be causing this change in XYLT1 expression. Pothacharoen et al. (2014) suggested using sesamin to increase anabolic factors to treat OA, as they showed it had anabolic effects on aggrecan production, in primary cultures. They looked at XYLT1 expression due to its potent cartilage repair potential and showed it was upregulated by sesamin (Pothacharoen et al. 2014). Despite this, high levels of XYLT1 provided a marker of OA severity in a murine model of posttraumatic osteoarthritis (McCoy et al. 2012). This suggests that overexpression may also

be detrimental to joint health, so research is needed to determine the optimum expression of XYLT1. Finally, XYLT1 was in the “Positive regulation of angiogenesis” sub-network but no literature currently links XYLT1, angiogenesis and OA. Exploring possible links may help explain why XYLT1 can also have a negative role in OA development.

8.3.1.4 FAM134B

The Reticulophagy Regulator 1 (FAM134B) gene encodes a cis-Golgi transmembrane protein, and is linked to the “Knee abnormalities” phenotype. However, there is no literature (that I am aware of) which links FAM134B to OA progression or development. Exploring if upregulation of FAM134B leads to knee abnormalities, or if it is a side effect of knee abnormalities, could potentially identify a novel mechanism of OA progression.

8.3.1.5 Conclusions

Analysing the sub-networks identified by PhenomeScape identified a number of genes for future study. The genes and sub-networks I have discussed are just a sub-section, and further analyses into the other genes would also undoubtedly find interesting connections to OA. However, this type of study shows both the advantages and disadvantages of looking at such a large dataset. I have now identified a number of genes for which further study would be interesting, but there are no established rules for identifying which would be the most sensible to peruse first.

Some of the genes identified also have interactions with TGF β , again highlighting its important role in OA progression. Further research into some of these genes may identify potential pathways that could be incorporated into my model.

8.3.2 Examining the context of my model in a global environment.

Overlaying my model genes to the complete OA network allowed me to see which other genes IL-1, OSM and TGF β may interact with. This provides a better understanding of how problems with the three cytokines could in turn lead to problems in other systems. Below I will discuss some of these genes and discuss what systems may be being altered by my model genes.

8.3.2.1 TGFBR1 and SMAD1

TGFBR1 is only directly linked to CD84, a neuronal protein also expressed in immune cells, which is important in both the adaptive and innate immune response (Zaiss et al. 2003). CD84 indirectly links TGFBR1 to multiple genes, most of which are already linked to SMAD1. This indicates that SMAD1 may affect multiple genes that are dysregulated in OA, and highlights the importance of catabolic TGF β signalling. The gene with the strongest connection to SMAD1 is EGF-Like Domain Multiple 7 (EGFL7); a gene that has been linked to calcium iron binding as well as Notch signalling (Zaiss et al. 2003). It is also believed to be important in angiogenesis; playing an important role in bone growth and remodelling that could lead to disease (Chim et al. 2013).

8.3.2.2 JunB

JunB was linked to the immediate early response 3 (IER3) gene which has been shown to be important in not only ERK signalling (Letourneux et al. 2006) but also plays a key role in cell stress; in particular apoptosis (Hamidi et al. 2012). Morinobu et al. (2016) showed that IER3 can induce apoptosis in RA patients leading to damage. They also showed TNF and IL-1 β increased IER3 in OA samples, which then modulated cytokine and chemokine mRNA expression in a similar way to in the RA samples. However, they could not confirm that it induced apoptosis in OA samples. Regulator of G-Protein Signalling 1 (RGS1) was also linked to JunB. RGS1 has been linked to the mechanical loading response (Eliasson et al. 2013), as well as pain in OA patients (Thakur et al. 2013), although the mechanism remains unclear.

8.3.2.3 c-Fos

c-Fos has four connections. The first, dual specificity phosphatase (DUSP1), is linked to DUSP16 which has been shown to dephosphorylate c-Fos (Caunt and Keyse 2013). Therefore, DUSP1 inclusion could be related to a similar action. c-Fos and Early Growth Response 1 (EGR1) have been shown to be co-regulated (Sukhatme et al. 1988) and both are expressed in chondrocytes in response to IL-1 (Goldring et al. 1994). EGR1 also has a role in development and has been shown to be activated in hypertonic chondrocytes (Levi et al. 1996). Re-initiation of developmental pathways and the maturation of chondrocytes can lead to

MMP-13 expression and cartilage degradation in OA (Dreier 2010). Work done previously in our group showed that Immediate Early Response 2 (IER2) has a role in IL-1+OSM-driven MMP-13 expression. Its removal with siRNA resulted in reduced MMP-13 expression after 24 hours (Macdonald 2013). The link demonstrated between c-Fos, IER2 and EGR1 could be a result of their role in inflammation-driven cartilage damage.

Also closely linked to c-Fos is ZFP36 Ring Finger Protein, a protein that binds to ARE-containing mRNAs to promote their degradation (M. Inada et al. 2004). The QIAGENs DECipherment Of DNA Elements (DECODE) programme also showed there is a c-Fos, c-Jun and AP-1 binding site on the ZFP36 promotor region (Kent et al. 2002). This suggests that c-Fos increases ZFP36 expression in OA, although the effect of this is not clear.

8.3.2.4 Conclusions

Overlaying my model genes gave me some biological insight into how exactly gene changes in my model can interact with a range of different pathways. It also identified some interactions that may not have been discovered without it. Specific gene interactions highlight how changes in genes from one pathway can then lead to crosstalk with other pathways, altering them and helping drive disease progression. Further exploration into these interactions and incorporating them into the model could help to identify interesting targets for future study and possible drug interventions.

8.3.2 Summary

- Overlaying knee specific data to my complete OA cytoscape network using PhenomeScape created 10 sub-networks that represent altered processes in knee OA. Future research into the genes in these pathways could provide a better understanding of how OA is developed.
- Overlaying my model genes to my complete cytoscape network allowed me to predict some OA associated genes that may be affected by IL-1, OSM and TGF β signalling. This helps to show how alterations in one signalling pathway can lead to other altered pathways and OA development. It also highlighted important pathways that should be considered, if not incorporated into the model in the future.
- The analyses presented in this chapter have identified a number of potential targets for future study. The challenge will be to choose the most sensible candidates to progress with.

Chapter 9 Final discussion

9.1 TGF β -mediated repression of IL-1+OSM-driven MMP-13 mRNA expression.

Matrix-degrading enzymes play important roles in the development of OA and of these, MMP-13 is believed to be the most important (Poole et al. 2002; L. Troeberg and H. Nagase 2012). TGF β has been shown in multiple studies to protect against the damaging effects of pro-inflammatory stimuli (Marie et al. 2006; Shull et al. 1992; Wang Hui et al. 2014). Throughout chapters 3 and 4 I confirmed that TGF β can reduce the IL-1+OSM-driven expression of MMP-1/13 mRNA in SW1353 cells and that this repressive effect is robust. Furthermore, I demonstrated that TGF β could mediate repression after 6 hours pre-treatment, even if it is was no longer present in the experiment. This effect, along with the initial delay in repression, led me to conclude that *de novo* synthesis of a tertiary mediator is required to mediate the effect. Model data presented in chapter 7 also showed TGF β reduced the variability in IL-1+OSM-driven MMP-13 mRNA upregulation that was seen with IL-1+OSM alone. Having these two layers of repression implies that TGF β has a vital role in reducing the effect of pro-inflammatory stimuli, allowing MMPs to regulate turnover (Masaki Inada et al. 2004), but preventing them from causing excess damage. Although TGF β affects a lot of non-canonical pathways (Hartsough and Mulder 1995; A. Nakao et al. 1997; Bhowmick et al. 2001), the SMAD2/3 pathway was my primary candidate to mediate the repressive effect due to the important role of SMAD2/3 in maintaining cartilage homeostasis (Gehua Zhen and Xu Cao 2014). Knockdown of ALK5 (upstream of SMAD2/3 (M.-J. Goumans et al. 2003)) showed TGF β was unable to mediate repression without this receptor.

9.1.1 How does TGF β mediate repression?

My data, as presented in chapter 5, suggest that TGF β can inhibit IL-1+OSM-driven MMP-13 mRNA upregulation through two methods: AP-1 complex competitive inhibition and increased instability of MMP-13 mRNA. In order to determine if both these components were necessary, I used a series of parameter estimations for different models, to see which could best fit the data. The literature suggested that there was a tertiary mediator leading to

competitive inhibition of the AP-1 complex that mediated MMP-13 mRNA repression (Emi Shimizu et al. 2010). We showed this by having JunB protein being synthesised upon addition of TGF β . This then bound to c-Jun, inhibiting the formation of c-Jun homodimer or heterodimer with c-Fos (Ponticos et al. 2009; Mauviel et al. 1996). Alone, this AP-1 competitive inhibition was not enough to replicate the experimental findings. This implied that something else was involved. Looking at the experimental data there was a large change in mRNA expression between 24 and 48 hours and so I hypothesised that this could be due to mRNA instability. I am unsure what would mediate this, so the model contained a dummy species that was increased with TGF β addition and could decrease MMP-13 mRNA stability. When the model was fitted with both components it not only replicated the observed data, but also correctly predicted the effect 6 hour TGF β pre-treatment would have on the system. This suggests that TGF β is affecting the system at two levels and cannot produce its effect without both mechanisms occurring together.

9.2 Alternative pro-inflammatory stimuli.

Throughout this thesis, IL-1+OSM has been used as a model of pro-inflammatory stimuli. However, there are other pro-inflammatory cytokines, with an established link to TGF β that could be incorporated into my model instead, or in addition to, IL-1+OSM. TNF- α synergises with OSM to upregulate MMPs, and this effect is repressed by TGF β , much the same as IL-1+OSM (Wang Hui et al. 2014). Interferon gamma (IFN- γ) expression is also known to be regulated by TGF β (Lin et al. 2005). I have shown that ALK5 is required for TGF β to have its protective effect on IL-1+OSM signalling, which has previously been shown to be more abundant in young cartilage, but the ALK1/ALK5 ratio moves towards ALK1 with age (Blaney Davidson et al. 2009). It has also been shown that following injury, OA changes appear sooner in older patients than they do in their younger counterparts (Roos et al. 1995). Whilst it is true that the structure of cartilage changes as it ages (Loeser 2010), it is also feasible that the reduction in ALK5 is restricting its ability to resist injury. If the regulation of TNF- α , IFN- γ , and possibly other unknown pro-inflammatory cytokines, are all mediated by ALK5, then the loss of this receptor with age could explain why

older cartilage is damaged more readily by injury, as a previously mechanism of reducing damage will now be lost.

9.3 Lack of MMP-13 in microarray data

Throughout this thesis I have discussed the importance of MMP-13 in the development of OA. However, MMP-13 was not present in the microarray network representative of OA in humans. It is difficult to ascertain the exact reason why this is, but I predict it is most likely a result of the way ARACNE infers interactions. ARACNE uses mutual information which measures how the state of one random variable affects another (Margolin et al. 2006). MMP-13 expression is normally the end point of a signalling cascade, therefore it does not directly affect the expression of other genes and is also upregulated by multiple different pathways (Fanjul-Fernández et al. 2010). This means that although MMP-13 may be upregulated in the samples, no individual gene provides meaningful information about the state of MMP-13 expression, or vice versa. Therefore, it is unlikely a single gene could have a significant ARACNE connection to MMP-13, as upregulation of multiple genes will effect MMP-13 expression and ARACNE cannot always determine the most important. It is also important to note the ARACNE programme was run in late 2015 so any genes linked to MMP-13 since 2016 will not be included; for example ATF3 (Chan et al. 2017).

9.4 Changing role of TGF β

9.4.1 ALK1/ALK5

Though the change in ALK1/ALK5 ratio with age is established (Blaney Davidson et al. 2009), the cause of the change is unknown. My model predicts, as originally presented in Wang Hui et al. (2014), that both ALK5 homodimers and ALK1/ALK5 heterodimers bind to TGF β to mediate their effect and are then inactivated by SMAD7. During this inactivation the receptors are degraded; both ALK5 and ALK1 are resynthesised in the model, but this degradation happens at a higher rate than resynthesis. Therefore, the overall number of receptors decreases. ALK5 is affected more by this process due to its abundance, which results in more ALK5 homodimers being activated, and subsequently degraded

(M.-J. Goumans et al. 2003). Furthermore, as ALK1 must be bound to ALK5 to mediate its effect (M.-J. Goumans et al. 2003), for every ALK1 degraded an ALK5 molecule also degrades. Therefore, it would be difficult for degradation of ALK1 to exceed degradation of ALK5. This is supported by research that shows SMAD7 can recruit E3 ubiquitin ligases, Smurf1 and Smurf2, which can in turn target ALK5 for degradation through the proteasomal pathway (Yan et al. 2009). ALK1 may also avoid degradation as it has been suggested the ALK1 pathway is predominantly regulated by SMAD6 (König et al. 2005), rather than SMAD7.

There are many other processes that could be responsible for the change in the ALK1/ALK5 ratio. For example, receptor shedding is important for signal cessation by removal of functioning receptors (Levine 2004), as well as providing soluble cytokine receptors which have antagonist properties by binding excess cytokines (Levine 2004). Shedding of the LRP1 receptor can be increased under certain conditions such as chronic inflammation (Yamamoto et al. 2017). If shedding of TGF β type I receptors also increased with age, it would conceivably have a greater effect on ALK5, again due to its abundance and because ALK1 binds to ALK5. Though this hypothesis is different to that currently in the model, the basic concept is similar and the model could be adapted to fit it. Research into the change in ALK1/ALK5 ratio is currently ongoing but testing hypotheses using a model could help understand if, or how, something could drive the changes seen with age.

An attempt to overexpress ALK 1 in chapter 6 highlighted how delicate the ALK1/ALK5 balance is. Knocking out ALK5 removed the effect of both receptors, as ALK5 is required for ALK1 to signal (M.-J. Goumans et al. 2003). Overexpressing ALK1 allowed it to mediate increased ID1 expression. However, MMP-13 could not be upregulated, which would be expected if TGF β was predominantly signalling through ALK1 (Blaney Davidson et al. 2009), therefore ALK5 still appeared to be the dominant receptor. Understanding of the sensitive balance between the receptors will be important for any future treatments that target these receptors. This was demonstrated in chapter 7

where the timing of theoretical treatments had a clear impact on how much effect they had on the system.

9.4.2 Effects of clock genes

A circadian rhythm (CR) is a roughly 24 hour cycle affecting the physiological processes of living beings. CR is a fundamental regulatory factor in many aspects of biology such as: sleep, metabolism and blood pressure (Laposky et al. 2008). Clock genes are responsible for mediating the CR in these processes, several of which were shown to be disrupted during early cartilage degeneration in a murine model (Gossan et al. 2013). Recent publications have also linked an altered CR with OA. Akagi et al. (2017) found that two key CR genes were altered in OA cartilage: Brain and Muscle ARNT-Like 1 (BMAL1) or Nuclear Receptor Subfamily 1 Group D Member 1 (NR1D1). They also found that knockdown of either BMAL1 or NR1D1 affected the TGF β signalling pathway, but they found no difference in the levels of SMAD2/3 or SMAD1/5/8 (Akagi et al. 2017). Michal Dudek et al. (2016) also linked altered CR to TGF β signalling. However, they looked specifically at BMAL1 showing that a knockout of BMAL1 corresponded with an increase in SMAD1/5/8 phosphorylation and a decrease in SMAD2/3 phosphorylation. This change may have been the result of a change in ALK1 expression, as the BMAL1 knockout showed a different expression pattern; in wild type mice ALK1 expression was cyclic whilst in the BMAL1 knockout ALK1 was constantly upregulated (Michal Dudek et al. 2016). How these changes across the day change the effect of TGF β on pro-inflammatory stimuli could be interesting as it suggests the timing of an event could affect how the body deals with it. For example if a pro-inflammatory event occurred at 9am, when ALK1 levels are high (Michal Dudek et al. 2016), it may cause a longer response than at 9pm, when ALK1 levels are reduced (Michal Dudek et al. 2016). In chapter 5 my data suggested that age results in a prolonged pro-inflammatory response in the presence of TGF β than the younger counterpart. As BMAL1 appears to affect SMAD phosphorylation and type I receptor composition (Michal Dudek et al. 2016), it could alter the TGF β effect on pro-inflammatory stimuli in a similar way to ageing.

9.5 How TGF β links to key OA pathways

Despite the important role TGF β plays in OA development (addressed in chapters 1 and 3), there are many other inflammatory pathways that play a role. Exploring the interactions between these pathways may be important in understanding OA as a whole. chapter 8 presented a way of combining modelled genes with a large scale bioinformatic study. This method identified a number of genes that interact with the model, highlighting in particular notch signalling. Notch signalling has been shown to synergise with SMAD3 signalling. This interaction is direct, as notch signalling can attract SMAD3 to DNA binding sites to effect transcription (Blokzijl et al. 2003).

PhenomeScope analysis also showed the range of sub-networks that represent processes involved in OA development, as well as gene lists to help uncover how these may be mediated. For example it identified a sub-network responsible for insulin signalling, which is interesting as diabetes has recently been linked with an increased risk of OA (Louati et al. 2015). Currently the reason for this link is not understood, so genes in the sub-network may help to uncover how a change in insulin signalling could lead to OA development. These types of analyses highlight the complexity of OA but also provide a structure that will hopefully lead to a more detailed understanding of the disease.

9.6 Therapeutic targets

As discussed in more detail in chapter 4, Chen et al. (2015) argued that inhibition of TGF β , rather than activation, should be considered for treatment. They used TGFBR2 inhibitors to delay OA development after DMM surgery (Chen et al. 2015). They later showed that TGF β was low in cartilage of wild type mice preDMM surgery (Fang et al. 2017). My model allowed me to test predictions about potential therapeutic targets, which highlighted future considerations in design of therapeutics. Gehua Zhen et al. (2013) also showed that targeting TGF β could attenuate OA development in mice. This study used an anti-TGF β antibody, 1D11. Incorporating this into the model showed that treatments had to be given multiple times and at regular intervals to have positive effects. This is in agreement with murine data from Xie et al. (2016)

which showed systematic neutralisation of TGF β with 1D11 was more effective if given three times a week when compared to once or twice.

The model also predicted that 1D11 could lead to an increase in MMP-13 when administered only once, as the reduced level of TGF β will primarily signal through ALK1. This was in agreement with Fang et al. (2017) who suggested TGF β may work in a dose-dependent manner, as either above or below a certain threshold it will lead to damage. However, there were no signs of extra joint damage with reduced 1D11 administration in the Xie et al. (2016) study. The model predicted that after 1D11 treatment(s), TGF β would lose the protective effect against pro-inflammatory stimuli and the timing of 1D11 administration(s) was important for the desired effects. I am unaware of any study that has addressed these predictions but they may be important considerations in the development of an anti-TGF β drug treatment.

9.7 Alterations with hindsight

Reflecting on the data collected throughout my thesis allowed me to assess what could have been done differently.

9.7.1 ALK1 overexpression

Attempting to over-express ALK1 in the SW1353 cell line was a large part of my PhD. Despite some success, it did not produce the results originally expected, such as upregulating MMP-13, which prevented me from drawing any firm conclusions. This appears to be because SW1353 cell were not the correct cell line for over-expression. The levels of ALK5 in these cells appear insurmountably higher than ALK1. Attempting these experiments in another cell line, such as the C28/I2 used by Finnsen et al. (2010), may have allowed the over-expression experiments to be more successful. However, it would have required repeating all experiments performed on the SW1353 cell to confirm the behaviour was the same, which there was insufficient time to do.

9.7.2 Ambition in early stages

Originally, I aimed to build a model of different inflammatory pathways and then combine these to give an overview of inflammation in OA. This project proved to be too ambitious; in hindsight focussing on one pathway from the start would

have given me more time to explore more of the elements discussed in future work.

9.8 Future work

9.8.1 Incorporating other pathways into the model

The interaction of other inflammatory pathways with TGF β is interesting as they also regularly affect SMAD signalling. Incorporating these pathways into the model may help explain why TGF β moves towards ALK1 signalling with age, or reveal a target area to help reverse these changes. For example, WNT signalling, as discussed in chapter 1, can affect the expression of genes that skew TGF β signalling towards ALK1 signalling (M. H. van den Bosch et al. 2014). Incorporating WNT into the model may help to explain how this shift occurs. Notch signalling also synergises with SMAD3 (Blokzijl et al. 2003), so looking at how this synergy could affect TGF β signalling (especially with age) could reveal some interesting interactions.

I would also like to look at how TGF β interacts with other pro-inflammatory cytokines. It has already been shown that TGF β can repress TNF- α and IFN- γ responses (Lin et al. 2005; Wang Hui et al. 2014). Identifying if there are more pro-inflammatory responses TGF β represses, and if ALK5 is also required for these interactions, could highlight how important the loss of ALK5 with age is. For example, repeating the IL-1+OSM \pm TGF β experiments with a range of different cytokines could show how many cytokine responses TGF β can repress.

9.8.2 Exploring computational predictions

Examining the complete OA network by overlaying my model genes and using PhenomeScape analysis produced a large list of potential genes for further study. The next step would be to confirm that these genes are upregulated in OA tissues before choosing the most interesting candidates to continue studying.

9.8.3 Importance of cycling TGF or clock genes incorporated into model

Changes in the expression of the CR gene BMAL1 appears to have similar effects on TGF β signalling as ageing. Changing the current model to show how

BMAL1 changes throughout the day, and how this affects pro-inflammatory stimuli may help better understand the importance of CR in OA. Incorporating ageing into this model may show how changes in TGF β signalling with age can be affected by changes in BMAL1.

9.8.4 Examine model predictions experimentally

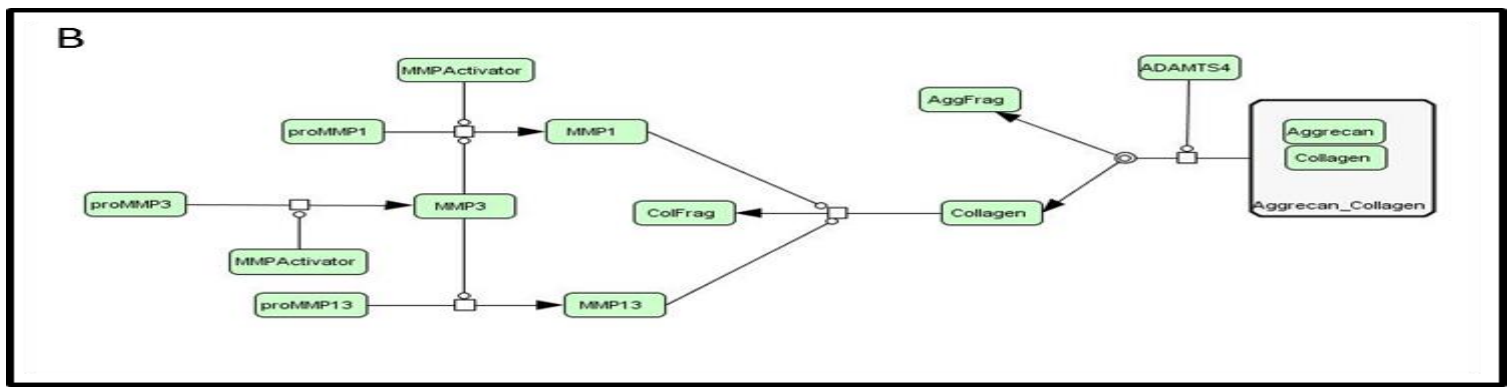
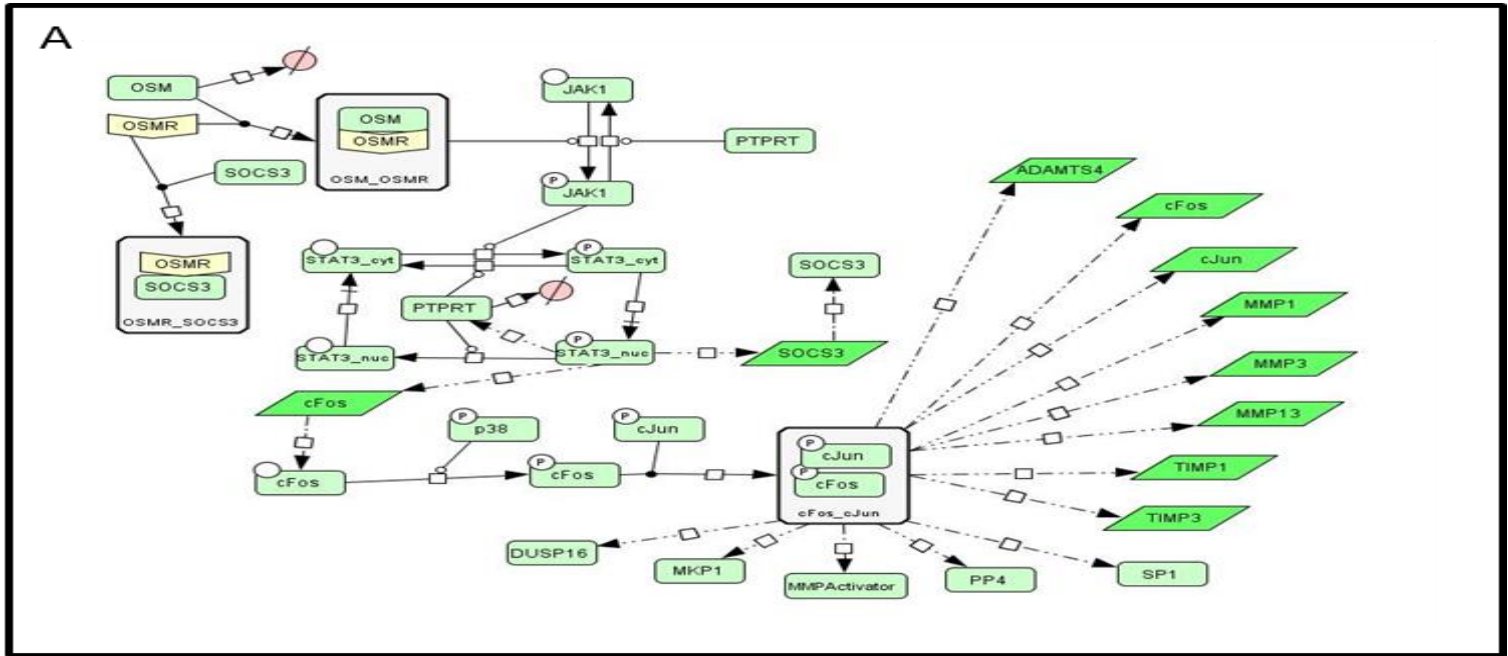
In the model JunB provides competitive inhibition to c-Jun, preventing formation of c-Jun homodimers and c-Jun/c-Fos heterodimers after IL-1+OSM treatment. DNA affinity pull down assays would allow specific examination at the binding site of MMP-13, to help determine if there is reduced c-Jun/c-Fos heterodimer binding when TGF β is present. As mentioned in chapter 2 ATF3 is believed to have an important role downstream of c-Jun/c-Fos (Chan et al. 2017), so measuring its binding may be significant.

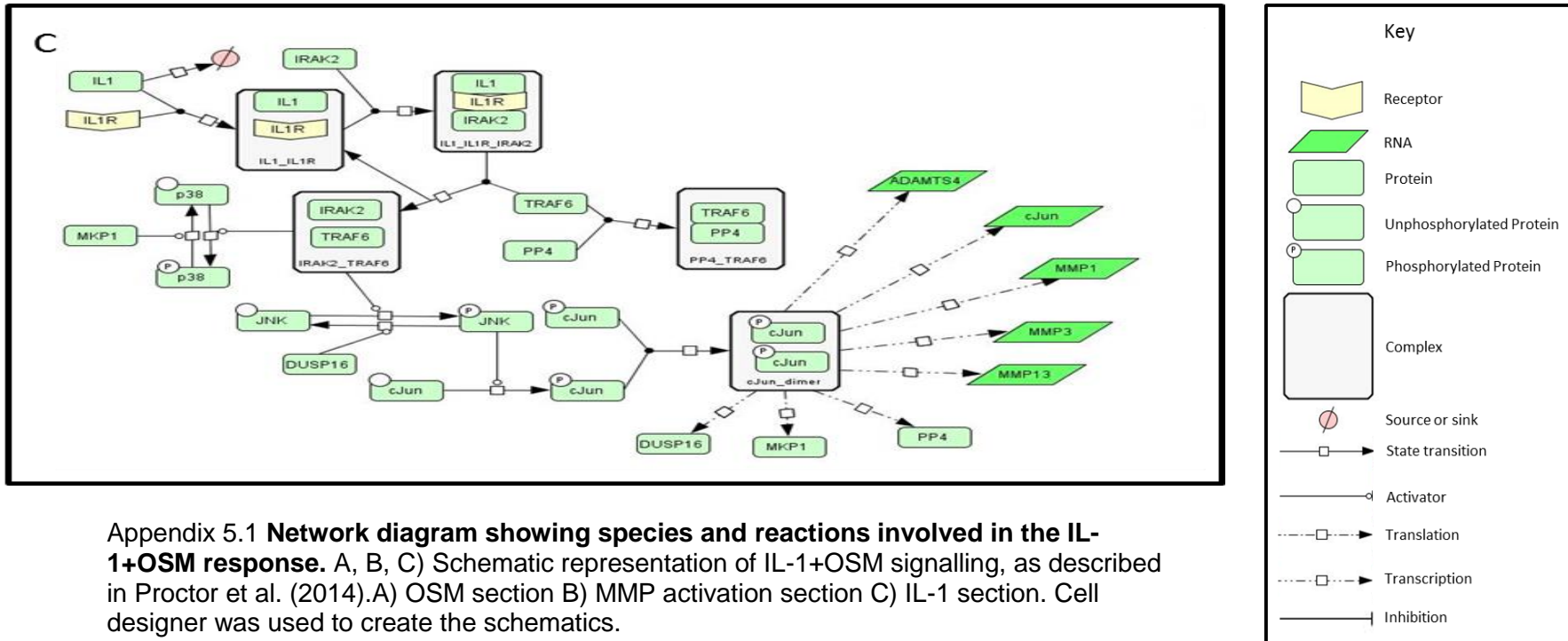
As discussed in chapter 5, JunB is not the only protein that may be important in the competitive inhibition to c-Jun. For this reason siRNA against JunB may be able to determine its importance in this process.

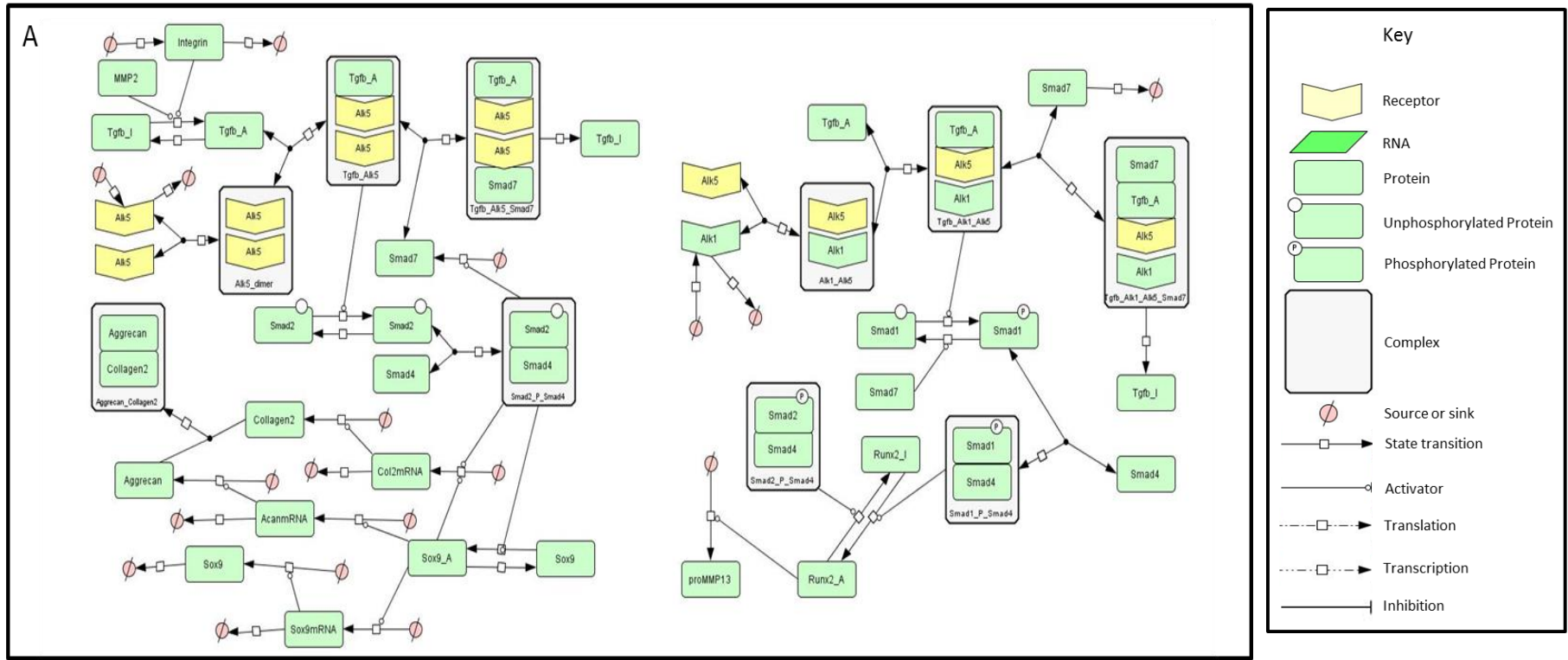
The model also predicted that TGF β could induce degradation of MMP-13 mRNA. However, the cause of this is unclear. In chapter 5 some possible genes are discussed, exploring these with siRNA may reduce the repressive effect of TGF β . I also think it may be worth performing a microRNA screen on IL-1+OSM \pm TGF β samples, as these have been known to alter mRNA stability (Valinezhad Orang et al. 2014).

The prediction that TGF β can reduce variability to an inflammatory response was presented in chapter 8. Confirming this prediction experimentally could be difficult, but could identify a novel role of TGF β with important implications. Single cell experiments could be interesting as they would allow you to measure the stochasticity of the response in lone cells as well as the complete population, for example single cell RNA-sequencing (Svensson et al. 2017).

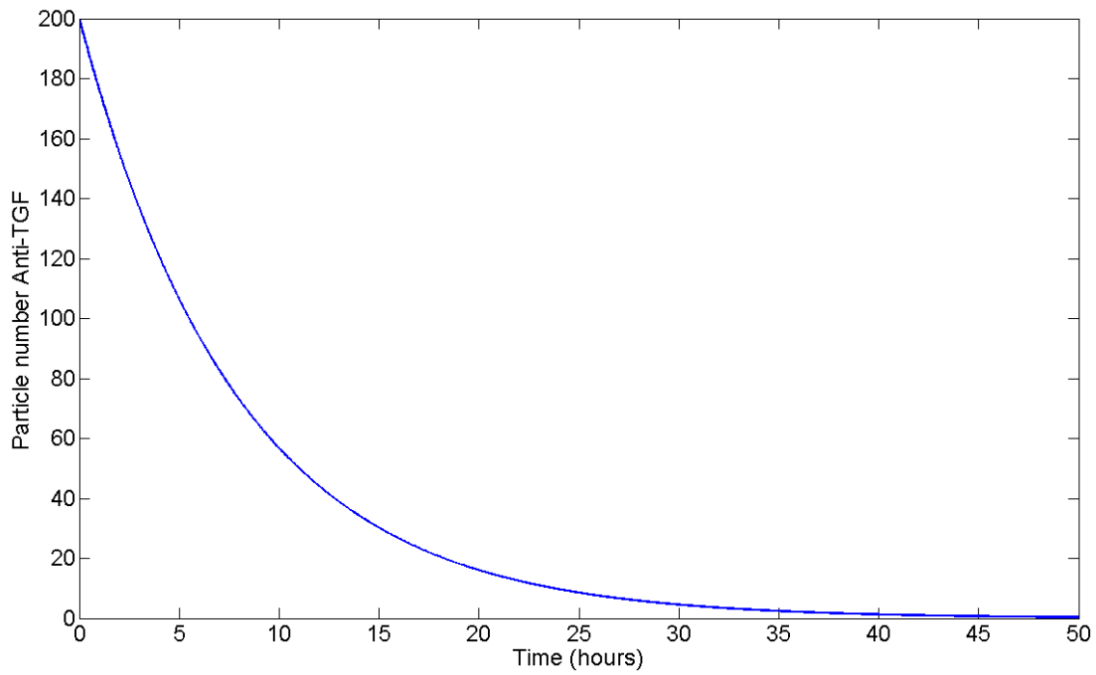
Chapter 10 Appendix



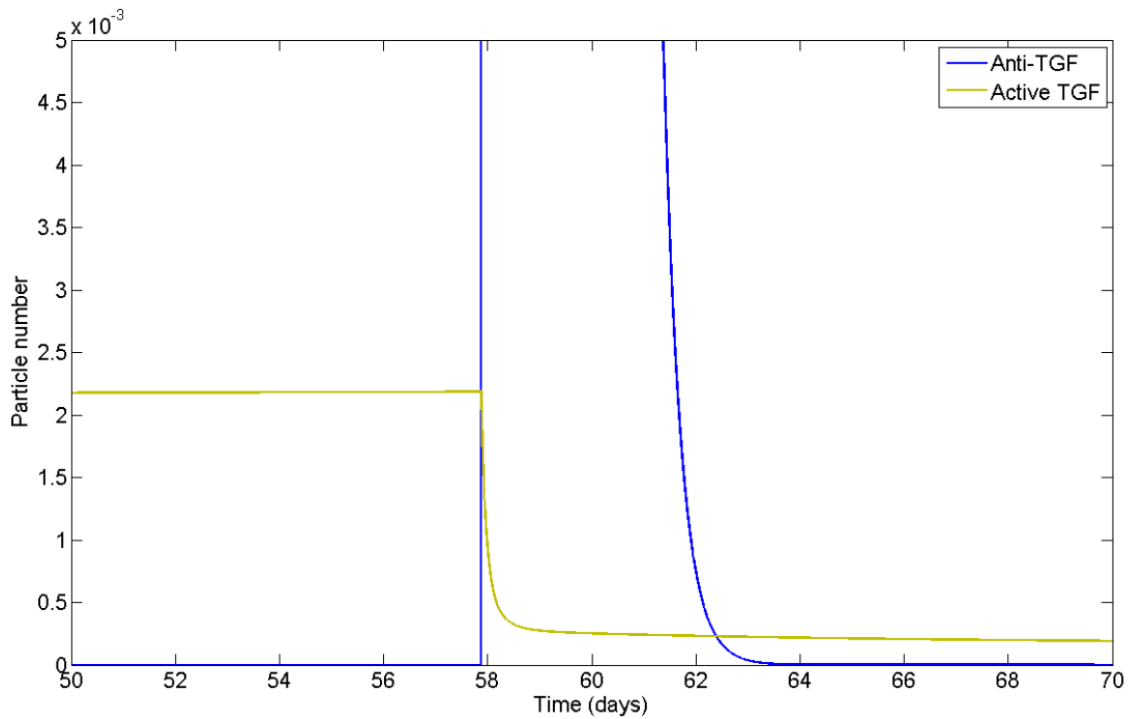




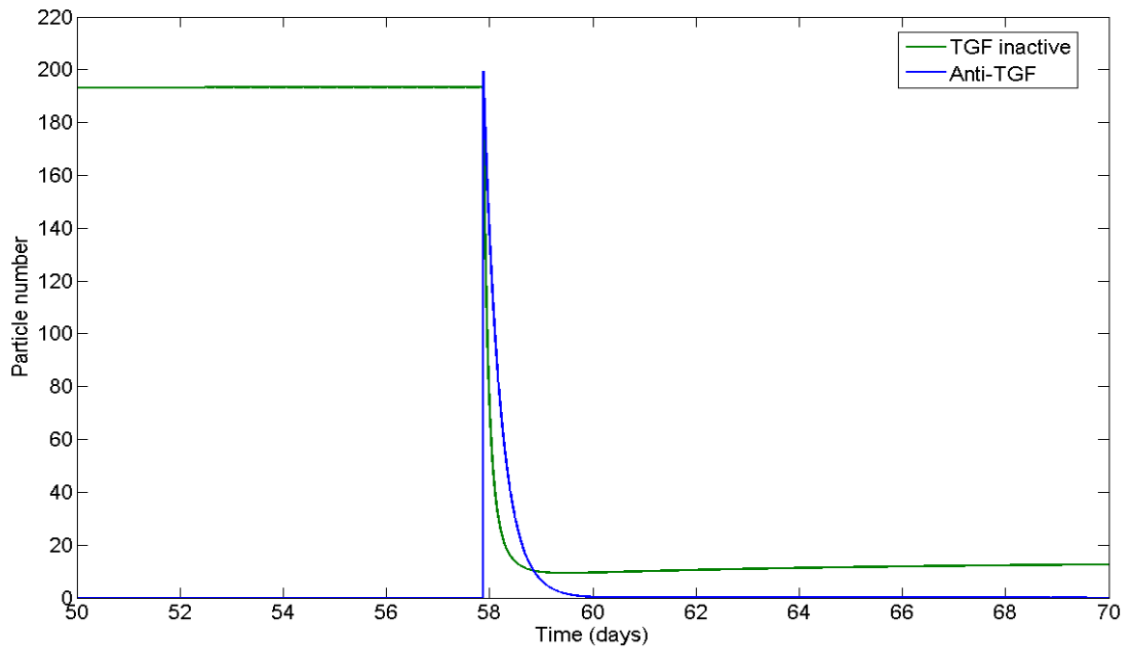
Appendix 5.2 **Network diagram showing all the species and reactions involved in the TGFβ pathway.** A) Schematic representation of the TGFβ component from the model presented in Wang Hui et al. (2014). CellDesigner was used to create the schematic.



Appendix 7.1 **Degradation of Anti-TGF**. Deterministic simulation results showing the degradation of Anti-TGF across 50 hours simulation time. The simulation was run using COPASI.



Appendix 7.2 **Effect of Anti-TGF on active TGF β** . Deterministic simulation results showing the effect Anti-TGF has on the levels of active TGF β . Ran across 70 days simulation time. The simulation was run using COPASI.



Appendix 7.3 **Effect of Anti-TGF on inactive TGF β** . Deterministic simulation results showing the effect Anti-TGF has on the levels of inactive TGF β . Ran across 70 days simulation time. The simulation was run using COPASI.

References

- Abramson and Amin (2002) Blocking the effects of IL-1 in rheumatoid arthritis protects bone and cartilage. *Rheumatology* 41/9: 972-980.
- Afrakhte, Morén, Jossan, Itoh, Sampath, Westermarck, Heldin, Heldin and ten Dijke (1998) Induction of inhibitory Smad6 and Smad7 mRNA by TGF- β family members. *Biochemical and Biophysical Research Communications* 249/2: 505-511.
- Akagi, Akatsu, Fisch, Alvarez-Garcia, Teramura, Muramatsu, Saito, Sasho, Su and Lotz (2017) Dysregulated circadian rhythm pathway in human osteoarthritis: NR1D1 and BMAL1 suppression alters TGF- β signaling in chondrocytes. *Osteoarthritis and Cartilage* 25/6: 943-951.
- Albro, Cigan, Nims, Yeroushalmi, Oungouljian, Hung and Ateshian (2012) Shearing of Synovial Fluid Activates Latent TGF- β . *Osteoarthritis Cartilage* 20/11: 1374-1382.
- Andia and Maffulli (2013) Platelet-rich plasma for managing pain and inflammation in osteoarthritis. *Nature Reviews Rheumatology* 9/12: 721-730.
- Attur, Palmer, Al-Mussawir, Dave, Teixeira, Rifkin, Appleton, Beier and Abramson (2009) F-spondin, a neuroregulatory protein, is up-regulated in osteoarthritis and regulates cartilage metabolism via TGF-beta activation. *FASEB Journal* 23/1: 79-89.
- Baarsma, Spanjer, Haitsma, Engelbertink, Meurs, Jonker, Timens, Postma, Kerstjens and Gosens (2011) Activation of WNT/beta-catenin signaling in pulmonary fibroblasts by TGF-beta(1) is increased in chronic obstructive pulmonary disease. *PloS One* 6/9: e25450.
- Balbín, Fueyo, Knäuper, López, Alvarez, Sánchez, Quesada, Bordallo, Murphy and López-Otín (2001) Identification and enzymatic characterization of two diverging murine counterparts of human interstitial collagenase (MMP-1) expressed at sites of embryo implantation. *Journal of Biological Chemistry* 276/13: 10253-10262.
- Barksby, Hui, Wappler, Peters, Milner, Richards, Cawston and Rowan (2006) Interleukin-1 in combination with oncostatin M up-regulates multiple genes in chondrocytes: Implications for cartilage destruction and repair. *Arthritis & Rheumatology* 54/2: 540-550.
- Baugé, Girard, Lhuissier, Bazille and Boumediene (2014) Regulation and role of TGF β signaling pathway in aging and osteoarthritis joints. *Aging and Disease* 5/6: 394.
- Baum, Fundel-Clemens, Kreuz, Kontermann, Weith, Mennerich and Rippmann (2010) Off-target analysis of control siRNA molecules reveals important differences in the cytokine profile and inflammation response of human fibroblasts. *Oligonucleotides* 20/1: 17-26.
- Bellehumeur, Blanchet, Fontaine, Bourcier and Akoum (2009) Interleukin 1 regulates its own receptors in human endometrial cells via distinct mechanisms. *Human Reproduction* 24/9: 2193-2204.
- Berenbaum (2004) Signaling transduction: target in osteoarthritis. *Current Opinion in Rheumatology* 16/5: 616-622.
- Berenbaum (2013) Osteoarthritis as an inflammatory disease (osteoarthritis is not osteoarthrosis!). *Osteoarthritis and Cartilage* 21/1: 16-21.
- Bhowmick, Ghiassi, Bakin, Aakre, Lundquist, Engel, Arteaga and Moses (2001) Transforming growth factor-beta1 mediates epithelial to mesenchymal transdifferentiation through a RhoA-dependent mechanism. *Molecular Biology of the Cell* 12/1: 27-36.
- Bierie and Moses (2006) Tumour microenvironment: TGFbeta: the molecular Jekyll and Hyde of cancer. *Nature Reviews: Cancer* 6/7: 506-520.
- Bitzer, von Gersdorff, Liang, Dominguez-Rosales, Beg, Rojkind and Böttinger (2000) A mechanism of suppression of TGF- β /SMAD signaling by NF- κ B/RelA. *Genes and Development* 14/2: 187-197.

- Black, Castner, Slack, Tocker, Eisenman, Jacobson, Delaney, Winters, Hecht and Bendele (2006) A14 INJECTED TIMP-3 PROTECTS CARTILAGE IN A RAT MENISCAL TEAR MODEL. *Osteoarthritis and Cartilage* 14: S23-S24. Available at [http://dx.doi.org/10.1016/S1063-4584\(07\)60467-1](http://dx.doi.org/10.1016/S1063-4584(07)60467-1), accessed 2017/06/13.
- Blaney Davidson, Remst, Vitters, van Beuningen, Blom, Goumans, van den Berg and van der Kraan (2009) Increase in ALK1/ALK5 ratio as a cause for elevated MMP-13 expression in osteoarthritis in humans and mice. *J Immunol* 182/12: 7937-7945.
- Blaney Davidson, van der Kraan and van den Berg (2007) TGF-beta and osteoarthritis. *Osteoarthritis and Cartilage* 15/6: 597-604.
- Blaney Davidson, Vitters, van den Berg and van der Kraan (2006) TGF beta-induced cartilage repair is maintained but fibrosis is blocked in the presence of Smad7. *Arthritis Research & Therapy* 8/3: R65.
- Blokzijl, Dahlqvist, Reissmann, Falk, Moliner, Lendahl and Ibáñez (2003) Cross-talk between the Notch and TGF- β signaling pathways mediated by interaction of the Notch intracellular domain with Smad3. *The Journal of cell biology* 163/4: 723-728.
- Blom, van Lent, Holthuysen, van der Kraan, Roth, van Rooijen and van den Berg (2004) Synovial lining macrophages mediate osteophyte formation during experimental osteoarthritis. *Osteoarthritis and Cartilage* 12/8: 627-635.
- Brew, Dinakarandian and Nagase (2000) Tissue inhibitors of metalloproteinases: evolution, structure and function. *Biochimica et Biophysica Acta* 1477/1-2: 267-283.
- Buckwalter, Mankin and Grodzinsky (2005) Articular cartilage and osteoarthritis. *Instructional Course Lectures* 54: 465-480.
- Buckwalter, Rosenberg and Hunziker (1990) Articular cartilage: composition, structure, response to injury, and methods of facilitating repair. *Articular cartilage and knee joint function: basic science and arthroscopy*: 19-56.
- Buschmann, Kim, Wong, Frank, Hunziker and Grodzinsky (1999) Stimulation of aggrecan synthesis in cartilage explants by cyclic loading is localized to regions of high interstitial fluid flow. *Archives of Biochemistry and Biophysics* 366/1: 1-7.
- Campbell, Wojta, Novak and Hamilton (1994) Cytokine modulation of plasminogen activator inhibitor-1 (PAI-1) production by human articular cartilage and chondrocytes. Down-regulation by tumor necrosis factor alpha and up-regulation by transforming growth factor-B basic fibroblast growth factor. *Biochimica et Biophysica Acta* 1226/3: 277-285.
- Cao, Wei, Zhang, Guo, Zhang, Li, Sun, Sun, Wang, Li and Wei (2014) Decreased histone deacetylase 4 is associated with human osteoarthritis cartilage degeneration by releasing histone deacetylase 4 inhibition of runt-related transcription factor-2 and increasing osteoarthritis-related genes: a novel mechanism of human osteoarthritis cartilage degeneration. *Arthritis Res Ther* 16/6: 491.
- Castrogiovanni and Musumeci (2016) Which is the Best Physical Treatment for Osteoarthritis? *Journal of Functional Morphology and Kinesiology* 1/1: 54. Available at <http://www.mdpi.com/2411-5142/1/1/54>.
- Caunt and Keyse (2013) Dual-specificity MAP kinase phosphatases (MKPs). *The FEBS journal* 280/2: 489-504.
- Cawston, Curry, Summers, Clark, Riley, Life, Spaul, Goldring, Koshy and Rowan (1998) The role of oncostatin M in animal and human connective tissue collagen turnover and its localization within the rheumatoid joint. *Arthritis & Rheumatology* 41/10: 1760-1771.
- Cawston, Ellis, Humm, Lean, Ward and Curry (1995) Interleukin-1 and oncostatin M in combination promote the release of collagen fragments from bovine nasal cartilage in culture. *Biochem Biophys Res Commun* 215/1: 377-385.
- Cerdà-Costa and Xavier Gomis-Rüth (2014) Architecture and function of metallopeptidase catalytic domains. *Protein Science* 23/2: 123-144.

- Chambers, Halford, Geltz, Villamizar, Gross, Embalabala, Gershburg and Wilber (2015) A system for creating stable cell lines that express a gene of interest from a bidirectional and regulatable herpes simplex virus type 1 promoter. *PLoS One* 10/3: e0122253.
- Chambers, Kirkpatrick, Evans, Gorski, Foster and Borghaei (2013) IL-4 inhibition of IL-1 induced Matrix Metalloproteinase-3 (MMP-3) expression in human fibroblasts involves decreased AP-1 activation via negative crosstalk involving of Jun N-terminal Kinase (JNK). *Exp Cell Res* 319/10: 1398-1408.
- Chan, Macdonald, Litherland, Wilkinson, Skelton, Europe-Finner and Rowan (2017) Cytokine-induced MMP13 Expression in Human Chondrocytes Is Dependent on Activating Transcription Factor 3 (ATF3) Regulation. *Journal of Biological Chemistry* 292/5: 1625-1636.
- Chang, Yang, Li, Chen and Dai (2011) Age-related biological characterization of mesenchymal progenitor cells in human articular cartilage. *Orthopedics* 34/8: e382-e388.
- Chavez, Coricor, Perez, Seo and Serra (2017) SOX9 protein is stabilized by TGF- β and regulates PAPS2 mRNA expression in chondrocytes. *Osteoarthritis and Cartilage* 25/2: 332-340.
- Chen, Macica, Nasiri and Broadus (2008) Regulation of articular chondrocyte proliferation and differentiation by indian hedgehog and parathyroid hormone-related protein in mice. *Arthritis and Rheumatism* 58/12: 3788-3797.
- Chen, Mian, Fu, Zhao, Yang, Li and Xu (2015) Attenuation of the progression of articular cartilage degeneration by inhibition of TGF- β 1 signaling in a mouse model of osteoarthritis. *The American journal of pathology* 185/11: 2875-2885.
- Chen, Thuillier, Chin and Alliston (2012) Chondrocyte-intrinsic Smad3 represses Runx2-inducible matrix metalloproteinase 13 expression to maintain articular cartilage and prevent osteoarthritis. *Arthritis and Rheumatism* 64/10: 3278-3289.
- Chen, Zhang, Yi and Xia (2012) Increased apoptosis in human knee osteoarthritis cartilage related to the expression of protein kinase B and protein kinase C δ in chondrocytes. *Folia Histochemica et Cytobiologica* 50/1: 137-143.
- Chim, Tickner, Chow, Kuek, Guo, Zhang, Rosen, Erber and Xu (2013) Angiogenic factors in bone local environment. *Cytokine Growth Factor Rev* 24/3: 297-310. Available at <http://www.ncbi.nlm.nih.gov/pubmed/23611723>.
- Chubinskaya, Hakimiyan, Pacione, Yanke, Rappoport, Aigner, Rueger and Loeser (2007) Synergistic effect of IGF-1 and OP-1 on matrix formation by normal and OA chondrocytes cultured in alginate beads. *Osteoarthritis and Cartilage* 15/4: 421-430.
- Chun, Oh, Yang and Park (2008) Wnt signaling in cartilage development and degeneration. *BMB Rep* 41/7: 485-494.
- Clark, Swingler, Sampieri and Edwards (2008) The regulation of matrix metalloproteinases and their inhibitors. *Int J Biochem Cell Biol* 40/6-7: 1362-1378.
- Clements, Price, Chambers, Visco, Poole and Mason (2003) Gene deletion of either interleukin-1 β , interleukin-1 β -converting enzyme, inducible nitric oxide synthase, or stromelysin 1 accelerates the development of knee osteoarthritis in mice after surgical transection of the medial collateral ligament and partial medial meniscectomy. *Arthritis & Rheumatology* 48/12: 3452-3463.
- Clutterbuck, Asplin, Harris, Allaway and Mobasheri (2009) Targeting matrix metalloproteinases in inflammatory conditions. *Current Drug Targets* 10/12: 1245-1254.
- Coleman, Widmyer, Leddy, Utturkar, Spritzer, Moorman, Guilak and DeFrate (2013) Diurnal variations in articular cartilage thickness and strain in the human knee. *Journal of Biomechanics* 46/3: 541-547.
- Correa and Lietman (2017) Articular cartilage repair: Current needs, methods and research directions. *Seminars in Cell and Developmental Biology* 62: 67-77. Available at <http://www.ncbi.nlm.nih.gov/pubmed/27422331>.

- Cravero, Carlson, Im, Yammani, Long and Loeser (2009) Increased expression of the Akt/PKB inhibitor TRB3 in osteoarthritic chondrocytes inhibits insulin-like growth factor 1–mediated cell survival and proteoglycan synthesis. *Arthritis and Rheumatism* 60/2: 492-500.
- D'Souza, Meloty-Kapella and Weinmaster (2010) Canonical and non-canonical Notch ligands. *Curr Top Dev Biol* 92: 73-129.
- Daub and Merks (2015) Cell-based computational modeling of vascular morphogenesis using Tissue Simulation Toolkit. *Methods in Molecular Biology* 1214: 67-127.
- Davidson, Turan, Egginton and Falciani (2016) Multilevel functional genomics data integration as a tool for understanding physiology: a network biology perspective. *J Appl Physiol (1985)* 120/3: 297-309.
- Davidson, Remst, Vitters, van Beuningen, Blom, Goumans, van den Berg and van der Kraan (2009) Increase in ALK1/ALK5 ratio as a cause for elevated MMP-13 expression in osteoarthritis in humans and mice. *The Journal of Immunology* 182/12: 7937-7945.
- Davidson, Scharstuhl, Vitters, Van der Kraan and Van Den Berg (2005) Reduced transforming growth factor-beta signaling in cartilage of old mice: role in impaired repair capacity. *Arthritis Research & Therapy* 7/6: R1338.
- de Larco and Todaro (1978) Growth factors from murine sarcoma virus-transformed cells. *Proc Natl Acad Sci U S A* 75/8: 4001-4005.
- Dinarello (1988) Biology of interleukin 1. *Faseb j* 2/2: 108-115.
- Dingle, Page Thomas, King and Bard (1987) In vivo studies of articular tissue damage mediated by catabolin/interleukin 1. *Annals of the Rheumatic Diseases* 46/7: 527-533.
- Dolan, Nelson, Zupanic, Smith and Shanley (2013) Systems modelling of NHEJ reveals the importance of redox regulation of Ku70/80 in the dynamics of dna damage foci. *PLoS One* 8/2: e55190.
- Dolan, Zupanic, Nelson, Hall, Miwa, Kirkwood and Shanley (2015) Integrated stochastic model of DNA damage repair by non-homologous end joining and p53/p21-mediated early senescence signalling. *PLoS Computational Biology* 11/5: e1004246.
- Dong, Drissi, Chen, Chen, Zuscik, Schwarz and O'Keefe (2005) Wnt-mediated regulation of chondrocyte maturation: modulation by TGF-beta. *Journal of Cellular Biochemistry* 95/5: 1057-1068.
- Dozin, Malpeli, Camardella, Cancedda and Pietrangelo (2002) Response of young, aged and osteoarthritic human articular chondrocytes to inflammatory cytokines: molecular and cellular aspects. *Matrix Biology* 21/5: 449-459.
- Dreier (2010) Hypertrophic differentiation of chondrocytes in osteoarthritis: the developmental aspect of degenerative joint disorders. *Arthritis Research & Therapy* 12/5: 216.
- Dudek, Gossan, Yang, Im, Ruckshanthi, Yoshitane, Li, Jin, Wang and Boudiffa (2016) The chondrocyte clock gene Bmal1 controls cartilage homeostasis and integrity. *The Journal of clinical investigation* 126/1: 365.
- Dudek, Gossan, Yang, Im, Ruckshanthi, Yoshitane, Li, Jin, Wang, Boudiffa, Bellantuono, Fukada, Boot-Handford and Meng (2016) The chondrocyte clock gene Bmal1 controls cartilage homeostasis and integrity. *Journal of Clinical Investigation* 126/1: 365-376.
- Dunker and Kriegelstein (2000) Targeted mutations of transforming growth factor-beta genes reveal important roles in mouse development and adult homeostasis. *European Journal of Biochemistry* 267/24: 6982-6988.
- Dunn, Soul, Anand, Schwartz, Boot-Handford and Hardingham (2016) Gene expression changes in damaged osteoarthritic cartilage identify a signature of non-chondrogenic and mechanical responses. *Osteoarthritis and Cartilage* 24/8: 1431-1440.

- Dunn, Soul, Anand, Schwartz, Boot-Handford and Hardingham (2016) Gene expression changes in damaged osteoarthritic cartilage identify a signature of non-chondrogenic and mechanical responses. *Osteoarthritis and Cartilage* 24/8: 1431-1440.
- Edgar, Domrachev and Lash (2002) Gene Expression Omnibus: NCBI gene expression and hybridization array data repository. *Nucleic acids research* 30/1: 207-210.
- Edgar, Domrachev and Lash (2002) Gene Expression Omnibus: NCBI gene expression and hybridization array data repository. *Nucleic Acids Research* 30/1: 207-210.
- Eliasson, Andersson, Hammerman and Aspenberg (2013) Primary gene response to mechanical loading in healing rat Achilles tendons. *J Appl Physiol (1985)* 114/11: 1519-1526. Available at <http://www.ncbi.nlm.nih.gov/pubmed/23519232>.
- Fang, Xiao, Chen and Zhao (2017) Conditional removal of the canonical TGF- β 1 signaling delays condylar cartilage degeneration induced by a partial discectomy in mice. *PLoS One* 12/5: e0177826.
- Fang, Xu, Li and Zhao (2016) Roles of TGF-beta 1 signaling in the development of osteoarthritis. *Histology and Histopathology* 31/11: 1161-1167.
- Fanjul-Fernández, Folgueras, Cabrera and López-Otín (2010) Matrix metalloproteinases: evolution, gene regulation and functional analysis in mouse models. *Biochimica et Biophysica Acta (BBA)-Molecular Cell Research* 1803/1: 3-19.
- Federici, Kutner, Zhang, Kuroda, Tordo, Boulis and Reiser (2009) Comparative analysis of HIV-1-based lentiviral vectors bearing lyssavirus glycoproteins for neuronal gene transfer. *Genetic Vaccines and Therapy* 7/1: 1.
- Finsson, Chi, Bou-Gharios, Leask and Philip (2012) TGF- β signaling in cartilage homeostasis and osteoarthritis. *Front Biosci (Schol Ed)* 4: 251-268.
- Finsson, Parker, Chi, Hoemann, Goldring, Antoniou and Philip (2010) Endoglin differentially regulates TGF- β -induced Smad2/3 and Smad1/5 signalling and its expression correlates with extracellular matrix production and cellular differentiation state in human chondrocytes. *Osteoarthritis and Cartilage* 18/11: 1518-1527.
- Fosang, Last, Knäuper, Murphy and Neame (1996) Degradation of cartilage aggrecan by collagenase-3 (MMP-13). *FEBS Letters* 380/1-2: 17-20.
- Franceschi, Bonafe, Valensin, Olivieri, De Luca, Ottaviani and De Benedictis (2000) Inflammaging. An evolutionary perspective on immunosenescence. *Annals of the New York Academy of Sciences* 908: 244-254.
- Fukumoto, Sperling, Sanyal, Fitzsimmons, Reinholz, Conover and O'Driscoll (2003) Combined effects of insulin-like growth factor-1 and transforming growth factor-beta1 on periosteal mesenchymal cells during chondrogenesis in vitro. *Osteoarthritis and Cartilage* 11/1: 55-64.
- Funahashi, Morohashi, Kitano and Tanimura (2003) CellDesigner: a process diagram editor for gene-regulatory and biochemical networks. *Biosilico* 1/5: 159-162.
- Galloway, Murphy, Sandy, Gavrilovic, Cawston and Reynolds (1983) Purification and characterization of a rabbit bone metalloproteinase that degrades proteoglycan and other connective-tissue components. *Biochemical Journal* 209/3: 741-752.
- Gay, Schwartz, Sylvia and Boyan (2004) Lysophospholipid regulates release and activation of latent TGF-beta1 from chondrocyte extracellular matrix. *Biochimica et Biophysica Acta* 1684/1-3: 18-28.
- Ge and Greenspan (2006) BMP1 controls TGF β 1 activation via cleavage of latent TGF β -binding protein. *The Journal of cell biology* 175/1: 111-120.
- Gendron, Kashiwagi, Hughes, Caterson and Nagase (2003) TIMP-3 inhibits aggrecanase-mediated glycosaminoglycan release from cartilage explants stimulated by catabolic factors. *FEBS Letters* 555/3: 431-436.

- Gentleman, Carey, Bates, Bolstad, Dettling, Dudoit, Ellis, Gautier, Ge and Gentry (2004) Bioconductor: open software development for computational biology and bioinformatics. *Genome biology* 5/10: R80.
- Gervasi, Bianchi-Smiraglia, Cummings, Zheng, Wang, Liu and Bakin (2012) JunB contributes to Id2 repression and the epithelial-mesenchymal transition in response to transforming growth factor-beta. *J Cell Biol* 196/5: 589-603. Available at <http://www.ncbi.nlm.nih.gov/pubmed/22391036>.
- Gillespie (1976) A general method for numerically simulating the stochastic time evolution of coupled chemical reactions. *Journal of computational physics* 22/4: 403-434.
- Glasson, Askew, Sheppard, Carito, Blanchet, Ma, Flannery, Kanki, Wang and Peluso (2004) Characterization of and osteoarthritis susceptibility in ADAMTS-4-knockout mice. *Arthritis & Rheumatology* 50/8: 2547-2558.
- Glasson, Askew, Sheppard, Carito, Blanchet, Ma, Flannery, Peluso, Kanki and Yang (2005) Deletion of active ADAMTS5 prevents cartilage degradation in a murine model of osteoarthritis. *Nature* 434/7033: 644-648.
- Goldring (2012) Articular cartilage degradation in osteoarthritis. *HSS Journal* 8/1: 7-9.
- Goldring, Birkhead, Suen, Yamin, Mizuno, Glowacki, Arbiser and Apperley (1994) Interleukin-1 beta-modulated gene expression in immortalized human chondrocytes. *Journal of Clinical Investigation* 94/6: 2307.
- Goldring and Otero (2011) Inflammation in osteoarthritis. *Current opinion in rheumatology* 23/5: 471.
- Goodrich, Hidaka, Robbins, Evans and Nixon (2007) Genetic modification of chondrocytes with insulin-like growth factor-1 enhances cartilage healing in an equine model. *Journal of Bone and Joint Surgery (British Volume)* 89/5: 672-685.
- Gossan, Zeef, Hensman, Hughes, Bateman, Rowley, Little, Piggins, Rattray and Boot-Handford (2013) The circadian clock in murine chondrocytes regulates genes controlling key aspects of cartilage homeostasis. *Arthritis & Rheumatology* 65/9: 2334-2345.
- Goumans, Valdimarsdottir, Itoh, Lebrin, Larsson, Mummery, Karlsson and ten Dijke (2003) Activin receptor-like kinase (ALK)1 is an antagonistic mediator of lateral TGFbeta/ALK5 signaling. *Mol Cell* 12/4: 817-828.
- Goumans, Valdimarsdottir, Itoh, Lebrin, Larsson, Mummery, Karlsson and Ten Dijke (2003) Activin receptor-like kinase (ALK) 1 is an antagonistic mediator of lateral TGFβ/ALK5 signaling. *Molecular Cell* 12/4: 817-828.
- Goumans, Valdimarsdottir, Itoh, Rosendahl, Sideras and ten Dijke (2002) Balancing the activation state of the endothelium via two distinct TGF-beta type I receptors. *EMBO Journal* 21/7: 1743-1753.
- Gravallese, Pettit, Lee, Madore, Manning, Tsay, Gaspar, Goldring, Goldring and Oettgen (2003) Angiopoietin-1 is expressed in the synovium of patients with rheumatoid arthritis and is induced by tumour necrosis factor α. *Annals of the Rheumatic Diseases* 62/2: 100-107.
- Greene and Loeser (2015) Aging-related Inflammation in Osteoarthritis. *Osteoarthritis and Cartilage* 23/11: 1966-1971.
- Griner and Kazanietz (2007) Protein kinase C and other diacylglycerol effectors in cancer. *Nat Rev Cancer* 7/4: 281-294.
- Hall, Young, Waters, Rowan, Chantry, Edwards and Clark (2003) The comparative role of activator protein 1 and Smad factors in the regulation of Timp-1 and MMP-1 gene expression by transforming growth factor-beta 1. *J Biol Chem* 278/12: 10304-10313.
- Hamanishi, Hashima, Satsuma and Tanaka (1996) Protein kinase C activator inhibits progression of osteoarthritis induced in rabbit knee joints. *Journal of Laboratory and Clinical Medicine* 127/6: 540-544.

- Hamidi, Algul, Cano, Sandi, Molejon, Riemann, Calvo, Lomberk, Dagorn, Weih, Urrutia, Schmid and Iovanna (2012) Nuclear protein 1 promotes pancreatic cancer development and protects cells from stress by inhibiting apoptosis. *J Clin Invest* 122/6: 2092-2103. Available at <http://www.ncbi.nlm.nih.gov/pubmed/22565310>.
- Hartsough and Mulder (1995) Transforming growth factor beta activation of p44mapk in proliferating cultures of epithelial cells. *Journal of Biological Chemistry* 270/13: 7117-7124.
- Hasdemir, Hoefsloot and Smilde (2015) Validation and selection of ODE based systems biology models: how to arrive at more reliable decisions. *BMC Systems Biology* 9: 32.
- Hata, Lagna, Massagué and Hemmati-Brivanlou (1998) Smad6 inhibits BMP/Smad1 signaling by specifically competing with the Smad4 tumor suppressor. *Genes and Development* 12/2: 186-197.
- Hayashi, Abdollah, Qiu, Cai, Xu, Grinnell, Richardson, Topper, Gimbrone and Wrana (1997) The MAD-related protein Smad7 associates with the TGF β receptor and functions as an antagonist of TGF β signaling. *Cell* 89/7: 1165-1173.
- Hendriks, Griffiths, Benson, Kenyon, Lazzara, Swinton, Beck, Hickinson, Beusmans, Lauffenburger and de Graaf (2006) Decreased internalisation of erbB1 mutants in lung cancer is linked with a mechanism conferring sensitivity to gefitinib. *Systems Biology* 153/6: 457-466.
- Hiraki, Shukunami, Iyama and Mizuta (2001) Differentiation of chondrogenic precursor cells during the regeneration of articular cartilage. *Osteoarthritis and Cartilage* 9: S102-S108.
- Hiramatsu, Iwai, Yoshikawa and Tsumaki (2011) Expression of dominant negative TGF-beta receptors inhibits cartilage formation in conditional transgenic mice. *Journal of Bone and Mineral Metabolism* 29/4: 493-500.
- Hoops, Sahle, Gauges, Lee, Pahle, Simus, Singhal, Xu, Mendes and Kummer (2006) COPASI—a COMplex PATHway Simulator. *Bioinformatics* 22/24: 3067-3074.
- Hoops, Sahle, Gauges, Lee, Pahle, Simus, Singhal, Xu, Mendes and Kummer (2006) COPASI—a complex pathway simulator. *Bioinformatics* 22/24: 3067-3074.
- Hopwood, Tsykin, Findlay and Fazzalari (2007) Microarray gene expression profiling of osteoarthritic bone suggests altered bone remodelling, WNT and transforming growth factor-beta/bone morphogenic protein signalling. *Arthritis Research & Therapy* 9/5: R100.
- Horiki, Imamura, Okamoto, Hayashi, Murai, Myoui, Ochi, Miyazono, Yoshikawa and Tsumaki (2004) Smad6/Smurf1 overexpression in cartilage delays chondrocyte hypertrophy and causes dwarfism with osteopenia. *Journal of Cell Biology* 165/3: 433-445.
- Hosaka, Saito, Sugita, Hikata, Kobayashi, Fukai, Taniguchi, Hirata, Akiyama, Chung and Kawaguchi (2013) Notch signaling in chondrocytes modulates endochondral ossification and osteoarthritis development. *Proceedings of the National Academy of Sciences of the United States of America* 110/5: 1875-1880.
- Houard, Goldring and Berenbaum (2013) Homeostatic Mechanisms in Articular Cartilage and Role of Inflammation in Osteoarthritis. *Curr Rheumatol Rep* 15/11: 375.
- Huang, Sherman and Lempicki (2009) Systematic and integrative analysis of large gene lists using DAVID bioinformatics resources. *Nature protocols* 4/1: 44-57.
- Hucka, Finney, Sauro, Bolouri, Doyle, Kitano, Arkin, Bornstein, Bray, Cornish-Bowden, Cuellar, Dronov, Gilles, Ginkel, Gor, Goryanin, Hedley, Hodgman, Hofmeyr, Hunter, Juty, Kasberger, Kremling, Kummer, Le Novère, Loew, Lucio, Mendes, Minch, Mjolsness, Nakayama, Nelson, Nielsen, Sakurada, Schaff, Shapiro, Shimizu, Spence, Stelling, Takahashi, Tomita, Wagner and Wang (2003) The systems biology markup language (SBML): a medium for representation and exchange of biochemical network models.

- Bioinformatics* 19/4: 524-531. Available at <http://dx.doi.org/10.1093/bioinformatics/btg015>.
- Hugle, Geurts, Nuesch, Muller-Gerbl and Valderrabano (2012) Aging and osteoarthritis: an inevitable encounter? *J Aging Res* 2012: 950192.
- Hui, Cawston and Rowan (2003) Transforming growth factor beta 1 and insulin-like growth factor 1 block collagen degradation induced by oncostatin M in combination with tumour necrosis factor alpha from bovine cartilage. *Annals of the Rheumatic Diseases* 62/2: 172-174.
- Hui, Rowan and Cawston (2000) Transforming growth factor beta1 blocks the release of collagen fragments from bovine nasal cartilage stimulated by oncostatin M in combination with IL-1alpha. *Cytokine* 12/6: 765-769.
- Hui, Young, Rowan, Xu, Cawston and Proctor (2014) Oxidative changes and signalling pathways are pivotal in initiating age-related changes in articular cartilage. *Annals of the Rheumatic Diseases*: annrheumdis-2014-206295.
- Hui, Young, Rowan, Xu, Cawston and Proctor (2014) Oxidative changes and signalling pathways are pivotal in initiating age-related changes in articular cartilage. *Annals of the Rheumatic Diseases*.
- Ijiri, Zerbini, Peng, Correa, Lu, Walsh, Zhao, Taniguchi, Huang and Otu (2005) A novel role for GADD45 β as a mediator of MMP-13 gene expression during chondrocyte terminal differentiation. *Journal of Biological Chemistry* 280/46: 38544-38555.
- Ikeda, Mabuchi, Fukuda, Hiraoka, Kawakami, Yamamoto, Machida, Takatori, Kawaguchi and Nakamura (2001) Identification of sequence polymorphisms in two sulfation-related genes, PAPSS2 and SLC26A2, and an association analysis with knee osteoarthritis. *Journal of Human Genetics* 46/9: 538-543.
- Im, Muddasani, Natarajan, Schmid, Block, Davis, van Wijnen and Loeser (2007) Basic fibroblast growth factor stimulates matrix metalloproteinase-13 via the molecular cross-talk between the mitogen-activated protein kinases and protein kinase Cdelta pathways in human adult articular chondrocytes. *Journal of Biological Chemistry* 282/15: 11110-11121.
- Imamura (1997) Smad6 inhibits signaling by the TGF-beta superfamily. *Nature* 389: 549-551.
- Inada, Wang, Byrne, Rahman, Miyaura, Lopez-Otin and Krane (2004) Critical roles for collagenase-3 (Mmp13) in development of growth plate cartilage and in endochondral ossification. *Proc Natl Acad Sci U S A* 101/49: 17192-17197. Available at <http://www.ncbi.nlm.nih.gov/pubmed/15563592>.
- Inada, Wang, Byrne, Rahman, López-Otín and Krane (2004) Critical roles for collagenase-3 (Mmp13) in development of growth plate cartilage and in endochondral ossification. *Proc Natl Acad Sci U S A* 101/49: 17192-17197.
- Irizarry, Hobbs, Collin, Beazer-Barclay, Antonellis, Scherf and Speed (2003) Exploration, normalization, and summaries of high density oligonucleotide array probe level data. *Biostatistics* 4/2: 249-264.
- Itoh, Landström, Hermansson, Itoh, Heldin, Heldin and ten Dijke (1998) Transforming growth factor β 1 induces nuclear export of inhibitory Smad7. *Journal of Biological Chemistry* 273/44: 29195-29201.
- Janusz, Hookfin, Brown, Hsieh, Heitmeyer, Taiwo, Natchus, Pikul, Almstead and Peng (2006) Comparison of the pharmacology of hydroxamate- and carboxylate-based matrix metalloproteinase inhibitors (MMPi) for the treatment of osteoarthritis. *Inflammation Research* 55/2: 60-65.
- Ji and Yan (2017) Mathematical and Computational Modeling in Complex Biological Systems. 2017: 5958321.
- Johnson, Li and Rabinovic (2007) Adjusting batch effects in microarray expression data using empirical Bayes methods. *Biostatistics* 8/1: 118-127.

- Jonason, Xiao, Zhang, Xing and Chen (2009) Post-translational regulation of Runx2 in bone and cartilage. *Journal of Dental Research* 88/8: 693-703.
- Jotanovic, Mihelic, Sestan and Dembic (2012) Role of interleukin-1 inhibitors in osteoarthritis: an evidence-based review. *Drugs and Aging* 29/5: 343-358.
- Kashiwagi, Tortorella, Nagase and Brew (2001) TIMP-3 is a potent inhibitor of aggrecanase 1 (ADAM-TS4) and aggrecanase 2 (ADAM-TS5). *Journal of Biological Chemistry* 276/16: 12501-12504.
- Kavsak, Rasmussen, Causing, Bonni, Zhu, Thomsen and Wrana (2000) Smad7 binds to Smurf2 to form an E3 ubiquitin ligase that targets the TGF β receptor for degradation. *Molecular Cell* 6/6: 1365-1375.
- Kelwick, Desanlis, Wheeler and Edwards (2015) The ADAMTS (A Disintegrin and Metalloproteinase with Thrombospondin motifs) family. *Genome Biology* 16/1: 113.
- Kent, Sugnet, Furey, Roskin, Pringle, Zahler and Haussler (2002) The human genome browser at UCSC. *Genome research* 12/6: 996-1006.
- Kim, Chung, Woo, Jung, Lee, Moon, Suh-Kim and Baik (2010) Differential regulation of proliferation and differentiation in neural precursor cells by the Jak pathway. *Stem Cells* 28/10: 1816-1828.
- Kini and Nandeesh (2012) Physiology of bone formation, remodeling, and metabolism. In *Radionuclide and hybrid bone imaging*, 29-57. Springer.
- Kinoshita, Saito, Tomita, Makita, Yoshida, Ghadami, Yamada, Kondo, Ikegawa, Nishimura, Fukushima, Nakagomi, Saito, Sugimoto, Kamegaya, Hisa, Murray, Taniguchi, Niikawa and Yoshiura (2000) Domain-specific mutations in TGF β 1 result in Camurati-Engelmann disease. *Nature Genetics* 26/1: 19-20.
- Kizawa, Kou, Iida, Sudo, Miyamoto, Fukuda, Mabuchi, Kotani, Kawakami, Yamamoto, Uchida, Nakamura, Notoya, Nakamura and Ikegawa (2005) An aspartic acid repeat polymorphism in asporin inhibits chondrogenesis and increases susceptibility to osteoarthritis. *Nature Genetics* 37/2: 138-144.
- Kjeldsen, Johnsen, Sengeløv and Borregaard (1993) Isolation and primary structure of NGAL, a novel protein associated with human neutrophil gelatinase. *Journal of Biological Chemistry* 268/14: 10425-10432.
- Klamt, Saez-Rodriguez and Gilles (2007) Structural and functional analysis of cellular networks with CellNetAnalyzer. *BMC Systems Biology* 1: 2.
- Köhler, Doelken, Ruef, Bauer, Washington, Westerfield, Gkoutos, Schofield, Smedley and Lewis (2013) Construction and accessibility of a cross-species phenotype ontology along with gene annotations for biomedical research. *F1000Research* 2.
- Kohn, Dong, Mirando, Jesse, Honjo, Zuscik, O'Keefe and Hilton (2012) Cartilage-specific RBP κ -dependent and -independent Notch signals regulate cartilage and bone development. *Development* 139/6: 1198-1212.
- König, Kögel, Rami and Prehn (2005) TGF- β 1 activates two distinct type I receptors in neurons. *The Journal of cell biology* 168/7: 1077-1086.
- Kopan and Ilgan (2009) The canonical Notch signaling pathway: unfolding the activation mechanism. *Cell* 137/2: 216-233.
- Kuruvilla, Shah, Hochwald, Liggitt, Palladino and Thorbecke (1991) Protective effect of transforming growth factor beta 1 on experimental autoimmune diseases in mice. *Proceedings of the National Academy of Sciences of the United States of America* 88/7: 2918-2921.
- Laposky, Bass, Kohsaka and Turek (2008) Sleep and circadian rhythms: key components in the regulation of energy metabolism. *FEBS Letters* 582/1: 142-151.
- Lark, Gordy, Weidner, Ayala, Kimura, Williams, Mumford, Flannery, Carlson and Iwata (1995) Cell-mediated Catabolism of Aggrecan EVIDENCE THAT CLEAVAGE AT THE

- “AGGRECANASE” SITE (Glu-Ala) IS A PRIMARY EVENT IN PROTEOLYSIS OF THE INTERGLOBULAR DOMAIN. *Journal of Biological Chemistry* 270/6: 2550-2556.
- Le Novere, Hucka, Mi, Moodie, Schreiber, Sorokin, Demir, Wegner, Aladjem and Wimalaratne (2009) The systems biology graphical notation. *Nature biotechnology* 27/8: 735-741.
- Lee, Fitzgerald, Dimicco and Grodzinsky (2005) Mechanical injury of cartilage explants causes specific time-dependent changes in chondrocyte gene expression. *Arthritis Rheum* 52/8: 2386-2395.
- Lee, Lee, Nah, Lee, Yang, Kim, Chun, Hong and Kim (2008) Association of TIMP-4 gene polymorphism with the risk of osteoarthritis in the Korean population. *Rheumatology International* 28/9: 845-850.
- Lee, Song, Hwang, Yi, Oh, Lee, Choi, Choi and Kim (2001) Regeneration of hyaline cartilage by cell-mediated gene therapy using transforming growth factor β 1-producing fibroblasts. *Human Gene Therapy* 12/14: 1805-1813.
- Lee, Zimmer, Lee and Park (2006) Colored Petri net modeling and simulation of signal transduction pathways. *Metab Eng* 8/2: 112-122.
- Leivonen, Lazaridis, Decock, Chantry, Edwards and Kahari (2013) TGF-beta-elicited induction of tissue inhibitor of metalloproteinases (TIMP)-3 expression in fibroblasts involves complex interplay between Smad3, p38alpha, and ERK1/2. *PLoS One* 8/2: e57474.
- Letourneau, Rocher and Porteu (2006) B56-containing PP2A dephosphorylate ERK and their activity is controlled by the early gene IEX-1 and ERK. *Embo j* 25/4: 727-738.
- Levi, Topilko, Schneider-Maunoury, Lasagna, Mantero, Cancedda and Charnay (1996) Defective bone formation in Krox-20 mutant mice. *Development* 122/1: 113-120.
- Levine (2004) Mechanisms of soluble cytokine receptor generation. *The Journal of Immunology* 173/9: 5343-5348.
- Li, Wei, Li, Chen, Wang, Jiao, Wang, Wei, Zhang and Wei (2015) The Role of miRNAs in Cartilage Homeostasis. *Curr Genomics* 16/6: 393-404.
- Li, Yin, Gao, Cheng, Pavlos, Zhang and Zheng (2013) Subchondral bone in osteoarthritis: insight into risk factors and microstructural changes. *Arthritis Research & Therapy* 15/6: 223.
- Li, Yin, Gao, Cheng, Pavlos, Zhang and Zheng (2013) Subchondral bone in osteoarthritis: insight into risk factors and microstructural changes. *Arthritis Research & Therapy* 15/6: 223.
- Lin, Madan, Yoon, Fang, Yan, Kim, Hwang, Hood and Foltz (2010) Massively parallel signature sequencing and bioinformatics analysis identifies up-regulation of TGFBI and SOX4 in human glioblastoma. *PLoS One* 5/4: e10210.
- Lin, Martin, Xia and Gorham (2005) TGF- β 1 uses distinct mechanisms to inhibit IFN- γ expression in CD4+ T cells at priming and at recall: differential involvement of Stat4 and T-bet. *The Journal of Immunology* 174/10: 5950-5958.
- Lin, Sun, Jiang, Hong and Zheng (2013) Sirt2 suppresses inflammatory responses in collagen-induced arthritis. *Biochem Biophys Res Commun* 441/4: 897-903. Available at <http://www.ncbi.nlm.nih.gov/pubmed/24211200>.
- Linn and Sokoloff (1965) MOVEMENT AND COMPOSITION OF INTERSTITIAL FLUID OF CARTILAGE. *Arthritis and Rheumatism* 8: 481-494.
- Litherland, Elias, Hui, Macdonald, Catterall, Barter, Farren, Jefferson and Rowan (2010) Protein kinase C isoforms zeta and iota mediate collagenase expression and cartilage destruction via STAT3- and ERK-dependent c-fos induction. *Journal of Biological Chemistry* 285/29: 22414-22425.
- Little, Barai, Burkhardt, Smith, Fosang, Werb, Shah and Thompson (2009) Matrix metalloproteinase 13-deficient mice are resistant to osteoarthritic cartilage erosion but not chondrocyte hypertrophy or osteophyte development. *Arthritis & Rheumatology* 60/12: 3723-3733.
- Little, Hughes, Curtis, Janusz, Bohne, Wang-Weigand, Taiwo, Mitchell, Otterness and Flannery (2002) Matrix metalloproteinases are involved in C-terminal and interglobular domain

- processing of cartilage aggrecan in late stage cartilage degradation. *Matrix Biology* 21/3: 271-288.
- Little, Meeker, Golub, Lawlor, Farmer, Smith and Fosang (2007) Blocking aggrecanase cleavage in the aggrecan interglobular domain abrogates cartilage erosion and promotes cartilage repair. *Journal of Clinical Investigation* 117/6: 1627.
- Little, Mittaz, Belluoccio, Rogerson, Campbell, Meeker, Bateman, Pritchard and Fosang (2005) ADAMTS-1–Knockout mice do not exhibit abnormalities in aggrecan turnover in vitro or in vivo. *Arthritis & Rheumatology* 52/5: 1461-1472.
- Liu, Chen, Mirando, Wang, Zuscik, O’Keefe and Hilton (2015) A dual role for NOTCH signaling in joint cartilage maintenance and osteoarthritis. *Science signaling* 8/386: ra71.
- Loeser (2010) Age-related changes in the musculoskeletal system and the development of osteoarthritis. *Clinics in Geriatric Medicine* 26/3: 371-386.
- Loeser, Carlson, Del Carlo and Cole (2002) Detection of nitrotyrosine in aging and osteoarthritic cartilage: Correlation of oxidative damage with the presence of interleukin-1beta and with chondrocyte resistance to insulin-like growth factor 1. *Arthritis and Rheumatism* 46/9: 2349-2357.
- Lories, Daans, Derese, Matthys, Kasran, Tylzanowski, Ceuppens and Luyten (2006) Noggin haploinsufficiency differentially affects tissue responses in destructive and remodeling arthritis. *Arthritis and Rheumatism* 54/6: 1736-1746.
- Louati, Vidal, Berenbaum and Sellam (2015) Association between diabetes mellitus and osteoarthritis: systematic literature review and meta-analysis. *RMD open* 1/1: e000077.
- Loughlin, Dowling, Chapman, Marcelline, Mustafa, Southam, Ferreira, Ciesielski, Carson and Corr (2004) Functional variants within the secreted frizzled-related protein 3 gene are associated with hip osteoarthritis in females. *Proceedings of the National Academy of Sciences of the United States of America* 101/26: 9757-9762.
- Lu, Sun, Ge, Teng and Jiang (2014) Histone deacetylase 4 alters cartilage homeostasis in human osteoarthritis. *BMC Musculoskeletal Disorders* 15.
- Luyten, Tylzanowski and Lories (2009) Wnt signaling and osteoarthritis. *Bone* 44/4: 522-527.
- Macdonald (2013) Synergistic transcriptional regulation of collagenase gene expression in chondrocytes. Newcastle University.
- Madej, van Caam, van der Kraan and Buma (2013) Old and Young Articular Cartilage Respond Equivalently for Physiological and Excessive Loading by Activation of Protective Tgf-Beta Signaling. *Osteoarthritis and Cartilage* 21: S107-S108. Available at <Go to ISI>://WOS:000317942300217.
- Mahjoub, Sassi, Driss, Laadhar, Allouche, Hamdoun, Romdhane, Sellami and Makni (2012) Expression patterns of Notch receptors and their ligands in human osteoarthritic and healthy articular cartilage. *Tissue and Cell* 44/3: 182-194.
- Margolin, Nemenman, Basso, Wiggins, Stolovitzky, Dalla Favera and Califano (2006) ARACNE: an algorithm for the reconstruction of gene regulatory networks in a mammalian cellular context. *BMC bioinformatics* 7/1: S7.
- Mariani, Pulsatelli and Facchini (2014) Signaling pathways in cartilage repair. *Int J Mol Sci* 15/5: 8667-8698.
- Marie, Liggitt and Rudensky (2006) Cellular mechanisms of fatal early-onset autoimmunity in mice with the T cell-specific targeting of transforming growth factor-beta receptor. *Immunity* 25/3: 441-454. Available at <http://www.ncbi.nlm.nih.gov/pubmed/16973387>.
- Maroudas (1979) Physicochemical properties of articular cartilage. *Adult articular cartilage*: 215-290.
- Martel-Pelletier, Alaaeddine and Pelletier (1999) Cytokines and their role in the pathophysiology of osteoarthritis. *Frontiers in Bioscience* 4: D694-703.

- Martel-Pelletier, Boileau, Pelletier and Roughley (2008) Cartilage in normal and osteoarthritis conditions. *Best Practice & Research Clinical Rheumatology* 22/2: 351-384.
- Massaous and Hata (1997) TGF- β signalling through the Smad pathway. *Trends in Cell Biology* 7/5: 187-192.
- Massova, Kotra, Fridman and Mobashery (1998) Matrix metalloproteinases: structures, evolution, and diversification. *The FASEB Journal* 12/12: 1075-1095.
- Mauviel, Chung, Agarwal, Tamai and Uitto (1996) Cell-specific induction of distinct oncogenes of the Jun family is responsible for differential regulation of collagenase gene expression by transforming growth factor-beta in fibroblasts and keratinocytes. *J Biol Chem* 271/18: 10917-10923. Available at <http://www.ncbi.nlm.nih.gov/pubmed/8631909>.
- McCoy, Falgowski, Srinivasan, Thompson, Selva and Kirn-Safran (2012) Serum xylosyltransferase 1 level increases during early posttraumatic osteoarthritis in mice with high bone forming potential. *Bone* 51/2: 224-231.
- Meng, Ma, Ma and Xu (2005) Microarray analysis of differential gene expression in temporomandibular joint condylar cartilage after experimentally induced osteoarthritis. *Osteoarthritis and Cartilage* 13/12: 1115-1125.
- Millward-Sadler and Salter (2004) Integrin-dependent signal cascades in chondrocyte mechanotransduction. *Annals of Biomedical Engineering* 32/3: 435-446.
- Milner, Elliott and Cawston (2001) Activation of procollagenases is a key control point in cartilage collagen degradation: interaction of serine and metalloproteinase pathways. *Arthritis Rheum* 44/9: 2084-2096.
- Mitchell, Pobre, Mulivor, Grinberg, Castonguay, Monnell, Solban, Ucran, Pearsall and Underwood (2010) ALK1-Fc inhibits multiple mediators of angiogenesis and suppresses tumor growth. *Molecular Cancer Therapeutics* 9/2: 379-388.
- Mobasheri, Barrett-Jolley, Carter, Martin-Vasallo, Schulze-Tanzil and Shakibaei (2005) Functional Roles of Mechanosensitive Ion Channels, ss1 Integrins and Kinase Cascades in Chondrocyte Mechanotransduction. In A. Kamkin and I. Kiseleva, eds: *Mechanosensitivity in Cells and Tissues*. Moscow: Academia
- Academia Publishing House Ltd.
- Morinobu, Tanaka, Nishimura, Takahashi, Kageyama, Miura, Kurosaka, Saegusa and Kumagai (2016) Expression and Functions of Immediate Early Response Gene X-1 (IEX-1) in Rheumatoid Arthritis Synovial Fibroblasts. *PLoS One* 11/10: e0164350. Available at <http://www.ncbi.nlm.nih.gov/pubmed/27736946>.
- Morris, Apeltsin, Newman, Baumbach, Wittkop, Su, Bader and Ferrin (2011) clusterMaker: a multi-algorithm clustering plugin for Cytoscape. *BMC Bioinformatics* 12/1: 436.
- Morris, Cs-Szabo and Cole (2010) Characterization of TIMP-3 in human articular talar cartilage. *Connective Tissue Research* 51/6: 478-490.
- Morrisette-Thomas, Cohen, Fulop, Riesco, Legault, Li, Milot, Dusseault-Belanger and Ferrucci (2014) Inflamm-aging does not simply reflect increases in pro-inflammatory markers. *Mechanisms of Ageing and Development* 139: 49-57.
- Mort and Billington (2001) Articular cartilage and changes in arthritis: matrix degradation. *Arthritis Res* 3/6: 337-341.
- Nakamura, Kamihagi, Satakeda, Katayama, Pan, Okamoto, Noshiro, Takahashi, Yoshihara and Shimmei (1996) Enhancement of SPARC (osteonectin) synthesis in arthritic cartilage: increased levels in synovial fluids from patients with rheumatoid arthritis and regulation by growth factors and cytokines in chondrocyte cultures. *Arthritis & Rheumatology* 39/4: 539-551.
- Nakao, Afrakhte, Moren and Nakayama (1997) Identification of Smad7, a TGF-beta-inducible antagonist of TGF-beta signalling. *Nature* 389/6651: 631.

- Nakao, Imamura, Souchelnytskyi, Kawabata, Ishisaki, Oeda, Tamaki, Hanai, Heldin, Miyazono and ten Dijke (1997) TGF-beta receptor-mediated signalling through Smad2, Smad3 and Smad4. *EMBO Journal* 16/17: 5353-5362.
- Neuhold, Killar, Zhao, Sung, Warner, Kulik, Turner, Wu, Billingham and Meijers (2001) Postnatal expression in hyaline cartilage of constitutively active human collagenase-3 (MMP-13) induces osteoarthritis in mice. *Journal of Clinical Investigation* 107/1: 35.
- Ng, Chiu, Rabie and Hagg (2006) Repeated mechanical loading enhances the expression of Indian hedgehog in condylar cartilage. *Frontiers in Bioscience* 11: 943-948.
- Nicklas and Saiz (2013) Computational modelling of Smad-mediated negative feedback and crosstalk in the TGF-beta superfamily network. *J R Soc Interface* 10/86: 20130363.
- Nishimura, Hata, Matsubara, Wakabayashi and Yoneda (2012) Regulation of bone and cartilage development by network between BMP signalling and transcription factors. *Journal of Biochemistry* 151/3: 247-254.
- Olex, Turkett, Fetrow and Loeser (2014) Integration of gene expression data with network-based analysis to identify signaling and metabolic pathways regulated during the development of osteoarthritis. *Gene* 542/1: 38-45.
- Pai, Rymer, Chang and Sharma (1997) Effect of age and osteoarthritis on knee proprioception. *Arthritis and Rheumatism* 40/12: 2260-2265.
- Pan, Yu, Chen, Li, Wu, Wan, Ma and Sun (2008) Sox9, a key transcription factor of bone morphogenetic protein-2-induced chondrogenesis, is activated through BMP pathway and a CCAAT box in the proximal promoter. *Journal of Cellular Physiology* 217/1: 228-241.
- Panoulas, Douglas, Smith, Stavropoulos-Kalinoglou, Metsios, Nightingale and Kitas (2009) Transforming growth factor-beta1 869T/C, but not interleukin-6 -174G/C, polymorphism associates with hypertension in rheumatoid arthritis. *Rheumatology* 48/2: 113-118.
- Papathanasiou, Malizos and Tsezou (2012) Bone morphogenetic protein-2-induced Wnt/beta-catenin signaling pathway activation through enhanced low-density-lipoprotein receptor-related protein 5 catabolic activity contributes to hypertrophy in osteoarthritic chondrocytes. *Arthritis Research & Therapy* 14/2: R82.
- Park and Choi (2016) The Effects of Adherence to Non-Steroidal Anti-Inflammatory Drugs and Factors Influencing Drug Adherence in Patients with Knee Osteoarthritis. 31/5: 795-800.
- Passos, Nelson, Wang, Richter, Simillion, Proctor, Miwa, Olijslagers, Hallinan and Wipat (2010) Feedback between p21 and reactive oxygen production is necessary for cell senescence. *Molecular Systems Biology* 6/1: 347.
- Pedersen, Hagedorn, Lindholm and Lindow (2014) A Kinetic Model Explains Why Shorter and Less Affine Enzyme-recruiting Oligonucleotides Can Be More Potent. *Mol Ther Nucleic Acids* 3: e149.
- Pedrozo, Schwartz, Gomez, Ornoy, Xin-Sheng, Dallas, Bonewald, Dean and Boyan (1998) Growth plate chondrocytes store latent transforming growth factor (TGF)-beta 1 in their matrix through latent TGF-beta 1 binding protein-1. *Journal of Cellular Physiology* 177/2: 343-354.
- Petzold (1983) Automatic selection of methods for solving stiff and nonstiff systems of ordinary differential equations. *SIAM journal on scientific and statistical computing* 4/1: 136-148.
- Plater-Zyberk, Buckton, Thompson, Spaul, Zanders, Papworth and Life (2001) Amelioration of arthritis in two murine models using antibodies to oncostatin M. *Arthritis and Rheumatism* 44/11: 2697-2702.

- Pombo-Suarez, Castaño-Oreja, Calaza, Gomez-Reino and Gonzalez (2009) Differential upregulation of the three transforming growth factor beta isoforms in human osteoarthritic cartilage. *Annals of the Rheumatic Diseases* 68/4: 568-571.
- Ponticos, Harvey, Ikeda, Abraham and Bou-Gharios (2009) JunB mediates enhancer/promoter activity of COL1A2 following TGF-beta induction. *Nucleic Acids Research* 37/16: 5378-5389.
- Poole, Kobayashi, Yasuda, Lavery, Mwale, Kojima, Sakai, Wahl, El-Maadawy, Webb, Tchetina and Wu (2002) Type II collagen degradation and its regulation in articular cartilage in osteoarthritis. *Ann Rheum Dis* 61 Suppl 2: ii78-81. Available at <http://www.ncbi.nlm.nih.gov/pubmed/12379630>.
- Pothacharoen, Najarus, Settakorn, Mizumoto, Sugahara and Kongtawelert (2014) Effects of sesamin on the biosynthesis of chondroitin sulfate proteoglycans in human articular chondrocytes in primary culture. *Glycoconjugate Journal* 31/3: 221-230.
- Poulet, Ulici, Stone, Pead, Gburcik, Constantinou, Palmer, Beier, Timmons and Pitsillides (2012) Time-series transcriptional profiling yields new perspectives on susceptibility to murine osteoarthritis. *Arthritis & Rheumatology* 64/10: 3256-3266.
- Pratta, Yao, Decicco, Tortorella, Liu, Copeland, Magolda, Newton, Trzaskos and Arner (2003) Aggrecan protects cartilage collagen from proteolytic cleavage. *Journal of Biological Chemistry* 278/46: 45539-45545.
- Proctor and Gartland (2016) Simulated interventions to ameliorate age-related bone loss indicate the importance of timing. *Frontiers in Endocrinology* 7.
- Proctor and Gray (2008) Explaining oscillations and variability in the p53-Mdm2 system. *BMC Systems Biology* 2/1: 75.
- Proctor, Macdonald, Milner, Rowan and Cawston (2014) A computer simulation approach to assessing therapeutic intervention points for the prevention of cytokine-induced cartilage breakdown. *Arthritis Rheumatol* 66/4: 979-989.
- Queirolo, Galli, Masselli, Borzi, Martini, Vitale, Gobbi, Carubbi and Mirandola (2016) PKCepsilon is a regulator of hypertrophic differentiation of chondrocytes in osteoarthritis. *Osteoarthritis and Cartilage* 24/8: 1451-1460. Available at <http://www.ncbi.nlm.nih.gov/pubmed/27072078>.
- Radin, Paul and Rose (1972) Role of mechanical factors in pathogenesis of primary osteoarthritis. *Lancet* 1/7749: 519-522.
- Rahmati, Mobasheri and Mozafari (2016) Inflammatory mediators in osteoarthritis: A critical review of the state-of-the-art, current prospects, and future challenges. *Bone* 85: 81-90.
- Ramaswamy, Sohn, Eberhardt and Serra (2012) Altered responsiveness to TGF- β results in reduced Paps2 expression and alterations in the biomechanical properties of mouse articular cartilage. *Arthritis Research & Therapy* 14/2: R49.
- Regan, Flannelly, Bowler, Tran, Nicks, Carbone, Glueck, Heijnen, Mason and Crapo (2005) Extracellular superoxide dismutase and oxidant damage in osteoarthritis. *Arthritis and Rheumatism* 52/11: 3479-3491.
- Resat, Petzold and Pettigrew (2009) Kinetic modeling of biological systems. *Methods in Molecular Biology* 541: 311-335.
- Responte, Lee, Hu and Athanasiou (2012) Biomechanics-driven chondrogenesis: from embryo to adult. *FASEB Journal* 26/9: 3614-3624.
- Rhodes, Yu, Shanker, Deshpande, Varambally, Ghosh, Barrette, Pandey and Chinnaiyan (2004) Large-scale meta-analysis of cancer microarray data identifies common transcriptional profiles of neoplastic transformation and progression. *Proceedings of the National Academy of Sciences of the United States of America* 101/25: 9309-9314.
- Rhodes, Yu, Shanker, Deshpande, Varambally, Ghosh, Barrette, Pandey and Chinnaiyan (2004) Large-scale meta-analysis of cancer microarray data identifies common transcriptional

- profiles of neoplastic transformation and progression. *Proceedings of the National Academy of Sciences of the United States of America* 101/25: 9309-9314.
- Richards (2013) The enigmatic cytokine oncostatin m and roles in disease. *ISRN Inflamm* 2013: 512103.
- Rigoglou and Papavassiliou (2013) The NF-kappaB signalling pathway in osteoarthritis. *International Journal of Biochemistry and Cell Biology* 45/11: 2580-2584.
- Roberts, Anzano, Lamb, Smith and Sporn (1981) New class of transforming growth factors potentiated by epidermal growth factor: isolation from non-neoplastic tissues. *Proc Natl Acad Sci U S A* 78/9: 5339-5343.
- Roberts, Anzano, Wakefield, Roche, Stern and Sporn (1985) Type beta transforming growth factor: a bifunctional regulator of cellular growth. *Proc Natl Acad Sci U S A* 82/1: 119-123.
- Roberts, Sporn, Assoian, Smith, Roche, Wakefield, Heine, Liotta, Falanga, Kehrl and et al. (1986) Transforming growth factor type beta: rapid induction of fibrosis and angiogenesis in vivo and stimulation of collagen formation in vitro. *Proc Natl Acad Sci U S A* 83/12: 4167-4171.
- Rock and Kono (2008) The inflammatory response to cell death. *Annu Rev pathmechdis Mech Dis* 3: 99-126.
- Roos, Adalberth, Dahlberg and Lohmander (1995) Osteoarthritis of the knee after injury to the anterior cruciate ligament or meniscus: the influence of time and age. *Osteoarthritis and Cartilage* 3/4: 261-267.
- Rosselot, Vasilatos-Younken and Leach (1994) Effect of growth hormone, insulin-like growth factor I, basic fibroblast growth factor, and transforming growth factor beta on cell proliferation and proteoglycan synthesis by avian postembryonic growth plate chondrocytes. *Journal of Bone and Mineral Research* 9/3: 431-439.
- Saeed, Sharov, White, Li, Liang, Bhagabati, Braisted, Klapa, Currier and Thiagarajan (2003) TM4: a free, open-source system for microarray data management and analysis. *Biotechniques* 34/2: 374.
- Sanchez-Adams, Leddy, McNulty, O'Connor and Guilak (2014) The Mechanobiology of Articular Cartilage: Bearing the Burden of Osteoarthritis. *Curr Rheumatol Rep* 16/10: 451.
- Sandy and Verscharen (2001) Analysis of aggrecan in human knee cartilage and synovial fluid indicates that aggrecanase (ADAMTS) activity is responsible for the catabolic turnover and loss of whole aggrecan whereas other protease activity is required for C-terminal processing in vivo. *Biochemical Journal* 358/3: 615-626.
- Sapolsky, Altman, Woessner and Howell (1973) The action of cathepsin D in human articular cartilage on proteoglycans. *Journal of Clinical Investigation* 52/3: 624.
- Sassi, Gadgadi, Laadhar, Allouche, Murali, Zandieh-Doulabi, Hamdoun, Nulend, Makni and Sellami (2014) Notch signaling is involved in human articular chondrocytes de-differentiation during osteoarthritis. *Journal of Receptor and Signal Transduction Research* 34/1: 48-57.
- Sassi, Laadhar, Allouche, Achek, Kallel-Sellami, Makni and Sellami (2014) WNT signaling and chondrocytes: from cell fate determination to osteoarthritis physiopathology. *Journal of Receptor and Signal Transduction Research* 34/2: 73-80.
- Scanzello and Goldring (2012) The role of synovitis in osteoarthritis pathogenesis. *Bone* 51/2: 249-257.
- Schadt, Linderman, Sorenson, Lee and Nolan (2010) Computational solutions to large-scale data management and analysis. *Nat Rev Genet* 11/9: 647-657.
- Scharstuhl, Glansbeek, van Beuningen, Vitters, van der Kraan and van den Berg (2002) Inhibition of endogenous TGF-beta during experimental osteoarthritis prevents osteophyte formation and impairs cartilage repair. *Journal of Immunology* 169/1: 507-514.

- Scharstuhl, van Beuning, Vitters, van der Kraan and van den Berg (2002) Loss of transforming growth factor counteraction on interleukin 1 mediated effects in cartilage of old mice. *Annals of the Rheumatic Diseases* 61/12: 1095-1098.
- Schlaak, Pfers, Meyer Zum Buschenfelde and Marker-Hermann (1996) Different cytokine profiles in the synovial fluid of patients with osteoarthritis, rheumatoid arthritis and seronegative spondylarthropathies. *Clinical and Experimental Rheumatology* 14/2: 155-162.
- Schlichting, Dehne, Mans, Endres, Stuhlmüller, Sittinger, Kaps and Ringe (2014) Suitability of porcine chondrocyte micromass culture to model osteoarthritis in vitro. *Molecular Pharmaceutics* 11/7: 2092-2105.
- Schmierer, Tournier, Bates and Hill (2008) Mathematical modeling identifies Smad nucleocytoplasmic shuttling as a dynamic signal-interpreting system. *Proceedings of the National Academy of Sciences of the United States of America* 105/18: 6608-6613.
- Schmierer, Tournier, Bates and Hill (2008) Mathematical modeling identifies Smad nucleocytoplasmic shuttling as a dynamic signal-interpreting system. *Proceedings of the National Academy of Sciences* 105/18: 6608-6613.
- Schuttler, Reiche, Altenburger and Busch (2017) The Transcriptome of the Zebrafish Embryo After Chemical Exposure: A Meta-Analysis. *Toxicological Sciences* 157/2: 291-304.
- Selvamurugan, Kwok and Partridge (2004) Smad3 interacts with JunB and Cbfa1/Runx2 for transforming growth factor-beta1-stimulated collagenase-3 expression in human breast cancer cells. *J Biol Chem* 279/26: 27764-27773. Available at <http://www.ncbi.nlm.nih.gov/pubmed/15084595>.
- Sen and Packer (1996) Antioxidant and redox regulation of gene transcription. *The FASEB journal* 10/7: 709-720.
- Settle, Vickery, Nemirovskiy, Vidmar, Bendele, Messing, Ruminski, Schnute and Sunyer (2010) Cartilage degradation biomarkers predict efficacy of a novel, highly selective matrix metalloproteinase 13 inhibitor in a dog model of osteoarthritis: confirmation by multivariate analysis that modulation of type II collagen and aggrecan degradation peptides parallels pathologic changes. *Arthritis & Rheumatology* 62/10: 3006-3015.
- Shannon, Markiel, Ozier, Baliga, Wang, Ramage, Amin, Schwikowski and Ideker (2003) Cytoscape: a software environment for integrated models of biomolecular interaction networks. *Genome research* 13/11: 2498-2504.
- Shao, Wang, Welter and Ballock (2012) Primary cilia modulate Ihh signal transduction in response to hydrostatic loading of growth plate chondrocytes. *Bone* 50/1: 79-84.
- Shen, Abu-Amer, O'Keefe and McAlinden (2017) Inflammation and epigenetic regulation in osteoarthritis. *Connective Tissue Research* 58/1: 49-63.
- Shen, Li and Chen (2014) TGF-beta signaling and the development of osteoarthritis. *Bone Res* 2.
- Shimizu, Selvamurugan, Westendorf, Olson and Partridge (2010) HDAC4 represses matrix metalloproteinase-13 transcription in osteoblastic cells, and parathyroid hormone controls this repression. *Journal of Biological Chemistry* 285/13: 9616-9626.
- Shimizu, Selvamurugan, Westendorf, Olson and Partridge (2010) HDAC4 represses matrix metalloproteinase-13 transcription in osteoblastic cells, and parathyroid hormone controls this repression. *Journal of Biological Chemistry* 285/13: 9616-9626.
- Shingleton, Jones, Xu, Cawston and Rowan (2006) Retinoic acid and oncostatin M combine to promote cartilage degradation via matrix metalloproteinase-13 expression in bovine but not human chondrocytes. *Rheumatology* 45/8: 958-965.
- Shull, Ormsby, Kier, Pawlowski, Diebold, Yin, Allen, Sidman, Proetzel, Calvin and et al. (1992) Targeted disruption of the mouse transforming growth factor-beta 1 gene results in multifocal inflammatory disease. *Nature* 359/6397: 693-699. Available at <http://www.ncbi.nlm.nih.gov/pubmed/1436033>.

- Sieker, Proffen, Waller, Chin, Karamchedu, Akelman, Perrone, Kiapour, Konrad and Murray (2017) Transcriptional Profiling of Articular Cartilage in a Porcine Model of Early Post-traumatic Osteoarthritis. *Journal of Orthopaedic Research*.
- Silman AJ (2001) *Epidemiology of the Rheumatic Diseases*. 2nd. New York: Oxford University Press.
- Silver and Maroudas (1975) Measurement of PH and Ionic Composition of Pericellular Sites [and Discussion]. *Philosophical Transactions of the Royal Society of London B: Biological Sciences* 271/912: 261-272.
- Song, D Tortorella, Malfait, Alston, Yang, Arner and Griggs (2007) Aggrecan degradation in human articular cartilage explants is mediated by both ADAMTS-4 and ADAMTS-5. *Arthritis & Rheumatology* 56/2: 575-585.
- Song, Hong, Oh, Yi, Choi, Lee, Park, Han, Suh and Lee (2004) Regeneration of hyaline articular cartilage with irradiated transforming growth factor β 1-producing fibroblasts. *Tissue Engineering* 10/5-6: 665-672.
- Sophia Fox, Bedi and Rodeo (2009) The basic science of articular cartilage: structure, composition, and function. *Sports health* 1/6: 461-468.
- Sophia Fox, Bedi and Rodeo (2009) The basic science of articular cartilage: structure, composition, and function. *Sports Health* 1/6: 461-468.
- Soul, Dunn, Hardingham, Boot-Handford and Schwartz (2016) PhenomeScape: a cytoscape app to identify differentially regulated sub-networks using known disease associations. *Bioinformatics* 32/24: 3847-3849.
- Stannus, Jones, Blizzard, Cicuttini and Ding (2013) Associations between serum levels of inflammatory markers and change in knee pain over 5 years in older adults: a prospective cohort study. *Annals of the Rheumatic Diseases* 72/4: 535-540.
- Strobel, Loparic, Wendt, Schenk, Candrian, Lindberg, Moldovan, Barbero and Martin (2010) Anabolic and catabolic responses of human articular chondrocytes to varying oxygen percentages. *Arthritis Research & Therapy* 12/2: R34.
- Su, Kuchinsky, Morris, States and Meng (2010) GLay: community structure analysis of biological networks. *Bioinformatics* 26/24: 3135-3137.
- Subramanian, Tamayo, Mootha, Mukherjee, Ebert, Gillette, Paulovich, Pomeroy, Golub and Lander (2005) Gene set enrichment analysis: a knowledge-based approach for interpreting genome-wide expression profiles. *Proceedings of the National Academy of Sciences* 102/43: 15545-15550.
- Sukhatme, Cao, Chang, Tsai-Morris, Stamenkovich, Ferreira, Cohen, Edwards, Shows and Curran (1988) A zinc finger-encoding gene coregulated with c-fos during growth and differentiation, and after cellular depolarization. *Cell* 53/1: 37-43.
- Suri and Walsh (2012) Osteochondral alterations in osteoarthritis. *Bone* 51/2: 204-211.
- Sutton, Clutterbuck, Harris, Gent, Freeman, Foster, Barrett-Jolley and Mobasher (2009) The contribution of the synovium, synovial derived inflammatory cytokines and neuropeptides to the pathogenesis of osteoarthritis. *Veterinary Journal* 179/1: 10-24.
- Svensson, Natarajan, Ly, Miragaia, Labalette, Macaulay, Cvejic and Teichmann (2017) Power analysis of single-cell RNA-sequencing experiments. *Nature methods*.
- Swingler, Waters, Davidson, Pennington, Puente, Darrah, Cooper, Donell, Guile and Wang (2009) Degradome expression profiling in human articular cartilage. *Arthritis Research & Therapy* 11/3: R96.
- Takai, Kishimoto, Inoue and Nishizuka (1977) Studies on a cyclic nucleotide-independent protein kinase and its proenzyme in mammalian tissues. I. Purification and characterization of an active enzyme from bovine cerebellum. *J Biol Chem* 252/21: 7603-7609.

- Tang, Wu, Lei, Pang, Wan, Shi, Zhao, Nagy, Peng, Hu, Feng, Van Hul, Wan and Cao (2009) TGF-beta1-induced migration of bone mesenchymal stem cells couples bone resorption with formation. *Nature Medicine* 15/7: 757-765.
- Tanos, Marinissen, Leskow, Hochbaum, Martinetto, Gutkind and Coso (2005) Phosphorylation of c-Fos by members of the p38 MAPK family role in the AP-1 response to UV light. *Journal of Biological Chemistry* 280/19: 18842-18852.
- Team (2013) R: A language and environment for statistical computing. R Foundation for Statistical Computing, Vienna, Austria.[WWW document]. URL <http://www.R-project.org/>[Accessed December 24, 2013].
- Thakur, Dawes and McMahon (2013) Genomics of pain in osteoarthritis. *Osteoarthritis Cartilage* 21/9: 1374-1382. Available at <http://www.ncbi.nlm.nih.gov/pubmed/23973152>.
- Thijssen, van Caam and van der Kraan (2014) Obesity and osteoarthritis, more than just wear and tear: pivotal roles for inflamed adipose tissue and dyslipidaemia in obesity-induced osteoarthritis. *Rheumatology*: keu464.
- Thomas and Baneyx (1996) Protein misfolding and inclusion body formation in recombinant Escherichia coli cells overexpressing heat-shock proteins. *Journal of Biological Chemistry* 271/19: 11141-11147.
- Thoms, Dudek, Lafont and Murphy (2013) Hypoxia promotes the production and inhibits the destruction of human articular cartilage. *Arthritis and Rheumatism* 65/5: 1302-1312.
- Tian and Kreeger (2014) Analysis of the quantitative balance between insulin-like growth factor (IGF)-1 ligand, receptor, and binding protein levels to predict cell sensitivity and therapeutic efficacy. *BMC Systems Biology* 8/1: 98.
- Tortorella, Burn, Pratta, Abbaszade, Hollis, Liu, Rosenfeld, Copeland, Decicco and Wynn (1999) Purification and cloning of aggrecanase-1: a member of the ADAMTS family of proteins. *Science* 284/5420: 1664-1666.
- Toukap, Galant, Theate, Maudoux, Lories, Houssiau and Lauwerys (2007) Identification of distinct gene expression profiles in the synovium of patients with systemic lupus erythematosus. *Arthritis & Rheumatology* 56/5: 1579-1588.
- Troeberg and Nagase (2012) Proteases involved in cartilage matrix degradation in osteoarthritis. *Biochim Biophys Acta* 1824/1: 133-145. Available at <http://www.ncbi.nlm.nih.gov/pubmed/21777704>.
- Troeberg and Nagase (2012) Proteases involved in cartilage matrix degradation in osteoarthritis. *Biochimica et Biophysica Acta (BBA)-Proteins and Proteomics* 1824/1: 133-145.
- Tsuchida, Beekhuizen, Ct Hart, Radstake, Dhert, Saris, van Osch and Creemers (2014) Cytokine profiles in the joint depend on pathology, but are different between synovial fluid, cartilage tissue and cultured chondrocytes. *Arthritis Research & Therapy* 16/5: 441.
- Usami, Gunawardena, Iwamoto and Enomoto-Iwamoto (2016) Wnt signaling in cartilage development and diseases: lessons from animal studies. *Laboratory Investigation* 96/2: 186-196.
- Vadon-Le Goff, Hulmes and Moali (2015) BMP-1/tolloid-like proteinases synchronize matrix assembly with growth factor activation to promote morphogenesis and tissue remodeling. *Matrix Biology* 44: 14-23.
- Valdes, Spector, Tamm, Kisand, Doherty, Dennison, Mangino, Tamm, Kerna, Hart, Wheeler, Cooper, Lories, Arden and Doherty (2010) Genetic variation in the SMAD3 gene is associated with hip and knee osteoarthritis. *Arthritis and Rheumatism* 62/8: 2347-2352.
- Valinezhad Orang, Safaralizadeh and Kazemzadeh-Bavili (2014) Mechanisms of miRNA-mediated gene regulation from common downregulation to mRNA-specific upregulation. *International journal of genomics* 2014.

- van Beuningen, Glansbeek, van der Kraan and van den Berg (2000) Osteoarthritis-like changes in the murine knee joint resulting from intra-articular transforming growth factor-beta injections. *Osteoarthritis and Cartilage* 8/1: 25-33.
- van Caam, Madej, van Beuningen, Davidson and van der Kraan (2015) TGF-beta blocks chondrocyte hypertrophy and maintains cell viability in cultured cartilage explants but does not protect against proteoglycan loss. *Osteoarthritis and Cartilage* 23: A137-A138.
- van den Bosch, Blom, van Lent, van Beuningen, Blaney Davidson, van der Kraan and van den Berg (2014) Canonical Wnt signaling skews TGF-beta signaling in chondrocytes towards signaling via ALK1 and Smad 1/5/8. *Cell Signal* 26/5: 951-958.
- van den Bosch, Blom, van Lent, van Beuningen, Davidson, van der Kraan and van den Berg (2014) Canonical Wnt signaling skews TGF- β signaling in chondrocytes towards signaling via ALK1 and Smad 1/5/8. *Cellular Signalling* 26/5: 951-958.
- van der Kraan (2014) Age-related alterations in TGF beta signaling as a causal factor of cartilage degeneration in osteoarthritis. *Bio-Medical Materials and Engineering* 24/s1: 75-80.
- van der Kraan, Goumans, Davidson and Ten Dijke (2012) Age-dependent alteration of TGF- β signalling in osteoarthritis. *Cell and Tissue Research* 347/1: 257-265.
- van der Kraan and van den Berg (2007) Osteophytes: relevance and biology. *Osteoarthritis and Cartilage* 15/3: 237-244.
- van der Kraan and van den Berg (2008) Osteoarthritis in the context of ageing and evolution. Loss of chondrocyte differentiation block during ageing. *Ageing Res Rev* 7/2: 106-113.
- Van Meurs, Van Lent, Stoop, Holthuysen, Singer, Bayne, Mudgett, Poole, Billingham and Van Der Kraan (1999) Cleavage of aggrecan at the Asn341–Phe342 site coincides with the initiation of collagen damage in murine antigen-induced arthritis: A pivotal role for stromelysin 1 in matrix metalloproteinase activity. *Arthritis & Rheumatology* 42/10: 2074-2084.
- Verrecchia, Tacheau, Schorpp-Kistner, Angel and Mauviel (2001) Induction of the AP-1 members c-Jun and JunB by TGF-beta/Smad suppresses early Smad-driven gene activation. *Oncogene* 20/18: 2205-2211. Available at <http://www.ncbi.nlm.nih.gov/pubmed/11402315>.
- Vilar, Jansen and Sander (2006) Signal processing in the TGF-beta superfamily ligand-receptor network. *PLoS Computational Biology* 2/1: e3.
- Villiger and Lotz (1992) Differential expression of TGF beta isoforms by human articular chondrocytes in response to growth factors. *Journal of Cellular Physiology* 151/2: 318-325.
- Vogel and Marcotte (2012) Insights into the regulation of protein abundance from proteomic and transcriptomic analyses. *Nature reviews Genetics* 13/4: 227.
- Voit, Martens and Omholt (2015) 150 years of the mass action law. *PLoS Computational Biology* 11/1: e1004012.
- Vorburger and Hunt (2002) Adenoviral gene therapy. *The Oncologist* 7/1: 46-59.
- Wang, Rozelle, Lepus, Scanzello, Song, Larsen, Crish, Bebek, Ritter and Lindstrom (2011) Identification of a central role for complement in osteoarthritis. *Nature Medicine* 17/12: 1674-1679.
- Wang, Saadatpour and Albert (2012) Boolean modeling in systems biology: an overview of methodology and applications. *Physical Biology* 9/5: 055001.
- Wang, Shen, Jin, Im, Sandy and Chen (2011) Recent progress in understanding molecular mechanisms of cartilage degeneration during osteoarthritis. *Ann N Y Acad Sci* 1240: 61-69.
- Wang, Xu, Hunter and Ding (2015) Investigational drugs for the treatment of osteoarthritis. *Expert opinion on investigational drugs* 24/12: 1539-1556.

- Wann, Zuo, Haycraft, Jensen, Poole, McGlashan and Knight (2012) Primary cilia mediate mechanotransduction through control of ATP-induced Ca²⁺ signaling in compressed chondrocytes. *FASEB Journal* 26/4: 1663-1671.
- Waters and Baumgartner (2011) Sarcopenia and obesity. *Clinics in Geriatric Medicine* 27/3: 401-421.
- Wawra, Kuhl and Kestler (2007) Extended analyses of the Wnt/beta-catenin pathway: robustness and oscillatory behaviour. *FEBS Letters* 581/21: 4043-4048.
- Wegner, Bachmann, Schad, Lucarelli, Sahle, Nickel, Meyer, Klingmuller, Dooley and Kummer (2012) Dynamics and feedback loops in the transforming growth factor beta signaling pathway. *Biophysical Chemistry* 162: 22-34.
- Wei, Zhou, Wei, Zhang, Fleming, Terek, Pei, Chen, Liu and Wei (2012) Activation of Indian hedgehog promotes chondrocyte hypertrophy and upregulation of MMP-13 in human osteoarthritic cartilage. *Osteoarthritis and Cartilage* 20/7: 755-763.
- Wingfield, Palmer and Liang (2001) Folding and purification of insoluble (inclusion body) proteins from *Escherichia coli*. *Current protocols in protein science*: 6.5. 1-6.5. 30.
- Woessner (1973) Purification of cathepsin D from cartilage and uterus and its action on the protein-polysaccharide complex of cartilage. *Journal of Biological Chemistry* 248/5: 1634-1642.
- Woetzel, Huber, Kupfer, Pohlers, Pfaff, Driesch, Häupl, Koczan, Stiehl and Guthke (2014) Identification of rheumatoid arthritis and osteoarthritis patients by transcriptome-based rule set generation. *Arthritis Research & Therapy* 16/2: R84.
- Wu, Chen and Li (2016) TGF- β and BMP signaling in osteoblast, skeletal development, and bone formation, homeostasis and disease. *Bone research* 4: 16009.
- Xie, Tintani, Wang, Li, Zhen, Qiu, Wan, Crane, Chen and Cao (2016) Systemic neutralization of TGF- β attenuates osteoarthritis. *Annals of the New York Academy of Sciences* 1376/1: 53-64.
- Yaeger, Masi, de Ortiz, Binette, Tubo and McPherson (1997) Synergistic action of transforming growth factor-beta and insulin-like growth factor-I induces expression of type II collagen and aggrecan genes in adult human articular chondrocytes. *Experimental Cell Research* 237/2: 318-325.
- Yamamoto, Santamaria, Botkjaer, Dudhia, Troeberg, Itoh, Murphy and Nagase (2017) Inhibition of Shedding of Low-Density Lipoprotein Receptor-Related Protein 1 Reverses Cartilage Matrix Degradation in Osteoarthritis. *Arthritis & Rheumatology*.
- Yan, Liu and Chen (2009) Regulation of TGF-beta signaling by Smad7. *Acta Biochim Biophys Sin (Shanghai)* 41/4: 263-272.
- Yang, Chen, Xu, Li, Huang and Deng (2001) TGF-beta/Smad3 signals repress chondrocyte hypertrophic differentiation and are required for maintaining articular cartilage. *Journal of Cell Biology* 153/1: 35-46.
- Yang, Kim, Ryu, Oh, Chun, Kim, Min and Chun (2010) Hypoxia-inducible factor-2alpha is a catabolic regulator of osteoarthritic cartilage destruction. *Nature Medicine* 16/6: 687-693.
- Yeh, Chang, Chiang, Tsai, Chen, Wu, Chien and Chen (2009) Regulation of plasminogen activator inhibitor 1 expression in human osteoarthritic chondrocytes by fluid shear stress: role of protein kinase Calpha. *Arthritis and Rheumatism* 60/8: 2350-2361.
- Yu and Stamenkovic (2000) Cell surface-localized matrix metalloproteinase-9 proteolytically activates TGF-beta and promotes tumor invasion and angiogenesis. *Genes and Development* 14/2: 163-176.
- Yuan, Meng, Wang, Peng, Guo, Wang and Lu (2014) Bone-cartilage interface crosstalk in osteoarthritis: potential pathways and future therapeutic strategies. *Osteoarthritis and Cartilage* 22/8: 1077-1089.

- Zaiss, Hirtreiter, Rehli, Rehm, Kunz-Schughart, Andreesen and Hennemann (2003) CD84 expression on human hematopoietic progenitor cells. *Exp Hematol* 31/9: 798-805. Available at <http://www.ncbi.nlm.nih.gov/pubmed/12962726>.
- Zhang (2009) Non-Smad pathways in TGF-beta signaling. *Cell Research* 19/1: 128-139.
- Zhang, Feng and Derynck (1998) Smad3 and Smad4 cooperate with c-Jun/c-Fos to mediate TGF-beta-induced transcription. *Nature* 394/6696: 909-913.
- Zhao, Jin, Cui, Ren, Liu, Chen, Wong, Li, Fan, Rodriguez, Chang and Wong (2013) Novel modeling of cancer cell signaling pathways enables systematic drug repositioning for distinct breast cancer metastases. *Cancer Research* 73/20: 6149-6163.
- Zhao, Wang, Luo, Chen, Leung, Wen, Shah, Pan, Chiu, Cao and Lu (2016) Cartilage degeneration and excessive subchondral bone formation in spontaneous osteoarthritis involves altered TGF-beta signaling. *Journal of Orthopaedic Research* 34/5: 763-770.
- Zhen and Cao (2014) Targeting TGFβ Signaling in Subchondral Bone and Articular Cartilage Homeostasis. *Trends in Pharmacological Sciences* 35/5: 227-236.
- Zhen and Cao (2014) Targeting TGFβ signaling in subchondral bone and articular cartilage homeostasis. *Trends in Pharmacological Sciences* 35/5: 227-236.
- Zhen, Wen, Jia, Li, Crane, Mears, Askin, Frassica, Chang and Yao (2013) Inhibition of TGF-β signaling in subchondral bone mesenchymal stem cells attenuates osteoarthritis. *Nature Medicine* 19/6: 704.
- Zhen, Wen, Jia, Li, Crane, Mears, Askin, Frassica, Chang, Yao, Nayfeh, Johnson, Artemov, Chen, Zhao, Zhou, Cosgarea, Carrino, Riley, Sponseller, Wan, Lu and Cao (2013) Inhibition of TGF-β signaling in subchondral bone mesenchymal stem cells attenuates osteoarthritis. *Nature Medicine* 19/6: 704-712.
- Zhou, Chen, Lanske, Fleming, Terek, Wei, Zhang, Wang, Li and Wei (2014) Disrupting the Indian hedgehog signaling pathway in vivo attenuates surgically induced osteoarthritis progression in Col2a1-CreERT2; Ihhfl/fl mice. *Arthritis Research & Therapy* 16/1: R11.
- Zi, Feng, Chapnick, Dahl, Deng, Klipp, Moustakas and Liu (2011) Quantitative analysis of transient and sustained transforming growth factor-beta signaling dynamics. *Molecular Systems Biology* 7: 492.